UNIVERSITY OF SOUTHAMPTON

PHOTOCHEMISTRY OF SOME CYCLOPENTADIENYL CARBONYL COMPLEXES OF CHROMIUM, MOLYBDENUM, TUNGSTEN, IRON AND RUTHENIUM ISOLATED IN FROZEN GAS MATRICES AT 12K

by

Khalil Assaad Mahmoud

A Dissertation Submitted to
The University of Southampton
In Fulfilment of the Requirements
for the Degree of Doctor
of Philosophy

November 1983

ذكرى

الى الوالدين

To

My Parents

This dissertation describes work carried out in the Department of Chemistry of the University of Southampton between October 1980 and September 1983. It is the result of my own work and, unless specifically stated to the contrary in the text, includes nothing which is the result of work done in collaboration.

None of the presented work has been previously submitted for a degree by me in this or any University.

K.A. Mahmoud

November 1983

ACKNOWLEDGEMENTS

I wish to take this opportunity to express my sincere gratitude and thanks to the following:

My supervisor, Dr. Antony Rest, for his friendship, help, guidance and encouragement throughout this project.

Dr. Helmut Alt, friend and colleague, University of Bayreuth (West Germany) for preparing many of the complexes studied in this project.

Professor Wolfgang Malisch, University Würzburg (West Germany) for preparing the arsenic and antimony substituted complexes.

Dr. Ramaier Narayanaswamy, friend and colleague, for his help during the early stages of this project.

All of my friends, both inside and outside the Department, especially Eileen, Maheer and Bahzad for checking the text.

The Lebanese University, Faculty of Science, for financial support.

Finally I would particularly like to thank Mrs. Glenda North for her diligent and careful typing of an often difficult manuscript.

CONTENTS

INDEX OF FIGURES

PAGE

INDEX OF TABLES

UNIVERSITY OF SOUTHAMPTON

ABSTRACT

FACULTY OF SCIENCE

CHEMISTRY

Doctor of Philosophy

PHOTOCHEMISTRY OF SOME CYCLOPENTADIENYL CARBONYL COMPLEXES OF CHROMIUM, MOLYBDENUM, TUNGSTEN, IRON AND RUTHENIUM ISOLATED IN FROZEN GAS MATRICES AT 12K

By Khalil Assaad Mahmoud

Photochemical processes of a variety of cyclopentadienyl transition metal carbonyl complexes of general formula $(\eta^5\text{-}C_5H_5)M(CO)_nR$ (n = 3, M = Cr, Mo, W; n = 2, M = Fe, Ru; R = alkyl), $(\eta^5\text{-}C_5H_5)M(CO)_nX$ (n = 3, M = Mo, W; X = Cl, AsR_2, SbR_2; n = 2, M = Fe, Ru: X = Cl) and $(\eta^5\text{-}C_5H_5)_2Fe_2(CO)_4$ have been studied for the first time at 12K using primarily infrared spectroscopy together with ^{13}CO labelling.

Photoejection of CO from $(\eta^5\text{-}C_5H_5)M(CO)_3R$ complexes (M = Cr, Mo, W; R = CH_3, CF_3, $COCF_3$) results in the formation of the 16-electron species $(\eta^5\text{-}C_5H_5)M(CO)_2R$. Evidence is also found for α-H and α-F elimination in the complexes $(\eta^5\text{-}C_5H_5)Cr(CO)_3CH_3$ and $(\eta^5\text{-}C_5H_5)Mo(CO)_3CF_3$ respectively, and for the fluoroalkyl migration to the metal in the complex $(\eta^5\text{-}C_5H_5)Mo(CO)_3COCF_3$.

Photolysis of $(\eta^5\text{-}C_5H_5)M(CO)_3H$ complexes (M = Cr, Mo, W) in Ar and CH_4 matrices generates the 16-electron species $(\eta^5\text{-}C_5H_5)M(CO)_2H$. The reactivity of these species is apparent in their reactions with N_2 and C_2H_4 to produce $(\eta^5\text{-}C_5H_5)M(CO)_2(N_2)H$ and $(\eta^5\text{-}C_5H_5)M(CO)_2(C_2H_4)H$ derivatives. In CO matrices the observation of the radicals $(\eta^5\text{-}C_5H_5)M(CO)_3^{\cdot}$ and $HC\dot{O}$ is indicative of photo-induced metal-hydrogen bond cleavage. Irradiation of *trans*-$(\eta^5\text{-}C_5H_5)W(CO)_2(C_2H_4)H$ in CH_4 matrices causes *trans* $\rightleftarrows$ *cis* isomerisation, followed by insertion of C_2H_4 into the W-H bond to generate the 16-electron species $(\eta^5\text{-}C_5H_5)W(CO)_2C_2H_5$.

Irradiation of $(\eta^5\text{-}C_5R'_5)M(CO)_3$ alkyl complexes (M = Mo, W; R' = H, CH_3) results in the formation of the 16-electron intermediates $(\eta^5\text{-}C_5R'_5)M(CO)_2$ alkyl. For alkyl complexes with β-hydrogens, thermal and photochemical β-elimination reactions led to the conversion of $(\eta^5\text{-}C_5R'_5)M(CO)_2$ alkyl species into the olefin-hydrides $(\eta^5\text{-}C_5R'_5)M(CO)_2(\text{olefin})H$. Photolysis of the $(\eta^5\text{-}C_5H_5)W(CO)_3(\eta^1\text{-}R)$ complexes (R = C_3H_5, $CH_2C_6H_5$), led to CO dissociation and $\eta^1 \rightleftarrows \eta^3$ isomerisation.

Direct evidence for CO dissociation as a primary photoprocess for $(\eta^5\text{-}C_5H_5)M(CO)_2R$ complexes (M = Fe, Ru; R = CH_3, C_2H_5) was afforded by trapping the 16-electron species $(\eta^5\text{-}C_5H_5)Ru(CO)CH_3$ in a CH_4 matrix. Photolysis of $(\eta^5\text{-}C_5H_5)M(CO)_2C_2H_5$ complexes in CH_4 matrices afforded $(\eta^5\text{-}C_5H_5)Fe(CO)_2H$ and $(\eta^5\text{-}C_5H_5)Ru(CO)_2H$ together with $(\eta^5\text{-}C_5H_5)Ru(CO)(C_2H_4)H$, i.e. β-elimination. In CO matrices ring-slippage products, $(\eta^3\text{-}C_5H_5)M(CO)_3R$, were formed.

Irradiation of $(\eta^5\text{-}C_5H_5)M(CO)_3Cl$ complexes (M = Mo, W) in Ar and CH_4 matrices led to the 16-electron species $(\eta^5\text{-}C_5H_5)M(CO)_2Cl$. In CO matrices the formation of the ionic species $(\eta^5\text{-}C_5H_5)M(CO)_3^+$ and Cl^- occured and is indicative of photo-induced metal-chlorine bond cleavage. The $(\eta^5\text{-}C_5H_5)M(CO)_2Cl$ complexes (M = Fe, Ru) gave only the 16-electron species $(\eta^5\text{-}C_5H_5)M(CO)Cl$.

Evidence is presented for the formation of the 16-electron species $(\eta^5\text{-}C_5H_5)(CO)_2M\text{-}ER_2$ and the double bonded complexes $(\eta^5\text{-}C_5H_5)(CO)_2M{=}ER_2$ on irradiation of the transition metal substituted arsine and stibine complexes $(\eta^5\text{-}C_5H_5)(CO)_3M\text{-}ER_2$ (M = Mo, E = As, Sb; M = W, E = As). Photolysis of $(\eta^5\text{-}C_5H_5)_2Fe_2(CO)_4$ led to the formation of the novel species $(\eta^5\text{-}C_5H_5)_2Fe_2(\mu\text{-}CO)_3$ in CH_4 matrices and to non-bridged $(\eta^5\text{-}C_5H_5)_2Fe_2(CO)_4$ in CO matrices.

CHAPTER ONE

INTRODUCTION

1.1 Intermediates Proposed in Reactions Catalysed by Transition Metal Organometallic Complexes

Organotransition-metal complexes have been implicated as intermediates in many important chemical reactions, many of which are carried out on large scales as industrial processes, e.g. the hydroformylation of olefins which produces between 3.6 and 4.5 million tonnes of aldehydes or derivatives annually [1]. The ability of a transition metal to accommodate several different ligands in its co-ordination sphere is clearly important if it is to catalyse reactions between one or more substrates. Thus, in a hydroformylation reaction [2, 3] (Equation 1.1), the transition metal must be able to

$$RCH = CH_2 + CO + H_2 \xrightarrow{\text{Co or Rh}} RCH_2CH_2CHO + RCH(CH_3)CHO \qquad (1.1)$$

accommodate olefin, carbonyl and hydride within its co-ordination sphere during the course of the reaction together with any other non-participative ligands.

The ability of transition metals to exist in several oxidation states allows a wide range of complexes with other elements and compounds to be formed. However, perhaps more important than this is the ability to readily interchange between oxidation states during the course of chemical reactions and catalytic cycles. For example, in the rhodium catalysed hydrogenation reaction (Equation 1.2), the rhodium undergoes a I → III → I.

$$\overset{\text{I}}{Rh}ClL_2 \xrightarrow{H_2} \overset{\text{III}}{Rh}H_2ClL_2 \xrightarrow{RCH = CH_2} \overset{\text{III}}{Rh}H(RCH_2CH_2)ClL_2 \qquad (1.2)$$

$$\overset{\text{III}}{Rh}H(RCH_2CH_2)ClL_2 \xrightarrow[-RCH_2CH_3]{L = PPh_3} RhClL_2$$

oxidation state change for every catalytic cycle [4]. Similarly in hydrogenation reactions catalysed by $RuH(PPh_3)_2Cl$ the proposed mechanism involves

a II → IV → II oxidation state change for the ruthenium catalyst [3, 5].

The proposed catalytic cycle, e.g. the generalised cycle for hydroformylation (Scheme 1.1), involves a number of coordinatively saturated 18-electron species (I, III, V), for which stable model compounds have been isolated, and unstable coordinatively unsaturated 16-electron species (II, IV, VI). In order to verify such a catalytic cycle it is essential that evidence for the existence of species II, IV, and VI and any other potential intermediates should be sought.

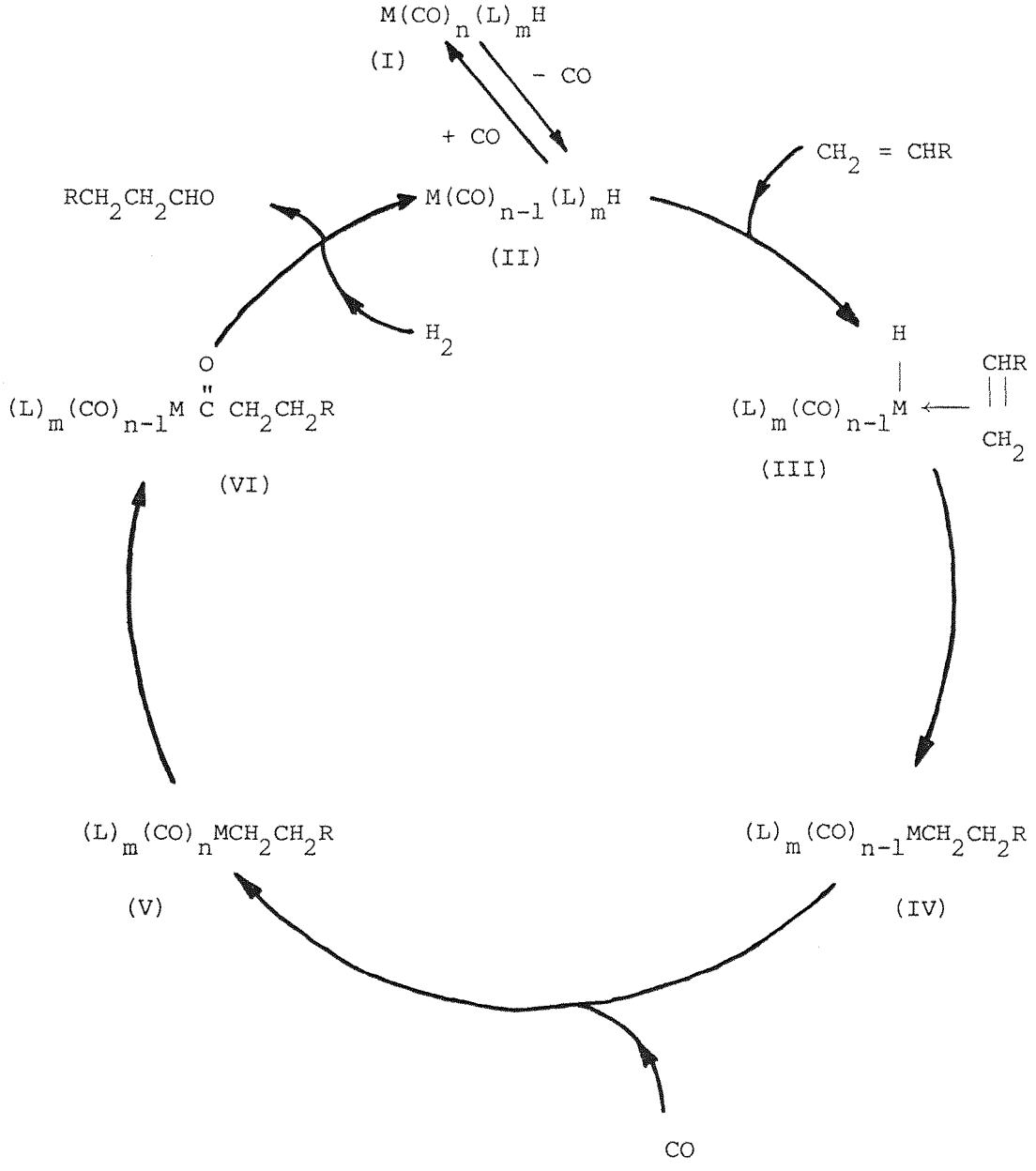

Scheme 1.1

In catalytic cycles two very important processes are insertion/ inter-ligand migration and elimination:

(a) Insertion/inter-ligand migration. In this process, two substrates, X and Y bonded to the metal centre combine to form an intermediate XY which remains bonded to the metal centre (Equation 1.3).

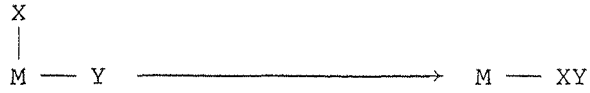

(1.3)

Such metal insertion or inter-ligand migration reactions are to be found in almost all catalytic systems. The vacant co-ordination site resulting from the migration can be filled by solvent or by incoming ligand. In catalytic systems where this particular process is important, e.g. carbonylation and hydroformylation, the incoming ligand is usually carbon monoxide. In small scale reactions, ligands such as $P(OPh)_3$ or PPh_3 are equally effective in promoting alkyl migration reactions.

(b) Elimination. When a substrate undergoes some fragmentation change such that it gives rise to a stable product, then such a process is described as elimination.

Metal alkyl complexes often readily convert to a metal-hydrido complex plus alkene by transfer of a hydrogen on the β-carbon alkyl unit to the metal (Equation 1.4). This process, β-elimination, is particularly significant in

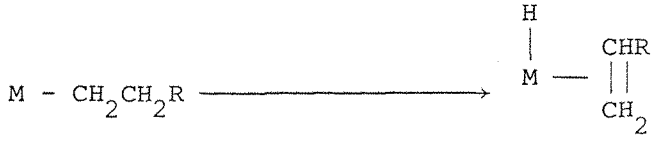

(1.4)

the transition-metal catalysed isomerisation of olefins and as a termination process in metal-catalysed alkene polymerization reactions. Essentially this type of elimination process is the reverse of the inter-ligand insertion reaction (Equation 1.5).

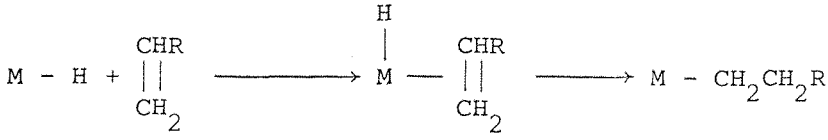

(1.5)

Although less well documented, eliminations involving a group in the α-position of the substrate can also occur. Such a process, known as α-elimination (Equation 1.6), has been proposed to occur in tungsten-methyl

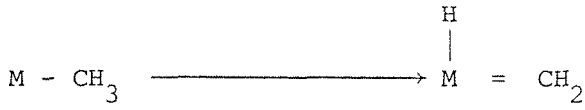

(1.6)

complexes [6]. Metal carbene ($M = CR_2$) complexes have been proposed as the active intermediates in tungsten and molybdenum catalysed metathesis reactions [7]. In 1973 Casey and Burkhardt reported [8] the synthesis and isolation of the metal-carbene complexes (I) with R = H, Ph. This complex is

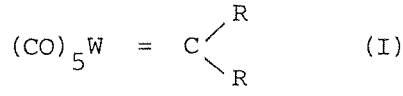

(I)

closer to the type of carbene species envisaged as taking part in metathesis reactions because it does not contain a hetero-atom bonded to carbene carbon. The significance of (I) to the mechanism of alkene metathesis was demonstrated by a model metathesis reaction (Equation 1.7) [9].

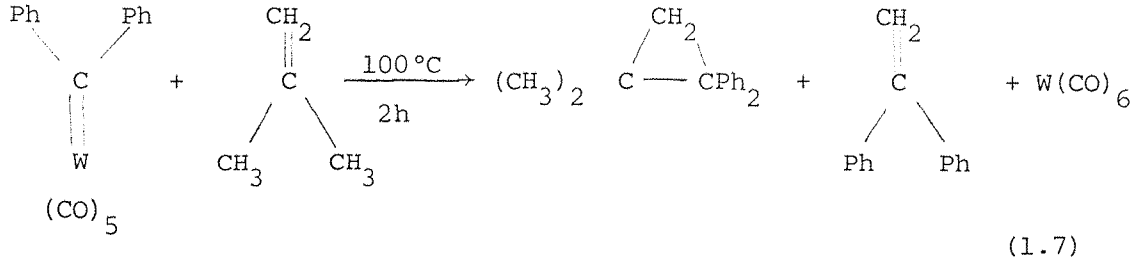

(1.7)

The use of light in a catalytic cycle has significant advantages. For example, light-induced loss of CO from $Fe(CO)_5$ [10], is one of the oldest known photoreactions of transition metal organometallic compounds (Equation 1.8).

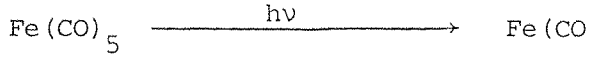

(1.8)

This process is undoubtedly the first step in the photochemical formation of a very active catalyst for the isomerisation, hydrogenation, and hydrosilation of alkenes [11]. The isomerisation of alkenes, for example, is believed to occur via a π-allyl hydride intermediate generated by the sequence indicated in Scheme 1.2

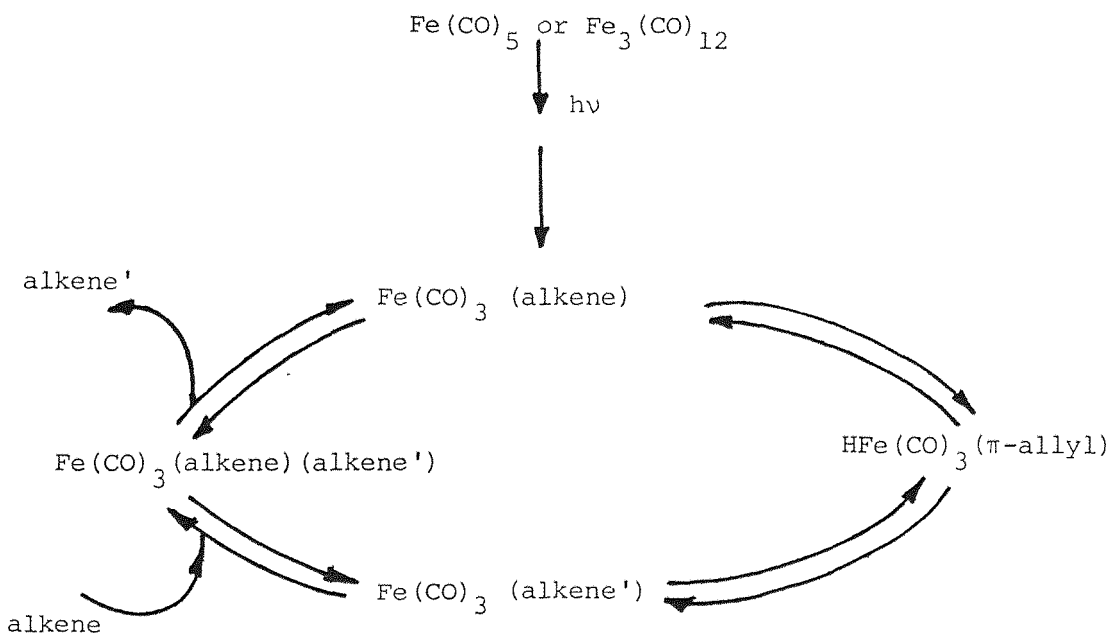

Scheme 1.2

1.2 Matrix Isolation Studies of Unstable Transition Metal Carbonyls and Related Species

Thermal reactions of organometallic complexes often involve the replacement of bound ligands as steps in the overall reaction processes, e.g. substitution reactions. For such substitution reactions, kinetic studies have established two broad categories of reactions: (i) those reactions which show a dependence solely on the concentration of the metal complex and (ii) others which show a dependence on the concentrations of the metal complex and of the incoming ligand. The former reactions are described as proceeding by

a dissociative mechanism with coordinatively unsaturated species, e.g. (I) in Scheme 1.3, postulated as reaction intermediates. The latter reactions are described as proceeding by an associative mechanism with expanded coordination number species, e.g. (II) in Scheme 1.3, postulated as intermediates.

Many organometallic compounds are not very thermodynamically stable so that the thermal energy required to effect their synthesis and to carry out reactions with them often leads to decomposition. However, uv-vis irradiation of the reaction mixture at ambient temperatures and/or lower temperatures, i.e. a photochemical reaction, often leads to a good yield of products. In the general photochemical reaction illustrated in Scheme 1.4, the absorption of energy to give an excited state, $M(CO)_nA^*$ leads to products (III'), (IV') and (V') which may be accounted for by proposing the existence of coordinatively unsaturated short-lived intermediate species (III) - (V).

Mechanisms for thermal and photochemical reactions could be put on firmer bases if evidence could be found for the existence of species such as (I) - (V), which have been proposed as reaction intermediates. Furthermore, if precise details of the structure, reactivity and bonding of such species could be determined, it should be possible to develop a better understanding of organometallic reactions. Such an understanding could lead to a rational and predictive approach to the reactions of organometallic complexes and, importantly, to establishing the validity or otherwise of catalytic cycles.

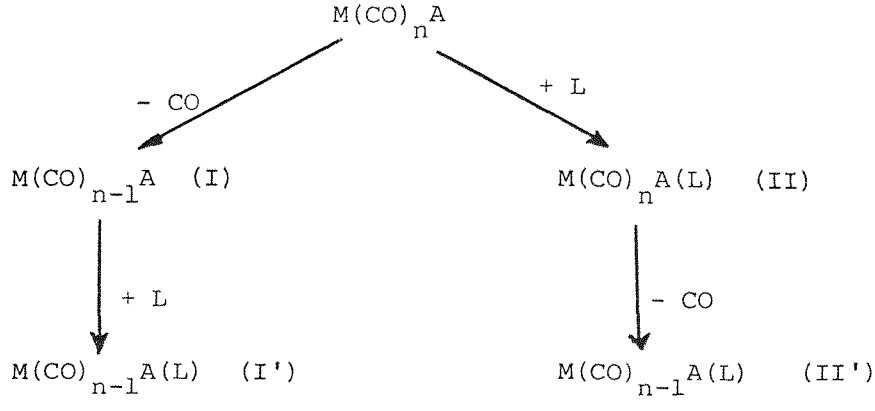

Scheme 1.3

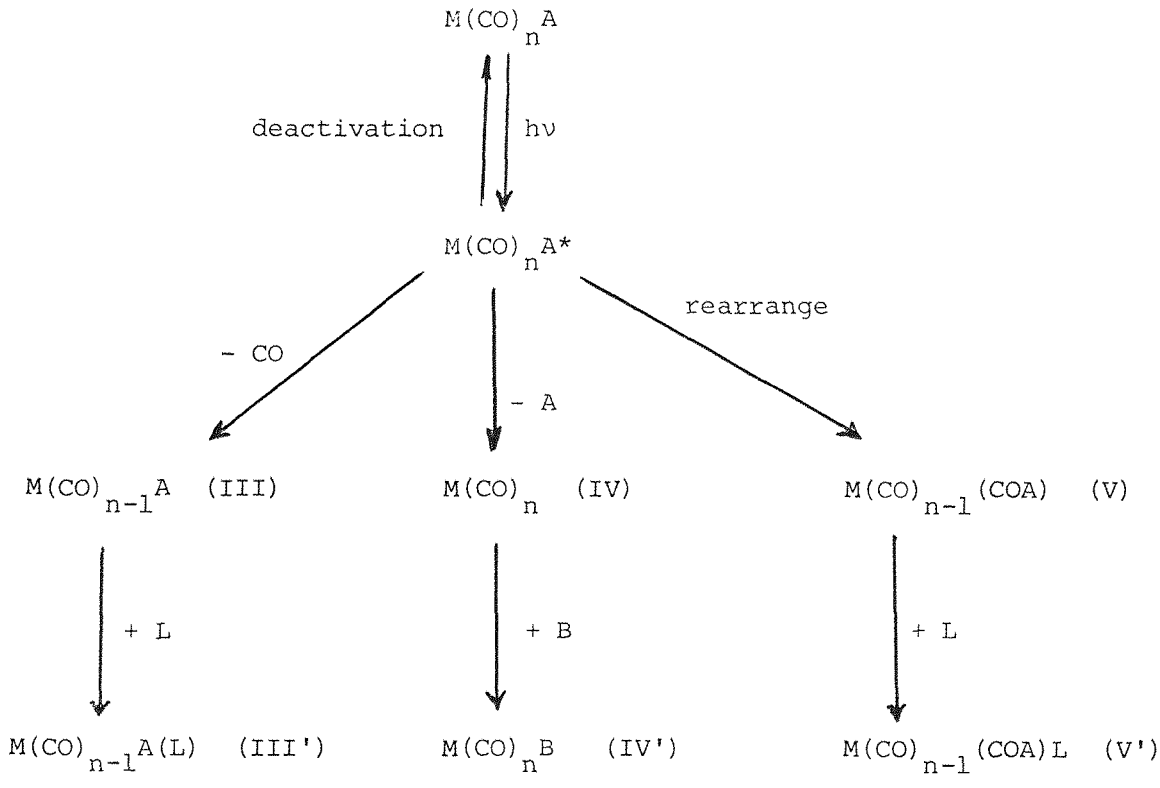

Scheme 1.4

Given that reaction intermediates and transition state species are highly reactive and very unstable, there are basically two ways of studying them:

(a) To observe them in their natural lifetime by rapid detection techniques, e.g. flash photolysis and pulse radiolysis;

(b) To prolong their life by quenching the species, once they have been formed, at low temperatures, e.g. matrix isolation spectroscopy.

For molecules with more than a few atoms approach (a), although capable of giving information about the lifetimes of species down to picoseconds, gives little information about the detailed structures of the species. This is because the very short lifetimes are measured using electronic absorption bands which are generally broad and structureless for organometallic complexes.

Approach (b), however, allows more leisure for spectroscopy and using the matrix isolation technique very detailed information about the structure of unstable species can be obtained.

The essential features of the matrix isolation technique [12, 13] are that (i) the unstable species are surrounded by large numbers of unreactive host matrix atoms or molecules which form a rigid array so that pairs of unstable species cannot come together for bimolecular reactions, and (ii) at low temperatures, and especially at temperatures in the range 4-25K, the unstable molecules themselves have very little internal energy and so cannot decompose by unimolecular reactions. Unstable species for matrix isolation spectroscopy are produced primarily either by some gas-phase reaction or process and then quenched on to the cold spectroscopic window or by decomposing stable molecules already isolated in the matrices using some form of irradiation. In order to generate the types of unstable species which have been proposed in reaction mechanisms, e.g. Schemes 1.3 and 1.4 the latter approach has been most widely used.

This thesis describes new applications of matrix isolation studies to the photochemistry of some cyclopentadienyl carbonyl complexes of chromium, molybdenum, tungsten, iron and ruthenium isolated in frozen gas matrices at 12K and provides evidence for dissociative and associative pathways and several types of intramolecular rearrangement. The new species obtained in this study are related to the intermediates proposed in catalytic cycles. For example, the observation of CO substitution by C_2H_4 followed by C_2H_4 insertion into a W-H bond in $(\eta^5\text{-}C_5H_5)W(CO)_2(C_2H_4)H$, c.f. (II) → (IV) in Scheme 1.1.

1.3 References

1. B. Cornils, R. Payer and K.C. Traenchner. *Hydrocarbon Processing*, 1975, 54(6), 83.

2. J. Falbe, *Carbon Monoxide in Organic Synthesis*, New York, 1970.

3. C. Masters, *Homogeneous Transition-Metal Catalysis*, Chapman and Hall, London, 1981.

4. L.H. Slaugh and R.D. Mullineaux, *U.S. Patent 3*, 1966, 239, 570; and ibid, *J. Organomet. Chem.*, 1968, 13, 469.

5. B.R. James, A.D. Rattray and D.K. Wang, *J. Chem. Soc. Chem. Commun.*, 1976, 792.

6. N.J. Cooper and M.L.H. Green, *J. Chem. Soc. Chem. Commun.*, 1974, 761.

7. N. Calderon, J.P. Lawrence and E.A. Ofstead, *Adv. Organomet. Chem.*, 1979, 17, 449.

8. C.P. Casey and T.J. Burkhardt, *J. Am. Chem. Soc.*, 1973, 95, 5833.

9. C.P. Casey and T.J. Burkhardt, *J. Am. Chem. Soc.*, 1974, 96, 7808.

10. J. Dewar and H.O. Jones, *Proc. Roy. Soc. London, Ser. A.*, 1905, 76, 558.

11. M.A. Schroeder and M.S. Wrighton, *J. Am. Chem. Soc.*, 1976, 98, 551 and *J. Organomet. Chem.*, 1977, 128, 345.

12. A.J. Barnes, W.J. Orville-Thomas, A. Müller and R. Gaufrès (Eds.), *"Matrix Isolation Spectroscopy"*, *NATO ASI Series*, D. Reidel Publ. Co., Dordrect, Holland, 1981.

13. M. Moskovits and G.A. Ozin, in *"Cryochemistry"*, John Wiley, 1976.

CHAPTER TWO

PHOTOCHEMISTRY OF THE COMPLEXES $(\eta^5\text{-}C_5H_5)M(CO)_3CH_3$ (M = Cr, Mo, W), $(\eta^5\text{-}C_5H_5)Mo(CO)_3CF_3$ AND $(\eta^5\text{-}C_5H_5)Mo(CO)_3COCF_3$ IN LOW TEMPERATURE GAS MATRICES AT 12K

2.1 INTRODUCTION

The primary process dominating the photochemistry of $(\eta^5\text{-}C_5H_5)M(CO)_3X$ (M = Cr, Mo, W; X = Cl, I, CH_3) complexes is the dissociative loss of CO [1 - 6]. Barnett and Treichel [1] first studied the photolysis of $(\eta^5\text{-}C_5H_5)M(CO)_3CH_3$ complexes (M = Mo, W) in the presence of PPh_3. Thermal substitution of carbon monoxide by phosphine was observed, but the reaction proceeded much faster under u.v. irradiation. The resultant yield of products, however, was lower due to photodecomposition. For the molybdenum complex, the principal products were $(\eta^5\text{-}C_5H_5)Mo(CO)_2(PPh_3)CH_3$ and $(\eta^5\text{-}C_5H_5)Mo(CO)_2(PPh_3)COCH_3$ complexes. Both products were believed to arise through initial photosubstitution of CO by PPh_3 with the acetyl derivative coming from a secondary thermal reaction with carbon monoxide (Equation 2.1). A similar process had been previously shown to lead to the acetyl derivative of $(\eta^5\text{-}C_5H_5)Fe(CO)_2CH_3$ [7]. The tungsten complex gave only photosubstitution of CO by PPh_3; no acetyl product could be isolated.

$$(\eta^5\text{-}C_5H_5)M(CO)_3CH_3 + PPh_3 \xrightarrow[-CO]{h\nu} (\eta^5\text{-}C_5H_5)M(CO)_2(PPh_3)CH_3$$

$$\downarrow \Delta, CO \qquad (2.1)$$

$$(\eta^5\text{-}C_5H_5)M(CO)_2(PPh_3)\overset{O}{\overset{\|}{C}}CH_3$$

In subsequent reports, Alt [8] confirmed Barnett and Treichel's observation of photosubstitution of $(\eta^5\text{-}C_5H_5)W(CO)_3CH_3$ with phosphine and phosphite ligands and showed an analogous photoreactivity pattern for

$(\eta^5\text{-}C_5H_5)Cr(CO)_3CH_3$. The chromium complex also gave the acetyl derivative $(\eta^5\text{-}C_5H_5)Cr(CO)_2(PPh_3)COCH_3$, presumably from a thermal reaction of the initially formed $(\eta^5\text{-}C_5H_5)Cr(CO)_2(PPh_3)CH_3$. Alt also observed that photolysis of the $(\eta^5\text{-}C_5H_5)M(CO)_3CH_3$ (M = Cr, Mo, W) complexes in pentane solution in the absence of excess ligand led to formation of the binuclear complexes $[(\eta^5\text{-}C_5H_5)M(CO)_3]_2$ and $[(\eta^5\text{-}C_5H_5)M(CO)_2]_2$ (Equation 2.2). Methane

$$(\eta^5\text{-}C_5H_5)M(CO)_3CH_3 \xrightarrow[300\ nm]{h\nu} [(\eta^5\text{-}C_5H_5)M(CO)_3]_2 + [(\eta^5\text{-}C_5H_5)M(CO)_2]_2 + CH_4 \qquad (2.2)$$

was identified as the gaseous product, and labelling studies [9] showed that abstraction of hydrogen from a cyclopentadienyl ligand had occured. It was suggested that homolysis of the $M\text{-}CH_3$ represented the primary photochemical event in these complexes. Photolysis of the $(\eta^5\text{-}C_5H_5)M(CO)_3CH_3$ complexes in $CHCl_3$ gave high yields of $[(\eta^5\text{-}C_5H_5)CrCl_2]_2$ for chromium and $(\eta^5\text{-}C_5H_5)M(CO)_3Cl$ complexes for Mo and W.

Severson et al. [10] have also examined the photoreactivity of $(\eta^5\text{-}C_5H_5)W(CO)_3R$ (R = CH_3, $CH_2C_6H_5$) and presented the most definitive mechanistic data. Their results essentially confirmed the observations of Treichel [1] and Alt [8], but their key result was in noting that the quantum yield of formation of $[(\eta^5\text{-}C_5H_5)W(CO)_3]_2$ from $(\eta^5\text{-}C_5H_5)W(CO)_3CH_3$ was greatly suppressed when the complex was irradiated under a CO atmosphere compared to when the photolysis was carried out under Ar. This strongly implicated CO dissociation as the primary photochemical event, rather than M - CH_3 homolysis, as suggested by Rausch and Alt [9]. Methane was suggested to arise from secondary thermal or photochemical reactions, but no further mechanistic experiments were reported. The overall mechanism was suggested [10] to be as shown in Equation 2.3.

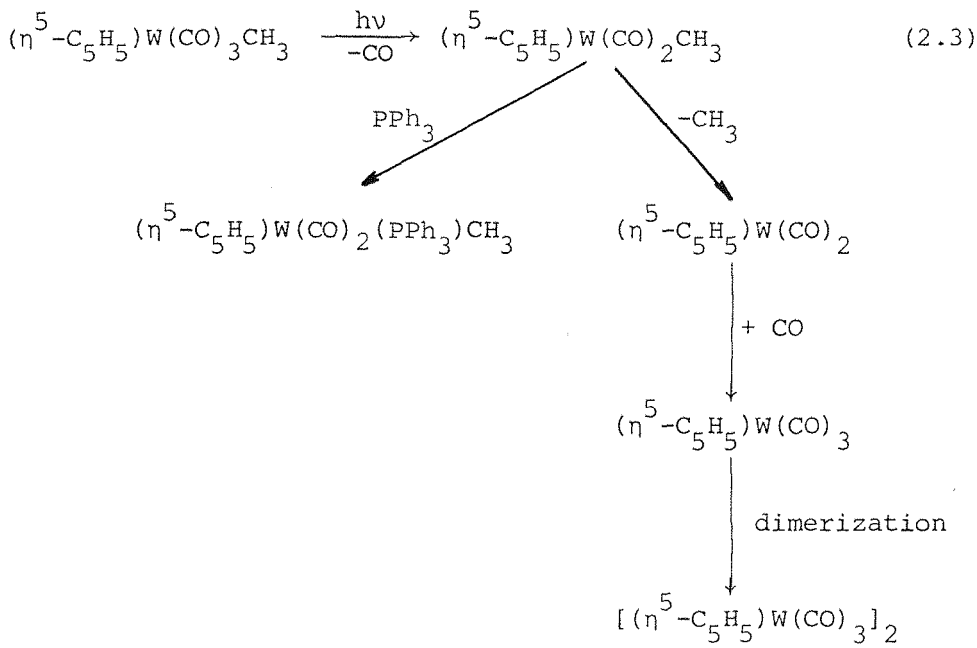

Since carbon monoxide is among the best of π-acceptor ligands, and coordinates virtually with all the transition metals, the ease of the migration-insertion reactions in which the alkyl metal carbonyl complexes are converted to acyl metal complexes, allows metal carbonyls to be effective carbonylation (acylating) agents for a variety of organic substrates. For example, the complexes $(\eta^5\text{-}C_5H_5)Mo(CO)_3R$ (R = CH_3, C_2H_5) react with ethylene at 100°C and with $(\eta^5\text{-}C_5H_5)Mo(CO)_3H$ at 25°C to yield ketones and aldehydes [11].

Using frozen gas matrices at 12K the work described in this chapter illustrates that the principal photoprocess for isolated $(\eta^5\text{-}C_5H_5)M(CO)_3CH_3$ (M = Cr, Mo, W) and $(\eta^5\text{-}C_5H_5)Mo(CO)_3CF_3$ molecules is ejection of CO to give the 16-electron species $(\eta^5\text{-}C_5H_5)M(CO)_2CH_3$ and $(\eta^5\text{-}C_5H_5)Mo(CO)_2CF_3$ respectively whose reactivity was demonstrated by their facile recombination with CO at ∿ 30K [12]. In addition to CO ejection the complexes $(\eta^5\text{-}C_5H_5)Cr(CO)_3CH_3$ and $(\eta^5\text{-}C_5H_5)Mo(CO)_3CF_3$ undergo α-hydride and α-fluoride migrations to give new carbene complexes $(\eta^5\text{-}C_5H_5)Cr(CO)_2(=CH_2)H$ and $(\eta^5\text{-}C_5H_5)Mo(CO)_2(=CF_2)F$ respectively. This chapter will also provide further evidence that the acyl group of the $(\eta^5\text{-}C_5H_5)Mo(CO)_3COCF_3$ complex can be decarbonylated photochemically to yield the corresponding alkyl complex $(\eta^5\text{-}C_5H_5)Mo(CO)_3CF_3$ [13]

via the coordinatively unsaturated 16-electron species, $(\eta^5\text{-}C_5H_5)Mo(CO)_2COCF_3$.

2.2 RESULTS

2.2.1 Photolysis of $(\eta^5\text{-}C_5H_5)M(CO)_3CH_3$ Complexes (M = Cr, Mo, W)* in CH_4, Ar and CO Matrices and of ^{13}CO-enriched $(\eta^5\text{-}C_5H_5)Mo(CO)_3CH_3$ in a CH_4 Matrix

The i.r. spectrum of $(\eta^5\text{-}C_5H_5)Mo(CO)_3CH_3$ isolated at high dilution in a CH_4 matrix is shown in Figure 2.1(a). The spectrum shows that although the $Mo(CO)_3CH_3$ fragment has a local C_s symmetry, i.e. three infrared-active CO stretching bands are expected, only a single low wavenumber band ($\sim$ 1940 cm^{-1}) is observed in addition to the high wavenumber symmetric (A') band ($\sim$ 2025 cm^{-1}, Table 2.1). The single low wavenumber band must, therefore, arise from an accidental coincidence between the A" and the lower A' bands.

Irradiation of the matrices with u.v. light (λ = 320 - 370 nm) giving light corresponding to the long wavelength absorption (Figure 2.2(a)) produced free CO ($\sim$ 2138 cm^{-1}) and two new bands at 1966.0 and 1880.1 cm^{-1} (Figure 2.1(b) and Figure 2.1(c)). The production of these two bands is accompanied by the decrease of parent molecule and an increase in the band of free CO. After irradiation with long-wavelength light (λ > 430 nm), c.f. the long wavelength tail (Figure 2.2(b)), or annealing the matrix for 3 minutes and then re-cooling to 12K, the new product bands were observed to decrease with the regeneration of $(\eta^5\text{-}C_5H_5)Mo(CO)_3CH_3$ bands (Figure 2.1(d)). The relative intensity of the new terminal CO stretching bands remained constant under a variety of photolysis conditions (time and wavelength of irradiation) indicating that the bands arose from a single product species. The dilution used (ca 1:2000) and the reversibility of the matrix reaction rule out the possibility of formation of polynuclear aggregate species, e.g.

---

*The chromium complex, $(\eta^5\text{-}C_5H_5)Cr(CO)_3CH_3$ showed different behaviour from the molybdenum and tungsten analogues and its photochemistry is described separately (see section 2.2.4).

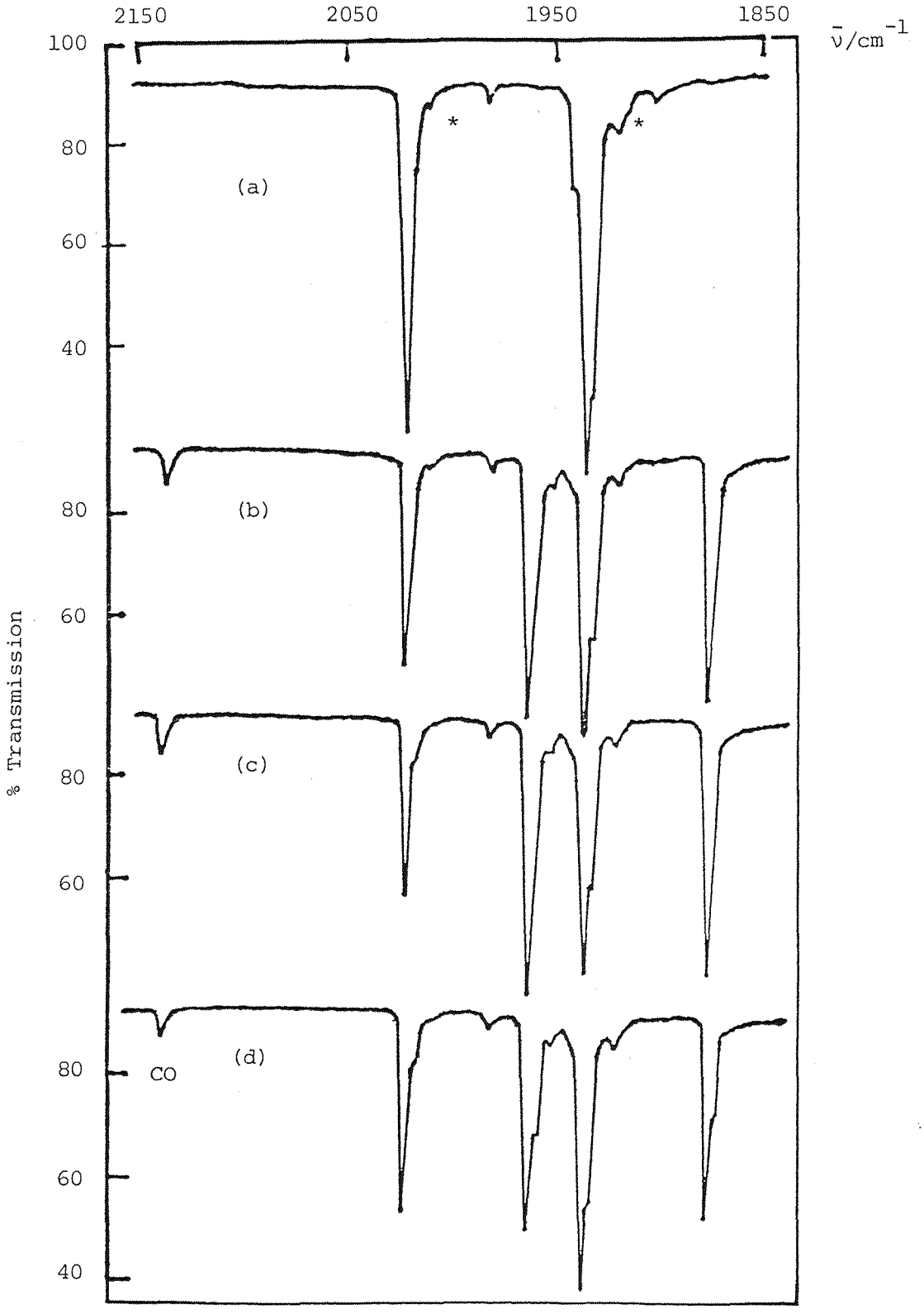

FIGURE 2.1 Infrared spectra from an experiment with $(\eta^5\text{-}C_5H_5)Mo(CO)_3CH_3$ isolated at high dilution in a CH_4 matrix at 12K: (a) after deposition, (b) after 15 min photolysis using (λ = 320 - 370 nm), (c) after further 15 min photolysis using (λ = 320 - 370 nm) and (d) after annealing the matrix to $\sim$ 30K. Bands marked * are due to $(\eta^5\text{-}C_5H_5)Mo(^{12}CO)_2(^{13}CO)CH_3$ in natural abundance.

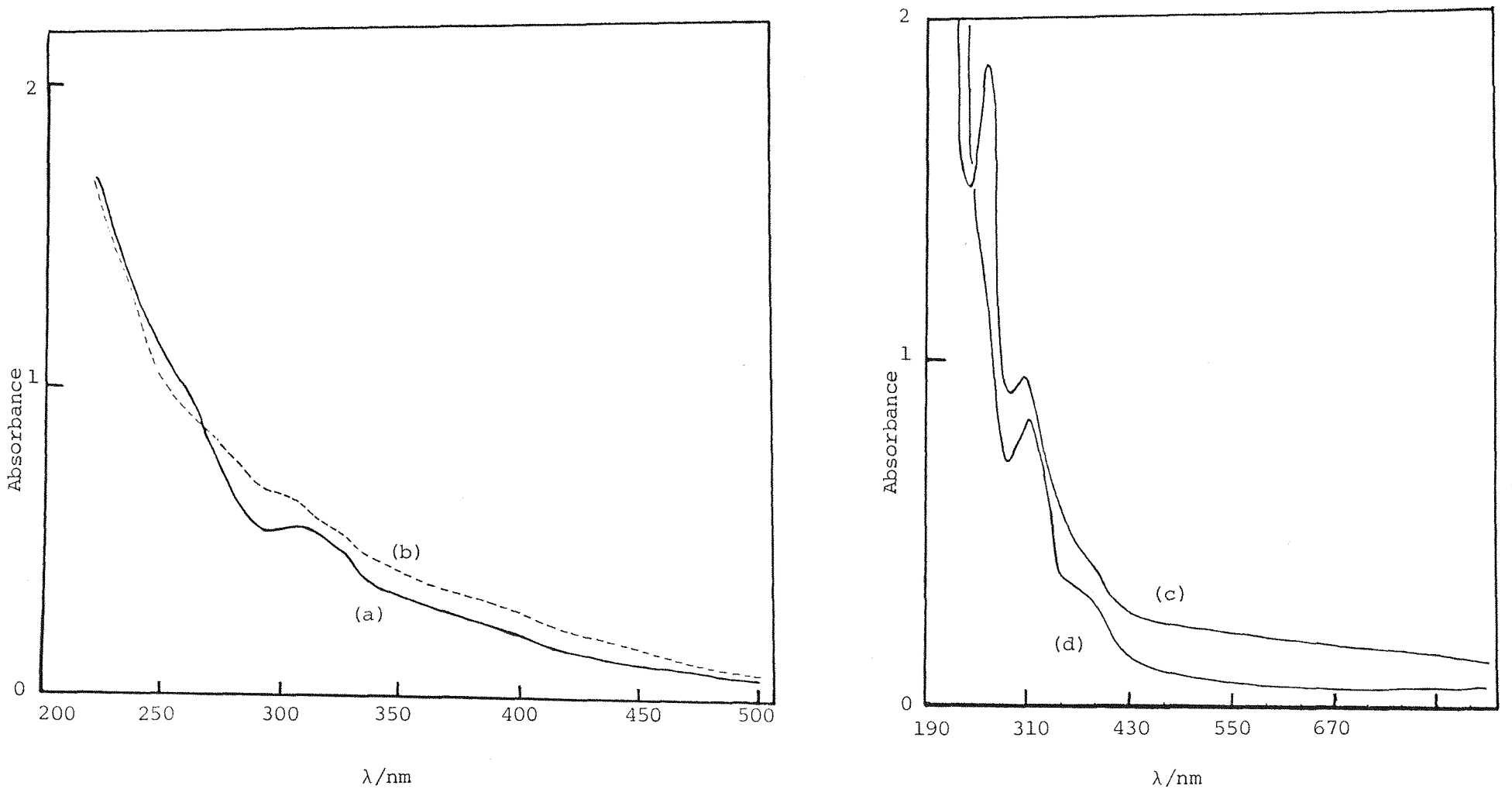

FIGURE 2.2 Ultraviolet/visible spectra of: (a) $(\eta^5\text{-}C_5H_5)Mo(CO)_3CH_3$ after deposition, (b) after 30 min photolysis using (λ = 320 - 370 nm), (c) $(\eta^5\text{-}C_5H_5)Mo(CO)_3CF_3$ after deposition and (d) $(\eta^5\text{-}C_5H_5)Mo(CO)_3COCF_3$ after deposition. All complexes were isolated at high dilution in CH_4 matrices.

$[(\eta^5\text{-}C_5H_5)Mo(CO)_3]_2$, as confirmed by separate matrix isolation studies of $[(\eta^5\text{-}C_5H_5)Mo(CO)_3]_2$ [14]. We, therefore, assign these new bands to the dicarbonyl complex $(\eta^5\text{-}C_5H_5)Mo(CO)_2CH_3$, the bands corresponding to the A' (1966.0 cm^{-1}) and A" (1880.1 cm^{-1}) terminal CO stretching modes with local C_s symmetry (Table 2.1).

Analogous results were obtained for Ar and CO matrices (Table 2.1) although the rates of photo-reactions were slower, as has been observed elsewhere [15, 16]. The tungsten complex, $(\eta^5\text{-}C_5H_5)W(CO)_3CH_3$, gave identical results in CH_4, Ar and CO matrices with the exception that a much higher yield of the unsaturated 16-electron species $(\eta^5\text{-}C_5H_5)W(CO)_2CH_3$ was observed in CO matrices compared to the low yield of $(\eta^5\text{-}C_5H_5)Mo(CO)_2CH_3$. Spectroscopic data for the new species is presented in Table 2.1.

The i.r. spectrum of ^{13}CO-enriched $(\eta^5\text{-}C_5H_5)Mo(CO)_3CH_3$ isolated in a pure CH_4 matrix (Figure 2.3(a)) shows bands due to the complexes $(\eta^5\text{-}C_5H_5)Mo(^{12}CO)_{3-n}(^{13}CO)_nCH_3$ (n = 0, 1, 2, 3), as confirmed by the excellent correspondence between observed and calculated [15 - 17] band positions (Table 2.2), obtained using an energy-factored force-field. Photolysis of the complexes using u.v. light (λ = 310 - 370 nm) gave new ^{13}CO-enriched product bands at 1947.8, 1852.7 and 1836.8 cm^{-1} in addition to the bands for the ^{12}CO species at 1965.9 and 1879.6 cm^{-1} (Figures 2.3(b) and 2.3(c)). In this case a good fit was obtained for the observed and calculated bands of a C_s $Mo(CO)_2$ fragment (Table 2.2). The photoproduct in Ar, CH_4 and CO matrices (see above) can, therefore, be conclusively assigned as $(\eta^5\text{-}C_5H_5)Mo(CO)_2CH_3$. The observed relative intensity of the two terminal bands (1.32 for A':A" and obtained by tracing and weighing the bands) was used to calculate a OC-Mo-CO angle of 82 ± 1° from the standard expression [18] $I_{sym}/I_{antisym} = \cot^2(\theta/2)$.

2.2.2 Photolysis of $(\eta^5\text{-}C_5H_5)M(CO)_3CH_3$ Complexes (M = Mo, W) and of ^{13}CO-enriched $(\eta^5\text{-}C_5H_5)Mo(CO)_3CH_3$ in N_2 Matrices

The i.r. spectrum of $(\eta^5\text{-}C_5H_5)Mo(CO)_3CH_3$ isolated in a pure N_2 matrix in the terminal CO stretching region (Table 2.1) is very similar to that in

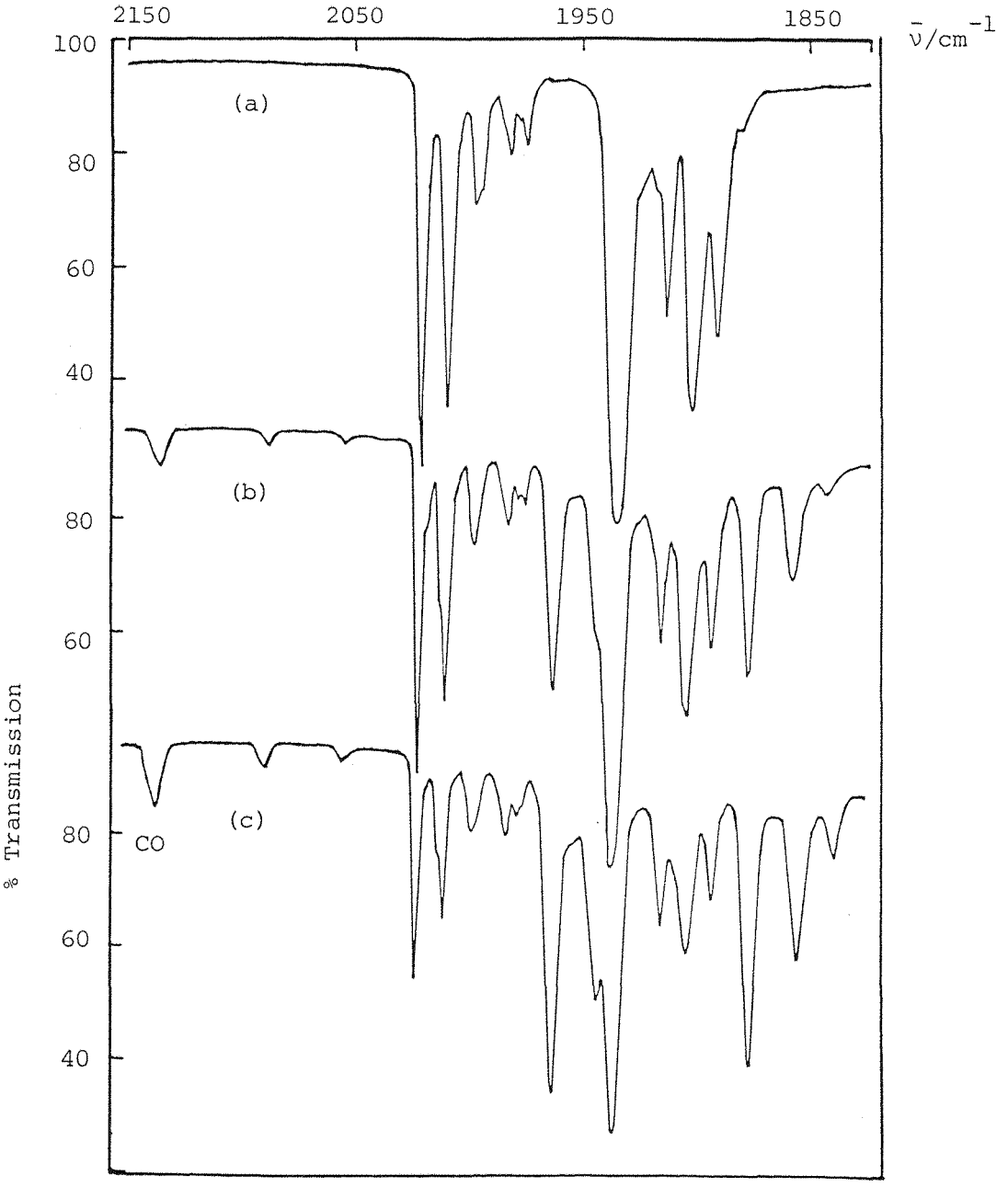

FIGURE 2.3 Infrared spectra from an experiment with ^{13}CO-enriched $(\eta^5\text{-}C_5H_5)Mo(CO)_3CH_3$ isolated at high dilution in a CH_4 matrix at 12K: (a) after deposition, (b) after 15 min photolysis using (λ = 320 - 370 nm), and (c) after further 50 min photolysis using the same energy filter (λ = 320 - 370 nm).

Ar, CO and CH_4 matrices. The two terminal CO stretching bands correspond to the A' (2028.6 cm^{-1}) and coincident A' + A" (1941.4 cm^{-1}) modes as before. A period of photolysis using u.v. light (λ = 320 - 370 nm), produced new i.r. bands (Table 2.1) at 2190.8, 2138.0, 1972.8, 1969.7, 1913.7 and 1884.4 cm^{-1}, of which the band at 2138.0 cm^{-1} corresponds to CO liberated by photolysis. All these bands increased with a constant relative intensity.

Taking into account the dilution and the subsequent reversibility of the primary photolysis step, these bands can be assigned to two mononuclear species. The bands at 1972.8 and 1884.4 cm^{-1} can be assigned as the terminal CO stretching modes of $(\eta^5\text{-}C_5H_5)Mo(CO)_2CH_3$ species by comparison of the band positions with those for CH_4, Ar and CO matrices (Table 2.1), together with their analogous reversal behaviour. The band at 2190.8 cm^{-1} can be assigned to a $^{14}N\text{-}^{14}N$ stretching mode and the bands at 1969.7 and 1912.7 cm^{-1} may be assigned to the terminal CO stretching modes of $(\eta^5\text{-}C_5H_5)Mo(CO)_2(N_2)CH_3$ (see below). Long wavelength irradiation using (λ > 430 nm) or annealing the matrix and re-cooling to 12K failed to reverse these primary photoproduct bands in contrast to the ready reversal of the bands due to $(\eta^5\text{-}C_5H_5)Mo(CO)_2CH_3$. The non-reversibility of the $(\eta^5\text{-}C_5H_5)Mo(CO)_2(N_2)CH_3$ complex is analogous to observations of other dinitrogen complexes, $(\eta^5\text{-}C_5H_5)Co(CO)(N_2)$ [17] and $(\eta^5\text{-}C_5H_5)Mn(CO)_2(N_2)$ [19] which have ν(NN) in the 2160 cm^{-1} region, and is in contrast to the behaviour of $(\eta^4\text{-}C_4H_4)Fe(CO)_2(N_2)$ [19] and other matrix-isolated dinitrogen complexes, e.g. $Ni(CO)_3(N_2)$ [20] and (tfa)Rh(CO)(N_2) [21] which have ν(NN) above 2200 cm^{-1}. Surprisingly, no $(\eta^5\text{-}C_5H_5)W(CO)_2(N_2)CH_3$ species was detected when the parent tungsten analogue was irradiated in N_2 matrices under similar conditions. Spectroscopic data for the new species is given in Table 2.1.

Photolysis of ^{13}CO-enriched $(\eta^5\text{-}C_5H_5)Mo(CO)_3CH_3$ isolated in a pure N_2 matrix using u.v. light (λ = 320 - 370 nm) gave the bands for the ^{12}CO species at 1969.7 and 1913.7 cm^{-1} (Table 2.1) and new ^{13}CO-enriched product bands at 1955.3, 1924.5, 1886.0 and 1871.4 cm^{-1} (Table 2.2). These bands were observed in addition to the bands due to complexes $(\eta^5\text{-}C_5H_5)Mo(^{12}CO)_{3-n}(^{13}CO)_nCH_3$ (n = 0, 1, 2, 3) and $(\eta^5\text{-}C_5H_5)Mo(^{12}CO)_{2-m}(^{13}CO)_mCH_3$ (m = 0, 1, 2). Irradiation with long wavelength light using (λ > 430 nm) or annealing the matrix for two minutes and then re-cooling to 12K, produced increase of bands

at 1955.3, 1924.5, 1886.0, 1871.4 and 2190.8 (ν_{NN}) cm^{-1} with corresponding decrease of bands of $(\eta^5\text{-}C_5H_5)Mo(^{12}CO)_{2-m}(^{13}CO)_mCH_3$ (m = 0, 1, 2) complexes. Using an energy-factored force-field fitting, a good correspondence was obtained between the observed and calculated bands of a $\underline{C_s}$ $Mo(CO)_2$ fragment (Table 2.2). Therefore, the photoproduct obtained in the N_2 matrices (see above) corresponding to the bands at 2190.8, 1969.7 and 1913.7 cm^{-1} can be assigned conclusively to the species $(\eta^5\text{-}C_5H_5)Mo(CO)_2(N_2)CH_3$. Two structures (I and II) can be drawn for the $Mo(CO)_2(N_2)CH_3$ fragment of this complex. On the basis of a comparison* of k_i obtained for this complex (43.3 Nm^{-1}) with k_i values for $(\eta^5\text{-}C_5H_5)Mo(CO)_3CH_3$ ($k_{12} = k_{cis}$ = 43.8 and $k_{23} = k_{trans}$ = 49.0 Nm^{-1}) it seems likely that $(\eta^5\text{-}C_5H_5)Mo(CO)_2(N_2)CH_3$ adopts structure I.

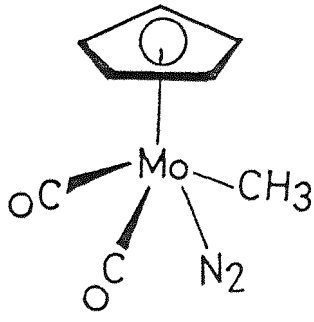

(I) *cis*

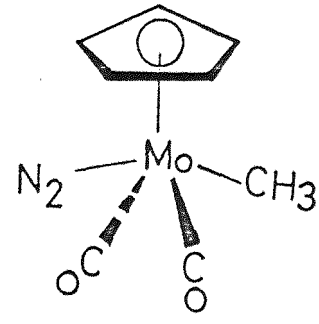

(II) *trans*

---

* Burdett [22] has concluded that for metal carbonyls containing other ligands, the use of carbonyl band intensities to calculate bond angles is not universally applicable. The method can only be a legitimate one in those molecules where vibrational coupling between the M-X and CO oscillators is small, e.g. $Mn(CO)_5Br$. Where coupling is intensive, the errors involved in the method may be unacceptable, e.g. $Mo(CO)_5(N_2)$. In our experience, however, where ν_{CO} and ν_{NN} or ν_{CO} and ν_{NO} bands are separated by $\underline{ca}$ 200 cm^{-1} bond angle calculations and energy-factored force field fittings of bands of ^{13}CO enriched species can be satisfactorily carried out without recourse to including perturbations from the N_2 and NO ligands, e.g. $(\eta^5\text{-}C_5H_5)Co(CO)(N_2)$ [17], $(\eta^5\text{-}C_5H_5)Mo(CO)_2(N_2)CH_3$ [12] and $Mn(CO)(NO)_2(NO^*)$ [23].

2.2.3 Photolysis of $(\eta^5\text{-}C_5H_5)M(CO)_3CH_3$ Complexes (M = Mo, W) in 5% C_2H_4 Doped CH_4 Matrices

The infrared spectrum of $(\eta^5\text{-}C_5H_5)Mo(CO)_3CH_3$ isolated at high dilution in a 5% C_2H_4 doped CH_4 matrix shows much broader bands than obtained in pure gas matrices (Figure 2.4(a)). The broadness of the bands is a common feature of all doped matrices and does not reflect a lack of isolation but rather that bulky substrate molecules are isolated in matrix cages with varying probabilities of dopant, orientations of substrate, and packing of host matrix molecules.

A period of photolysis of $(\eta^5\text{-}C_5H_5)Mo(CO)_3CH_3$ in a 5% C_2H_4 doped CH_4 matrix using u.v. light (λ = 320 - 370 nm) produced new bands at 2138.0, 1985.3, 1900.5, 1964.7 and 1876.5 cm^{-1} of which the band at 2138.0 cm^{-1} corresponds to CO liberated during photolysis (Figure 2.4(b)). Irradiation with visible light (λ > 430 nm) (Figure 2.4(c)), or annealing the matrix to ca 30K caused increases in bands at 2024.8, 1938.8, 1985.3 and 1900.5 cm^{-1} with corresponding decreases in bands at 1964.7 and 1876.5 cm^{-1}. Annealing the matrix also showed that the bands at 1964.7 and 1876.5 cm^{-1} (pair (1)) were not related to those at 1985.3 and 1900.5 cm^{-1} (pair (2)) because the former decreased in intensity whereas the latter increased together with slight increases in the intensities of the parent bands (Figure 2.4(c)). The more intense pair of bands, pair (1), (1964.7 and 1876.5 cm^{-1}), which reversed on annealing and long wavelength photolysis, can be assigned to the coordinatively unsaturated 16-electron species $(\eta^5\text{-}C_5H_5)Mo(CO)_2CH_3$ by comparison with those observed in CH_4 matrices (Table 2.1), and their analogous reversal behaviour. The pair of bands at higher wavenumber, pair (2) (1985.3 and 1900.5 cm^{-1}), are typical of a situation where a CO ligand has been replaced by another ligand, e.g., $(\eta^5\text{-}C_5H_5)Mo(CO)_2(N_2)CH_3$ (1969.7 and 1913.7 cm^{-1}) compared with $(\eta^5\text{-}C_5H_5)Mo(CO)_2CH_3$ (1972.8 and 1884.4 cm^{-1}). These bands can probably be assigned to the 18-electron species $(\eta^5\text{-}C_5H_5)Mo(CO)_2(C_2H_4)CH_3$. The band positions, at (1985.3 and 1900.5 cm^{-1}), are comparatively higher than those for *trans*-$(\eta^5\text{-}C_5H_5)Mo(CO)_2(C_2H_4)H$ (1974.8 and 1901.3 cm^{-1}) isolated in a CH_4 matrix (see Chapter 3) and *trans*-$(\eta^5\text{-}C_5H_5)Mo(CO)_2(C_2H_4)CH_3$ observed in solution (1977 and 1901 cm^{-1}) [6]. Therefore, the bands at (1985.3 and 1900.5 cm^{-1}) are probably best assigned to the *cis*-$(\eta^5\text{-}C_5H_5)Mo(CO)_2(C_2H_4)CH_3$.

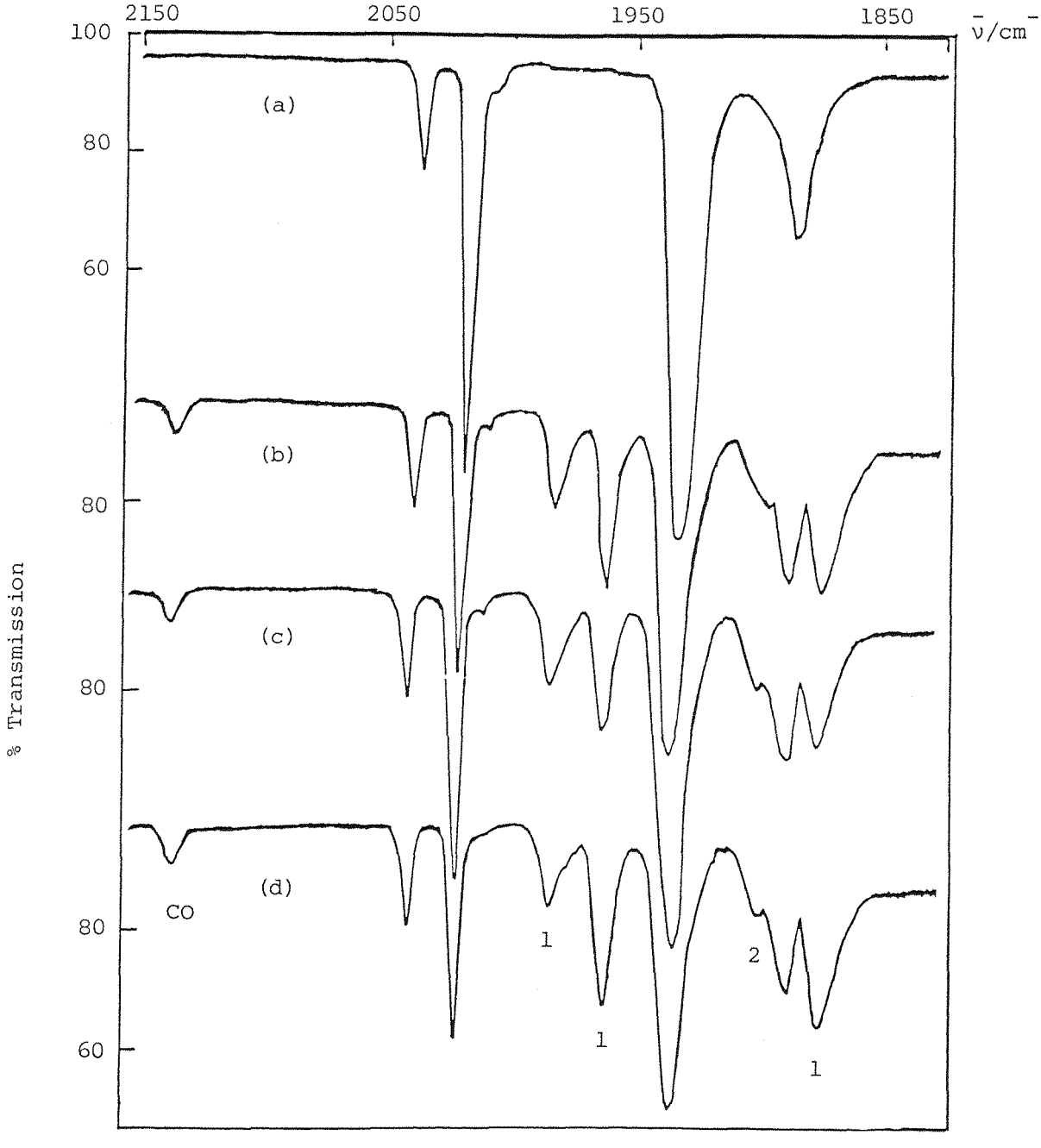

FIGURE 2.4 Infrared spectra from an experiment with $(\eta^5\text{-}C_5H_5)Mo(CO)_3CH_3$ isolated at high dilution in a 5% C_2H_4 doped CH_4 matrix at 12K: (a) after deposition, (b) after 10 min photolysis using (λ = 320 - 370 nm), (c) after reverse photolysis using (λ > 430 nm), and (d) after further 15 min photolysis using (λ = 320 - 370 nm).

Analogous results were obtained for $(\eta^5\text{-}C_5H_5)W(CO)_3CH_3$ isolated at high dilution in 5% C_2H_4 doped CH_4 matrices. Spectroscopic data for the new species are given in Table 2.1.

2.2.4 Photolysis of $(\eta^5\text{-}C_5H_5)Cr(CO)_3CH_3$ in CH_4, Ar, Co, N_2, 5% $^{13}CO/CH_4$ and 5% C_2H_4 Doped CH_4 Matrices

Infrared spectra from an experiment with $(\eta^5\text{-}C_5H_5)Cr(CO)_3CH_3$ isolated at high dilution (ca 1:2000 to 1:5000) in a pure CO matrix at 12K are shown in Figure 2.5. The spectrum before photolysis (Figure 2.5(a)) showed two strong bands in the terminal CO stretching region at 2012.5 and 1935.6 cm^{-1} together with weak bands (bands marked *) which arise from $(\eta^5\text{-}C_5H_5)Cr(^{12}CO)_2(^{13}CO)CH_3$ in natural abundance. Irradiation with visible light ($\lambda > 430$ nm) produced two new bands at 2020.0 and 1938.5 cm^{-1} (Figure 2.5(b)). Further irradiation with the same photolysis source enhanced the intensities of the new bands at the expense of the parent bands (Figure 2.5(c)). Annealing the matrix to ca 30K for two minutes and then re-cooling to 12K resulted in a reduction in the intensities of the new product bands and regeneration of the bands of the starting complex (Figure 2.5(d)). Similar bands together with a bands due to free CO were observed for CH_4, Ar, N_2 and even 5% C_2H_4 doped CH_4 matrices, in which the analogous Mo and W complexes gave $(\eta^5\text{-}C_5H_5)M(CO)_2(C_2H_4)CH_3$ complexes (M = Mo, W).

The high dilution used, the increasing and decreasing of the new bands with a constant relative intensity, and the reversibility of the primary photoreaction rule out a polynuclear species and indicate a single new product formed via a simple reaction process, viz ejection of a CO ligand. The large shift to lower wavenumbers of the bands for $(\eta^5\text{-}C_5H_5)Mo(CO)_2CH_3$ (ν_{CO} at 1966.0 and 1880.1 cm^{-1}; CH_4) compared with those for $(\eta^5\text{-}C_5H_5)Mo(CO)_3CH_3$ (ν_{CO} at 2023.9 and 1937.0 cm^{-1}; CH_4), however, enables the coordinately unsaturated 16-electron species, $(\eta^5\text{-}C_5H_5)Cr(CO)_2CH_3$ to be discounted. Similarly, separate experiments with $(\eta^5\text{-}C_5H_5)Cr(CO)_3H$ (ν_{CO} at 2016.7, 1943.6 and 1932.7 cm^{-1}) (see Chapter 4) in CO matrices at 12K ruled out this compound and its photoproducts $(\eta^5\text{-}C_5H_5)Cr(CO)_3^{\cdot}$ (ν_{CO} at 1986.3, 1910.4 and 1902.3 cm^{-1}) and $HCO^{\cdot}$ (ν_{CO} at 1859.2 cm^{-1}). In order to establish the identity of the new metal-containing product experiments were carried out

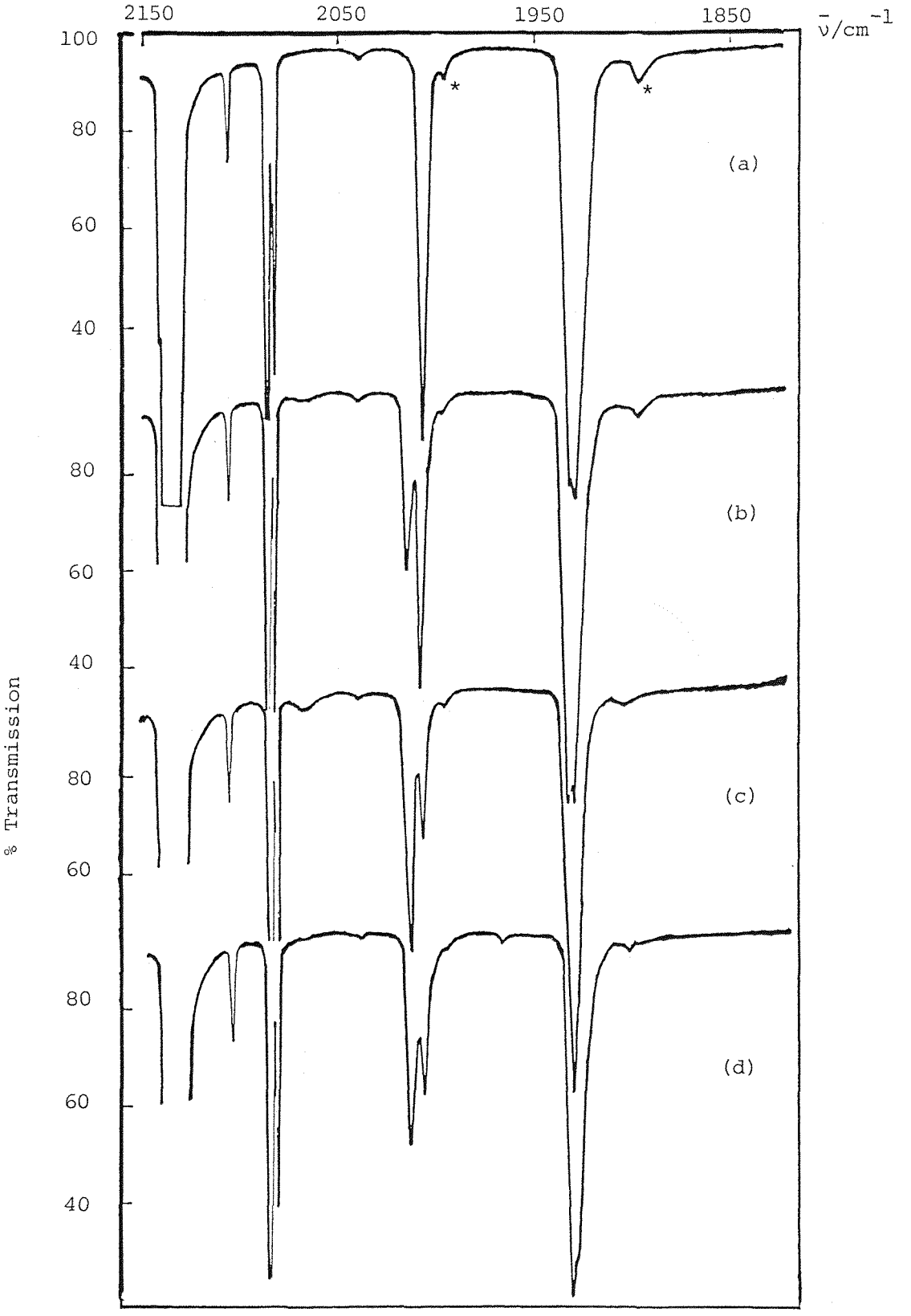

FIGURE 2.5 Infrared spectra from an experiment with $(\eta^5\text{-}C_5H_5)Cr(CO)_3CH_3$ isolated at high dilution in a CO matrix at 12K: (a) after deposition, (b) after 60 min photolysis with $\lambda > 430$ nm radiation, (c) after 180 min further photolysis using the same radiation, and (d) after annealing for 2 min. Bands marked (*) are due to $(\eta^5\text{-}C_5H_5)Cr(^{12}CO)_2(^{13}CO)CH_3$ present in natural abundance.

using 5% ^{13}CO doped CH_4 matrices. Initial brief irradiation caused some $^{13}CO/^{12}CO$ exchange in the parent complex but longer photolysis rapidly destroyed any $(\eta^5\text{-}C_5H_5)Cr(^{12}CO)_{3-n}(^{13}CO)_nCH_3$ complexes (n = 0 - 2) and produced new $^{13}CO/^{12}CO$ bands corresponding to the ^{12}CO photoproduct. The $^{13}CO/^{12}CO$ enrichment bands were subjected to an energy-factored force-field fitting procedure for metal carbonyl fragments, which has been described elsewhere [18]. Comparison of the observed and calculated band positions for the new species revealed that the bands arose from a $Cr(CO)_2$ fragment rather than a $Cr(CO)_3$ fragment (Table 2.2), which is consistent with the observation of free CO in CH_4 and Ar matrices. In order to produce higher wavenumber bands than for $(\eta^5\text{-}C_5H_5)Cr(CO)_3CH_3$ on ejection of a CO ligand some other π-acceptor ligand must have become coordinated to the metal. Since this ligand must have been previously coordinated to the metal in some form, it is proposed* that α-H elimination follows CO dissociation and that the new photoproduct is $(\eta^5\text{-}C_5H_5)Cr(CO)_2(CH_2)H$. Comparison of the interaction force constant (k_i = 66.6 Nm^{-1}) with those for $(\eta^5\text{-}C_5H_5)Mo(CO)_3CH_3$ (k_{cis} = 43.8 and k_{trans} = 49.0 Nm^{-1}) suggests that CO ligands and the hydride and methylene ligands are *trans* to one another. Support for the *trans* configuration is afforded by the observation that on complete photodestruction of $(\eta^5\text{-}C_5H_5)Cr(CO)_3CH_3$ the lower band of $(\eta^5\text{-}C_5H_5)Cr(CO)_2(CH_2)H$ is more intense than the upper band, i.e.

$$I_{antisym}/I_{sym} > 1.$$

Irradiation of $(\eta^5\text{-}C_5H_5)Cr(CO)_3CH_3$ in reactive gas matrices e.g. N_2 and C_2H_4 produced the same product $(\eta^5\text{-}C_5H_5)Cr(CO)_2(=CH_2)H$, i.e. no bands were observed for $(\eta^5\text{-}C_5H_5)Cr(CO)_2(N_2)CH_3$ and $(\eta^5\text{-}C_5H_5)Cr(CO)_2(C_2H_4)CH_3$ complexes in contrast to the formation of $(\eta^5\text{-}C_5H_5)Mo(CO)_2(L)CH_3$ (L = N_2, C_2H_4) and $(\eta^5\text{-}C_5H_5)W(CO)_2(C_2H_4)CH_3$ complexes.

Spectroscopic data for the new species is presented in Tables 2.1 and 2.2.

---

*It had been hoped to demonstrate the Cr-H bond using ν_{Cr-H} and the appropriate isotopic shift on deuteriation. However, ν_{Cr-H} in this species and $(\eta^5\text{-}C_5H_5)Cr(CO)_3H$ is extremely weak and so this means of verification proved impossible.

2.2.5 Photolysis of $(\eta^5\text{-}C_5H_5)Mo(CO)_3CF_3$ in CH_4 and N_2 Matrices

Infrared spectra from an experiment with $(\eta^5\text{-}C_5H_5)Mo(CO)_3CF_3$ (I) isolated at high dilution in a CH_4 matrix at ca 12K are shown in Figures 2.6 and 2.7. Irradiation with long wavelength radiation ($\lambda > 370$ nm) of a matrix, which was produced by co-condensing vapour from a sample of (I) held at 30°C with a vast excess of CH_4 (Figure 2.6(a)), resulted in the appearance of a large number of new bands: 2138.0, 2063.3, 2045.2, 1998.0, 1994.8, 1982.6, 1910.0, 1180.7, 1172.3, 1108.3, 1100.6, 1086.0 and 491 cm^{-1} (Figures 2.6(b) and 2.7(b)). Longer irradiation times with the same photolysis source produced further decreases in the bands of (I) (ν_{CO} at 2057.0, 1976.0 and 1970.3 cm^{-1} and ν_{CF} at 1065.0, 1055.3, 1032.5, 1018.0 and 1012.0 cm^{-1}) and increases in all the new product bands (Figures 2.6(c), 2.6(d) and 2.7(c), 2.7(d)). Subtraction of the scaled spectrum before photolysis from those after photolysis revealed (i) several obscured product bands in the terminal CO stretching region and (ii) that there were at least three photoproducts on the basis of growth and decay plots of bands. The bands at 1994.8 and 1910.0 cm^{-1} (set (1)) can be assigned to the 16-electron coordinatively unsaturated species $(\eta^5\text{-}C_5H_5)Mo(CO)_2CF_3$ (II) (ν_{CO} at 1994.8 and 1910.0 cm^{-1}) on the basis of reversal with visible light ($\lambda > 430$ nm) and the presence of free CO (band at 2138.0 cm^{-1}) in the matrix, features which had been observed on the photolytic formation of $(\eta^5\text{-}C_5H_5)Mo(CO)_2CH_3$. The remaining bands fall into two sets: set (2) at 2045.2, 1982.5, 1108.3, 1100.6 and 1086.0 cm^{-1} and set (3) at 2063.0, 1998.0, 1185.2, 1180.7, 1172.3 and a weak band at 491 cm^{-1}. Comparison of the CF stretching band positions for $Ru(=CF_2)(CO)_2(PPh_3)_2$ (ν_{CF} at 1083 and 980 cm^{-1}) and $Ru(CF_2H)Cl(CO)_2(PPh_3)_2$ (ν_{CF} at 980, 944, 928 and 911 cm^{-1} [24] shows that the CF stretching bands for the $M=CF_2$ fragment occur at higher wavenumbers than for the $M\text{-}CF_2H$ fragment. Both sets of new bands occur at higher wavenumbers than for (I) but it is the set (3) bands which occur at highest wavenumbers and additionally these bands correlate with two terminal CO stretching bands and the weak band at 491 cm^{-1}, which is very close to the position of ν_{ReF} (480 cm^{-1}) of $Re(CO)_5F$ [25, 26]. It seems reasonable, therefore to assign the set (3) bands to the difluoromethylene fluoride species $(\eta^5\text{-}C_5H_5)Mo(CO)_2(=CF_2)F$ (IV), which is an 18-electron compound. The other species (III), set (2) bands has CO stretching bands between those of (I) but below those of (IV) while the CF stretching

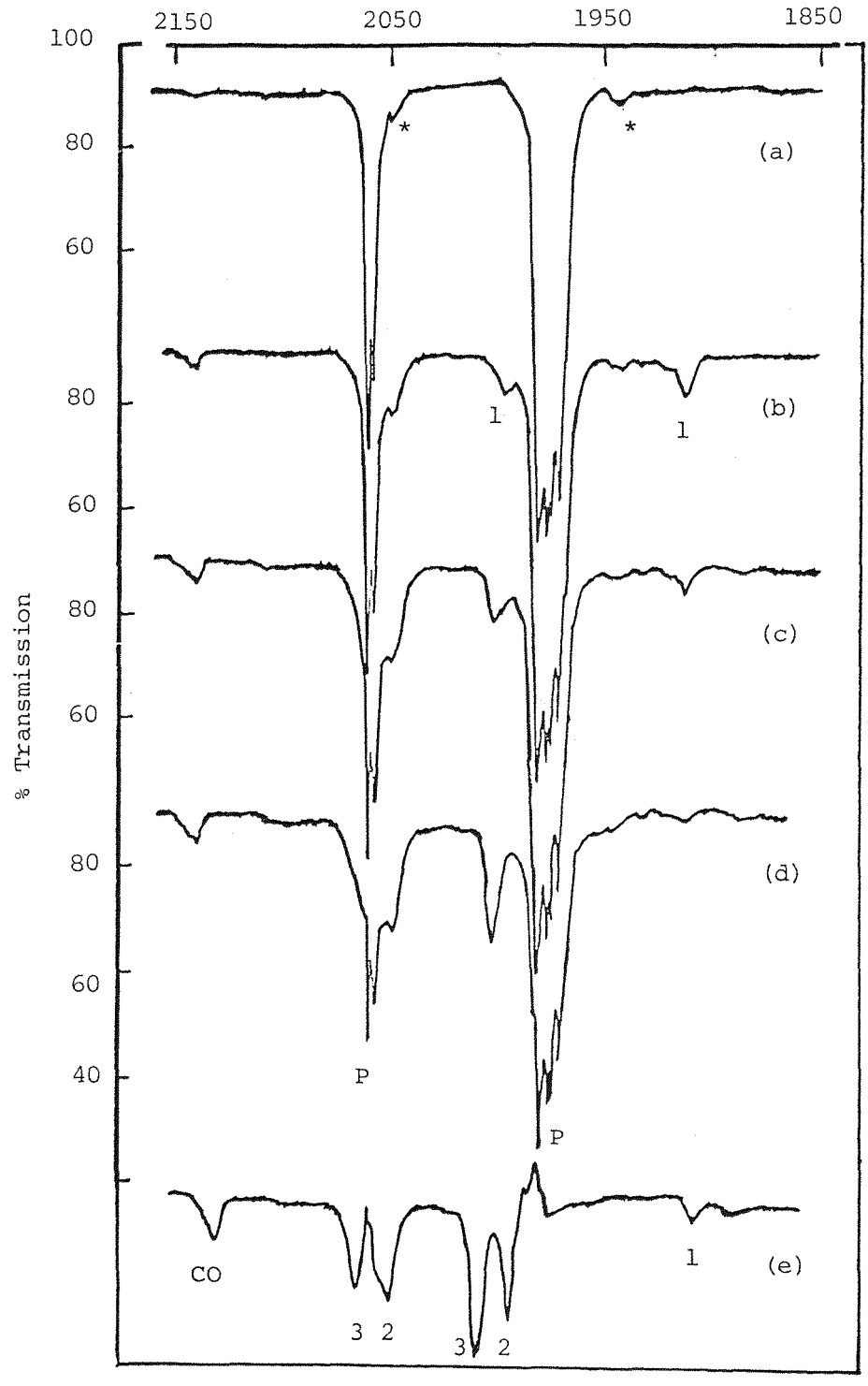

FIGURE 2.6 Infrared spectra (Nicolet 7199 FTIR) in the terminal CO stretching region from an experiment with $(\eta^5\text{-}C_5H_5)Mo(CO)_3CF_3$ isolated at high dilution in a CH_4 matrix at ca. 12K: (a) after deposition, (b) after 10 min. photolysis with low energy u.v. radiation (λ > 370 nm), (c) after further 20 min photolysis with the same source, (d) after another 40 min photolysis with the same source, and (e) subtraction of the spectrum before photolysis from that after photolysis, i.e. (d) - (a). Bands marked (*) are due to $(\eta^5\text{-}C_5H_5)Mo(^{12}CO)_2(^{13}CO)CF_3$ present in natural abundance. Bands marked (P) are due to $(\eta^5\text{-}C_5H_5)Mo(CO)_3CF_3$ and those marked (1) - (3) are due to photoproducts (see text).

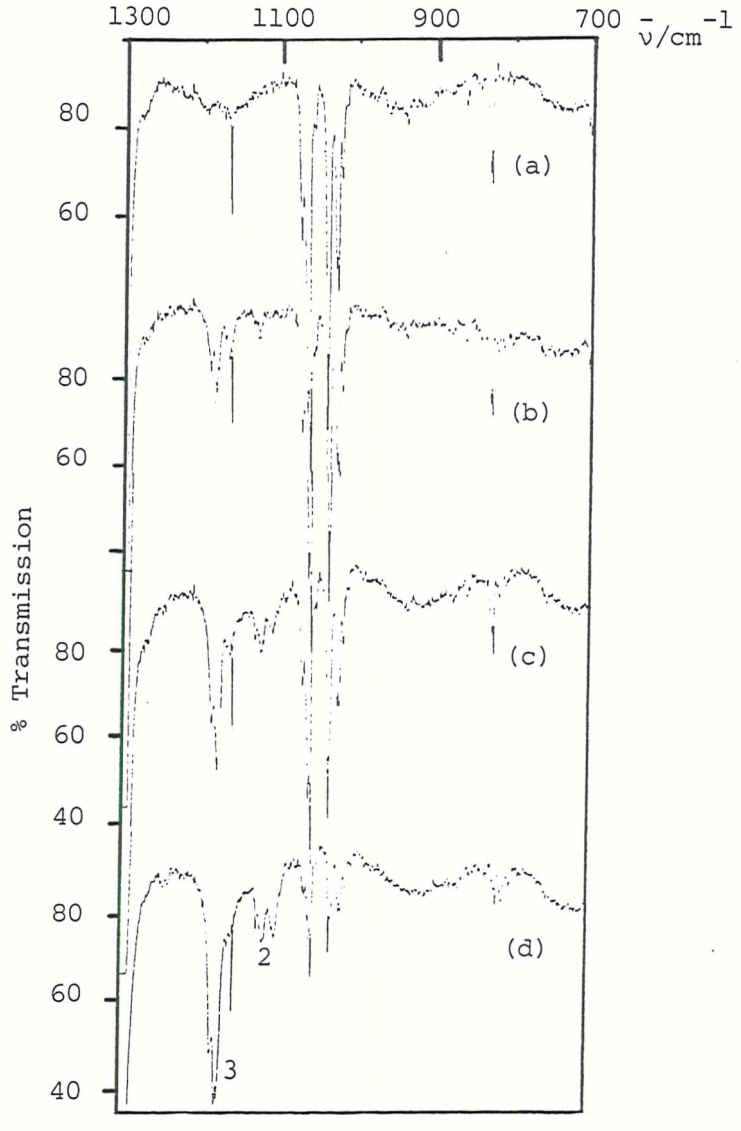

FIGURE 2.7 Infrared spectra (Nicolet 7199 FTIR) in the terminal C-F stretching region from an experiment with $(\eta^5\text{-}C_5H_5)Mo(CO)_3CF_3$ isolated at high dilution in a CH_4 matrix at ca. 12K: (a) after deposition, (b) after 10 min photolysis with low energy u.v. radiation ($\lambda > 370$ nm), (c) after further 20 min photolysis with the same energy source, and (d) after another 40 min photolysis with the same source. (Bands marked (1) - (3) are due to photoproducts (see text).

bands are above those of (I) but below those of (IV). These observations may be interpreted in terms of greater π back donation Mo → CO for (IV) than for (III) together with some strengthening of the CF bonds, perhaps as a result of increased M-C bond order. A possible structure for (III) together with a summary of the photoreactions are shown in Scheme 2.3. A precedent for an α-F to fill the vacant site in $(\eta^5\text{-}C_5H_5)Mo(CO)_2CF_3$ is found in the proposal that a β-H does something similar in the 16-electron coordinatively unsaturated species (V) [27].

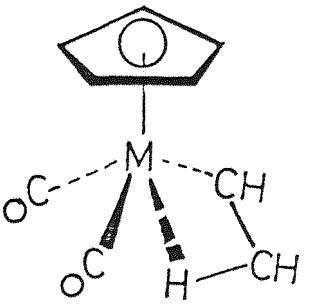

(V)

In addition to the bands due to the 16-electron species $(\eta^5\text{-}C_5H_5)Mo(CO)_2CF_3$ and $(\eta^5\text{-}C_5H_5)Mo(CO)_2(=CF_2)F$ complexes, irradiation of $(\eta^5\text{-}C_5H_5)Mo(CO)_3CF_3$ in nitrogen matrices produced some other bands at 2260.0, 2018.2 and 1938.3 cm^{-1} (Table 2.3). These bands are assigned to the dinitrogen species $(\eta^5\text{-}C_5H_5)Mo(CO)_2(N_2)CF_3$. The $\nu_{N\equiv N}$ stretching band for $(\eta^5\text{-}C_5H_5)Mo(CO)_2(N_2)CF_3$ (2260.0 cm^{-1}) occurs at a very similar wavenumber to those for $(\eta^5\text{-}C_5H_5)Mo(CO)_2(N_2)Cl$ (2240.8 cm^{-1}) (see Chapter 6).

Spectroscopic data for the new species is given in Table 2.3.

2.2.6 Photolysis of $(\eta^5\text{-}C_5H_5)Mo(CO)_3COCF_3$ in CH_4 and Ar Matrices

The i.r. spectrum of $(\eta^5\text{-}C_5H_5)Mo(CO)_3COCF_3$ isolated at high dilution in a CH_4 matrix before photolysis showed bands at 2046.5, 1976.8, 1962.0 and 1654.2 cm^{-1} in the CO stretching region and a 1257.5, 1238.7, 1194.5 and 1154.2 cm^{-1} in the C-F stretching region [24], (Table 2.3). Irradiation of the matrix with long wavelength radiation ($\lambda > 410$ nm) giving light corresponding to the electronic absorption (Figure 2.2(d)) produced a large number of new bands: 2138.0, 2057.3, 1976.0, 1970.3, 1891.4, 1065.0, 1055.3, 1032.5, 1018.0 and 1012.0 cm^{-1} (Table 2.3). Longer times of irradiation with the same energy filter ($\lambda > 410$ nm) resulted in an increase in the overall conversion of $(\eta^5\text{-}C_5H_5)Mo(CO)_3COCF_3$ into $(\eta^5\text{-}C_5H_5)Mo(CO)_3CF_3$ without increase in the weak band at 1891.4 cm^{-1}. The weak band at 1891.4 cm^{-1} and probably another band obscured by the lower parent band at 1976.0 cm^{-1} are assigned to the unsaturated 16-electron species $(\eta^5\text{-}C_5H_5)Mo(CO)_2COCF_3$, but no band attributable to the acetyl CO stretching vibration for the species $(\eta^5\text{-}C_5H_5)Mo(CO)_2COCF_3$ was observed. This is perhaps not surprising considering that the intensity of the terminal CO bands is weak and the acetyl CO stretching band at 1654.2 cm^{-1} in $(\eta^5\text{-}C_5H_5)Mo(CO)_3COCF_3$ is much weaker than the terminal CO stretching bands. Support for the assignment of the intermediate species as $(\eta^5\text{-}C_5H_5)Mo(CO)_2COCF_3$ is afforded by the observation of $(\eta^5\text{-}C_5H_5)Fe(CO)COCH_3$ and $Mn(CO)_4COCH_3$ in the photochemical decarbonylation of $(\eta^5\text{-}C_5H_5)Fe(CO)_2COCH_3$ [28] and $Mn(CO)_5COCH_3$ [29] respectively in matrices at 12K. The bands at 2057.0, 1976.0, 1970.3, 1065.0, 1055.3, 1032.5, 1018.0 and 1012.0 cm^{-1} (Table 2.3) were assigned to the fluoroalkyl derivative $(\eta^5\text{-}C_5H_5)Mo(CO)_3CF_3$ (see above section 2.2.5).

Analogous results were obtained for $(\eta^5\text{-}C_5H_5)Mo(CO)_3COCF_3$ isolated at high dilution in Ar matrices and spectroscopic data for the new species are given in Table 2.3.

2.3 DISCUSSION

The photoreactions of $(\eta^5\text{-}C_5H_5)M(CO)_3CH_3$ complexes (M = Mo, W) at high dilution in CH_4, Ar, CO, N_2 and 5% C_2H_4 doped CH_4 are summarised in Scheme 2.1.

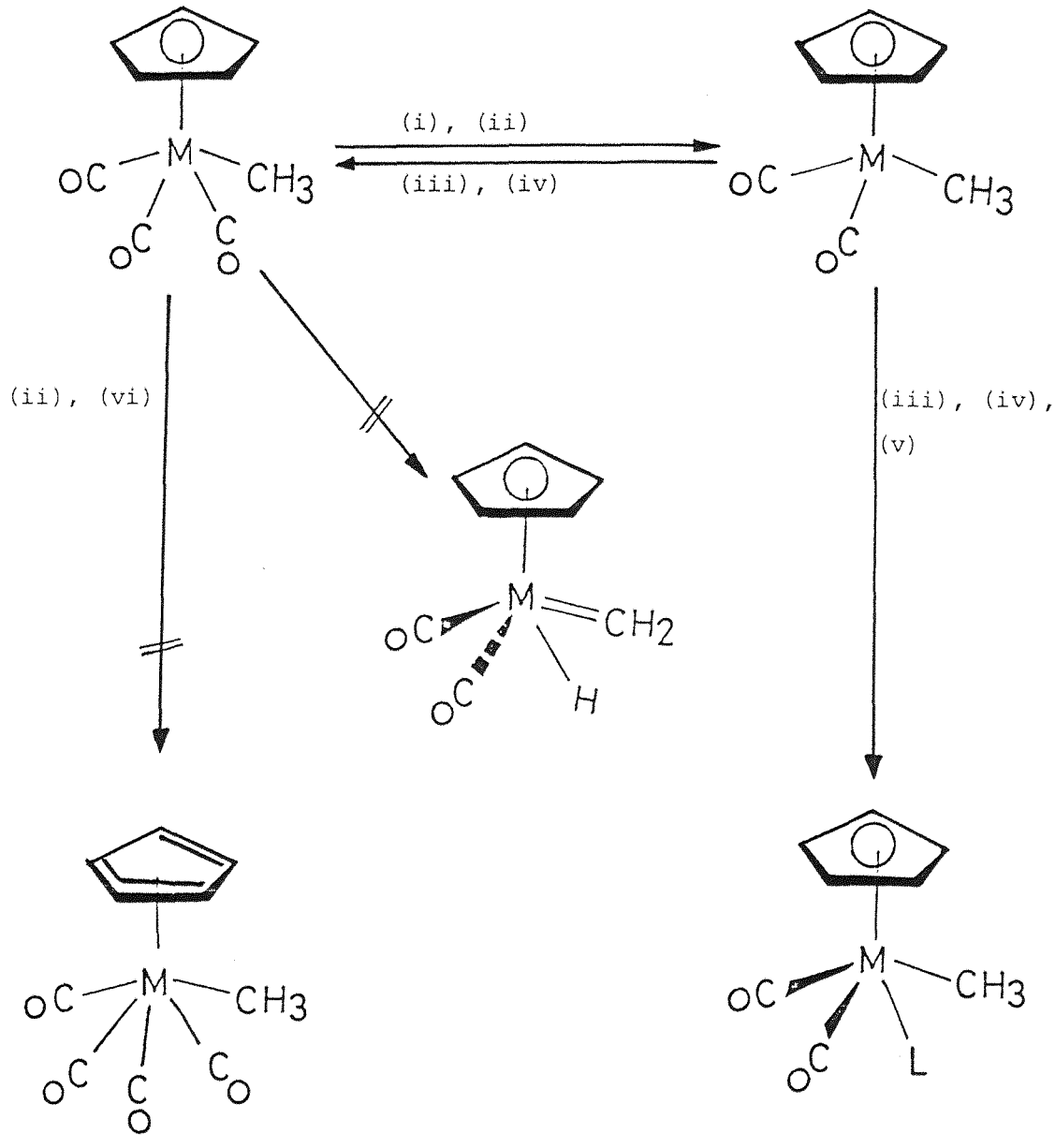

Scheme 2.1 (i) CH_4, Ar, CO, N_2, 5% C_2H_4/CH_4;
(ii) hν (310 < λ < 370 nm); (iii) hν (λ > 410 nm);
(iv) Annealing; (v) N_2, 5% C_2H_4/CH_4; (vi) CO.

The observation of the coordinatively unsaturated 16-electron species, $(\eta^5\text{-}C_5H_5)Mo(CO)_2CH_3$, even in a CO matrix, is consistent with the dissociative mechanism proposed [1 - 7] for ligand substitution reactions of $(\eta^5\text{-}C_5H_5)M(CO)_3CH_3$ complexes. For example, Tyler [30] reported that $(\eta^5\text{-}C_5H_5)W(CO)_3CH_3$ reacts photochemically with thf at -78°C to give $(\eta^5\text{-}C_5H_5)W(CO)_2(thf)CH_3$; solutions of this product are stable at -78°C but the complex decomposes to $[(\eta^5\text{-}C_5H_5)W(CO)_3]_2$ and $(\eta^5\text{-}C_5H_5)W(CO)_3CH_3$ upon warming to room temperature. The irradiation of $(\eta^5\text{-}C_5H_5)W(CO)_3CH_3$ at 77K in a hydrocarbon matrix (toluene or hexane) [27] containing PPh_3 followed by warm up to 298K resulted in formation of $(\eta^5\text{-}C_5H_5)W(CO)_2(PPh_3)CH_3$ (Equation 2.4).

$$(\eta^5\text{-}C_5H_5)W(CO)_3CH_3 + PPh_3 \xrightarrow[77K]{h\nu/-CO} (\eta^5\text{-}C_5H_5)W(CO)_2(PPh_3)CH_3 \qquad (2.4)$$

The observed product identified at 77K was the unsaturated 16-electron species $(\eta^5\text{-}C_5H_5)W(CO)_2CH_3$ and there was no evidence for a radical pathway, probably because of its low quantum yield and ready recombination of radicals in the frozen environment. Irradiation of $(\eta^5\text{-}C_5H_5)M(CO)_3CH_3$ (M = Mo, W) in CO matrices showed that the generation of the unsaturated 16-electron species $(\eta^5\text{-}C_5H_5)M(CO)_2CH_3$ takes place in spite of the availability of excess nucleophiles and is much more facile for M = W than for M = Mo. This may indicate that M-CO dissociation is more easier for the tungsten complex, $(\eta^5\text{-}C_5H_5)W(CO)_3CH_3$, than for the molybdenum analogue. In the CO matrix, no evidence was obtained for the formation of expanded coordination number species, e.g. $(\eta^3\text{-}C_5H_5)M(CO)_4CH_3$, possibly for steric reasons, in contrast to the expanded coordination number species $(\eta^3\text{-}C_5H_5)Co(CO)_3$ and $(\eta^3\text{-}C_5H_5)Fe(CO)_3CH_3$ produced from the complexes $(\eta^5\text{-}C_5H_5)Co(CO)_2$ [17] and $(\eta^5\text{-}C_5H_5)Fe(CO)_2CH_3$ [28] respectively.

In CH_4, Ar and CO gas matrices at 12K, no evidence was obtained for the homolysis of Mo-CH_3 bond forming radicals, whereas in solution evidence for a radical pathway comes from the formation of the dimer $[(\eta^5\text{-}C_5H_5)Mo(CO)_3]_2$ [6, 8, 9]. Interestingly, in the ^{13}CO exchange reaction the dimer complex was obtained in addition to the ^{13}CO-enriched dimer. Other evidence for

the importance of a primary photoprocess involving radicals comes from e.s.r. studies of the photolysis of $(\eta^5\text{-}C_5H_5)M(CO)_3CH_3$ (M = Cr, Mo and W) complexes in hydrocarbon solvents [31]. In this work the e.s.r. spectra were interpreted as being most consistent with a radical anion species, $(\eta^5\text{-}C_5H_5)Mo(CO)_2CH_3^{-\cdot}$, rather than the expected radical species $(\eta^5\text{-}C_5H_5)Mo(CO)_3^{\cdot}$, although this species was postulated as possibly being the primary photoproduct in a reaction scheme. In contrast to the gas matrix observations described above, in a p.v.c. polymer matrix at 12 - 298K both CO dissociation and Mo-CH_3 bond cleavage reactions occured [32]. The evidence for the latter process comes from the disappearance of bands due to $(\eta^5\text{-}C_5H_5)Mo(CO)_3CH_3$ together with the growth of bands due to $(\eta^5\text{-}C_5H_5)Mo(CO)_3Cl$ [32]. One of the reasons for the failure to observe radical species in gas matrices could be that unlike the polymer matrix, there are no secondary reaction processes, e.g. Cl abstraction, that can lead to product stabilisation. Additionally the small gas matrix molecules can pack tightly around a substrate molecule to create a 'tight cage' [33] in which the radicals produced on photolysis are unable to diffuse far enough apart to prevent a thermal back reaction. In contrast the bulky polymer chains form a 'loose cage' from which the CH_3 radical can escape. Support for the latter explanation can also be drawn from the fact that trapping of a radical species following photolysis of an organometallic compound in gas matrices has only been observed [34 - 36] when $H^{\cdot}$ has been ejected (Equations 2.5 - 2.8).

$$HCo(CO)_4 \xrightarrow[Ar]{h\nu} Co(CO)_4^{\cdot} + H^{\cdot} + HCo(CO)_3 + CO \qquad (2.5)$$

$$HCo(CO)_4 \xrightarrow[CO]{h\nu} Co(CO)_4^{\cdot} + HCO^{\cdot} \qquad (2.6)$$

$$(\eta^5\text{-}C_5H_5)_2ReH \xrightarrow[CO]{h\nu} (\eta^5\text{-}C_5H_5)_2Re + HCO^{\cdot} \qquad (2.7)$$

$$(\eta^5\text{-}C_5H_5)M(CO)_3H \xrightarrow[CO]{h\nu} (\eta^5\text{-}C_5H_5)M(CO)_3^{\cdot} + HCO^{\cdot} \qquad (2.8)$$

(M = Cr, Mo, W).

The formation of $(\eta^5\text{-}C_5H_5)Mo(CO)_2(N_2)CH_3$ in nitrogen matrices could be envisaged to occur via the 16-electron species $(\eta^5\text{-}C_5H_5)Mo(CO)_2CH_3$ which can add a N_2 molecule (Equations 2.9 and 2.10).

$$(\eta^5\text{-}C_5H_5)Mo(CO)_3CH_3 \xrightarrow[+N_2]{h\nu/-CO} (\eta^5\text{-}C_5H_5)Mo(CO)_2CH_3 \qquad (2.9)$$

$$(\eta^5\text{-}C_5H_5)Mo(CO)_2CH_3 \xrightarrow{+N_2} (\eta^5\text{-}C_5H_5)Mo(CO)_2(N_2)CH_3 \qquad (2.10)$$

The observation of $(\eta^5\text{-}C_5H_5)Mo(CO)_2CH_3$ as well as $(\eta^5\text{-}C_5H_5)Mo(CO)_2(N_2)CH_3$ on photolysis of $(\eta^5\text{-}C_5H_5)Mo(CO)_3CH_3$ in N_2 matrices suggests that $(\eta^5\text{-}C_5H_5)Mo(CO)_2(N_2)CH_3$ may be very difficult to prepare in a conventional reaction. This is in contrast to the complexes $(\eta^5\text{-}C_5H_5)Mn(CO)_2(N_2)$ and $(\eta^6\text{-}C_6H_6)Cr(CO)_2(N_2)$ which have been produced by photolysis in N_2 matrices [19] and also characterised by elemental analysis following reactions in solution [37]. Other contraindications for the preparation of $(\eta^5\text{-}C_5H_5)Mo(CO)_2(N_2)CH_3$ are the relatively high value of ν_{NN} (2190.8 cm^{-1}) compared to values of 2175.3 and 2148.4 cm^{-1} for $(\eta^5\text{-}C_5H_5)Mn(CO)_2(N_2)$ and $(\eta^6\text{-}C_6H_6)Cr(CO)_2(N_2)$ respectively, and the formation in solution of radicals leading to $[(\eta^5\text{-}C_5H_5)Mo(CO)_3]_2$ (see above). However, the tungsten analogue $(\eta^5\text{-}C_5H_5)W(CO)_3CH_3$ failed to react under the same conditions during irradiation in nitrogen matrices. Barnett and Treichel studied the reactions of $(\eta^5\text{-}C_5H_5)M(CO)_3CH_3$ complexes (M = Mo, W) with phosphine ligands and observed that the $(\eta^5\text{-}C_5H_5)Mo(CO)_3CH_3$ complex reacts with PPh_3 to yield mixtures of the two new compounds $(\eta^5\text{-}C_5H_5)Mo(CO)_2(PPh_3)CH_3$ and $(\eta^5\text{-}C_5H_5)Mo(CO)_2(PPh_3)COCH_3$ [1]. The tungsten complex $(\eta^5\text{-}C_5H_5)W(CO)_3CH_3$ is much less reactive towards PPh_3 substitution; no acetyl substitution product was isolated, but low conversion to $(\eta^5\text{-}C_5H_5)W(CO)_2(PPh_3)CH_3$ occured. The complex $(\eta^5\text{-}C_5H_5)Mo(CO)_3CH_3$ reacts with 1,2-bis(diphenylphosphine) ethane to yield $[(\eta^5\text{-}C_5H_5)Mo(CO)_2(COCH_3]_2$-μ-diphos in low yields. However, the tungsten compound $(\eta^5\text{-}C_5H_5)W(CO)_3CH_3$ failed to react under the same or more drastic conditions. This is consistent with our finding in nitrogen matrices. However, both complexes $(\eta^5\text{-}C_5H_5)M(CO)_3CH_3$ (M = Mo, W) reacted with C_2H_4 during irradiation in 5% C_2H_4 doped CH_4 matrices but again the tungsten compound $(\eta^5\text{-}C_5H_5)W(CO)_3CH_3$ was less reactive than the molybdenum analogue. The photosub-

stitution of ethylene ligand take place in the *cis* position to give the *cis*-$(\eta^5\text{-}C_5H_5)M(CO)_2(C_2H_4)CH_3$ isomers (M = Mo, W) (Equation 2.11).

$$(\eta^5\text{-}C_5H_5)M(CO)_3CH_3 \xrightarrow[-CO]{h\nu/+C_2H_4} \textit{cis}\text{-}(\eta^5\text{-}C_5H_5)M(CO)_2(C_2H_4)CH_3 \qquad (2.11)$$

In solution it has been shown that [6] one CO ligand in $(\eta^5\text{-}C_5H_5)W(CO)_3CH_3$ can be replaced photochemically by ethylene to give *trans*-$(\eta^5\text{-}C_5H_5)W(CO)_2(C_2H_4)CH_3$. Thermally the complexes $(\eta^5\text{-}C_5H_5)Mo(CO)_3R$ (R = CH_3, C_2H_5) react with ethylene at 100°C and with $(\eta^5\text{-}C_5H_5)Mo(CO)_3H$ at 25 - 50°C to yield ketones and aldehydes [11].

The photoreactions of $(\eta^5\text{-}C_5H_5)Cr(CO)_3CH_3$ in different gas matrices are summarised in Scheme 2.2 In contrast to the photochemistry of $(\eta^5\text{-}C_5H_5)M(CO)_3CH_3$ complexes (M = Mo, W) in low temperature matrices, irradiation of the $(\eta^5\text{-}C_5H_5)Cr(CO)_3CH_3$ resulted in the formation of the carbene-hydride species $(\eta^5\text{-}C_5H_5)Cr(CO)_2(=CH_2)H$. Irradiation of $(\eta^5\text{-}C_5H_5)Cr(CO)_3CH_3$ in solution in presence of PPh_3 led to migration of the methyl group from Cr to CO and introduction of the phosphine, to give an acyl chromium complex, $(\eta^5\text{-}C_5H_5)Cr(CO)_2(PPh_3)COCH_3$ (Equation 2.12), presumably from a thermal

$$(\eta^5\text{-}C_5H_5)Cr(CO)_3CH_3 \xrightarrow[h\nu]{PPh_3} (\eta^5\text{-}C_5H_5)Cr(CO)_2(PPh_3)COCH_3 \qquad (2.12)$$

reaction of the initially formed $(\eta^5\text{-}C_5H_5)Cr(CO)_2(PPh_3)CH_3$ [1]. However, irradiation of $(\eta^5\text{-}C_5H_5)Cr(CO)_3CH_3$ in low temperature matrices, in presence of external ligand L (L = N_2, C_2H_4) led to the formation of the carbene complex $(\eta^5\text{-}C_5H_5)Cr(CO)_2(=CH_2)H$; i.e. neither the photosubstitution products e.g. $(\eta^5\text{-}C_5H_5)Cr(CO)_2(L)CH_3$ (L = N_2, C_2H_4) nor the acyl chromium complex $(\eta^5\text{-}C_5H_5)Cr(CO)_2(L)COCH_3$ were observed. Similar reversible α-hydrogen abstraction from the methyl groups of $Co(PPh_3)_3CH_3$ and $Rh(PPh_3)_3CH_3$ involving intermediate carbene-hydride complexes, e.g. $CH_2{=}MH_3(PPh_3)_3$ has recently been demonstrated [38], (Equation 2.13), (M = Co, Rh).

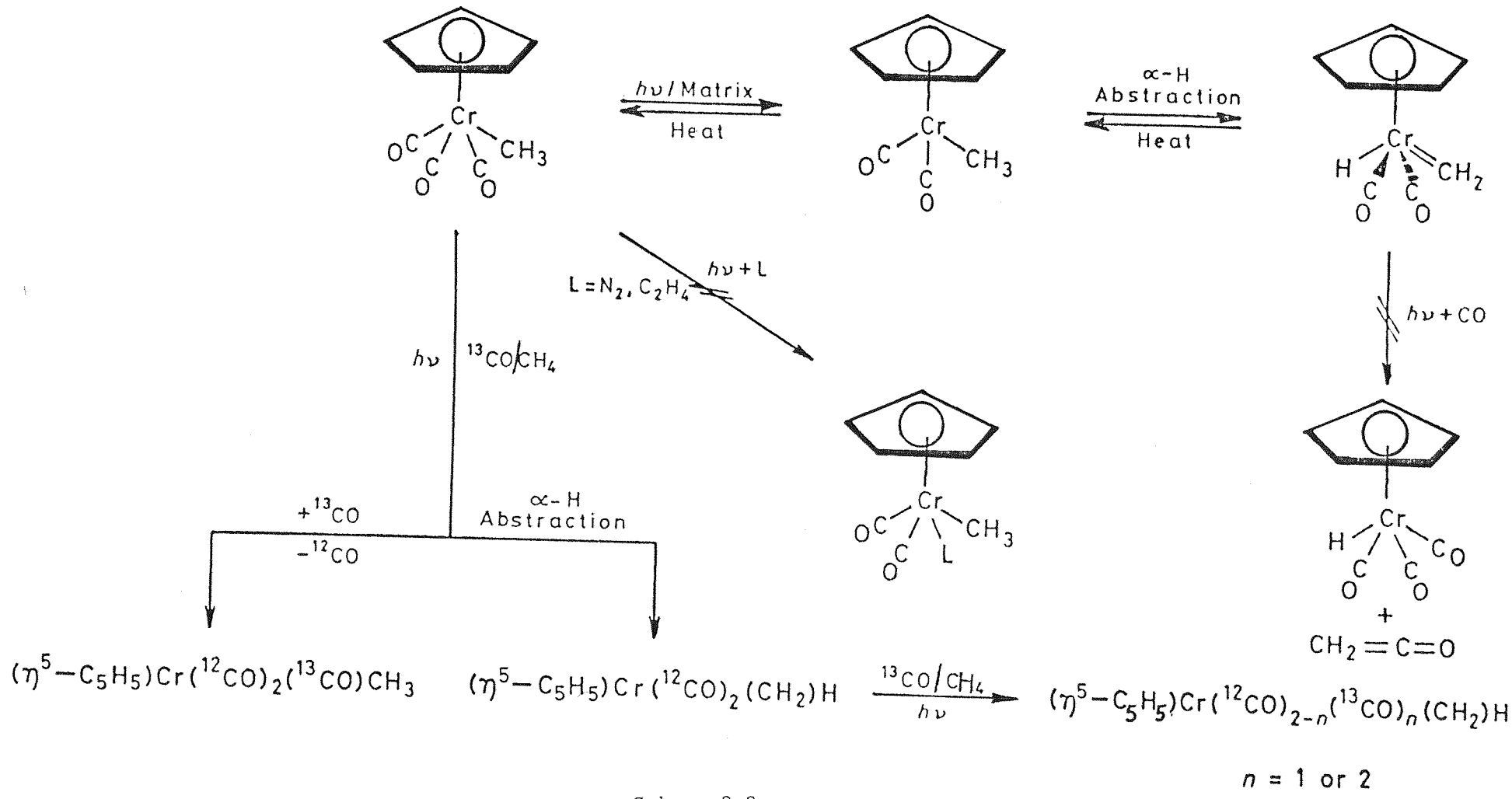
hν / Matrix
Heat
α-H
Abstraction
Heat
hν + L
L = N2, C2H4
hν + CO
hν
13CO/CH4
+13CO
-12CO
α-H
Abstraction
(η5−C5H5)Cr(12CO)2(13CO)CH3
(η5−C5H5)Cr(12CO)2(CH2)H
13CO/CH4
hν
(η5−C5H5)Cr(12CO)2-n(13CO)n(CH2)H
n = 1 or 2
CH2=C=O

Scheme 2.2

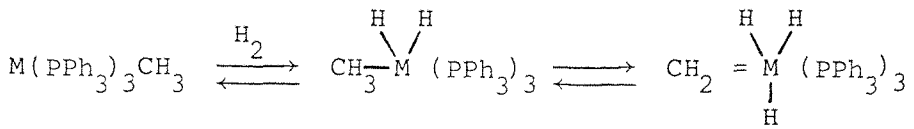

(2.13)

Reversible elimination of a hydrogen from carbons which are in β-positions relative to transition metals has been widely established to occur and to be important in catalytic reactions, e.g. olefin isomerisation. Although less well documented, elimination involving carbons in the α-positions may also occur (Equation 2.14) and may be important in generating active

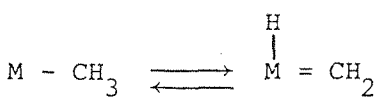

(2.14)

intermediates in metal catalysed disproportionation reactions [39, 40]. Strong evidence for α-elimination is the isolation of $[(\eta^5\text{-}C_5H_5)_2W(CD_2P(C_6H_5)(CH_3)_2)D]^+$ from the reaction of $[(\eta^5\text{-}C_5H_5)_2W(\eta^2\text{-}C_2H_4)CD_3]^+$ with $P(C_6H_5)(CH_3)_2$ [41]. It was proposed that the product arose via an equilibrium between two cationic intermediates (Equation 2.15). Evidence for

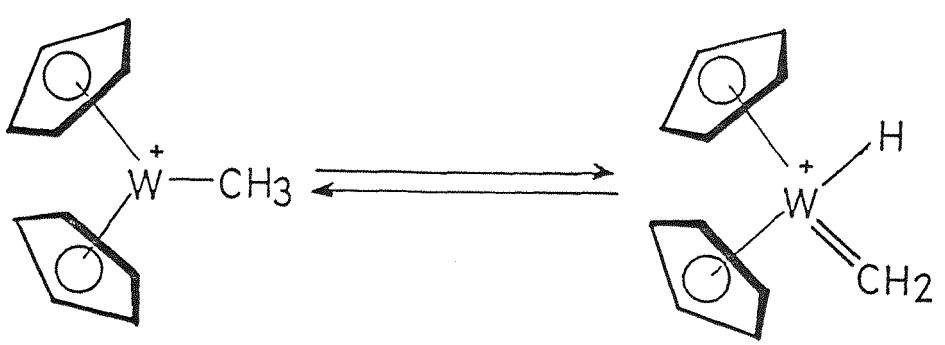

(2.15)

α-elimination for the chromium complexes $(C_6H_5CH_2CH_2CD_2CH_2)_3Cr.3THF$ and $(C_6H_5CH_2CH_2CH_2CD_2)_3Cr.3THF$ is inferred from the presence of $C_6H_5CH_2CH_2CD{=}CHD$ among the products. The presence of CH_2CD_2 and, after hydrolysis, of HD from the decomposition of $(CD_3)_3Cr.3THF$ also indicates a α-H elimination pathway [42]; a transitory carbene complex has been suggested as an intermediate [43]. Since as carbene $:CH_2$ capable of acting as a ligand in certain organotransition metal complexes, the lone pair electrons in $:CH_2$ could act as a donor pair and the vacant p_z carbon orbital would be available for back-donation of electrons from the metal. The species could thus

be classified with carbon monoxide and triphenylphosphine as far as donor-acceptor capabilities are concerned and could, in principle, replace such ligands in their stable complexes [44]. The validity of this reasoning is demonstrated through the isolation of $(\eta^5\text{-}C_5H_5)Cr(CO)_2(=CH_2)H$ in low temperature matrices.

The $^{12}CO \longrightarrow {}^{13}CO$ exchange reaction of $(\eta^5\text{-}C_5H_5)Cr(CO)_2(=CH_2)H$ is consistent with the proposed CO dissociation of carbene complexes and reaction of the coordinatively unsaturated intermediates with ^{13}CO and olefins, and their roles in the olefin metathesis reactions, e.g. $(CO)_5W=C(C_6H_5)_2$, $(CO)_5W=C(C_6H_5)H$ and $(CO)_5M=C(OCH_3)C_6H_5$ (M = Cr, Mo, W) complexes [45, 46].

In view of the increasing interest in the nature of proposed α-H abstraction and α-H elimination processes (Equation 2.12), Green et al. [47] showed that the decomposition pathways of α-abstraction and α-elimination, both leading to the titanium-methylidene intermediate $(\eta^5\text{-}C_5Me_5)_2Ti=CH_2$ from the $(\eta^5\text{-}C_5Me_5)_2Ti(CH_3)_2$ complex (Equation 2.16).

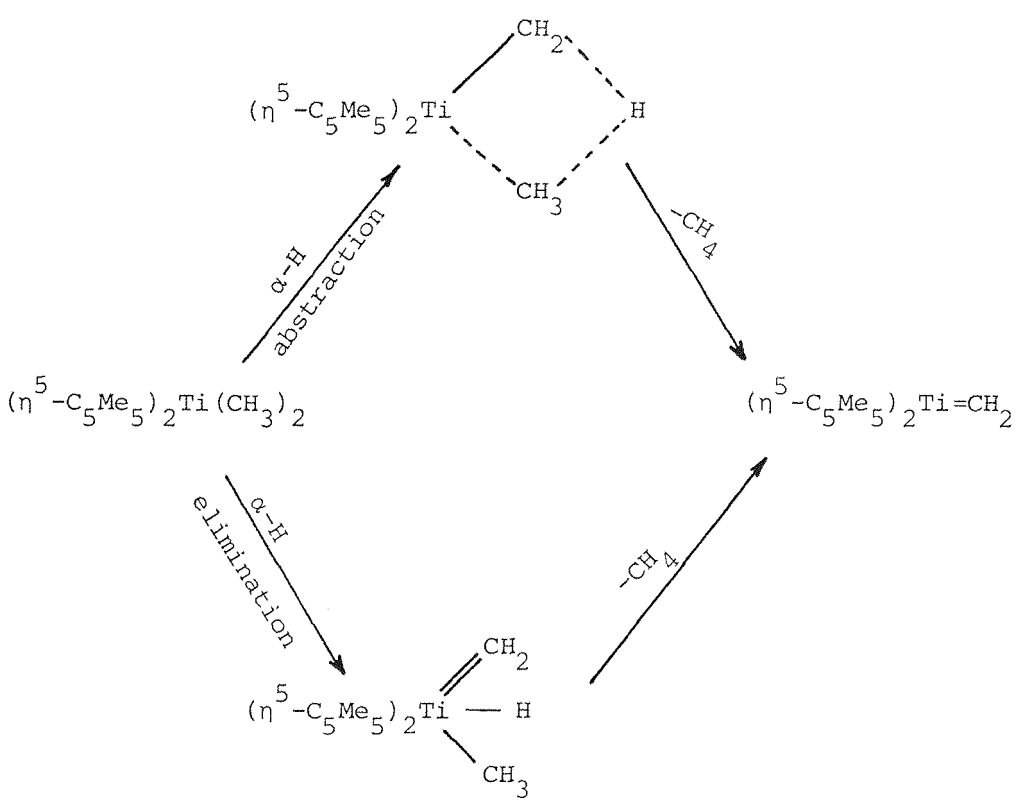

(2.16)

Very recently difluoromethylene (difluorocarbene) complexes were also reported for the first time, e.g. $RuCl_2(=CF_2)(CO)(PPh_3)_2$ [48] and $Ru(=CF_2)(CO)_2(PPh_3)_2$ [24]. The latter complex was formed from the reaction of $Ru(CO)_2(PPh_3)_3$ with $Cd(CF_3)_2(MeOCH_2CH_2OMe)$ and it was proposed that an intermediate product was $Ru(CF_3)(CdCF_3)(CO)_2(PPh_3)_2$ [24], which underwent an elimination reaction, although the nature of the elimination reaction was not determined.

Matrix isolation evidence for α-F elimination for $(\eta^5\text{-}C_5H_5)Mo(CO)_3CF_3$ now sheds light on the formation of the fluorocarbene complex, $Ru(=CF_2)(CO)_2(PPh_3)_2$, via the fluoroalkyl complex, $Ru(CF_3)(CdCF_3)(CO)_2(PPh_3)_2$. The photoreactions of $(\eta^5\text{-}C_5H_5)Mo(CO)_3CF_3$ in CH_4 and N_2 matrices are summarised in Scheme 2.3.

Similar results were obtained on photolysis of $Mn(CO)_5CF_3$ [49] in gas matrices at ca. 12K, i.e. formation of $Mn(CO)_4CF_3$ c.f. $Mn(CO)_4CH_3$ [15] and $Mn(=CF_2)F(CO)_4$, while photolysis of the trifluoroacetyl derivatives gave the coordinatively unsaturated 16-electron species $(\eta^5\text{-}C_5H_5)Mo(CO)_2COCF_3$ (II) and $Mn(CO)_4COCF_3$ c.f. $Mn(CO)_4COCH_3$ [15] species which went on to give $(\eta^5\text{-}C_5H_5)Mo(CO)_3CF_3$ and $Mn(CO)_5CF_3$ respectively.

Transition metal carbonyl complexes containing an acyl group can often be decarbonylated either on heating or photolysis to give the corresponding alkyl [50]. This process is termed decarbonylation. A general mechanistic scheme for decarbonylation is shown in equations 2.17 and 2.18.

$$(OC)_n\overset{O}{\overset{\|}{M}}CR \xrightarrow[\text{heat}]{h\nu \text{ or}} (OC)_{n-1}\overset{O}{\overset{\|}{M}}CR + CO \qquad (2.17)$$

$$(OC)_{n-1}\overset{O}{\overset{\|}{M}}CR \xrightarrow{\text{rearrangement}} (OC)_nMR \qquad (2.18)$$

The photoreactions of $(\eta^5\text{-}C_5H_5)Mo(CO)_3COCF_3$ isolated at high dilution in CH_4 and Ar matrices are shown in Scheme 2.4. The decarbonylation of $(\eta^5\text{-}C_5H_5)Mo(CO)_3COCF_3$ should occur via the reverse of the carbonylation reaction, i.e. dissociative loss of CO followed by a fluoromethyl migration to the

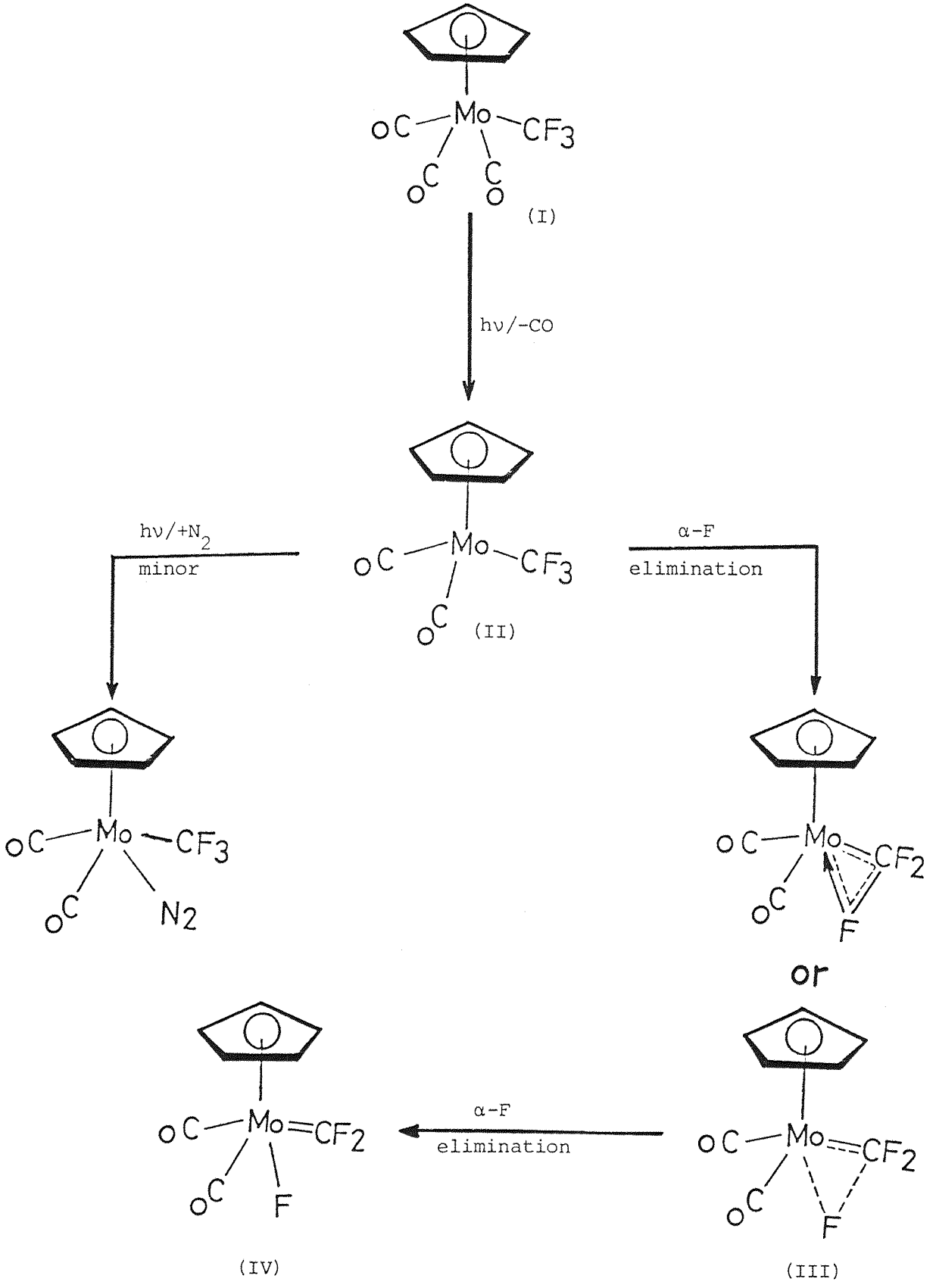

Scheme 2.3

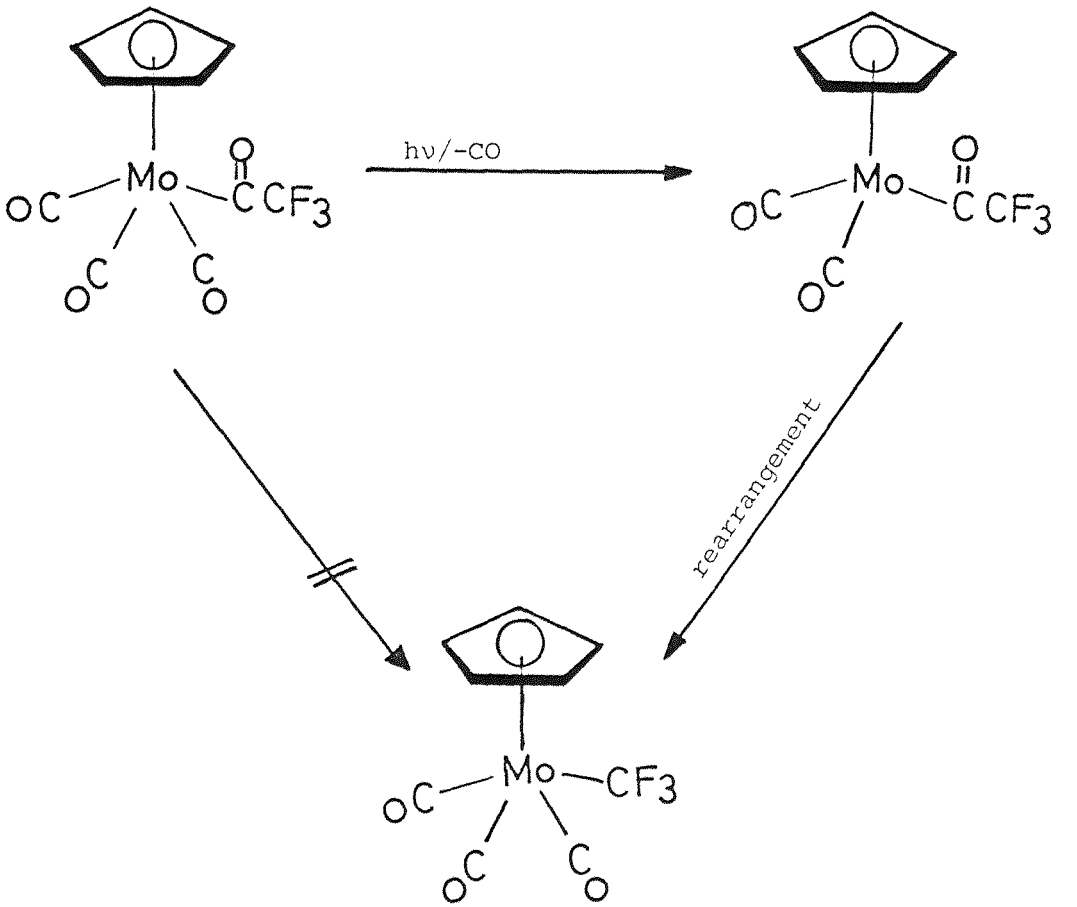

Scheme 2.4

vacant coordination site at the metal. The formation of $(\eta^5\text{-}C_5H_5)Mo(CO)_3CF_3$ from $(\eta^5\text{-}C_5H_5)Mo(CO)_3COCF_3$ via the 16-electron species $(\eta^5\text{-}C_5H_5)Mo(CO)_2COCF_3$ is supported by the presence of weak bands due to the very unstable 16-electron species $(\eta^5\text{-}C_5H_5)Mo(CO)_2COCF_3$. The observed decarbonylation of $(\eta^5\text{-}C_5H_5)Mo(CO)_3COCF_3$ in matrices is consistent with the thermal decarbonylation reaction which affords the only route to $(\eta^5\text{-}C_5H_5)Mo(CO)_3CF_3$ [13]. Interestingly, the complex, $(\eta^5\text{-}C_5H_5)Mo(CO)_3COCF_3$, was tested for its reaction with $Rh(PPh_3)_3Cl$. Upon abstraction of a terminal CO from $(\eta^5\text{-}C_5H_5)Mo(CO)_3COCF_3$, substitution by PPh_3 occured more rapidly than migration of the

of the CF_3 group. A 70% yield of $(\eta^5\text{-}C_5H_5)Mo(CO)_2(PPh_3)COCF_3$ was obtained [13, 51].

2.4 CONCLUSIONS

The photoreactions of $(\eta^5\text{-}C_5H_5)M(CO)_3CH_3$ complexes (M = Cr, Mo, W) in CH_4, Ar, CO, N_2 and 5% C_2H_4 doped CH_4 matrices at 12K indicate that the principal reactive intermediate in the thermal and photochemical solution substitution reactions is probably the coordinatively unsaturated species $(\eta^5\text{-}C_5H_5)M(CO)_2CH_3$. The reactions, therefore, involve dissociative mechanisms rather than associative mechanisms [17], c.f. (Equation 2.19).

$$(\eta^5\text{-}C_5H_5)Co(CO)_2 + CO \underset{h\nu'}{\overset{h\nu}{\rightleftharpoons}} (\eta^3\text{-}C_5H_5)Co(CO)_3 \qquad (2.19)$$

In addition to CO dissociation the chromium complex, $(\eta^5\text{-}C_5H_5)Cr(CO)_3CH_3$, showed α-hydrogen elimination to form the carbene-hydride complex $(\eta^5\text{-}C_5H_5)Cr(CO)_2(=CH_2)H$ for the first time, where only the 16-electron species $(\eta^5\text{-}C_5H_5)M(CO)_2CH_3$ were observed for molybdenum and tungsten.

Irradiation of $(\eta^5\text{-}C_5H_5)Mo(CO)_3CF_3$ also gave in addition to the 16-electron species $(\eta^5\text{-}C_5H_5)Mo(CO)_2CF_3$ the novel carbene-fluoride complex $(\eta^5\text{-}C_5H_5)Mo(CO)_2(=CF_2)F$ as a result of α-fluoride elimination.

Irradiation of $(\eta^5\text{-}C_5H_5)Mo(CO)_3COCF_3$ generated the fluoroalkyl derivative $(\eta^5\text{-}C_5H_5)Mo(CO)_3CF_3$ probably as a result of the terminal CO dissociation followed by a fluoromethyl migration onto the vacant coordination site at the metal.

Table 2.1 Infrared band positions (cm^{-1}) observed in the CO stretching region for $(\eta^5\text{-}C_5H_5)M(CO)_3CH_3$ complexes (M = Cr, Mo, W) and its photoproducts in various gas matrices at 12K.

Complex	CH_4	Ar	N_2	CO	5% C_2H_4/CH_4
$(\eta^5\text{-}C_5H_5)Cr(CO)_3CH_3$	2013.5 1937.2	2020.7 1946.3	2015.5 1939.2	2013.5 1936.6	2011.3 1936.8
$(\eta^5\text{-}C_5H_5)Mo(CO)_3CH_3$	2023.4 1937.9	2030.7 1945.8	2028.6 1941.4	2025.8 1945.2)[a] 1938.8)[a]	2021.8 1935.8
$(\eta^5\text{-}C_5H_5)W(CO)_3CH_3$	2020.8 1929.6	- -	2024.7 1933.8	2020.8 1932.2)[a] 1928.5)[a]	2020.0 1928.6
$(\eta^5\text{-}C_5H_5)Cr(CO)_2CH_3$	g	g	g	g	g
$(\eta^5\text{-}C_5H_5)Mo(CO)_2CH_3$	1966.0 1880.1	1972.0 1886.0	1972.8 1884.4	1962.4)[b] 1876.8)[b]	1964.7 1876.5
$(\eta^5\text{-}C_5H_5)W(CO)_2CH_3$	1953.8 1861.0	- -	1957.6 1864.7	1950.8 1861.3	1952.6 1860.5
$(\eta^5\text{-}C_5H_5)Cr(CO)_2(N_2)CH_3$			d		
$(\eta^5\text{-}C_5H_5)Mo(CO)_2(N_2)CH_3$			1969.7[c] 1913.7		
$(\eta^5\text{-}C_5H_5)W(CO)_2(N_2)CH_3$			d		
$(\eta^5\text{-}C_5H_5)Cr(CO)_2(C_2H_4)CH_3$					e
$(\eta^5\text{-}C_5H_5)Mo(CO)_2(C_2H_4)CH_3$	-	-	-	-	1985.3 1900.5
$(\eta^5\text{-}C_5H_5)W(CO)_2(C_2H_4)CH_3$					1983.5 f
$(\eta^5\text{-}C_5H_5)Cr(CO)_2(=CH_2)H$	2019.3 1938.3	2023.8 1943.1	2031.5 1940.2	2020.0 1938.5	2017.2 1937.2

.../Continued

Table 2.1 (Continued)

[a] Matrix splitting

[b] Long photolysis time required

[c] ν_{N_2} at 2190.8 cm^{-1}

[d] No reaction

[e] No reaction

[f] Band obscured by the band of the ethylene gas.

[g] Very weak bands

Table 2.2 Observed and calculated band positions (cm^{-1}) of terminal CO stretching bands in an experiment with ^{13}CO-enriched sample of $(\eta^5\text{-}C_5H_5)Mo(CO)_3CH_3$ in CH_4 and N_2 matrices, and of $(\eta^5\text{-}C_5H_5)Cr(CO)_3CH_3$ in 5% ^{13}CO doped CH_4 matrices at 12K.

Complex		ν_{CO}	Observed	Calculated
$(\eta^5\text{-}C_5H_5)Mo(^{12}CO)_3CH_3$ [a]	C_s	A'	2025.4	2025.5
		A'+A"	1940.1	1939.9
$(\eta^5\text{-}C_5H_5)Mo(^{12}CO)_2(^{13}CO)CH_3$	C_s	A'	2016.0	2016.3
		b A"	1939.2[c]	1939.9
		A'	1906.6[d]	1905.4
	C_1	A	2013.2	2013.8
		e A	1939.2[c]	1939.9
		A	1906.6[d]	1907.8
$(\eta^5\text{-}C_5H_5)Mo(^{12}CO)(^{13}CO)_2CH_3$	C_1	A	2001.0[g]	2002.3
		f A	1918.4	1918.7
		A	h	1896.7
	C_s	A'	1998.9	1998.9
		j A"	1921.4	1922.0
		A"	h	1896.8
$(\eta^5\text{-}C_5H_5)Mo(^{13}CO)_3CH_3$	C_s	A'	1980.6	1980.5
		A'+A"	1896.5	1896.7
$(\eta^5\text{-}C_5H_5)Mo(^{12}CO)_2CH_3$	C_s	A'	1965.9	1965.3
		A"	1879.6	1879.1
$(\eta^5\text{-}C_5H_5)Mo(^{12}CO)(^{13}CO)CH_3$	C_1	A	1947.8	1948.5
		A	1852.7	1853.2

..../Continued

Table 2.2 (Continued)

Complex	ν_{CO}	Observed	Calculated
$(\eta^5\text{-}C_5H_5)Mo(^{13}CO)_2CH_3$	A'	h	1921.6
C_s	A"	1836.8	1837.3
$(\eta^5\text{-}C_5H_5)Mo(^{12}CO)_2(N_2)CH_3$ [k]	A'	1969.7	1969.0
C_s	A"	1913.7	1913.8
$(\eta^5\text{-}C_5H_5)Mo(^{12}CO)(^{13}CO)(N_2)CH_3$	A	1955.3	1954.6
C_1	A	1886.0	1885.1
$(\eta^5\text{-}C_5H_5)Mo(^{13}CO)_2(N_2)CH_3$	A'	1924.5	1925.2
C_s	A"	1871.4	1871.3
$(\eta^5\text{-}C_5H_5)Cr(^{12}CO)_3CH_3$ [l]	A'	2011.5	2011.5
C_s	A'+A"	1935.7	1935.7
$(\eta^5\text{-}C_5H_5)Cr(^{12}CO)_2(^{13}CO)CH_3$	(A'	m	2002.7
C_s	b(A"	n	1935.5
	(A'	p	1900.7
	(A	1998.5	1996.3
C_1	e(A	n	1936.3
	(A	p	1906.1
$(\eta^5\text{-}C_5H_5)Cr(^{12}CO)(^{13}CO)_2CH_3$	(A	q	1992.8
C_1	f(A	r	1909.4
	(A	s	1893.3
	(A'	1985.2	1984.8 [v]
C_s	j(A'	v	1917.9
	(A"	s	1892.5
$(\eta^5\text{-}C_5H_5)Cr(^{13}CO)_3CH_3$	A'	w	1966.3
C_s	A'+A"		1892.1

.../Continued

Table 2.2 (Continued)

Complex	ν_{CO}	Observed	Calculated
$(\eta^5\text{-}C_5H_5)Cr(^{12}CO)_2(CH_2)H^{x}$			
$\underline{C_s}$	$\underline{A}'$	2016.5	2015.6
	$\underline{A}''$	1933.0	1932.0
$(\eta^5\text{-}C_5H_5)Cr(^{12}CO)(^{13}CO)(CH_2)H$			
$\underline{C_1}$	$\underline{A}$	1998.5	1998.6
	$\underline{A}$	1905.8	1905.1
$(\eta^5\text{-}C_5H_5)Cr(^{13}CO)_2(CH_2)H$			
$\underline{C_s}$	$\underline{A}'$	1969.8	1970.4
	$\underline{A}''$	1888.0	1889.0

[a] Refined energy-factored force constants for $(\eta^5\text{-}C_5H_5)Mo(CO)_3CH_3$: K_1 = 1559.5, K_2 = 1569.3, k_{12} = 43.8 and k_{23} = 49.0 Nm^{-1} as defined by the diagram

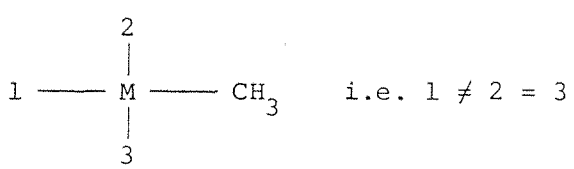

i.e. 1 ≠ 2 = 3

Refined energy-factored force constants for $(\eta^5\text{-}C_5H_5)Mo(CO)_2CH_3$: K = 1493.5 and k_i = 67.0 Nm^{-1}.

[b] ^{13}CO in position 1.

[c] Band obscured by bands of $(\eta^5\text{-}C_5H_5)Mo(CO)_3CH_3$.

[d] Broad band arising probably from two components at 1905 and 1908 cm^{-1}.

[e] ^{13}CO in position 2.

[f] ^{12}CO in position 2.

[g] Component of broad band centred at 2000 cm^{-1}.

[h] Band obscured by bands of ^{13}CO-enriched $(\eta^5\text{-}C_5H_5)Mo(CO)_3CH_3$.

[j] ^{12}CO in position 1.

[k] Refined energy-factored constants for $(\eta^5\text{-}C_5H_5)Mo(CO)_2(N_2)CH_3$: K = 1523.0 and k_i = 43.3 Nm^{-1}.

.../Continued

Table 2.2 (Continued)

[l] Refined energy-factored force constants for $(\eta^5\text{-}C_5H_5)Cr(CO)_3CH_3$: K_1 = 1568.0, K_2 = 1546.7, k_{12} = 42.6 and k_{23} = 32.0 Nm^{-1} as defined by the numbering above in (a).

[m] Unresolved band, obscured with the band of $(\eta^5\text{-}C_5H_5)Cr(^{12}CO)(^{13}CO)(CH_2)H$ at 1998.6 cm^{-1}.

[n] Obscured by the lower parent band at 1935.7 cm^{-1}.

[p] Obscured by the band of $(\eta^5\text{-}C_5H_5)Cr(^{12}CO)(^{13}CO)(CH_2)H$ at 1905.1 cm^{-1}.

[q] Obscured by the band of $(\eta^5\text{-}C_5H_5)Cr(^{12}CO)(^{13}CO)(CH_2)H$ at 1998.6 cm^{-1}.

[r] Obscured band.

[s] Obscured band.

[v] Very weak.

[w] Very weak bands were observed for $(\eta^5\text{-}C_5H_5)Cr(^{12}CO)(^{13}CO)_2CH_3$, but no $(\eta^5\text{-}C_5H_5)Cr(^{13}CO)_3CH_3$ species was generated.

[x] Refined energy-factored force constants for $(\eta^5\text{-}C_5H_5)Cr(CO)_2(CH_2)H$: K = 1574.6 and k_i = 66.6 Nm^{-1}.

Table 2.3 Infrared band positions (cm^{-1}) for $(\eta^5\text{-}C_5H_5)Mo(CO)_3CF_3$ and $(\eta^5\text{-}C_5H_5)Mo(CO)_3COCF_3$ complexes and their photoproducts in CH_4, Ar and N_2 matrices.

Complex	ν_{CO}			ν_{CF}
	CH_4	Ar	N_2	CH_4
$(\eta^5\text{-}C_5H_5)Mo(CO)_3CF_3$ (I)	2057.3 1976.0)[a] 1970.3)	2063.5 1983.2)[a] 1976.0)	2059.7 1978.5)[a] 1973.2)	1065.0 1055.3 1032.5 1018.0)[a] 1012.0)
$(\eta^5\text{-}C_5H_5)Mo(CO)_2CF_3$ (II)	1994.8 1910.0	1998.6 1914.7	1997.6 1914.5	b
$(\eta^5\text{-}C_5H_5)Mo(CO)_2(FCF_2)$ (III)	2045.2 1982.6	2051.6 1987.1	2049.5 1984.1	1108.3 1100.6 1086.0
$(\eta^5\text{-}C_5H_5)Mo(CO)_2(=CF_2)F$ (IV)	2063.3 1998.0	2068.3 2002.5	2065.8 2000.3	1185.2 1180.7 1172.3
$(\eta^5\text{-}C_5H_5)Mo(CO)_2(N_2)CF_3$			2018.2[c] 1938.3	
$(\eta^5\text{-}C_5H_5)Mo(CO)_3COCF_3$	2046.5 1976.8) 1962.0)[a] 1654.2[d]	2051.7 1976.8) 1962.0)[a] 1658.5[d]	-	1257.2 1238.3 1194.5 1154.2
$(\eta^5\text{-}C_5H_5)Mo(CO)_2COCF_3$	e 1891.4[f]	e 1896.2		-

.../Continued

Table 2.3 (Continued)

[a] Matrix splitting.

[b] The ν_{C-F} bands of $(\eta^5\text{-}C_5H_5)Mo(CO)_2CF_3$ are probably much weaker than the ν_{CO} bands. There are weak bands at 828.0, 820.0 and 808.0 cm^{-1}, but no evidence showed if these bands were related to any ν_{CO} stretching bands. The fact that they grew in intensity ruled out impurity bands arising from the CsI window.

[c] $\nu_{N\equiv N}$ at 2260.0 cm^{-1}.

[d] ν_{COCF_3}.

[e] Band obscured by the lower parent band at 1976.8 cm^{-1}.

[f] Very weak.

2.5 REFERENCES

1. K.W. Barnett and P.M. Treichel, *Inorg. Chem.*, 1967, 6, 294.

2. R.J. Haines, R.S. Nyholm and M.H.B. Stiddard, *J. Chem. Soc. (A).*, 1967, 94.

3. R.B. King, C.W. Howk and K.H. Pannell, *Inorg. Chem.*, 1969, 8, 1042.

4. R.B. King, W.C. Zipperer and M. Ishaq, *Inorg. Chem.*, 1972, 11, 1361.

5. A.J. Gingell, A. Harris, A.J. Rest and R.N. Turner, *J. Organomet. Chem.*, 1976, 121, 205.

6. H.G. Alt, *J. Organomet. Chem.*, 1977, 124, 167.

7. P.M. Treichel, R.L. Shubkin, K.W. Barnett and D. Reichard, *Inorg. Chem.*, 1966, 5, 1177.

8. H.G. Alt and J.A. Schwarzle, *J. Organomet. Chem.*, 1978, 162, 45.

9. M.D. Rausch, T.E. Gismondi, H.G. Alt and J.A. Schwarzle, *Z. Naturforsch.*, 1977, 32B, 998.

10. R.G. Severson and A. Wojcicki, *J. Organomet. Chem.*, 1978, 157, 173.

11. T. Yoshida, T. Okano, Y. Ueda and S. Otsuka, *J. Am. Chem. Soc.*, 1981, 103, 3411.

12. K.A. Mahmoud, R. Narayanaswamy and A.J. Rest, *J. Chem. Soc. Dalton Trans.*, 1981, 2199.

13. J.J. Alexander and A. Wojcicki, *Inorg. Chem.*, 1973, 12, 74.

14. R.H. Hooker, K.A. Mahmoud and A.J. Rest, *J. Organomet. Chem.*, 1983, in press.

15. T.M. McHugh and A.J. Rest, *J. Chem. Soc. Dalton trans.*, 1980, 2323.

16. M. Poliakoff, *J. Chem. Soc. Faraday II*, 1977, 569.

17. O. Crichton, A.J. Rest and D.J. Taylor, *J. Chem. Soc. Dalton Trans.*, 1980, 167.

18. P.S. Braterman, *"Metal Carbonyl Spectra"*, Academic Press, London, 1975.

19. A.J. Rest, J.R. Sodeau and D.J. Taylor, *J. Chem. Soc. Dalton Trans.*, 1978, 651.

20. A.J. Rest, *J. Organomet. Chem.*, 1972, 40, C76.

21. A.M.F. Brouwers, A. Oskam, R. Narayanaswamy and A.J. Rest, *Inorg. Chim. Acta Letters.*, 1981, 53(5), L205.

22. J.K. Burdett, *Inorg. Chem.*, 1981, 20, 2607.

23. O. Crichton and A.J. Rest, *J. Chem. Soc. Dalton Trans.*, 1977, 986.

24. G.R. Clark, S.V. Hoskins, T.C. Jones and W.R. Roper, *J. Chem. Soc. Chem. Comm.*, 1983, 719.

25. T.A. O'Donnell, K.A. Phillips and A.B. Waugh, *Inorg. Chem.*, 1973, 12, 1435.

26. D.M. Bruce, A.J. Hewitt, J.H. Holloway, R.D. Peacock and I.L. Wilson, *J. Chem. Soc. Dalton Trans.*, 1976, 2230.

27. R.J. Kaslauskas and M.S. Wrighton, *J. Amer. Chem. Soc.*, 1980, 102, 1727 and 1982, 104, 6005.

28. D.J. Fettes, R. Narayanaswamy and A.J. Rest, *J. Chem. Soc. Dalton Trans.*, 1981, 2311.

29. T.M. McHugh and A.J. Rest, *J. Chem. Soc. Dalton Trans.*, 1980, 2323.

30. D.R. Tyler, *Inorg. Chem.*, 1981, 7, 2257.

31. E. Samuel, M.D. Rausch, T.E. Gismondi, E.A. Mintz and C. Giannotti, *J. Organomet. Chem.*, 1979, 172, 309.

32. R.B. Hitam, R.H. Hooker, K.A. Mahmoud, R. Narayanaswamy and A.J. Rest, *J. Organomet. Chem.*, 1981, 222, C9.

33. B. Meyer, *"Low Temperature Spectroscopy"*, Elsevier, New York, 1971.

34. R.L. Sweany, *Inorg. Chem.*, 1980, 19, 3512.

35. J. Chetwynd-Talbot, P. Grebenik and R.N. Perutz, *J. Chem. Soc. Chem. Commun.*, 1981, 452.

36. K.A. Mahmoud, A.J. Rest and H.G. Alt, *J. Chem. Soc. Dalton Trans.*, 1983, accepted for publication.

37. D. Sellmann, *Angew. Chem. Int. Edn.*, 1971, 10, 919; D. Sellmann and G. Maisel, *Z. Naturforsch*, 1972, B27, 465.

38. L. Sunpu and A. Yamamoto, *J. Chem. Soc. Chem. Commun.*, 1974, 9.

39. J.P. Collmann and L.S. Hegedus, *"Principles and Applications of Organo Transition Metal Chemistry"*, University Science Books, Mill Valley, California, 1980.

40. C. Masters, *"Homogeneous Transition Metal Catalysis"*, Chapman and Hall, London 1981.

41. N.J. Cooper and M.L.H. Green, *J. Chem. Soc. Chem. Commun.*, 1974, 761; *J. Chem. Soc. Dalton Trans.*, 1979, 1121.

42. C. Baird, *J. Organomet. Chem.*, 1974, 64, 289.

43. J.R.C. Light and H.H. Zeiss, *J. Organomet. Chem.*, 1970, 21, 391.

44. P.W. Jolley and R. Pettit, *J. Am. Chem. Soc.*, 1966, 88, 5044.

45. C.P. Casey, L.D. Albin and T.J. Burkhardt, *J. Am. Chem. Soc.*, 1977, 99, 2534; *ibid* 1979, 101, 7282.

46. C.P. Casey and M.C. Cesa, *Organometallics*, 1982, 1, 87.

47. C. McDade, J.C. Green and J.E. Bercaw, *Organometallics*, 1982, 1, 1629.

48. G.R. Clark, S.V. Hoskins and W.R. Roper, *J. Organomet. Chem.*, 1982, 234, C9.

49. K.A. Mahmoud, A.J. Rest and I. Whitwell, unpublished work.

50. A. Wojcicki, *Advan. Organomet. Chem.*, 1974, 12, 31.

51. J.J. Alexander, *J. Am. Chem. Soc.*, 1975, 97, 1729.

CHAPTER THREE

PHOTOCHEMISTRY OF THE HYDRIDO COMPLEXES OF THE TYPE $(\eta^5\text{-}C_5H_5)M(CO)_3H$ (M = Cr, Mo, W) AND OF $(\eta^5\text{-}C_5H_5)W(CO)_2(C_2H_4)H$ IN DIFFERENT GAS MATRICES AT 12 K

3.1 INTRODUCTION

Transition metal hydrido complexes play important roles in a variety of reactions: (i) they provide hydrogens for organic or organometallic hydrogenation reactions [1, 2], (ii) olefins may insert into the metal-hydrogen bond generating alkyl derivatives [3 - 5], (iii) they represent efficient catalysts in hydroformylation reactions [6] and other catalytic processes [7, 8], e.g. isomerisation, polymerization, deuter ation and hydrosilation. Transition metal hydrido complexes are also useful synthetic intermediates, are promising as hydrogen and energy storage systems, and have been proposed as important intermediates for obtaining molecular hydrogen from water [9]. Additionally, transition metal hydrido complexes are highly reactive intermediates in the thermal or photo-induced β-hydrogen elimination process of transition metal alkyl complexes [10 - 12]. One reason for this versatile reactivity is the fact that the hydride ligand has only small steric requirements; even as a one-electron donor a hydride ligand can function as a bridging ligand between two or three transition metal atoms [13]. Since metal-hydrogen bonds are considered stronger than metal-carbon bonds [14], selective reactions can be expected for hydrido carbonyl complexes. So far, however, photochemical reactions have only been described for a few hydrido complexes [15], e.g. $(\eta^5\text{-}C_5H_5)_2ReH$ [16], $(\eta^5\text{-}C_5H_5)_2MH_2$ (M = Mo, W) [17 - 20], $M(CO)_5H$ (M = Mn, Re) [21] and $Co(CO)_4H$ [22] in both solution and low temperature matrices, and $IrClH_2(PPh_3)_3$ [23], $IrH_3(PPh_3)_2$ [24], and $(\eta^5\text{-}C_5Me_5)Os(CO)_2H$ [25] in solution only.

In order to gain more insight into the basic steps of the photochemistry of transition metal hydrido complexes we chose the compounds $(\eta^5\text{-}C_5H_5)M(CO)_3H$ (M = Cr, Mo, W) and an olefin derivative $(\eta^5\text{-}C_5H_5)W(CO)_2(C_2H_4)H$ for photolysis

studies in different gas matrices at 12K. We compare those results with studies in solution, e.g. Hoffman and Brown [26] have postulated that the facile thermal and photo-induced reactions of $(\eta^5\text{-}C_5H_5)W(CO)_3H$ with tri-n-butylphosphine both proceed chiefly via radical intermediates rather than by CO dissociation. The $(\eta^5\text{-}C_5H_5)Cr(CO)_3H$ complex shows different photochemical behaviour from the molybdenum and tungsten analogues and its results are described separately.

3.2 RESULTS*

3.2.1 Photolysis of $(\eta^5\text{-}C_5H_5)M(CO)_3H$ Complexes (M = Cr, Mo, W)** in Ar, CH_4, 5% $^{13}CO/CH_4$ and of ^{13}CO-enriched $(\eta^5\text{-}C_5H_5)W(CO)_3H$ in Ar Matrices at 12K

3.2.1(a) Photolysis of $(\eta^5\text{-}C_5H_5)M(CO)_3H$ (M = Mo, W) in CH_4, Ar and of ^{13}CO-enriched $(\eta^5\text{-}C_5H_5)W(CO)_3H$ in Ar Matrices at 12K

Infrared spectra from an experiment with $(\eta^5\text{-}C_5H_5)W(CO)_3H$ isolated at high dilution in an Ar matrix (ca 1:2000 - 1:5000) are shown in Figure 3.1. Before photolysis the spectrum in the terminal CO stretching region contains bands at 2032.2, 1946.1 and 1942.1 cm^{-1} (Figure 3.1(a), Table 3.1). The upper band is assigned as a symmetric A' stretch and the lower bands are assigned to overlapping A' (symmetric) and A" (antisymmetric) bands of a C_s symmetry complex by analogy with the bands observed in gas matrices for $(\eta^5\text{-}C_5R'_5)M(CO)_3R$ complexes (M = Mo, W; R = alkyl and aryl; R' = H, CH_3) [5, 27]. Irradiation of the matrix with u.v. radiation (λ = 230 - 410 nm) corresponding to the electronic absorption of $(\eta^5\text{-}C_5H_5)W(CO)_3H$ (Figure 3.2(a)) produced free CO (2138.5 cm^{-1}) and four new bands at 2004.8, 1908.0, 1966.7 and 1880.2 cm^{-1} (Figure 3.1(b)). Continued photolysis resulted in the latter bands and that of CO growing at the expense of the parent molecule bands. Prolonged irradiation with the same energy source (λ = 230 - 410 nm) resulted in a slight increase in the intensities of the bands at 2004.8 and

---

* Experimental details are given in Chapter 8

** The $(\eta^5\text{-}C_5H_5)Cr(CO)_3H$ shows different behaviour from the molybdenum and tungsten analogues and its photochemistry is described separately (see Sections 3.2.1(b) and 3.2.3(b)).

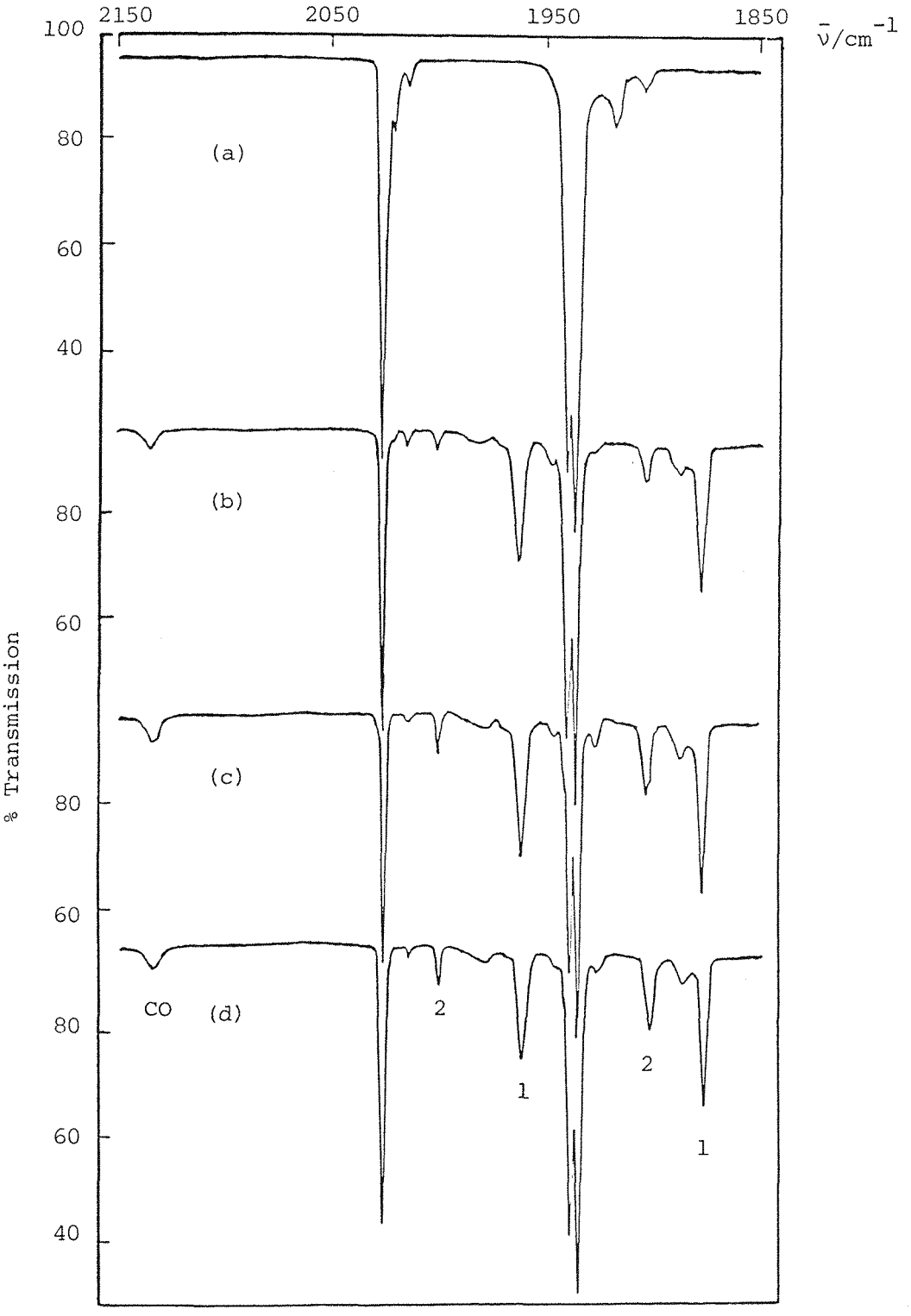

FIGURE 3.1 Infrared spectra from an experiment with $(\eta^5\text{-}C_5H_5)W(CO)_3H$ isolated in an Ar matrix at 12K: (a) after deposition, (b) after 75 min. photolysis using λ = 230 - 410 nm, (c) after further 20 min. photolysis using the same source, and (d) after 75 min. reversal using λ > 430 nm. Bands marked (*) are due to $(\eta^5\text{-}C_5H_5)W(^{12}CO)_2(^{13}CO)H$ present in natural abundance. Bands marked (1) and (2) derive from photoproducts (see text).

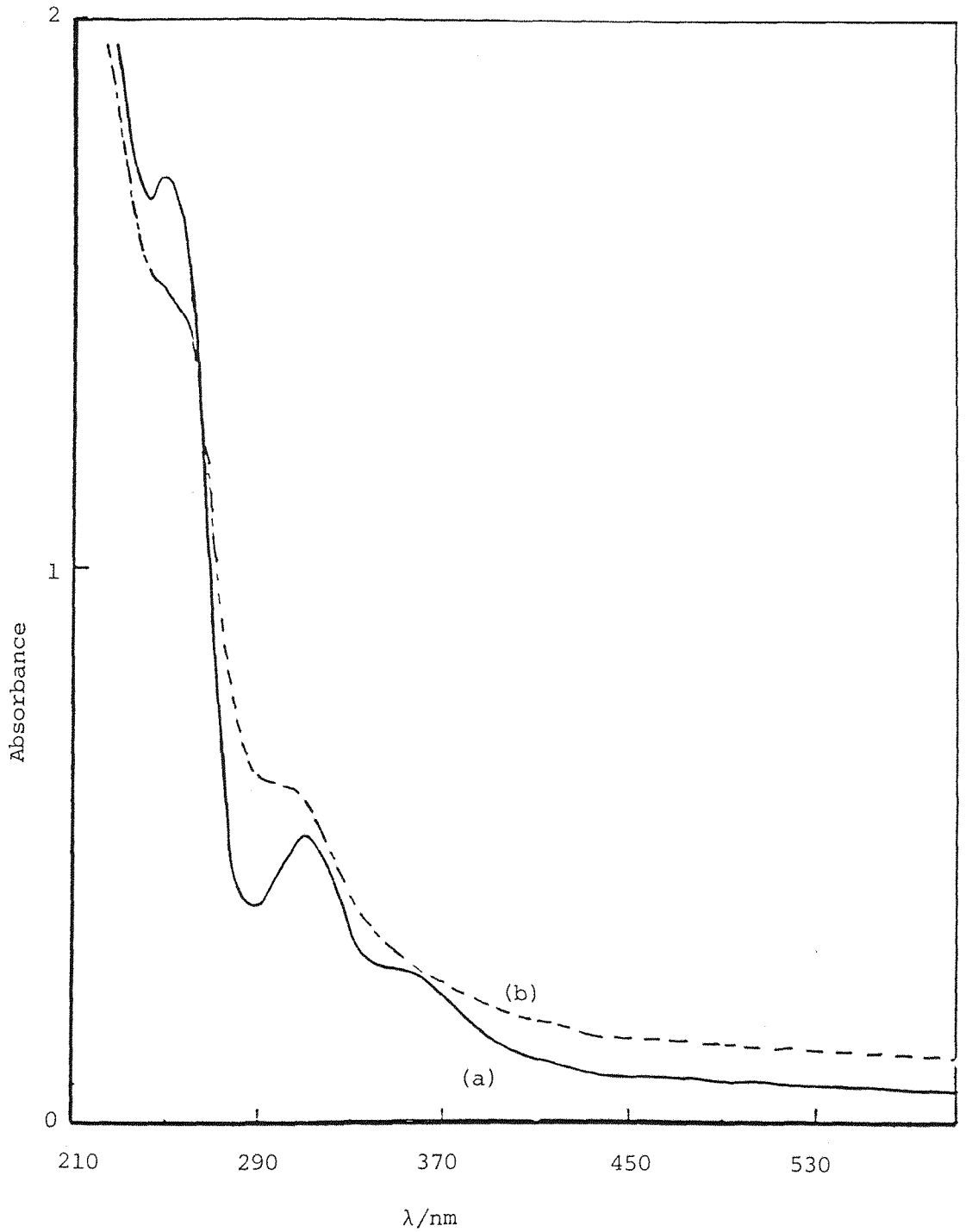

FIGURE 3.2 Ultraviolet/visible spectra from an experiment with $(\eta^5\text{-}C_5H_5)W(CO)_3H$ isolated at high dilution in an Ar matrix at 12K: (a) after deposition and (b) after 50 min. photolysis using $230 < \lambda < 410$ nm.

1908.0 cm^{-1}, whereas no changes were observed in the bands at 1966.7 and 1880.2 cm^{-1} (Figure 3.1(c)). Under steady irradiation conditions a stationary state was reached after 3 hours of irradiation in Ar matrices. Irradiation with visible light (λ > 430 nm) or annealing the matrix to ca. 35K (Figure 3.1(a)) demonstrated that the new photo-product bands belong to two different species. The first species was $(\eta^5\text{-}C_5H_5)W(CO)_2H$ (1966.7 and 1880.2 cm^{-1}; bands (1)), confirmed by ^{13}CO, and by comparison of the band positions with those observed on photolysis of $(\eta^5\text{-}C_5H_5)W(CO)_3H$ in CH_4 matrices. The second species was $(\eta^5\text{-}C_5H_5)W(CO)_3^{\bullet}$ (2004.8 and 1908.0 cm^{-1}; bands (2)), by comparison with the same species obtained in CO matrices (see Section 3.2.3 and Table 3.1).

Irradiation of $(\eta^5\text{-}C_5H_5)W(CO)_3H$ in the CH_4 matrices gave only the 16-electron intermediate $(\eta^5\text{-}C_5H_5)W(CO)_2H$ (see below) in a reversible process. The facile reversibility of the primary step shows that the W-H linkage is retained in the product species because if cleavage of the W-H bond had occurred H atoms would have been produced and these are known to diffuse freely in gas matrices at 4 - 30K [28]. Diffusion of H atoms would have precluded reversal of the primary step. The ejection of CO in the primary photolysis step with the retention of a W-H bond enables the new species to be identified as $(\eta^5\text{-}C_5H_5)W(CO)_2H$. This assignment was confirmed by an experiment with ^{13}CO-enriched $(\eta^5\text{-}C_5H_5)W(CO)_3H$ (see below). Analogous results were obtained for $(\eta^5\text{-}C_5H_5)Mo(CO)_3H$ isolated at high dilution in Ar and CH_4 matrices. Spectroscopic data for the new species are given in (Table 3.1).

The i.r. spectrum of ^{13}CO-enriched $(\eta^5\text{-}C_5H_5)W(CO)_3H$ isolated at high dilution in an Ar matrix at 12K shows bands due to the range of species $(\eta^5\text{-}C_5H_5)W(^{12}CO)_{3-n}(^{13}CO)_nH$ (n = 0 - 3) (Figure 3.3(a)). This is confirmed by an energy-factored force-field analysis of the observed and calculated band positions [27, 29, 30]. A very good fit was obtained using C_s symmetry (Table 3.2). Irradiation of the matrix with u.v. radiation (λ = 230 - 410 nm) gave new ^{13}CO-enriched product bands at 1965.9, 1950.1, 1879.5, 1854.5 and 1837.6 cm^{-1} (Figure 3.3(b)). In this case a good fit was obtained between the observed and calculated bands of a C_s $W(CO)_2$ fragments, i.e. $(\eta^5\text{-}C_5H_5)W(^{12}CO)_{2-m}(^{13}CO)_mH$ (m = 0 - 2) (Table 3.2). The photoproduct in Ar and CH_4 matrices (see above) can, therefore, be conclusively assigned as $(\eta^5\text{-}C_5H_5)M(CO)_2H$ (M = Mo, W).

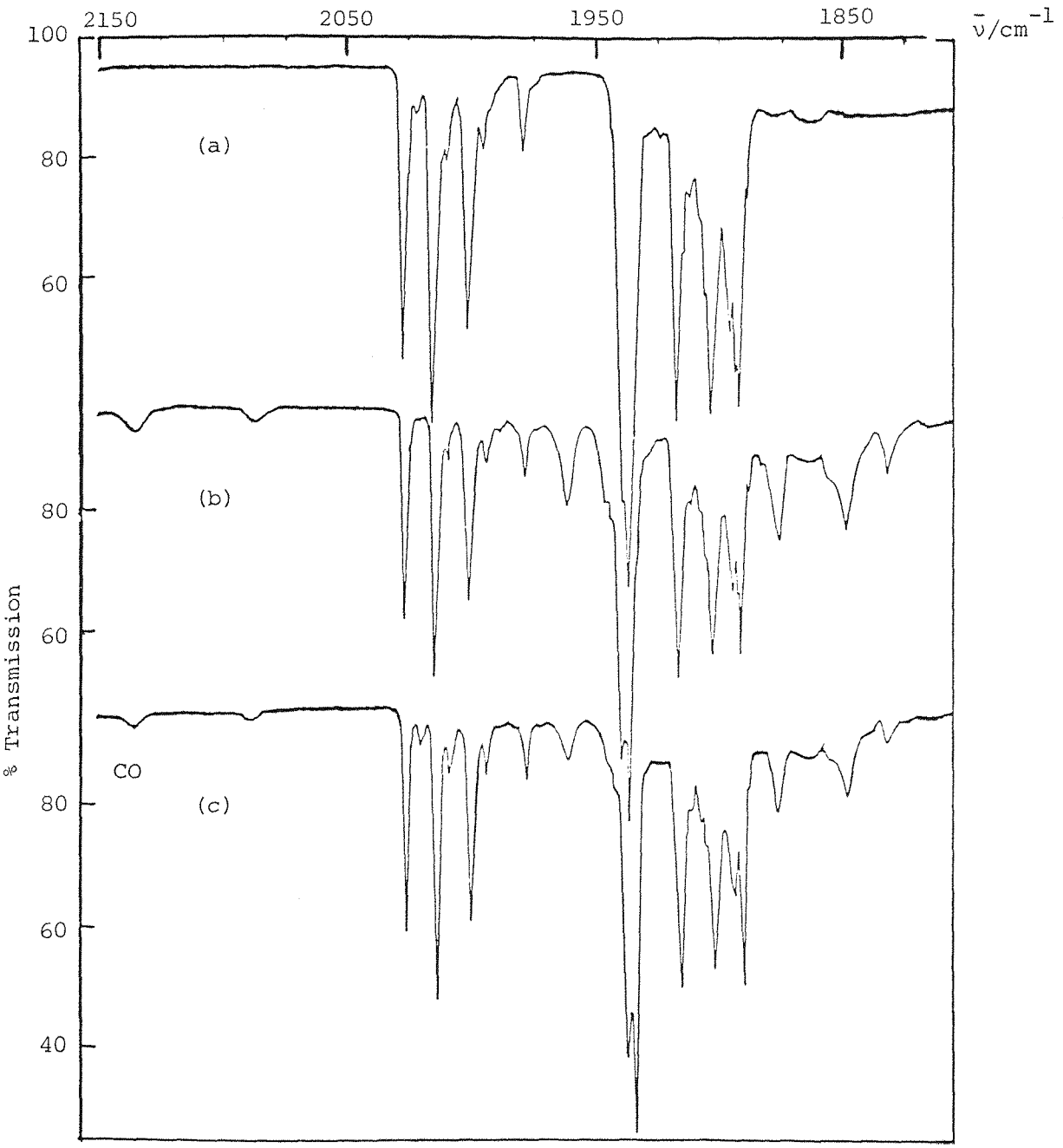

FIGURE 3.3 Infrared spectra from an experiment with ^{13}CO-enriched $(\eta^5\text{-}C_5H_5)W(CO)_3H$ isolated at high dilution in an Ar matrix at 12K: (a) after deposition, (b) after 45 min. photolysis using $290 < \lambda < 410$ nm radiation, and (c) after 2 min. annealing.

The observed relative intensities of the two bands for $(\eta^5\text{-}C_5H_5)W(^{12}CO)_2H$ (1.21:1) were obtained by tracing and weighing bands from spectra in absorbance mode. The ratio $I_{antisym}/I_{sym}$ (1.21:1) gave a OC-W-CO angle of ∿ 95° in the standard expression $I_{antisym}/I_{sym} = \tan^2(\theta/2)$ [30].

3.2.1(b) Photolysis of $(\eta^5\text{-}C_5H_5)Cr(CO)_3H$ in CH_4, Ar, and 5% $^{13}CO/CH_4$ Matrices at 12K

Infrared spectra from an experiment with $(\eta^5\text{-}C_5H_5)Cr(CO)_3H$ isolated at high dilution in a CH_4 matrix are shown in Figure 3.4. Before photolysis the spectrum in the terminal CO stretching region contains bands at 2016.4, 1941.8 and 1930.4 cm^{-1} (Figure 3.4(a), Table 3.1). Irradiation of the matrix with u.v. radiation (λ = 310 - 390 nm) produced free CO (2138.5 cm^{-1}) and five new bands at 2048.5, 1974.5, 1953.3, 1883.0 and 1855.5 cm^{-1} (Figure 3.4(b)). Irradiation with visible light (λ > 430 nm) or annealing the matrix decreased the intensity of the band at 2048.5 cm^{-1} and the band due to 'free' CO, and re-generated the bands due to the starting material, and slightly increased the intensities of the bands at 1974.5, 1953.3, 1883.0 and 1855.5 cm^{-1} (Figure 3.4(c)). Comparison of the growth and disappearance of bands in several experiments and under various times of photolysis with different energies of radiation identified that there were two pairs of new bands: (1) 1953.3 and 1855.5 cm^{-1}, (2) 1974.5 and 1883.0 cm^{-1}, and a single intense band at 2048.5 cm^{-1} (Figure 3.4(c)).

The (1) pair (1953.3 and 1855.5 cm^{-1}) can be assigned to the 16-electron coordinatively unsaturated species $(\eta^5\text{-}C_5H_5)Cr(CO)_2H$. The major photoproduct bands, pair (2) (1974.5 and 1883.0 cm^{-1}) could possibly be assigned to a ring-hydrogen to metal bridging species (I). However, the single band at 2048.5 cm^{-1} remains to be identified (see discussion).

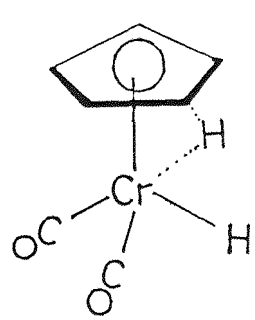

(I)

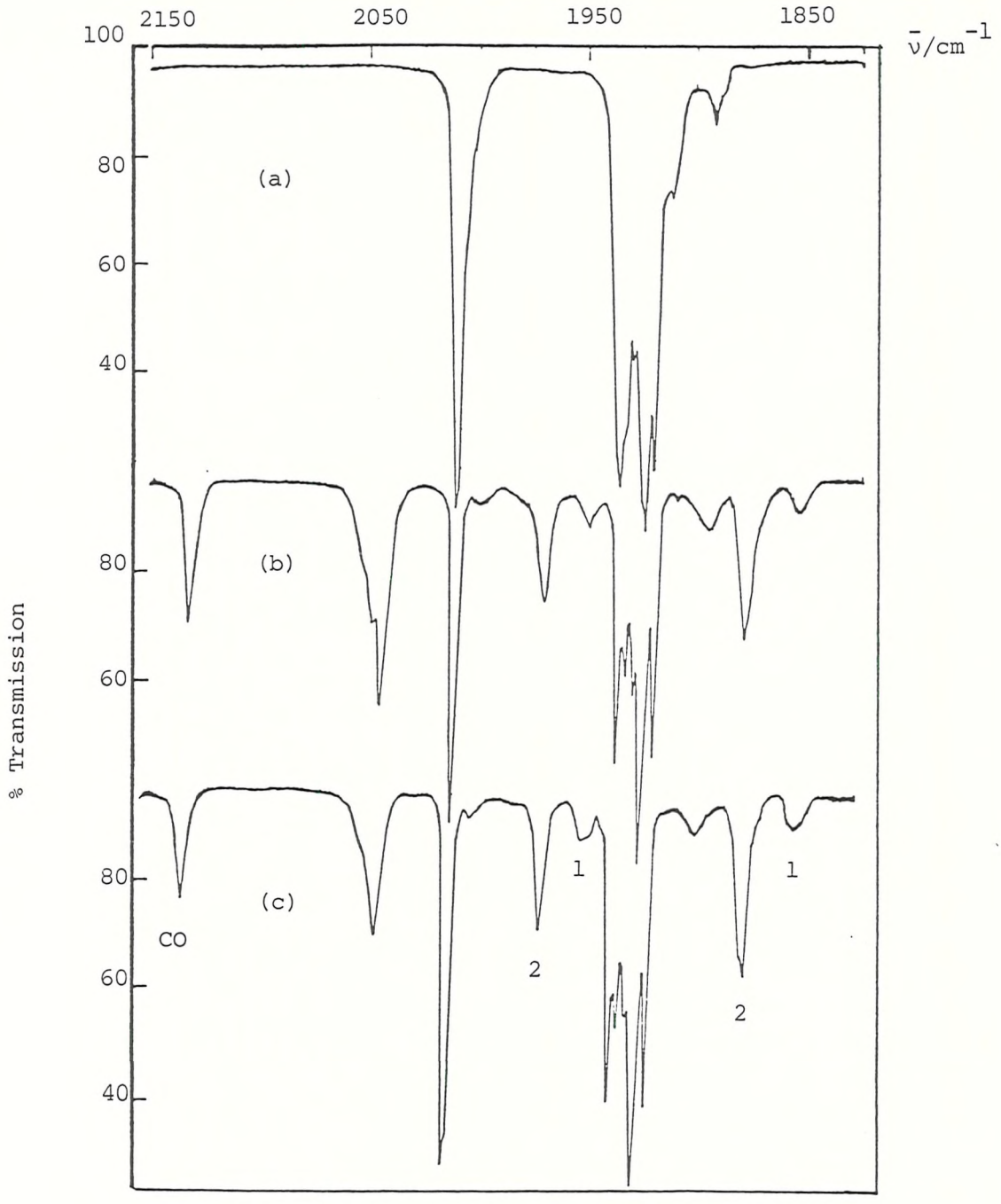

FIGURE 3.4 Infrared spectra from an experiment with $(\eta^5\text{-}C_5H_5)Cr(CO)_3H$ isolated in CH_4 matrix at 12K: (a) after deposition, (b) after 80 min. photolysis using λ = 310 - 390 nm, and (c) after 2 min. annealing. Bands marked (*) are due to $(\eta^5\text{-}C_5H_5)Cr(^{12}CO)_2(^{13}CO)H$ present in natural abundance. Bands marked (1) and (2) derive from photoproducts (see text).

The photogeneration of these new bands in a CH_4 matrix can also be observed in an Ar matrix under the same conditions. Before photolysis the i.r. spectrum of $(\eta^5\text{-}C_5H_5)Cr(CO)_3H$ isolated in an Ar matrix showed bands at 2021.2, 1949.7 and 1939.0 cm^{-1} (Table 3.1). Irradiation with u.v. light (λ = 310 - 390 nm) produced three i.r. bands at 2050.0, 1981.7 and 1888.0 cm^{-1} in addition to the band due to free CO at 2138 cm^{-1}. Longer times of irradiation with the same energy filter (λ = 320 - 390 nm) showed slight increases in the bands at 2050.0, 1981.7 and 1888.0 cm^{-1} while other new bands started to grow at 1986.5, 1913.3 and 1907.0 cm^{-1}. Annealing the matrix for 2 min. reduced the intensities of the bands at 2050.5, 1986.5, 1913.3 and 1907.0 cm^{-1}, and regenerated the bands due to the starting material whereas no changes in the intensities of the bands at 1981.7 and 1888.0 cm^{-1} were observed. Different photolysis conditions showed that these new bands (band sets (1) - (3) belong to three different species. The first has a single band at 2050.0 cm^{-1}, the second has two bands at 1981.7 and 1888.0 cm^{-1} and the third has bands at 1986.5, 1913.3 and 1907.0 cm^{-1} of which the latter pair could be a result of matrix splitting. The bands at 1986.5, 1913.3 and 1907.0 cm^{-1} may be assigned to the radical species $(\eta^5\text{-}C_5H_5Cr(CO)_3^{\cdot}$ by analogy with the species obtained from irradiation of $(\eta^5\text{-}C_5H_5)M(CO)_3H$ complexes (M = Mo, W) in Ar and CO matrices. The pair of bands at 1981.7 and 1888.0 cm^{-1} was assigned to species (I) obtained in a CH_4 matrix (see above) whereas the single band at 2050.0 cm^{-1} remains to be identified (see discussion).

The i.r. spectrum of $(\eta^5\text{-}C_5H_5)Cr(CO)_3H$ isolated at high dilution in a 5% ^{13}CO doped CH_4 matrix shows three strong bands at 2014.5, 1939.2 and 1929.0 cm^{-1} (Table 3.2). Irradiation of the matrix with u.v. light (λ = 320 - 390 nm) gave new ^{13}CO-enriched product bands due to the range of species $(\eta^5\text{-}C_5H_5)Cr(^{12}CO)_{3-n}(^{13}CO)_nH$ (n = 1 - 3; Table 3.2). This is confirmed by an energy-factored force-field analysis of the observed and calculated band positions. A very good fit was obtained using $\underline{C_s}$ symmetry. The observation of new ^{13}CO bands confirms that $^{12}CO \rightarrow {}^{13}CO$ exchange takes place, and that CO dissociation is the first step when the $(\eta^5\text{-}C_5H_5)Cr(CO)_3H$ complex is photolysed in gas matrices at 12K.

3.2.2 Photolysis of $(\eta^5\text{-}C_5H_5)M(CO)_3H$ (M = Cr, Mo, W) in N_2 Matrices at 12K

The i.r. spectrum of $(\eta^5\text{-}C_5H_5)W(CO)_3H$ isolated at high dilution in a N_2 matrix contains bands at 2029.5, 1942.5 and 1932.3 cm^{-1}. A period of photolysis using medium energy u.v. radiation (λ = 290 - 370 nm) produced new i.r. bands at 2163.5, 2138.0, 1972.7 and 1910.0 cm^{-1}, of which the band at 2138.0 cm^{-1} corresponds to free CO. Irradiation with long wavelength light (λ > 430 nm) caused little change in the intensities of the parent bands or new product bands; such long wavelength photolysis caused reversal of the forward step in the case of $(\eta^5\text{-}C_5H_5)W(CO)_3H$ (see Section 3.2.1(a)).

The band at 2163.5 cm^{-1} may be assigned as a N ≡ N stretching mode of an end-on coordinated dinitrogen ligand by analogy with bands for $(\eta^5\text{-}C_5H_5)Co(CO)(N_2)$ (ν_{NN} at 2164.6 cm^{-1} (N_2 matrix) [31], $(\eta^5\text{-}C_5H_5)Mn(CO)_2(N_2)$ (ν_{NN} at 2175.0 cm^{-1} (N_2 matrix) and 2169 cm^{-1} (n-hexane)) [32, 33], $(\eta^4\text{-}C_4H_4)Fe(CO)_2(N_2)$ (ν_{NN} at 2206.8 cm^{-1} (N_2 matrix)) [32], $Ni(CO)_3(N_2)$ (ν_{NN} at 2266 cm^{-1} (N_2 matrix)) [34], and $(\eta^5\text{-}C_5H_5)Mo(CO)_2(N_2)CH_3$ (ν_{NN} at 2190.8 cm^{-1} (N_2 matrix)) [27]. The bands at 1972.7 and 1910.0 cm^{-1} may be assigned as terminal CO stretching modes. Since the product is formed with the ejection of CO (band at 2138.0 cm^{-1}), it may be identified as $(\eta^5\text{-}C_5H_5)W(CO)_2(N_2)H$, cf. $(\eta^5\text{-}C_5H_5)Mo(CO)_2(N_2)CH_3$ (ν_{CO} at 1969.7 and 1913.7 cm^{-1}) [27]. This assignment was confirmed by photolysing $(\eta^5\text{-}C_5H_5)W(^{12}CO)_{3-n}(^{13}CO)_nH$ in a N_2 matrix and subjecting the resulting bands to an energy-factored force-field fitting procedure (see above). An excellent agreement between observed and calculated bands was obtained for a $M(CO)_2$ fragment (see Table 3.2).

Considering the relative intensities of the CO stretching bands of $(\eta^5\text{-}C_5H_5)W(CO)_2(N_2)H$, which may be assigned as the symmetric (1972.7 cm^{-1}) and antisymmetric (1910.0 cm^{-1}) modes of a C_s symmetry $W(CO)_2$ fragment, a OC-W-CO band angle can be calculated from the expression $I_{asym}/I_{sym} = \tan^2(\theta/2)$, c.f. $(\eta^5\text{-}C_5H_5)W(CO)_2H$. The value of the OC-W-CO angle was found to be 108° which is indicative of a *trans* geometry of the CO ligands. An alternative approach to assigning stereochemistry is via the calculation [30] of energy-factored CO interaction force constants k_i. For $(\eta^5\text{-}C_5H_5)W(CO)_2(N_2)H$ this gave a value of 49.2 Nm^{-1} for k_i and comparison of this value with k_i values for $(\eta^5\text{-}C_5H_5)W(CO)_3H$ ($k_{12} = k_{cis}$ = 43.9 Nm^{-1} and $k_{23} = k_{trans}$ = 51.9 Nm^{-1}; Table 3.2) confirmed the structure of the new species as *trans*-$(\eta^5\text{-}C_5H_5)W(CO)_2(N_2)H$.

Analagous results were obtained with $(\eta^5\text{-}C_5H_5)Mo(CO)_3H$ isolated at high dilution in N_2 matrices except that for this complex the forward photolysis to give $(\eta^5\text{-}C_5H_5)Mo(CO)_2(N_2)H$ could be reversed. Values of the OC-Mo-CO bond angle (102°) and the energy-factored CO-interaction force constant (k_i = 49.7 Nm^{-1}) confirmed the structure as *trans*-$(\eta^5\text{-}C_5H_5)Mo(CO)_2(N_2)H$ (see above). Spectroscopic data for the new dinitrogen complexes is given in (Table 3.1).

In contrast to the behaviour of $(\eta^5\text{-}C_5H_5)M(CO)_3H$ (M = Mo, W) complexes, no $\nu_{N\equiv N}$ was observed due to $(\eta^5\text{-}C_5H_5)Cr(CO)_2(N_2)H$ during irradiation of $(\eta^5\text{-}C_5H_5)Cr(CO)_3H$ in a nitrogen matrix under the same conditions but instead bands analogous to those observed for CH_4 and Ar were produced (see Section 3.2.1(b)).

3.2.3(a) Photolysis of $(\eta^5\text{-}C_5H_5)M(CO)_3H$ (M = Mo, W) Complexes in ^{12}CO and ^{13}CO and of ^{13}CO-enriched $(\eta^5\text{-}C_5H_5)W(^{12}CO)_3H$ in ^{13}CO:^{12}CO (25:75) Matrices at 12K

The i.r. spectrum of $(\eta^5\text{-}C_5H_5)Mo(CO)_3H$ isolated at high dilution in a ^{12}CO matrix is shown in (Figure 3.5(a)). Irradiation of the matrix with u.v. light (λ = 230 - 390 nm) resulted in the growth of four new bands at 2008.9, 1915.5, 1908.4 and 1859.1 cm^{-1} (Figure 3.5(b)). Longer times of irradiation with u.v. light caused the four bands to grow, together with an additional band at 1985.1 cm^{-1} (Figures 3.5(c) and 3.5(d)). Prolonged photolysis reduced the yield of the band at 1859.1 cm^{-1}. Irradiation with low energy light (λ > 430 nm) caused the pairs of bands at 2008.9 and 1915.5, 1908.4 cm^{-1} (bands (2)) to decrease slightly with regeneration of the bands due to the starting material (Figure 3.5(e)). Annealing the matrix for 2 min. and then recooling to 12K, showed that the new product bands were observed to decrease with the regeneration of bands due to $(\eta^5\text{-}C_5H_5)Mo(CO)_3H$ (Figure 3.5(f)). The relative intensity of the new terminal CO stretching bands remained constant under a variety of photolysis conditions (time and wavelength of radiation), indicating that the bands belong to the same product species. Annealing the matrix caused a change in the shape of the lower 1915.5/1908.4 cm^{-1} band and so this doublet is probably due to matrix splitting [21] (Table 3.1).

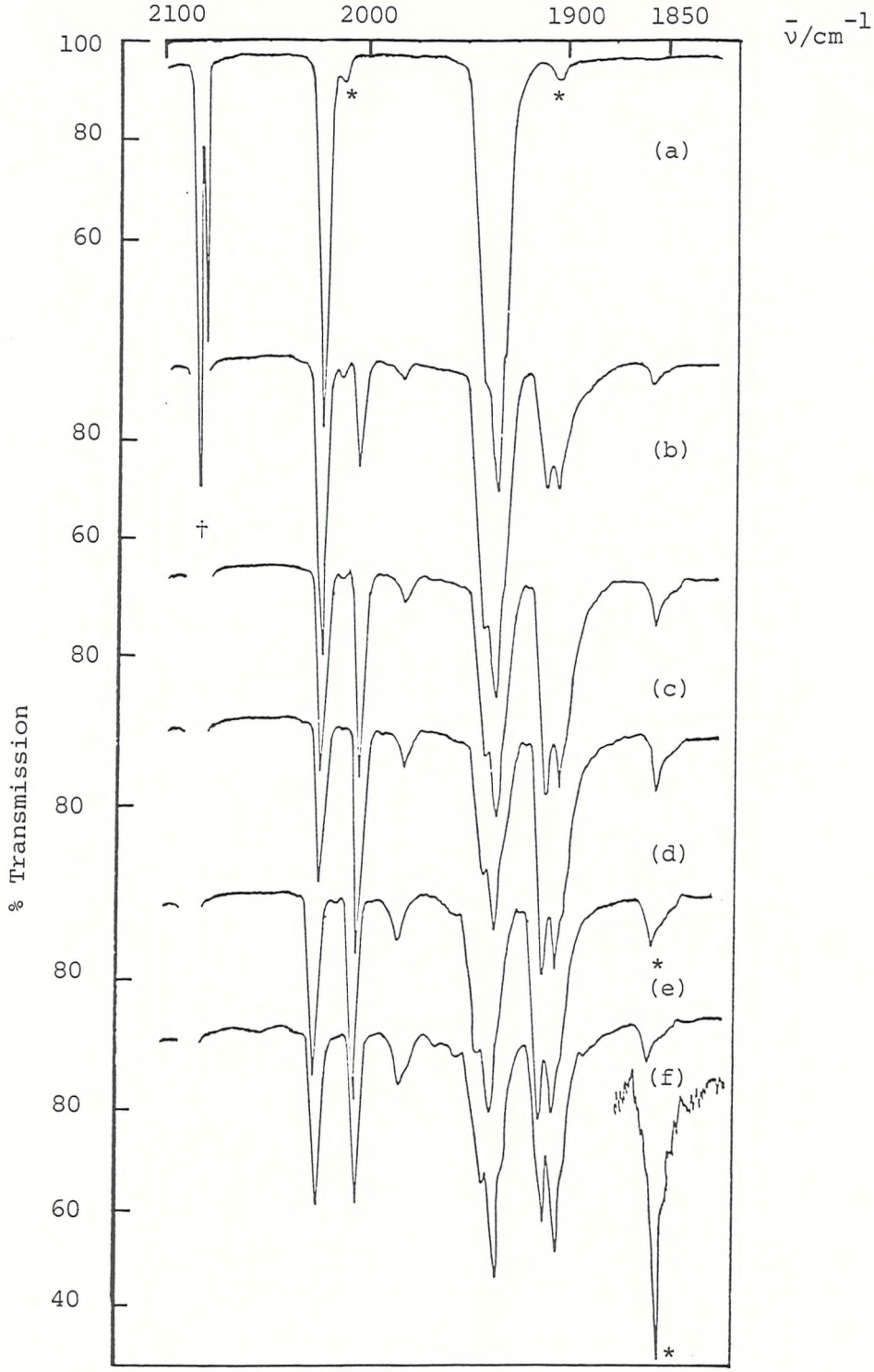

FIGURE 3.5 Infrared spectra from an experiment with $(\eta^5\text{-}C_5H_5)Mo(CO)_3H$ isolated at high dilution in a CO matrix at 12K: (a) after deposition, (b) after 15 min. photolysis using $230 < \lambda < 390$ nm radiation, (c) after 30 min. further photolysis using the same source, (d) after further 30 min. photolysis using the same source, (e) after annealing to 30K for 2 min. Bands marked (*) are due to $(\eta^5\text{-}C_5H_5)Mo(^{12}CO)_2(^{13}CO)H$ present in natural abundance, those marked (†) to ^{13}CO, and that marked * is assigned to the $H^{12}CO$ radical and is expanded 5 times.

In order to establish the nature of the metal-containing product, experiments were carried out using ^{13}CO-enriched $(\eta^5\text{-}C_5H_5)W(CO)_3H$ in a mixed $^{13}CO/^{12}CO$ (25:75) matrix which employed the same photolysis sources used previously for $(\eta^5\text{-}C_5H_5)W(CO)_3H$ in pure ^{12}CO. Irradiation of the matrix with u.v. light (λ = 230 - 390 nm) produced a number of bands which were seen in the terminal CO stretching region for $(\eta^5\text{-}C_5H_5)W(CO)_3H$ in ^{12}CO together with a new band at very much lower wavenumbers, (1817.0 cm^{-1}) (Table 3.2). Irradiation of $(\eta^5\text{-}C_5H_5)M(CO)_3H$ in ^{13}CO matrices gave all the bands due to $(\eta^5\text{-}C_5H_5)M(^{12}CO)_{3-n}(^{13}CO)_nH$ (n = 1 - 3) and for the ^{13}CO-enriched new photoproducts.

By analogy with the hydrides $HCo(CO)_4$ [22] and $HM(CO)_5$ (M = Mn, Re) [21] which give the radicals $HCO^{\cdot}$ and $Co(CO)_4^{\cdot}$ and $HCO^{\cdot}$ and $M(CO)_5^{\cdot}$ on photolysis at 4 - 20K, it might be expected that $(\eta^5\text{-}C_5H_5)Mo(CO)_3H$ would give $HCO^{\cdot}$ and $(\eta^5\text{-}C_5H_5)Mo(CO)_3^{\cdot}$. Indeed the band at 1859.1 cm^{-1}, which shows the appropriate ^{13}CO shift in ^{13}CO doped matrices, corresponding to the band position for $HCO^{\cdot}$ reported previously (1860 cm^{-1}) [21, 22]. The shift of this band to 1817.0 cm^{-1} is exactly what is predicted for the replacement of a ^{12}C by a ^{13}C atoms, i.e. $H^{13}CO$. The bands at 2008.9, 1915.5 and 1908.4 cm^{-1} may then be assigned to $(\eta^5\text{-}C_5H_5)Mo(CO)_3^{\cdot}$ with $\underline{C}_{3v}$ local symmetry for the $Mo(CO)_3$ fragment. This was confirmed by the studies of $(\eta^5\text{-}C_5H_5)M(CO)_3H$ (M = Mo, W) complexes and ^{13}CO-enriched complexes in mixed $^{12}CO/^{13}CO$ matrices (see above). The resulting band patterns were subjected to an energy-factored force-field fitting procedure and satisfactory agreement between observed and calculated bands for a $\underline{C}_{3v}$ symmetry $M(CO)_3$ fragment was observed (Table 3.2), i.e. $(\eta^5\text{-}C_5H_5)M(^{12}\overline{CO})_{3-n}(^{13}CO)_n^{\cdot}$ (n = 0 - 3) [35].

The remaining band at 1985.1 cm^{-1} corresponds exactly with the band position of $Mo(CO)_6$ isolated at high dilution in a CO matrix, i.e. extensive irradiation with u.v. light results in dissociation of the $\eta^5\text{-}C_5H_5$ ligand. A precedent for this is the conversion of $(\eta^5\text{-}C_5H_5)NiNO$ to $Ni(CO)_4$ by photolysis in a CO matrix at 20K [36].

Similar results were obtained with $(\eta^5\text{-}C_5H_5)W(CO)_3H$ isolated at high dilution in CO matrices. Interestingly neither the Mo nor W complexes gave any indication of the formation of $(\eta^5\text{-}C_5H_5)M(CO)_2H$ species as was found in CH_4 and Ar matrices. Spectroscopic data for the new species formed in CO matrices is given in Tables 3.1 and 3.2 .

3.2.3(b) Photolysis of $(\eta^5\text{-}C_5H_5)Cr(CO)_3H$ in CO Matrices at 12K

The i.r. spectrum of $(\eta^5\text{-}C_5H_5)Cr(CO)_3H$ isolated at high dilution in a CO matrix is shown in (Figure 3.6). Before photolysis the spectrum shows bands at 2016.7, 1943.6 and 1932.7 cm^{-1} (Figure 3.6(a)). Irradiation of the matrix with u.v. light (λ = 310 - 390 nm) produced new bands at 2050.5, 1976.3, 1904.2 and 1859.2 cm^{-1} (Figure 3.6(b)). Longer times of irradiation with the same energy light (λ = 310 - 390 nm), produced more new bands at 2023.2, 1986.3, 1910.4 and 1885.2 cm^{-1} (Figure 3.6(c)). Irradiation with visible light (λ > 430 nm), caused decreases in the intensities of all the new bands with the regeneration of the bands due to the starting material (Figure 3.6(d)). The bands at (1986.4 and 1910.4 cm^{-1}; bands (1)) are probably due to the terminal CO stretching bands of the radical species c.f. Mo and W and also $(\eta^5\text{-}C_5H_5)Cr(CO)_3^{\bullet}$. Since there is a band at 1859.2 cm^{-1} which may be assigned to the formyl radical $HC\dot{O}$ (see Section 3.2.3(a)). The bands at (2023.2 and 1902.3 cm^{-1}; bands (2)) may possibly be assigned to a species with reduced hapticity of C_5H_5 ring e.g. $(\eta^3\text{-}C_5H_5)Cr(CO)_4H$, while the band at 1976.2 cm^{-1} may be assigned to $Cr(CO)_6$ [37]. The band at 2040.5 cm^{-1} which was also observed during irradiation of $(\eta^5\text{-}C_5H_5)Cr(CO)_3H$ in Ar, CH_4 and N_2 matrices remains to be identified (Table 3.1).

3.2.4 Photolysis of $(\eta^5\text{-}C_5H_5)M(CO)_3H$ (M = Cr, Mo, W) in 5% C_2H_4 doped CH_4 Matrices at 12K

Infrared spectra from an experiment with $(\eta^5\text{-}C_5H_5)W(CO)_3H$ isolated at high dilution in a 5% C_2H_4 doped CH_4 matrix are shown in (Figure 3.7). Before photolysis the spectrum shows two broadened bands (2024.0 and 1932.5 cm^{-1}) (Figure 3.7(a)), whereas in pure Ar matrices sharper bands are observed together with a splitting of the lower wavenumber band (see Figure 3.1(a)). This band broadening is commonly experienced with 'mixed host' matrices and does not imply a lack of solute molecule isolation.

Irradiation with medium-energy u.v. radiation (λ = 290 - 370 nm) produced new terminal CO stretching i.r. bands at 1956.0 and 1874.5 cm^{-1} (Figure 3.7(b)). Longer irradiation times with the same radiation resulted in the appearance and growth of bands at 1986.2, 1974.0, 1945.3, 1927.8,

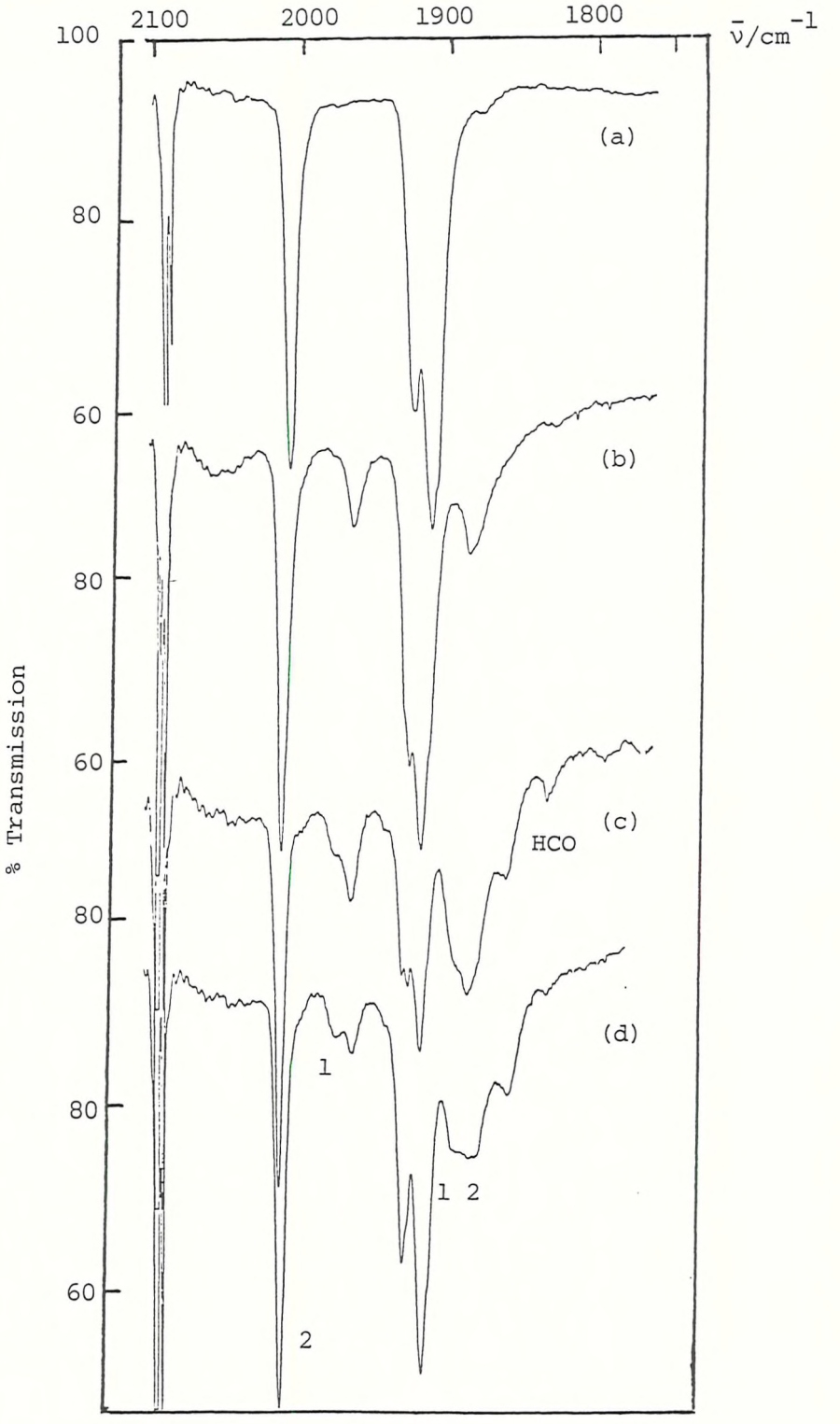

FIGURE 3.6 Infrared spectra from an experiment with $(\eta^5\text{-}C_5H_5)Cr(CO)_3H$ isolated in CO matrix at 12K: (a) after deposition, (b) after 5 min. photolysis using λ = 310 - 390 nm, (c) after further 13 min. photolysis using the same source, and (d) after 30 min. reversal using λ > 430 nm. Bands marked (1) and (2) derive from photoproducts (see text).

1897.5 and 1859.5 cm^{-1} (Figure 3.7(c)). Prolonged photolysis with the same energy radiation showed that the bands at 1956.0, 1945.3, 1874.7 and 1859.5 cm^{-1} increased more markedly than the other new bands while the bands of $(\eta^5\text{-}C_5H_5)W(CO)_3H$ continued to decrease. Irradiation with long wavelength radiation (λ > 430 nm) caused the bands at 1986.2, 1974.0, 1927.8 and 1897.5 cm^{-1} to increase dramatically while other bands decreased (Figure 3.7(d)). In these photolysis it was found that the lower band of $(\eta^5\text{-}C_5H_5)W(CO)_3H$ decreased more slowly than the upper band, indicating an overlapping growth of a new product band with the lower parent complex band.

Comparison of the band positions with those observed in photolysis of $(\eta^5\text{-}C_5H_5)W(CO)_3H$ in CH_4 matrices (see Section 3.2.1(a)), on photolysis of $(\eta^5\text{-}C_5H_5)W(CO)_3C_2H_5$ in CH_4 matrices (see Chapter 4), and deposition of an authentic sample of $(\eta^5\text{-}C_5H_5)W(CO)_2(C_2H_4)H$ in a CH_4 matrix (see Section 3.2.6), enabled a complete assignment to be made for all the new bands. The species observed were: $(\eta^5\text{-}C_5H_5)W(CO)_2H$ [1956.0 and 1874.5 cm^{-1}; bands (1)], $(\eta^5\text{-}C_5H_5)W(CO)_2(C_2H_5)$ [1945.3 and 1859.5 cm^{-1}; bands (2)], *cis*-$(\eta^5\text{-}C_5H_5)W(CO)_2(C_2H_4)H$ [1986.4 and 1927.8 cm^{-1}; bands (3)], and *trans*-$(\eta^5\text{-}C_5H_5)W(CO)_2(C_2H_4)H$ [1974.0 and 1897.5 cm^{-1}; bands (4)]. It is notable that the rate of formation of the *cis* and *trans* isomers of $(\eta^5\text{-}C_5H_5)W(CO)_2(C_2H_4)H$ depends on the rate of formation of the 16-electron species $(\eta^5\text{-}C_5H_5)W(CO)_2H$ and $(\eta^5\text{-}C_5H_5)W(CO)_2(C_2H_5)$ and these in turn are formed at a rate which is a function of the radiation used. This is illustrated in (Figures 3.7(e) and 3.7(f)), where photolysis with visible light (λ > 430 nm) causes the bands for $(\eta^5\text{-}C_5H_5)W(CO)_3H$ and for the ethylene complexes $(\eta^5\text{-}C_5H_5)W(CO)_2(C_2H_4)H$ to grow whereas irradiation with u.v. light results in the formation of the 16-electron species $(\eta^5\text{-}C_5H_5)W(CO)_2H$ and $(\eta^5\text{-}C_5H_5)W(CO)_2C_2H_5$.

Ultimately, prolonged photolysis produced a single new band at 1904.0 cm^{-1}, which was also observed on photolysis of $(\eta^5\text{-}C_5H_5)W(CO)_3C_2H_5$ and *trans*-$(\eta^5\text{-}C_5H_5)W(CO)_2(C_2H_4)H$. This band is tentatively assigned to the 16-electron $(\eta^5\text{-}C_5H_5)W(CO)(C_2H_4)H$ species.

Analogous results were obtained with $(\eta^5\text{-}C_5H_5)Mo(CO)_3H$ isolated at high dilution in 5% C_2H_4/CH_4 doped matrices with the exception that only the *trans* isomer was observed for Mo whereas both *cis*- and *trans*-$(\eta^5\text{-}C_5H_5)W(CO)_2(C_2H_4)H$ were

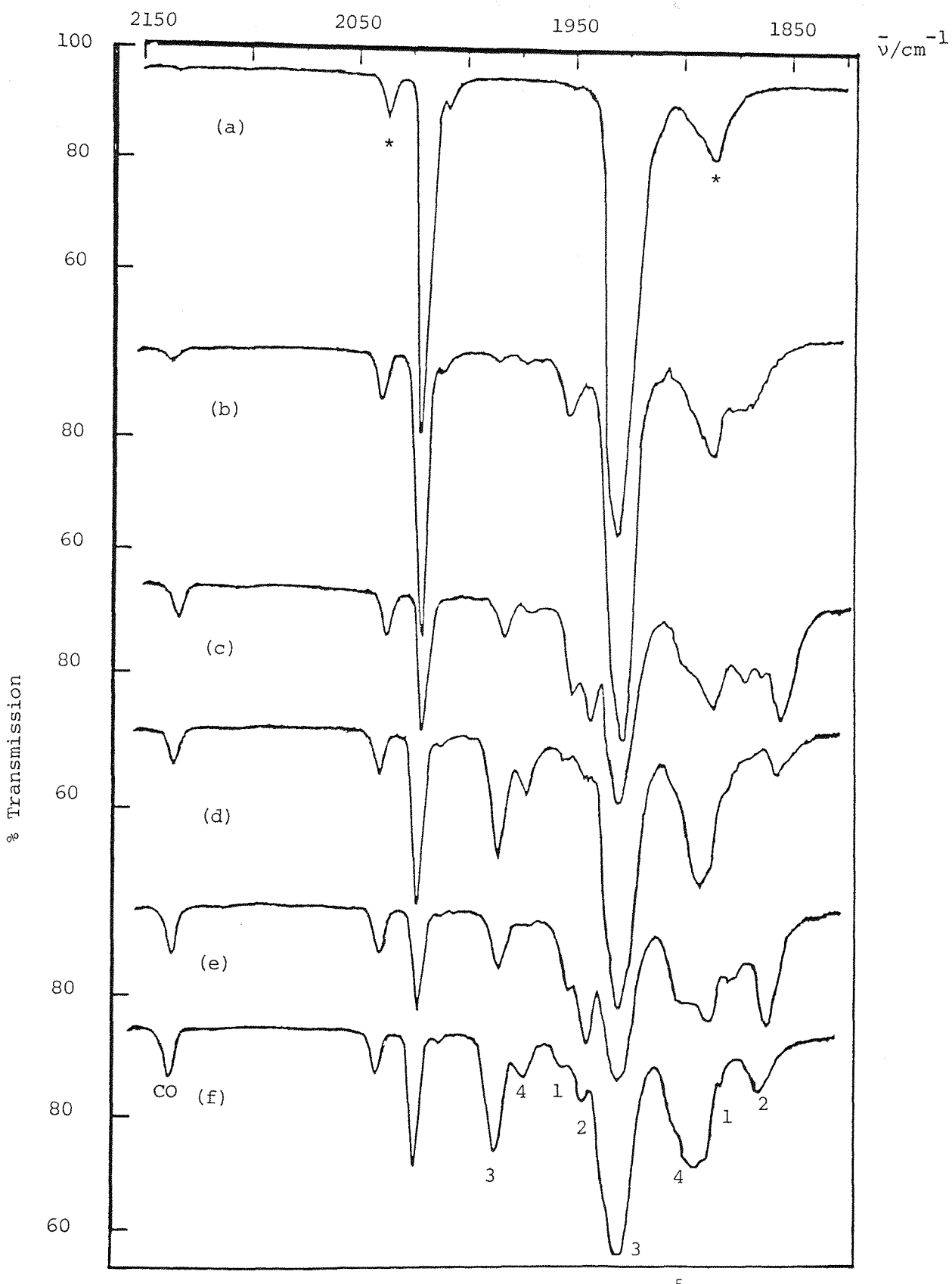

FIGURE 3.7 Infrared spectra from an experiment with $(\eta^5\text{-}C_5H_5)W(CO)_3H$ isolated at high dilution in a 5% C_2H_4/CH_4 doped matrix at 12K: (a) after deposition, (b) after 3 min. photolysis using $290 < \lambda < 370$ nm radiation, (c) after further 15 min. photolysis using the same source, (d) after 90 min. photolysis using $\lambda > 430$ nm radiation, (e) after 15 min. further photolysis using uv radiation ($290 < \lambda < 370$ nm), and (f) after further 30 min. photolysis using visible light ($\lambda > 430$ nm). Bands marked (*) are due to C_2H_4 in the matrix. Bands marked (1) to (4) derive from photoproducts (see text).

observed for W. Spectroscopic data for the new species is presented in (Table 3.1). It is important to note that all the intermediates in this photoreaction are also generated when the ethyl derivatives $(\eta^5\text{-}C_5H_5)W(CO)_3C_2H_5$ (M = Mo, W) are photolysed in CH_4 and CO matrices at 12K (see Chapter 4).

In contrast to the behaviour of the $(\eta^5\text{-}C_5H_5)M(CO)_3H$ (M = Mo, W) complexes, no reaction with ethylene was observed when the $(\eta^5\text{-}C_5H_5)Cr(CO)_3H$ was irradiated in 5% C_2H_4/CH_4 doped matrices under the same conditions.

3.2.5 Photolysis of $(\eta^5\text{-}C_5H_5)M(CO)_3H$ (M = Mo, W) in 3% C_2H_2 doped CH_4 Matrices at 12K

Infrared spectra from an experiment with $(\eta^5\text{-}C_5H_5)Mo(CO)_3H$ isolated in a 3% C_2H_2 doped CH_4 matrix at 12K are shown in (Figure 3.8). Before photolysis the spectrum (Figure 3.8(a)) shows two strong bands at 2027.7 and (1945.5, 1932.6)cm^{-1} (Table 3.1). Irradiation of the matrix with u.v. light (λ = 290 - 390 nm) produced two new bands at 1956.0 and 1880.8 cm^{-1} in addition to the band of free CO at 2138.0 cm^{-1} (Figure 3.8(b)). Further irradiation with the same energy light caused the appearance of further new bands at 2000.5, 1981.5 and 1906.3 cm^{-1} (Figure 3.8(c)). Prolonged photolysis showed that the pairs of bands at 1956.0 and 1880.8 cm^{-1} increased more rapidly than the other bands with the bands of $(\eta^5\text{-}C_5H_5)Mo(CO)_3H$ decreasing. Subsequent irradiation with low energy light (λ > 430 nm), caused the pair of bands at 1956.0 and 1880.8 cm^{-1} to decrease markedly and regenerated the bands due to the starting material with little or no change in the bands at 2000.5, 1981.5 and 1906.3 cm^{-1} (Figure 3.8(d)). Comparison of the band positions with those observed on photolysis of $(\eta^5\text{-}C_5H_5)Mo(CO)_3H$ in CH_4, CO and 5% C_2H_4/CH_4 matrices (see Table 3.1), enabled a complete assignment to be made for all the new bands. The species observed were: $(\eta^5\text{-}C_5H_5)Mo(CO)_2H$ [1956.0 and 1880.8 cm^{-1}; bands (1)], $(\eta^5\text{-}C_5H_5)Mo(CO)_3^{\cdot}$ [2000.5 and 1906.3 cm^{-1}; bands (2)], and *cis*-$(\eta^5\text{-}C_5H_5)Mo(CO)_2(C_2H_2)H$ [1981.5 cm^{-1} and the lower band is obscured under the lower band of the parent molecule; bands (3)].

Analogous results were obtained for $(\eta^5\text{-}C_5H_5)W(CO)_3H$ complex isolated at high dilution in 3% C_2H_2 doped CH_4 matrices. Spectroscopic data for the new species is given in (Table 3.1).

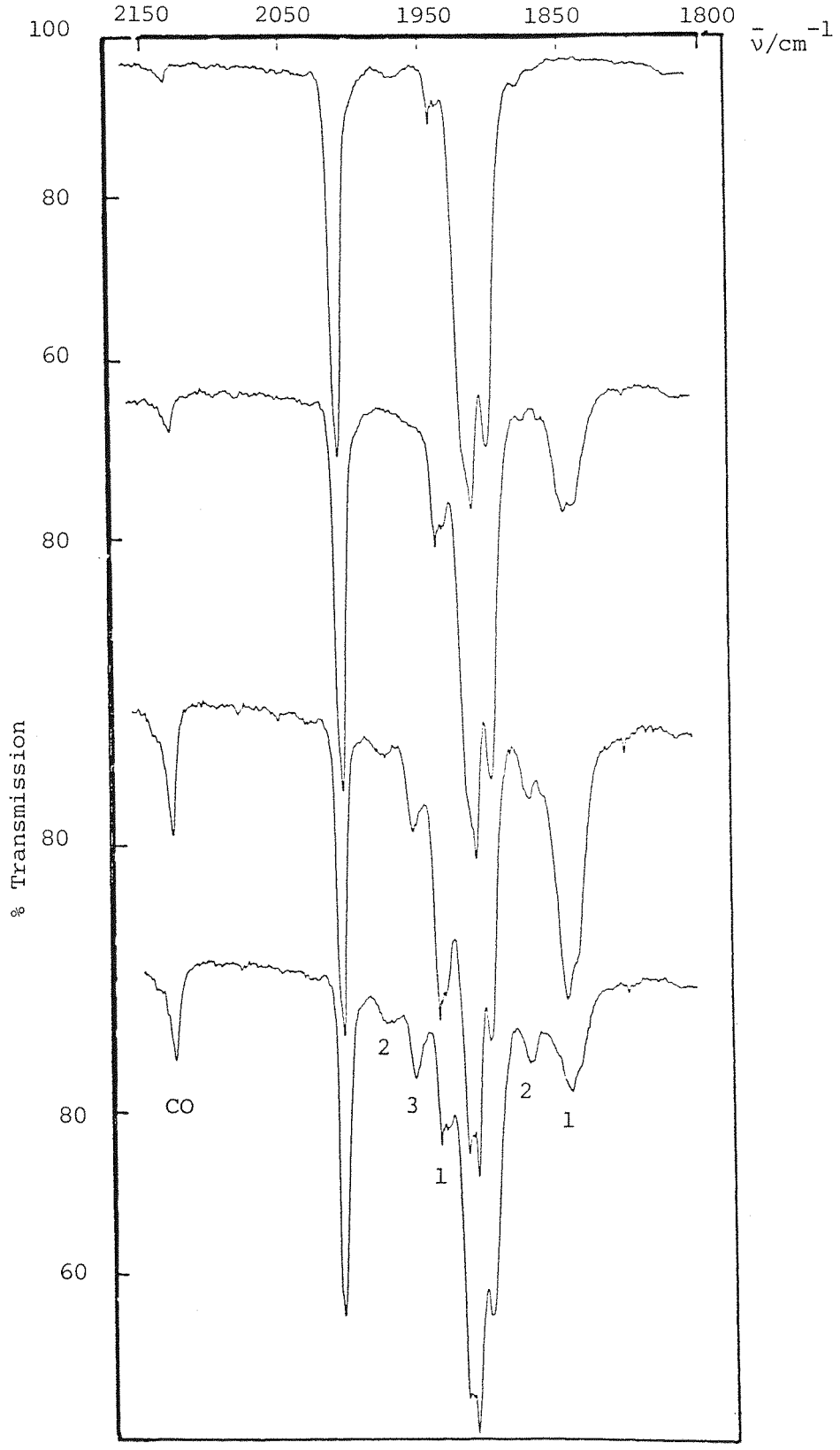

FIGURE 3.8 Infrared spectra from an experiment with $(\eta^5\text{-}C_5H_5)Mo(CO)_3H$ isolated in a 3% C_2H_2 doped CH_4 matrix at 12K: (a) after deposition, (b) after 15 min. photolysis using $290 < \lambda < 390$ nm, (c) after further 120 min. photolysis using the same source, and (d) after 45 min. reversal using $\lambda > 430$ nm. Bands marked (*) are due to C_2H_2 gas in the matrix. Bands marked (1) - (3) derive from photoproducts (see text).

3.2.6 Photolysis of *trans*-(η^5-C_5H_5)W(CO)$_2$(C_2H_4)H in CH_4 and CO Matrices at 12K

The i.r. spectrum produced on co-condensing (η^5-C_5H_5)W(CO)$_2$(C_2H_4)H with an excess of CH_4 at 12K shows two bands at 1974.3 and 1897.3 cm^{-1} in addition to bands arising from (η^5-C_5H_5)W(CO)$_3$H (†) and (η^5-C_5H_5)W(CO)$_3$$C_2H_5$ (*) present as impurities or disproportionation decomposition products (Figure 3.9(a)). The bands at 1974.3 and 1897.3 cm^{-1} correspond well with the i.r. bands in solution where a *trans* structure has been deduced on the basis of i.r. and n.m.r. spectroscopy [38]. Tracing and weighing the terminal CO stretching bands, from spectra recorded in absorbance mode, gave a OC-W-CO band angle of 112° [30], which also indicates a *trans* stereochemistry.

Photolysis with medium energy radiation (λ = 290 - 370 nm) resulted in the formation of new bands at 1987.6, 1947.8, 1928.5 and 1861.1 cm^{-1} (Figure 3.9(b)). Irradiation with visible light (λ > 430 nm) caused the bands at 1947.8 and 1861.1 cm^{-1} to decrease while the other two bands at 1987.6 and 1928.5 cm^{-1} increased (Figure 3.9(c)). Longer time irradiation with medium energy (λ = 310 - 370 nm) produced a significant increase in the bands at 1947.8 and 1861.1 cm^{-1} at the expense of the parent molecule bands (Figure 3.9(d)). Irradiation with visible light (λ > 430 nm) confirmed that the two sets of bands at (i) 1947.8 and 1861.1 and (ii) 1987.6 and 1928.5 cm^{-1} are due to two different species (Figure 3.9(e)) which are linked together in a reversible process (i) $\rightleftarrows$ (ii). Longer photolysis with higher energy radiation (λ = 290 - 370 nm) produced an intense single new band at 1904.0 cm^{-1} together with a band due to free CO at 2138 cm^{-1}.

By comparison with the species produced on photolysis of (η^5-C_5H_5)W(CO)$_3$$C_2H_5$ [5] the bands at 1947.8 and 1861.1 cm^{-1} (bands (1) may be assigned to (η^5-C_5H_5)W(CO)$_2$$C_2H_5$ and those at 1987.6 and 1928.5 cm^{-1} (bands (2)) may be assigned to *cis*-(η^5-C_5H_5)W(CO)$_2$(C_2H_4)H. Two possibilities exist for the band at 1904.1 cm^{-1} (band (3)). The 14-electron species (η^5-C_5H_5)W(CO)C_2H_5 or 16-electron species (η^5-C_5H_5)W(CO)(C_2H_4)H. The former contains an ethyl group which might be expected to undergo β-elimination to relieve the electronic unsaturation. Therefore, the band at 1904.1 cm^{-1} is assigned to the 16-electron monocarbonyl species (η^5-C_5H_5)W(CO)(C_2H_4)H.

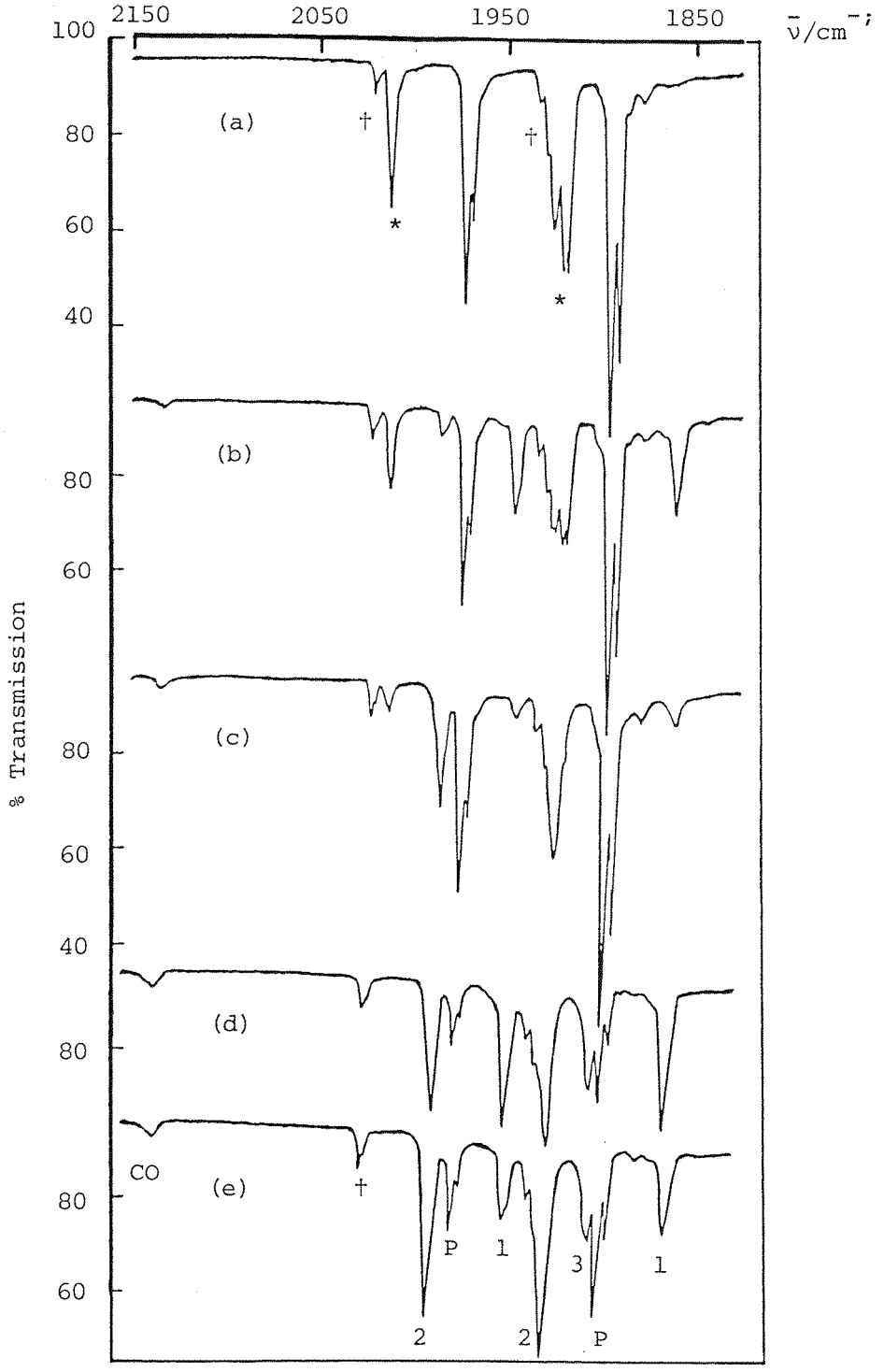

FIGURE 3.9 Infrared spectra from an experiment with *trans*-$(\eta^5\text{-}C_5H_5)W(CO)_2(C_2H_4)H$ isolated at high dilution in a CH_4 matrix at 12K: (a) after deposition, (b) after 10 min. photolysis using $290 < \lambda < 370$ nm radiation, (c) after 90 min. photolysis using visible light ($\lambda > 430$ nm), (d) after further 60 min. photolysis using $290 < \lambda < 370$ nm radiation, and (e) after further 30 min. photolysis using visible light ($\lambda > 430$ nm). Bands marked (*) are due to $(\eta^5\text{-}C_5H_5)W(CO)_3(C_2H_5)$ and those marked (†) are due to $(\eta^5\text{-}C_5H_5)W(CO)_3H$ present as decomposition impurities. Bands marked (1) to (3) derive from photoproducts (see text).

In CO matrices analogous products were observed with the difference that on extended photolysis the final product was $(\eta^5\text{-}C_5H_5)W(CO)_3H$ and no band was seen for $(\eta^5\text{-}C_5H_5)W(CO)(C_2H_4)H$.

3.3 DISCUSSION AND COMPARISON OF SOLUTION AND MATRIX PHOTOCHEMISTRY

The carbonyl-hydrido complexes $(\eta^5\text{-}C_5H_5)M(CO)_3H$ (M = Cr, Mo, W) and $(\eta^5\text{-}C_5H_5)W(CO)_2(C_2H_4)H$ represent an interesting series of complexes for photochemical studies because not only the carbonyl ligands but also the hydride ligands can be considered to be photolabile. The photoreactions of $(\eta^5\text{-}C_5H_5)M(CO)_3H$ (M = Cr, Mo, W) in frozen gas matrices (Ar, CH_4, N_2 and CO) are summarised in Scheme 3.1.

The primary process in the photolysis reaction of $(\eta^5\text{-}C_5H_5)M(CO)_3H$ complexes (M = Cr, Mo, W) in different gas matrices (Ar, CH_4, N_2) is the dissociative loss of one CO ligand and the formation of the unsaturated fragments $(\eta^5\text{-}C_5H_5)M(CO)_2H$ (M = Cr, Mo, W). These highly reactive species can be characterised by i.r. spectroscopy in CH_4 and Ar matrices. Rapid ^{13}CO exchange during the photolysis of $(\eta^5\text{-}C_5H_5)M(^{12}CO)_3H$ complexes (M = Cr, Mo, W) in matrices at 12K, leading to $(\eta^5\text{-}C_5H_5)M(^{12}CO)_{3-n}(^{13}CO)_nH$ (n = 1, 2 and ultimately 3), confirms that photo-induced dissociation and exchange of CO ligands is taking place during the irradiation in solution. However, in case of the chromium complex $(\eta^5\text{-}C_5H_5)Cr(CO)_3H$, the generation of the unsaturated 16-electron $(\eta^5\text{-}C_5H_5)Cr(CO)_2H$ species in CH_4 matrices was very moderate although two bands at 1974.5 and 1883.0 cm^{-1} were obtained during irradiation of $(\eta^5\text{-}C_5H_5)Cr(CO)_3H$ in CH_4 matrices. These bands are at comparatively high wavenumbers by analogy with $(\eta^5\text{-}C_5H_5)Mo(CO)_2H$ (1963.5 and 1885.2) cm^{-1} and $(\eta^5\text{-}C_5H_5)W(CO)_2H$ (1956.4 and 1872.0) cm^{-1} (Table 3.1). The irreversibility of the new bands corresponding to the reaction shown in Equation 3.1

$$(\eta^5\text{-}C_5H_5)Cr(CO)_3H \underset{h\nu'}{\overset{h\nu}{\rightleftharpoons}} (\eta^5\text{-}C_5H_5)Cr(CO)_2H + CO \qquad (3.1)$$

and the non reactivity of $(\eta^5\text{-}C_5H_5)Cr(CO)_3H$ with external ligands in matrices e.g. (L = N_2, C_2H_4), is probably due to hydrogen bridging between the

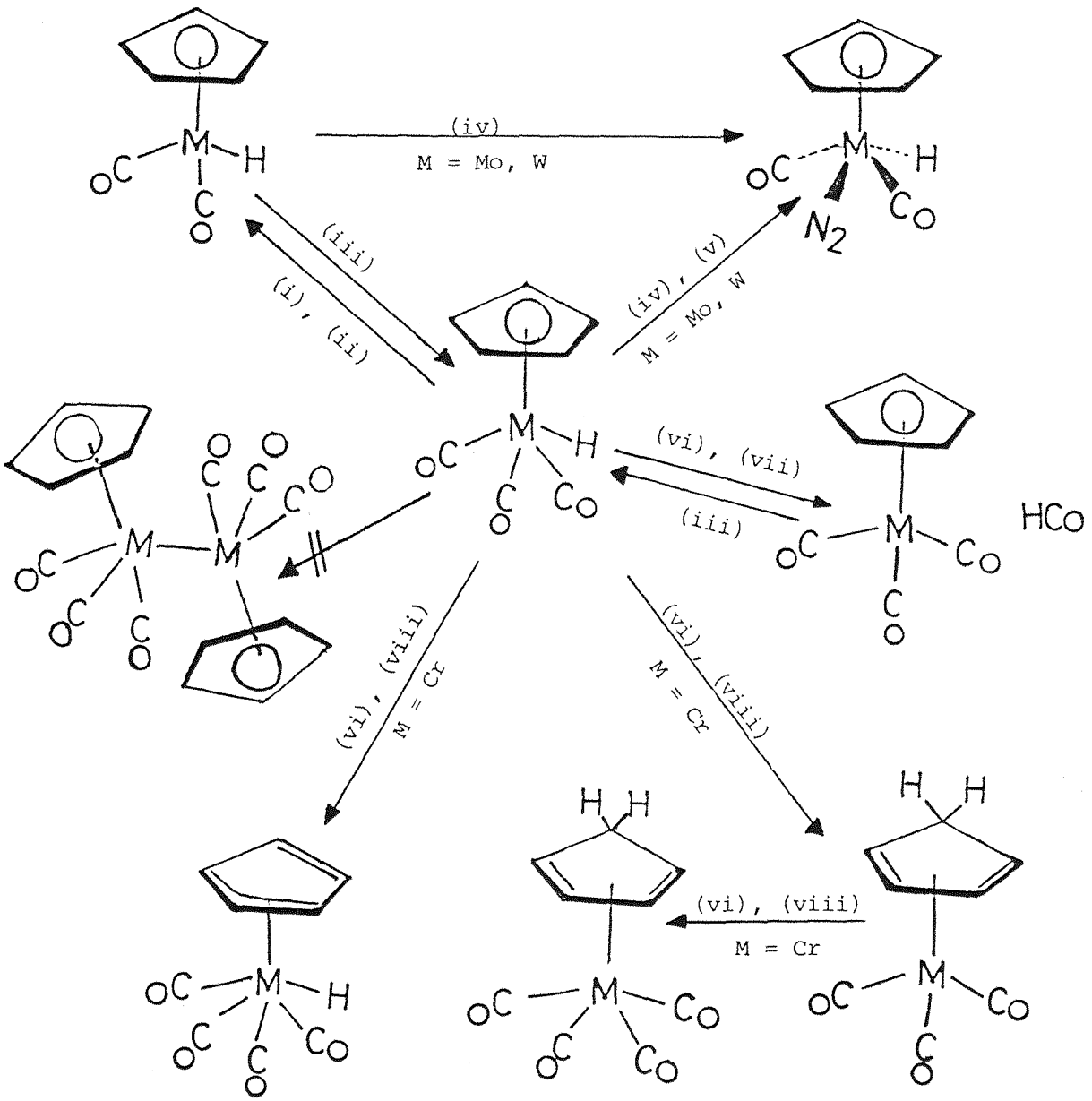

Scheme 3.1 (i) CH_4, Ar; (ii) hν (λ = 230 - 410 nm); (iii) hν (λ > 430 nm); (iv) N_2; (v) hν (λ = 290 - 370 nm); (vi) CO; (vii) hν (λ = 230 - 390 nm); (viii) hν (λ = 310 - 390 nm).

chromium metal and the ring species (I) in Equation 3.2.

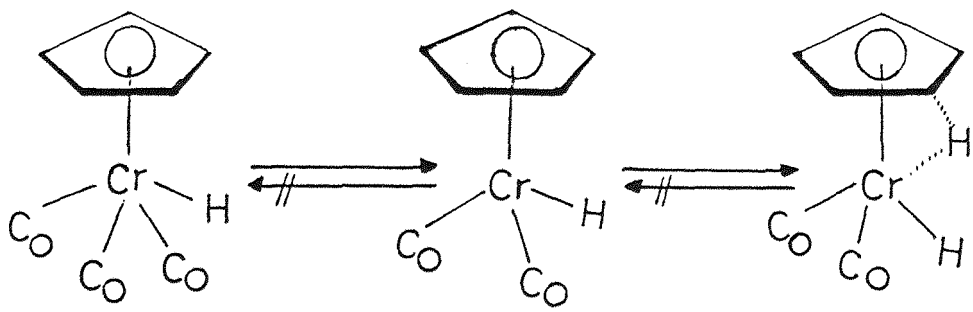

(I) (3.2)

One reason for proposing the species (I) is thermal instability of the 16-electron $(\eta^5\text{-}C_5H_5)Cr(CO)_2H$ intermediate even in low temperature matrices at 12K. It has been reported that for a series of hydride complexes in which the ligands are the same, the thermal stability generally increases with increasing atomic number of the metal. For example, $(\eta^5\text{-}C_5H_5)Cr(CO)_3H$ decomposes at 57° and $(\eta^5\text{-}C_5H_5)Mo(CO)_3H$ decomposes at 110° while $(\eta^5\text{-}C_5H_5)W(CO)_3H$ is stable up to 180° [39].

It is noteworthy that the 16-electron species $(\eta^5\text{-}C_5H_5)M(CO)_2H$ have been proposed in solution studies, especially the results from the photolysis of $(\eta^5\text{-}C_5H_5)W(CO)_3H$ [40], where dimerisation occurs to form $[(\eta^5\text{-}C_5H_5)M(CO)_2H]_2$ complexes (II). Subsequent photo-induced dehydrogenation could be responsible for the formation of $[(\eta^5\text{-}C_5H_5)M(CO)_2]_2$ complexes (III). The latter complexes are known to add carbon monoxide [41] in a dark reaction forming $[(\eta^5\text{-}C_5H_5)M(CO)_3]_2$ complexes (IV) (Scheme 3.2).

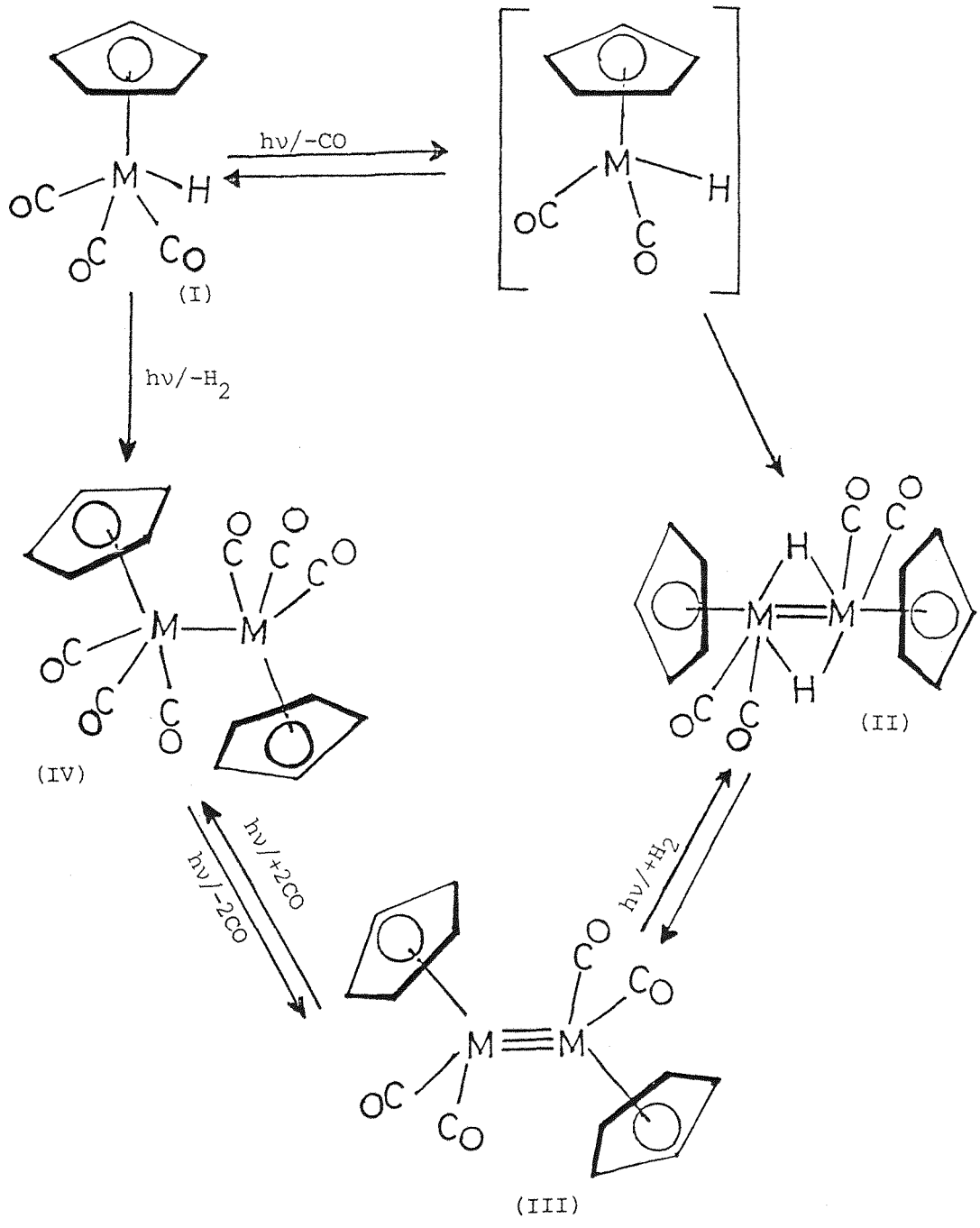

Scheme 3.2 M = Mo, W.

Similarly, Hoyano and Graham [25] demonstrated that when $(\eta^5\text{-}C_5Me_5)Os(CO)_2H$ was irradiated with a continuous H_2 purge of the solution, the new complexes (V and VI) were formed.

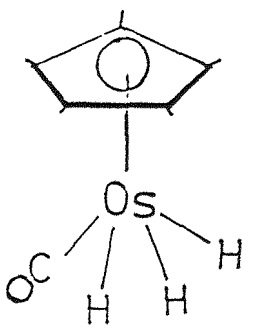

(V)

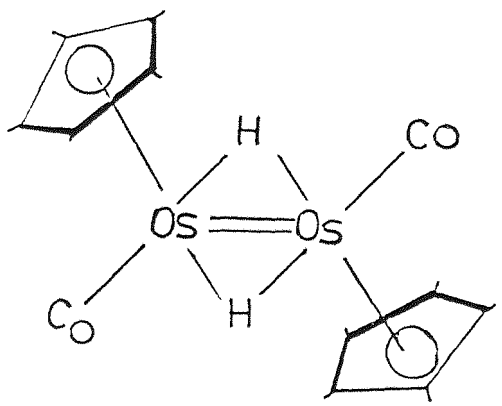

(VI)

The reaction shown in Equation 3.3 is effectively irreversible as CO is flushed from the system, while that in Equation 3.4 is expected to be reversible since H_2 elimination is a well recognized photochemical reaction of metal polyhydrides [23].

$$(\eta^5\text{-}C_5Me_5)Os(CO)_2H \longrightarrow (\eta^5\text{-}C_5Me_5)Os(CO)H + CO \qquad (3.3)$$

$$(\eta^5\text{-}C_5Me_5)Os(CO)H + H_2 \underset{\longleftarrow}{\xrightarrow{h\nu}} (\eta^5\text{-}C_5Me_5)Os(CO)H_3 \qquad (3.4)$$

A similar hydrogen-purged photolysis of $(\eta^5\text{-}C_5Me_5)Re(CO)_3$ gave the new pentamethyl analogue $(\eta^5\text{-}C_5Me_5)Re(CO)_2H_2$. The results summarized above demonstrate the synthetic utility of dihydrogen addition to 16-electron intermediates generated by loss of a carbonyl ligand through ultraviolet irradiation.

Irradiation of $(\eta^5\text{-}C_5H_5)M(CO)_3H$ (M = Mo, W) complexes in nitrogen matrices demonstrated the generation of the 16-electron species $(\eta^5\text{-}C_5H_5)M(CO)_2H$, which quickly reacted with N_2 to produce the $(\eta^5\text{-}C_5H_5)M(CO)_2(N_2)H$ complexes (Equations 3.5 and 3.6).

$$(\eta^5\text{-}C_5H_5)M(CO)_3H \underset{h\nu'/+CO}{\overset{h\nu/-CO}{\rightleftharpoons}} (\eta^5\text{-}C_5H_5)M(CO)_2H \qquad (3.5)$$

$$(\eta^5\text{-}C_5H_5)M(CO)_2H + N_2 \longrightarrow (\eta^5\text{-}C_5H_5)M(CO)_2(N_2)H \qquad (3.6)$$

The N ≡ N stretching band for $(\eta^5\text{-}C_5H_5)W(CO)_2(N_2)H$ (2163.5 cm^{-1}) occurs at very similar wavenumbers to those for $(\eta^5\text{-}C_5H_5)Mn(CO)_2(N_2)$ (2169.0 cm^{-1}) [32, 33], and $(\eta^6\text{-}C_6H_6)Cr(CO)_2(N_2)$ (2148 cm^{-1}) [42] which have been prepared by conventional techniques as well as in N_2 matrices. The comparability of $\nu_{N\equiv N}$ suggests a similar metal-dinitrogen bond strength, i.e. that $(\eta^5\text{-}C_5H_5)W(CO)_2(N_2)H$ might exist as a stable complex at ambient temperatures. Attempts to isolate $(\eta^5\text{-}C_5H_5)W(CO)_2(N_2)H$, by bubbling N_2 through n-pentane solutions of $(\eta^5\text{-}C_5H_5)W(CO)_3H$ and $(\eta^5\text{-}C_5H_5)W(CO)_2(C_2H_4)H$ while photolysing them, were unsuccessful [38]. A rapid decrease in intensity of the parent terminal CO stretching bands occurred but no new terminal CO stretching bands appeared. On the basis of $(\eta^5\text{-}C_5H_5)Mo(CO)_2(N_2)H$ (2192.0 cm^{-1}) the N ≡ N bond is stronger in this complex than in the W complex and, therefore, the metal-dinitrogen bond is predicted to be weaker [38]. An attempt [43] to prepare $(\eta^4\text{-}C_4H_4)Fe(CO)_2(N_2)$ (ν_{NN} at 2206.8 cm^{-1}), following successful matrix isolation experiments, led to the isolation of the novel iron dimer (VII).

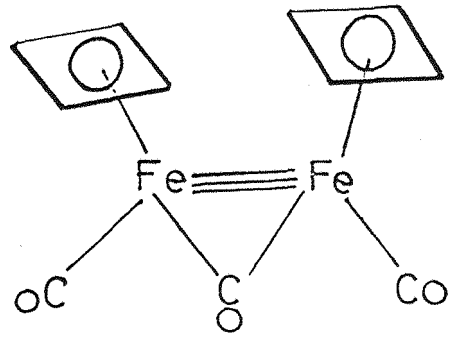

(VII)

An interesting feature of both Mo and W dinitrogen complexes is their *trans* stereochemistry deduced on the basis of OC-M-CO bond angles and energy-factored CO interaction force constants (see Section 3.2.2). The stereochemistry is analogous to *trans*-$(\eta^5\text{-}C_5H_5)Mo(CO)_2(C_2H_4)H$ in the case of Mo but not for W, where both *cis* and *trans* isomers are known in matrices at 12K; only $(\eta^5\text{-}C_5H_5)W(CO)_2(C_2H_4)H$ exists as a stable solid or in solutions at low temperatures. In case of the chromium complex, no evidence for $(\eta^5\text{-}C_5H_5)Cr(CO)_2(N_2)H$ was obtained when $(\eta^5\text{-}C_5H_5)Cr(CO)_3H$ was irradiated in N_2 matrices at 12K.

An alternative reaction path to CO ejection for metal carbonyl hydrides is M-H bond cleavage to give H atoms and radicals, e.g. $(\eta^5\text{-}C_5H_5)M(CO)_3^{\bullet}$ (M = Cr, Mo, W). Hoffman and Brown [26] have postulated that the facile thermal and photo-induced reactions of $(\eta^5\text{-}C_5H_5)W(CO)_3H$ with tri-n-butyl phosphine both proceed via radical intermediates. It was observed that photolysis (λ = 311 nm radiation) promoted substitution of $P(\underline{n}\text{-}C_4H_9)_3$ for CO (Equation 3.7).

$$(\eta^5\text{-}C_5H_5)W(CO)_3H + P(\underline{n}\text{-}C_4H_9)_3 \xrightarrow[-CO]{h\nu} (\eta^5\text{-}C_5H_5)W(CO)_2(P(\underline{n}\text{-}C_4H_9)_3)H \qquad (3.7)$$

The quantum yield for the overall substitution reaction varied from 6 to 30 suggesting a radical chain mechanism (Equation 3.8). Support for the initial W-H bond homolysis, which was thought to have a low quantum yield, came from a trapping experiment with $(C_6H_5)_3CCl$ (Equation 3.9),

$$(\eta^5\text{-}C_5H_5)W(CO)_3H \xrightarrow{h\nu} (\eta^5\text{-}C_5H_5)W(CO)_3 + H \qquad (3.8)$$

$$(\eta^5\text{-}C_5H_5)W(CO)_3H + (C_6H_5)_3CCl \xrightarrow{h\nu} (\eta^5\text{-}C_5H_5)W(CO)_3Cl + (C_6H_5)_3C\dot{} \qquad (3.9)$$

which gave complete conversion to $(\eta^5\text{-}C_5H_5)W(CO)_3Cl$, i.e. photoprocesses of metal carbonyl hydrides are not necessarily dominated by CO ejection. Some further evidence for this path could be derived from the observation that the final product when $(\eta^5\text{-}C_5H_5)Mo(CO)_3H$ is photolysed alone in n-pentane is the dimer $[(\eta^5\text{-}C_5H_5)Mo(CO)_3]_2$.

Irradiation of $(\eta^5\text{-}C_5H_5)M(CO)_3H$ (M = Cr, Mo, W) in CO matrices produced different photoproducts from those observed in Ar, N_2 and CH_4 matrices at 12K [38]. No evidence for radicals was found in CH_4 and N_2 matrices, but in CO matrices a band clearly assignable to the formyl radical ($H\dot{C}O$, 1860 cm^{-1}) [44] was observed together with terminal CO stretching bands which we assign to the radicals $(\eta^5\text{-}C_5H_5)M(CO)_3^{\cdot}$ (M = Cr, Mo, W). These observations are analogous to the detection of the radicals $M(CO)_5^{\cdot}$ (M = Mn, Re) on photolysis of $HMn(CO)_5$ [21] complexes (M = Mn, Re) and $Co(CO)_4^{\cdot}$ on photolysis of $HCo(CO)_4$ [22] and $(\eta^5\text{-}C_5H_5)_2Re$ on photolysis of $(\eta^5\text{-}C_5H_5)_2ReH$ [16] in CO matrices at 4 - 20K. Using e.s.r. spectroscopy the bond homolysis step was observed for $HCo(CO)_4$ in Ar matrices; such a step was not detectable using infrared spectroscopy because of the lower sensitivity of i.r. spectroscopy. It is interesting, therefore that irradiation of $(\eta^5\text{-}C_5H_5)M(CO)_3H$ complexes (M = Mo, W) in Ar matrices, produced the unsaturated 16-electron species $(\eta^5\text{-}C_5H_5)M(CO)_2H$, and the 17-electron radical species $(\eta^5\text{-}C_5H_5)M(CO)_3^{\cdot}$, where as in CO matrices M-H bond homolysis predominates (Equations 3.10 - 3.12).

$$(\eta^5\text{-}C_5H_5)M(CO)_3H \xrightarrow[\text{major}]{h\nu/Ar} (\eta^5\text{-}C_5H_5)M(CO)_2H + CO \quad (3.10)$$

$$(\eta^5\text{-}C_5H_5)M(CO)_3H \xrightarrow[\text{minor}]{h\nu/Ar} (\eta^5\text{-}C_5H_5)M(CO)_3^{\cdot} + H \quad (3.11)$$

$$(\eta^5\text{-}C_5H_5)M(CO)_3H \xrightarrow{h\nu/CO} (\eta^5\text{-}C_5H_5)M(CO)_3^{\cdot} + \dot{HCO} \quad (3.12)$$

Although no $(\eta^5\text{-}C_5H_5)M(CO)_2H$ species are detected in CO matrices, their presence can be inferred from the fact that when $(\eta^5\text{-}C_5H_5)M(CO)_3H$ complexes are photolysed in ^{13}CO doped ^{12}CO and ^{13}CO doped Ar matrices then exchange to form $(\eta^5\text{-}C_5H_5)M(^{12}CO)_{3-n}(^{13}CO)_nH$ complexes occurs much faster than the formation of $(\eta^5\text{-}C_5H_5)M(CO)_3^{\cdot}$ radicals. A similar result was observed with $HMn(CO)_5$ in ^{13}CO doped matrices [21]. It is also interesting that the reaction shown in Equation 3.13 should be reversed by visible radiation.

$$(\eta^5\text{-}C_5H_5)M(CO)_3H \underset{h\nu'}{\overset{h\nu/+\ CO}{\rightleftharpoons}} (\eta^5\text{-}C_5H_5)M(CO)_3^{\cdot} + \dot{HCO} \quad (3.13)$$

Such radiation is known to photodissociate $\dot{HCO}$ to give $\dot{H}$ atoms [45] and these could diffuse through the matrix and recombine with the $(\eta^5\text{-}C_5H_5)M(CO)_3^{\cdot}$ radicals. It is not clear from the above experiments whether the first step to produce radicals consists of the photo-induced formation of the 16-electron species $(\eta^5\text{-}C_5H_5)M(CO)_2H$ (Equations 3.14 - 3.16)

$$(\eta^5\text{-}C_5H_5)M(CO)_3H \xrightarrow{h\nu} (\eta^5\text{-}C_5H_5)M(CO)_2H + CO \quad (3.14)$$

$$(\eta^5\text{-}C_5H_5)M(CO)_2H \xrightarrow{h\nu} (\eta^5\text{-}C_5H_5)M(CO)_2^{\cdot} \quad (3.15)$$

$$(\eta^5\text{-}C_5H_5)M(CO)_2^{\cdot} + CO \xrightarrow{h\nu} (\eta^5\text{-}C_5H_5)M(CO)_3^{\cdot} \qquad (3.16)$$

that could undergo subsequent photo-induced M-H bond homolysis followed by fast uptake of one CO and formation of the radicals $(\eta^5\text{-}C_5H_5)M(CO)_3^{\cdot}$ (M = Mo, W), or whether the M-H bond fission occurs directly in the starting material [15]. Both processes seem possible but certainly no evidence could be found for the presence of $(\eta^5\text{-}C_5H_5)M(CO)_2H$ species in CO matrices. Comparing the photochemical reactivity of the Mo and W complexes in CO matrices reveals that the generation of the $(\eta^5\text{-}C_5H_5)M(CO)_3^{\cdot}$ radical is faster for Mo than for W using the same light source and the same period of irradiation. This suggests that the W-H bond is the stronger and is consistent with the supposition [39, 46] that the W-H bond energy is larger than the Mo-H bond energy.

In the case of the chromium complex $(\eta^5\text{-}C_5H_5)Cr(CO)_3H$, the generation of the radical $(\eta^5\text{-}C_5H_5)Cr(CO)_3^{\cdot}$ was to be expected, since the hydride complex $(\eta^5\text{-}C_5H_5)Cr(CO)_3H$, is a very active catalyst in the hydrogenation of conjugated dienes [47, 48]. Miyake and Kondo found that the hydrido chromium compound $(\eta^5\text{-}C_5H_5)Cr(CO)_3H$ reacted quantitatively with isoprene according to Equation 3.17.

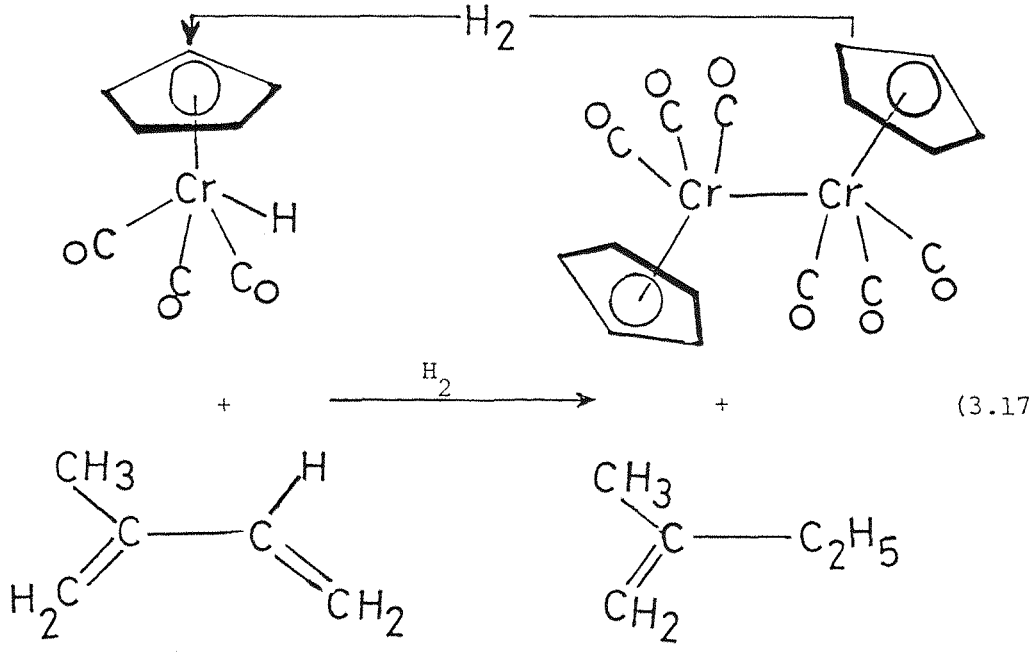

(3.17)

The dimer $[(\eta^5\text{-}C_5H_5)Cr(CO)_3]_2$ can be reconverted to the hydrido chromium compound by interaction with hydrogen (Equation 3.18),

$$(\eta^5\text{-}C_5H_5)Cr(CO)_3H \underset{+\ H_2}{\overset{-H_2}{\rightleftharpoons}} [(\eta^5\text{-}C_5H_5)Cr(CO)_3]_2 \qquad (3.18)$$

and, therefore, a catalytic cycle can be set up for the hydrogenation of dienes using either $(\eta^5\text{-}C_5H_5)Cr(CO)_3H$ or $[(\eta^5\text{-}C_5H_5)Cr(CO)_3]_2$ in the presence of hydrogen. This reaction does not occur with the molybdenum and tungsten dimers, and a catalytic cycle cannot be established. Various conjugated linear and cycle dienes, trienes, and tetraenes have, however, been hydrogenated with $[(\eta^5\text{-}C_5H_5)M(CO)_3]_2$ dimers as catalysts and of the Cr, Mo and W triad the chomium compound is reported to be the most active [47, 48]. Such behaviour suggests that the Cr-H bond is the weaker.

Another alternative pathway involving the hydride ligand could be migration to the $\eta^5\text{-}C_5H_5$ ring to produce the 16-electron species $(\eta^4\text{-}C_5H_6)M(CO)_3$ which could add a CO ligand from the matrix to give $(\eta^4\text{-}C_5H_6)M(CO)_4$ complexes. A precedent for hydride migration from a metal to a ring is the observation that photolysis of $(\eta^5\text{-}C_5H_5)_2ReH$ in a CO matrix at 12K and in solution leads to the formation of $(\eta^5\text{-}C_5H_5)(\eta^2\text{-}C_5H_6)Re(CO)_2$ [16, 49]. This complex is formed in a CO matrix via $(\eta^5\text{-}C_5H_5)(\eta^3\text{-}C_5H_5)Re(CO)H$ and $(\eta^5\text{-}C_5H_5)(\eta^1\text{-}C_5H_5)Re(CO)_2H$ (Scheme 3.3). In addition to the generation of the radical $(\eta^5\text{-}C_5H_5)Cr(CO)_3^{\cdot}$ species, irradiation of $(\eta^5\text{-}C_5H_5)Cr(CO)_3H$ in CO matrices produced bands at higher energy than the bands of the parent molecule (Table 3.1) and a band at 1976.2 due to $Cr(CO)_6$ [37]. Three possible photochemical reactions could be taking place for $(\eta^5\text{-}C_5H_5)Cr(CO)_3H$ in CO matrices: (a) H loss and this is confirmed by the presence of $HC\dot{O}$ radical, (b) ring slippage $\eta^5\text{-}C_5H_5 \longrightarrow \eta^3\text{-}C_5H_5$ and CO gain, and (c) metal to ring hydrogen migration and CO gain (Equations 3.19(a) - 3.19(c)). The first pathway takes place in CO and Ar matrices. Experiments in low temperature matrices do not always distinguish whether the increased coordination number occurs from step (b) or (c) of Equation 3.19, so this part of the mechanism remains unconfirmed. Such $(\eta^5\text{-}C_5H_5)$ to $(\eta^3\text{-}C_5H_5)$ de-coordination has been observed previously both in solution [16, 50] and in matrices [31]. Metal $\overset{\rightarrow}{\leftarrow}$ ring hydrogen migration was also reported for $(\eta^5\text{-}C_5H_5)(\eta^2\text{-}C_5H_6)Re(CO)_2$ [16, 49] in solution and low

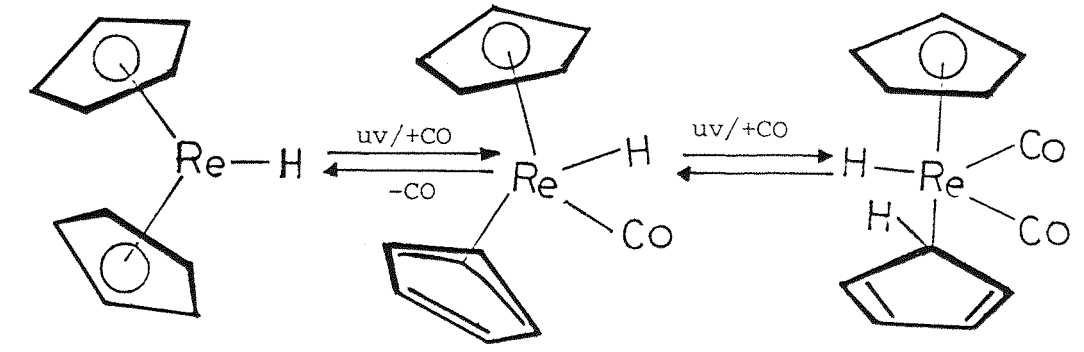

$(\eta^5\text{-}C_5H_5)_2ReH$ $(\eta^5\text{-}C_5H_5)(\eta^3\text{-}C_5H_5)Re(CO)H$ $(\eta^5\text{-}C_5H_5)(\eta^1\text{-}C_5H_5)Re(CO)_2$

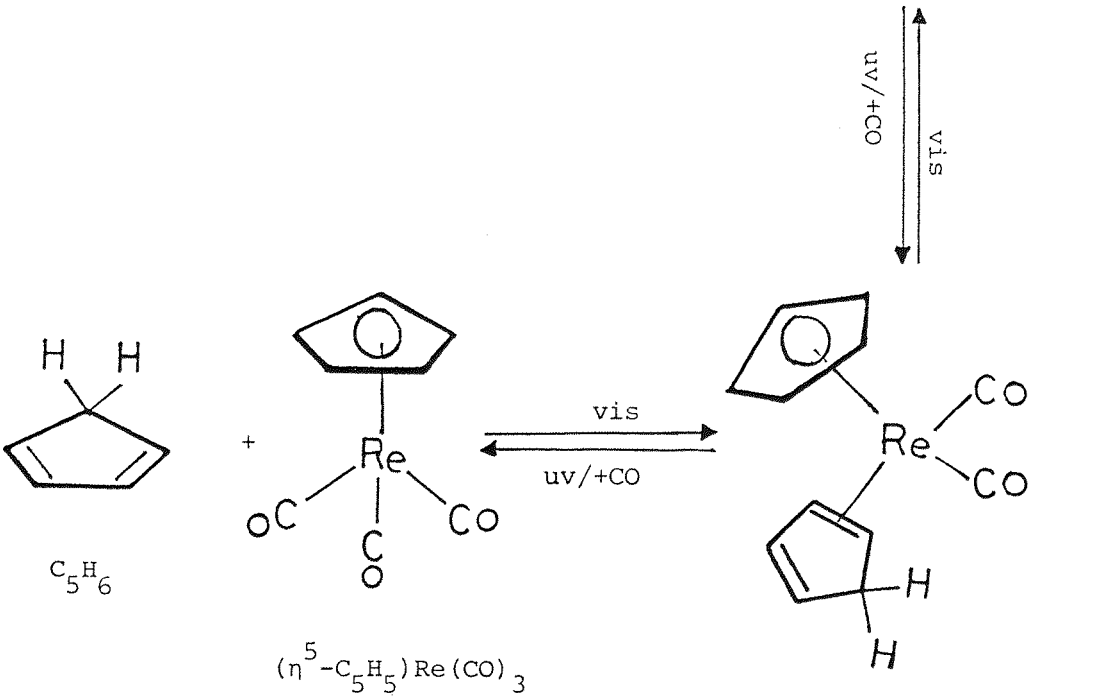

C_5H_6 $(\eta^5\text{-}C_5H_5)Re(CO)_3$ $(\eta^5\text{-}C_5H_5)(\eta^2\text{-}C_5H_6)Re(CO)_2$

Scheme 3.3

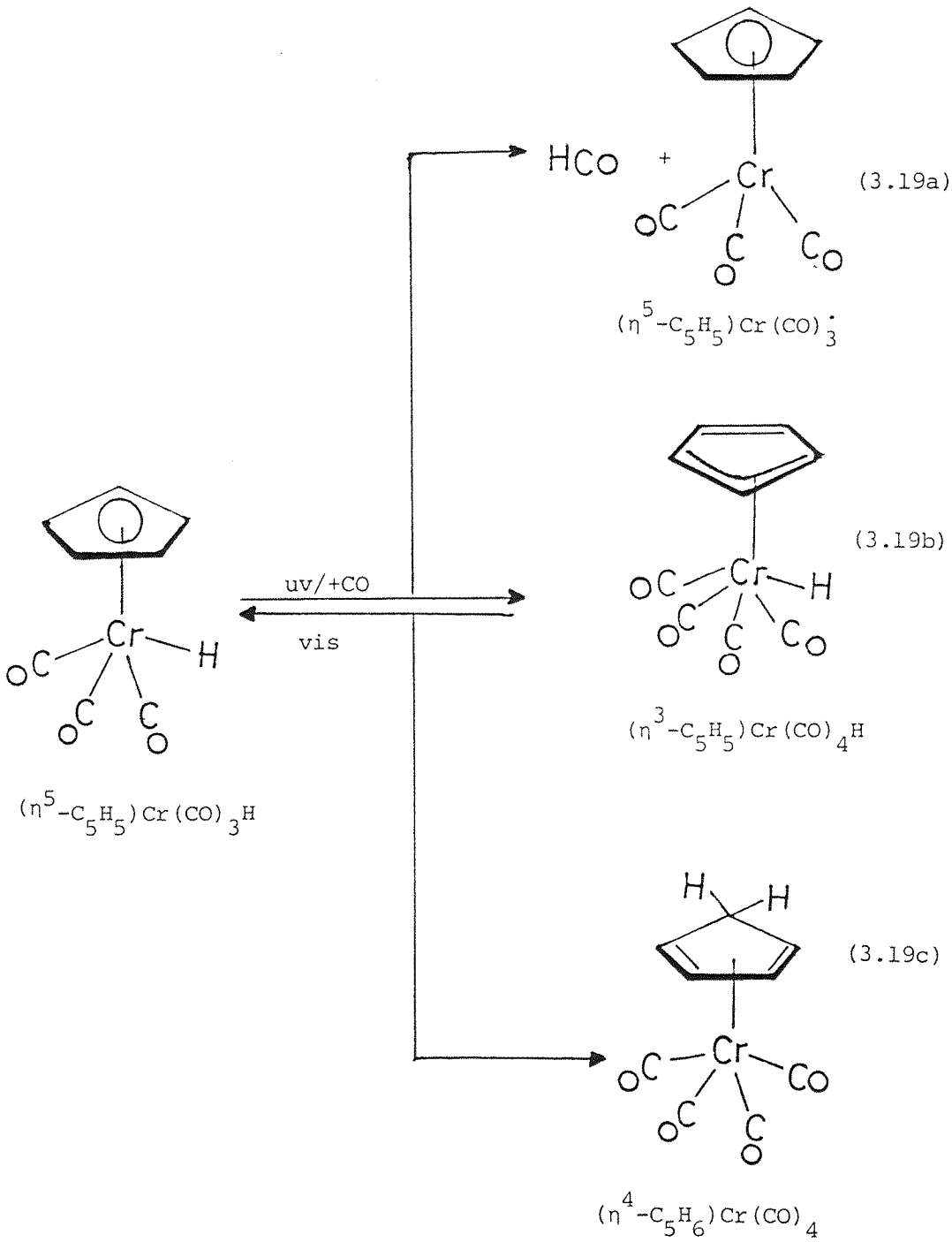
HCo
+
Cr
OC
C
O
Co
(3.19a)
$(\eta^5\text{-}C_5H_5)Cr(CO)_3^{\cdot}$
uv/+CO
vis
H
(3.19b)
$(\eta^3\text{-}C_5H_5)Cr(CO)_4H$
$(\eta^5\text{-}C_5H_5)Cr(CO)_3H$
(3.19c)
$(\eta^4\text{-}C_5H_6)Cr(CO)_4$

temperature matrices. Both steps (b) and (c) of Equation (3.19) lead ultimately to the generation of chromium hexacarbonyl $Cr(CO)_6$ as a result of ring decoordination. If $(\eta^3\text{-}C_5H_5)M(CO)_4H$ or $(\eta^4\text{-}C_5H_6)M(CO)_4$ complexes had been formed from $(\eta^5\text{-}C_5H_5)M(CO)_3H$ complexes (M = Mo, W) in CO matrices, bands would have been expected to appear at higher wavenumbers than those of $(\eta^5\text{-}C_5H_5)M(CO)_3H$. This is by analogy with the formation of $(\eta^3\text{-}C_5H_5)Fe(CO)_3CH_3$ [50] and $(\eta^3\text{-}C_5H_5)Co(CO)_3$ [31] from $(\eta^5\text{-}C_5H_5)Fe(CO)_2CH_3$ and $(\eta^5\text{-}C_5H_5)Co(CO)_2$ respectively in CO matrices at 12K and reflects the fact that increasing the number of CO ligands reduces the back-bonding for each CO ligand and this in turn strengthens the C-O bonds so that the bands are at higher wavenumbers. No such higher bands were observed but instead bands at lower wavenumbers assigned to the radicals $(\eta^5\text{-}C_5H_5)M(CO)_3^{\cdot}$ (M = Mo, W) were produced. That changes may occur in the ring-metal binding is evident from the observation of bands assigned to $M(CO)_6$ complexes (M = Mo, W), c.f. the conversion of $(\eta^5\text{-}C_5H_5)Ni(NO)$ to $Ni(CO)_4$ [36]. The conversion of $(\eta^5\text{-}C_5H_5)M(CO)_3H$ to $M(CO)_6$ is hardly likely to be a one step process but no intermediate stages could be seen.

The reactivity of the metal-hydrogen bond towards unsaturated organic molecules such as olefins, is central to many catalytic processes and can result in the formation of alkyl complexes (Equation 3.20).

$$M - H + \text{olefin} \longrightarrow M(\text{olefin})H \longrightarrow M - \text{alkyl} \qquad (3.20)$$

The reaction is reversible and is presumed to occur in two steps: (a) coordination of the unsaturated molecule to the metal (preceeded by ligand dissociation) and (b) transfer of the metal-hydrogen to the unsaturated molecule. The process is usually described either as an "addition" of the metal-hydrogen to the unsaturated molecule or as an "insertion" of the unsaturated molecule into the metal-hydrogen bond [51, 52]. The complexes $(\eta^5\text{-}C_5H_5)M(CO)_3H$ (M = Mo, W) undergo insertion of C_2F_4 affording the tetrafluoroethyl complex $(\eta^5\text{-}C_5H_5)M(CO)_3CF_2CF_2H$ [53] (Equation 3.21).

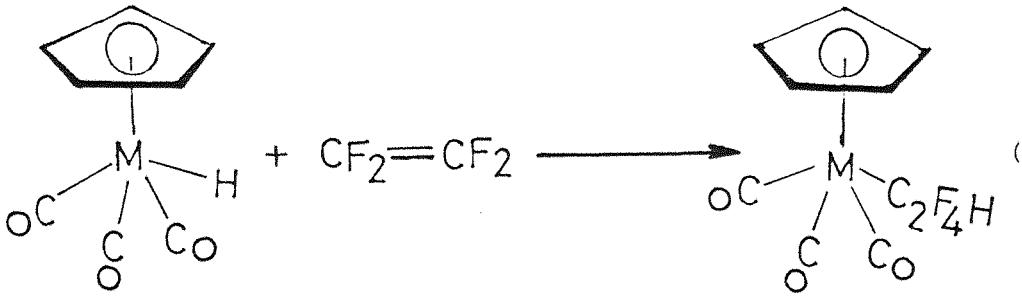

(3.21)

An illustration of the requirement for coordinative unsaturation in the reaction of a transition metal hydride with an olefin is provided by the reaction of the 18-electron complex $HCo(CO)_4$ with ethylene to give $C_2H_5Co(CO)_4$ [54] (Equation 3.22).

$$HCo(CO)_4 \underset{+CO}{\overset{-CO}{\rightleftharpoons}} HCo(CO)_3 \xrightarrow{+C_2H_4} HCo(CO)_3(CH_2 = CH_2)$$

$$\longrightarrow C_2H_5Co(CO)_3 \xrightarrow{+CO} C_2H_5Co(CO)_4 \longrightarrow \text{etc.} \qquad (3.22)$$

The photoreactions of $(\eta^5\text{-}C_5H_5)M(CO)_3H$ (M = Mo, W) in 5% C_2H_4 doped CH_4 matrices are summarised in (Scheme 3.4). The photolysis of $(\eta^5\text{-}C_5H_5)M(CO)_3H$ (M = Mo, W) in a 5% C_2H_4 doped CH_4 matrix leads to the formation of $(\eta^5\text{-}C_5H_5)M(CO)_2(C_2H_4)H$ complexes <u>via</u> $(\eta^5\text{-}C_5H_5)M(CO)_2H$ species. Interestingly even this route failed to produce any *cis* isomer for Mo whereas both *cis* and *trans* isomers were observed for W. It is noteworthy that reversible *cis* $\rightleftarrows$ *trans* isomerisation occurs for $(\eta^5\text{-}C_5H_5)W(CO)_2(C_2H_4)H$ in matrices at 12K (Scheme 3.4). At 77K Kazlauskas and Wrighton [12] were only able to observe the *trans* isomer of $(\eta^5\text{-}C_5H_5)W(CO)_2(C_2H_4)H$ by photolysis of $(\eta^5\text{-}C_5H_5)W(CO)_3C_2H_5$ whereas at 12K similar photolysis produced again *cis* and *trans* isomers (see Chapter 4). Photolysis of $(\eta^5\text{-}C_5H_5)Mo(CO)_3C_2H_5$ gave the *trans* isomer at 12 and 77K. Trimethyl-phosphine reacts instantly with *trans*-$(\eta^5\text{-}C_5H_5)W(CO)_2(C_2H_4)H$ in pentane solution forming a mixture of *cis* and *trans*-$(\eta^5\text{-}C_5H_5)W(CO)_2(PMe_3)H$ [55]. It is striking that only the olefin ligand is substituted by PMe_3 and not a carbonyl ligand. The photo-induced reaction of *trans*-$(\eta^5\text{-}C_5H_5)W(CO)_2(C_2H_4)H$ with the σ-donor thf gives only the corresponding *trans*-$(\eta^5\text{-}C_5H_5)W(CO)_2(thf)H$, indicating selective substitution of the olefin

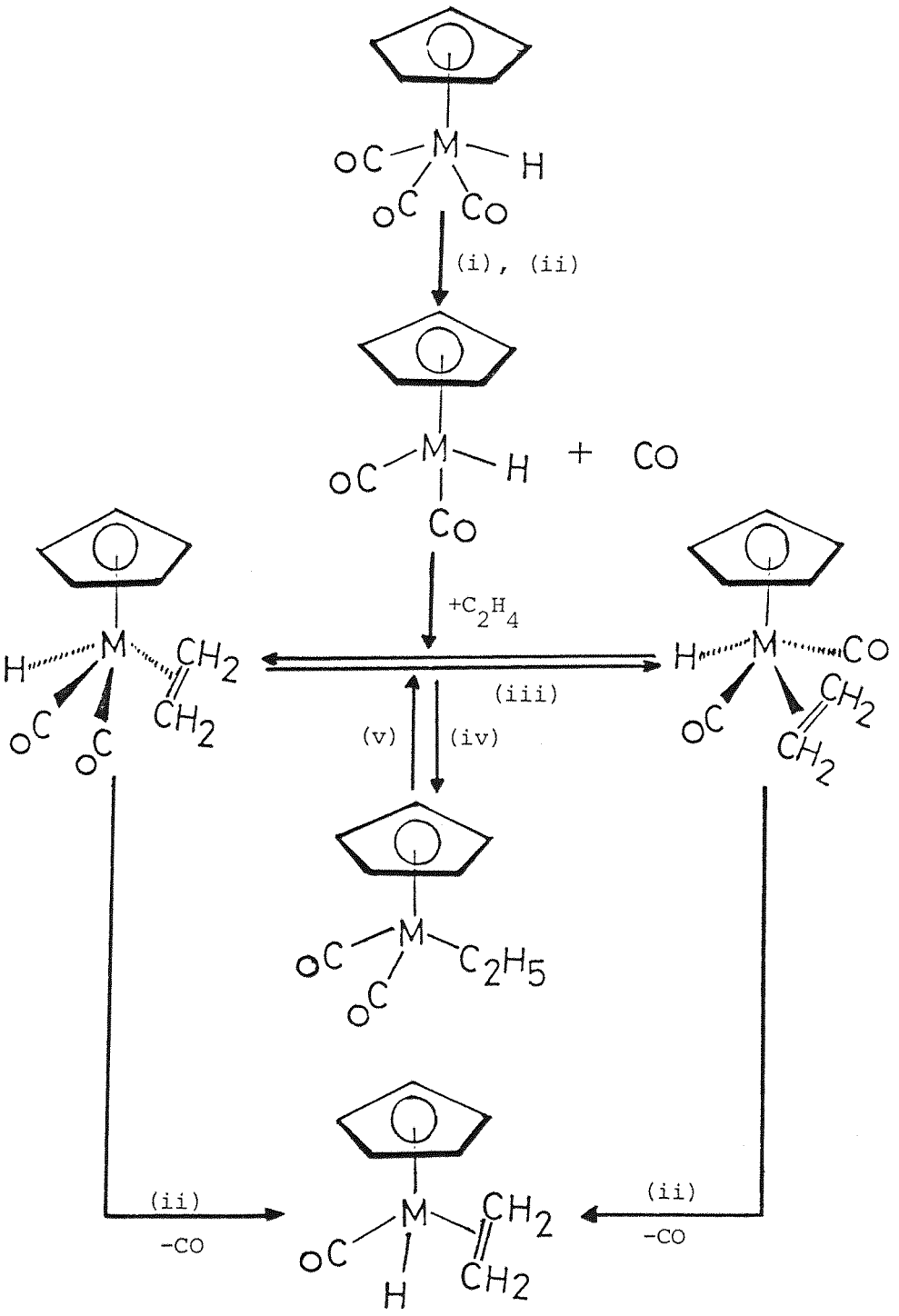

Scheme 3.4 (i) 5% C_2H_4 in CH_4; (ii) hν, $290 < \lambda < 370$ nm; (iii) hν = $\lambda > 370$ nm; (iv) hν, $310 < \lambda < 370$ nm; (v) hν, $\lambda > 430$ nm.

ligand without any change of the configuration. This is in striking contrast to the photolysis of $(\eta^5\text{-}C_5H_5)W(CO)_3H$ in thf solution where both *cis* and *trans* isomers are formed; $(\eta^5\text{-}C_5H_5)W(CO)_2(thf)H$ can be isolated and is stable at temperatures not higher than -20°C. It is noteworthy that prolonged photolysis of $(\eta^5\text{-}C_5H_5)M(CO)_3H$ in 5% C_2H_4 doped CH_4 matrices leads to the production of the 16-electron coordinatively unsaturated species $(\eta^5\text{-}C_5H_5)M(CO)_2C_2H_5$ (M = Mo, W; Scheme 3.4). This entails substitution of a CO by C_2H_4 and then insertion of the coordinated C_2H_4 into a M-H bond. Exactly these steps are proposed in the mechanism of the hydroformylation reaction [6, 56]. This is the first time intermediates corresponding to proposed insertion processes have been observed [57].

The addition of a metal-hydride to an alkyne may produce a vinyl metal complex (Equation 3.23).

$$M - H + HC \equiv CH \rightleftharpoons \underset{\underset{HC \equiv CH}{|}}{M - H} \rightleftharpoons M - CH = CH_2 \qquad (3.23)$$

For example, acetylene reacts with $HRhCl_2(PPh_3)_2$ to give a vinyl complex, $RhCl_2(PPh_3)_2(CH = CH_2)$ [58], but $HCo(CO)_4$ and acetylene give $Co_2(CO)_6(CH \equiv CH)$ [59]. Fluorinated acetylenes such as $CF_3C \equiv CCF_3$ give vinyl complexes upon reaction with hydride complexes such as $HMn(CO)_5$ [60, 61], $HRe(CO)_5$ [61], and $(\eta^5\text{-}C_5H_5)Fe(CO)_2H$ [61]. Irradiation of $(\eta^5\text{-}C_5H_5)M(CO)_3CH_3$ complexes in pentane solution in presence of acetylene [62, 63] gave formation of the metallocycle (Equation 3.24).

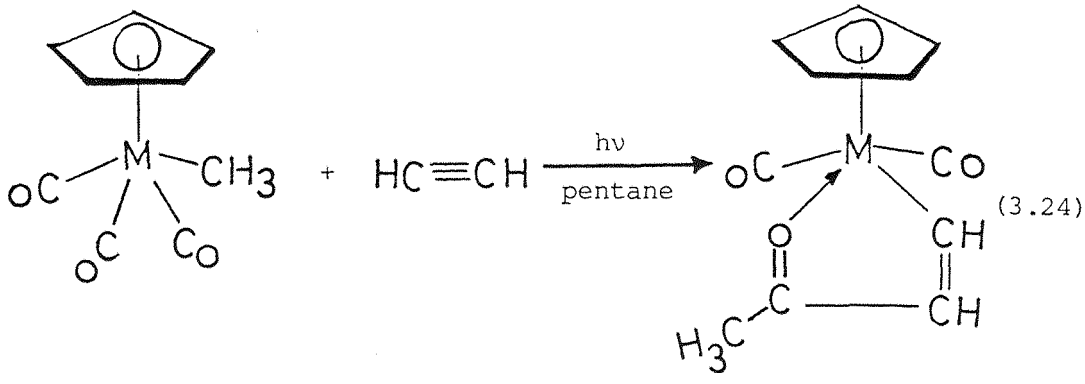

(3.24)

Irradiation of the hydride complexes $(\eta^5\text{-}C_5H_5)M(CO)_3H$ (M = Mo, W) in 3% C_2H_2 doped CH_4 matrices produced new species as shown in Scheme 3.5.

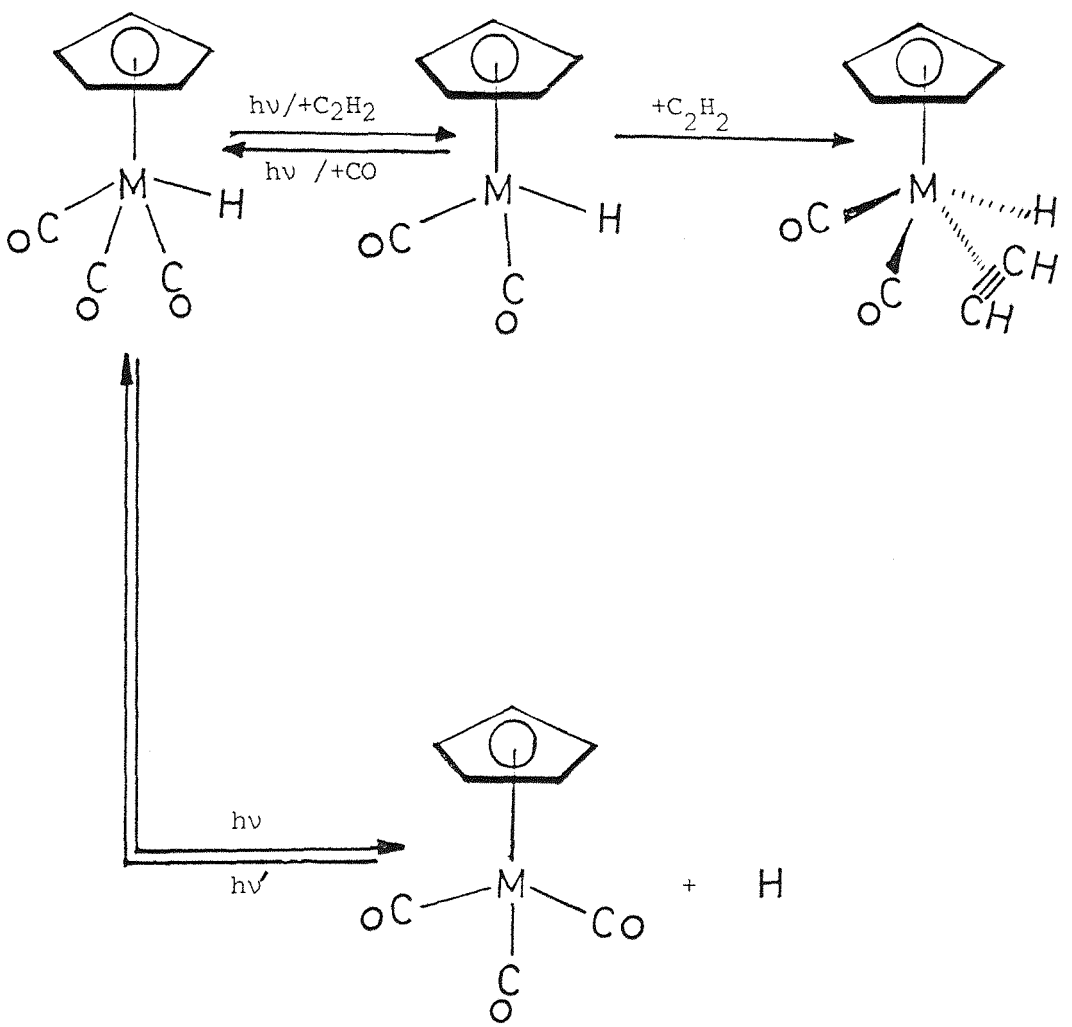

Scheme 3.5

The vinyl complex $(\eta^5\text{-}C_5H_5)M(CO)_2(CH=CH_2)$ could not be established because of the broadening of bands in the matrix. However, the presence of the unsaturated 16-electron intermediates $(\eta^5\text{-}C_5H_5)M(CO)_2H$ and the 18-electron $(\eta^5\text{-}C_5H_5)M(CO)_2(C_2H_2)H$ complexes is indicative of C_2H_2 behaving as a two-electron donor to the metal rather than a four-electron donor. The generation of a 16-electron intermediate $(\eta^5\text{-}C_5H_5)M(CO)_2H$, and its reaction with acetylene C_2H_2 is supported by the reaction of the $(\eta^5\text{-}C_5H_5)M(CO)_3H$ complexes with ethylene in gas matrices under the same conditions, and recently [64, 65] it has been shown that irradiation of toluene solutions of $(\eta^5\text{-}C_5H_5)_2MH_2$ (M = Mo, W) at either -78° or at room temperature in the presence of alkynes resulted in the formation of the respective alkyne complexes in essentially quantitative yield (Equation 3.25).

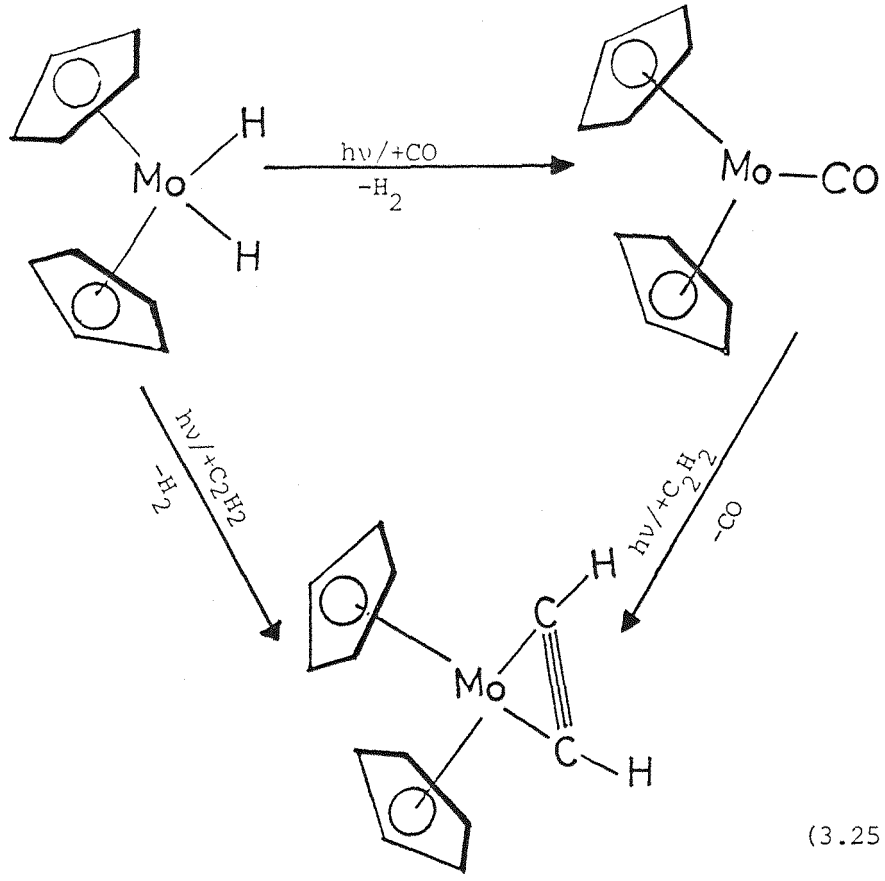

(3.25)

The formation of $(\eta^5\text{-}C_5H_5)M(CO)_2(C_2H_2)$ H with acetylene acting as a two-electron donor is in contrast to the coordination found for $W(CO)(C_2H_2)(S_2CNEt)_2$ where an 18-electron count requires a four-electron donor acetylene ligand [66].

3.4 CONCLUSIONS

Although only relatively few hydride complexes have been examined, several aspects concerning their photochemistry are becoming clear. Firstly, it appears that irradiation of complexes containing one hydride ligand, $M(CO)_mL_nH$, will lead to CO loss, as found for many metal carbonyls in Ar and CH_4 matrices at 12K, to give the coordinatively unsaturated 16-electron species $M(CO)_{m-1}L_nH$, e.g. $(\eta^5\text{-}C_5H_5)Mo(CO)_2H$. Such a process may often be reversed using visible light, i.e. there is an equilibrium (Equation 3.26).

$$(\eta^5\text{-}C_5H_5)M(CO)_3H \underset{h\nu'}{\overset{h\nu}{\rightleftharpoons}} (\eta^5\text{-}C_5H_5)M(CO)_2H + CO \qquad (3.26)$$

The reactivity of the $(\eta^5\text{-}C_5H_5)M(CO)_2H$ species was apparent from their reactions with N_2, C_2H_4 and C_2H_2 at 12K to produce *trans*-$(\eta^5\text{-}C_5H_5)M(CO)_2(N_2)H$ (M = Mo, W) complexes and both *cis* and *trans* isomers of $(\eta^5\text{-}C_5H_5)W(CO)_2(C_2H_4)H$ but only the *trans* isomer of $(\eta^5\text{-}C_5H_5)Mo(CO)_2(C_2H_4)H$. Secondly, irradiation in CO matrices can suppress the principle of CO loss photo-reaction pathway and allow a second pathway to be observed (Equation 3.27).

$$(\eta^5\text{-}C_5H_5)M(CO)_3H \underset{h\nu'}{\overset{h\nu/+CO}{\rightleftharpoons}} (\eta^5\text{-}C_5H_5)M(CO)_3^{\cdot} + \dot{H}CO \qquad (3.27)$$

The formation of $(\eta^5\text{-}C_5H_5)M(CO)_3^{\cdot}$ and $\dot{H}CO$ is indicative of photo-induced metal-hydrogen bond cleavage.

The chromium complex $(\eta^5\text{-}C_5H_5)Cr(CO)_3H$ gave different photo-products from the molybdenum and tungsten analogues. This is possibly due to the thermal instability of the 16-electron intermediate $(\eta^5\text{-}C_5H_5)Cr(CO)_2H$ even in low temperature matrices at 12K. In CO matrices, however, there are a

number of competing pathways. In addition to radical formation $(\eta^5\text{-}C_5H_5)Cr(CO)_3^{\cdot}$, $\eta^5\text{-}C_5H_5 \longrightarrow \eta^3\text{-}C_5H_5$ ring slippage or metal-hydride to ring transfer should be considered in the photochemical behaviour of $(\eta^5\text{-}C_5H_5)Cr(CO)_3H$. Additionally, substitution may lead to insertion.

Irradiation of *trans*-$(\eta^5\text{-}C_5H_5)W(CO)_2(C_2H_4)H$ in a CH_4 matrix gave the *cis* isomer as the primary product and this was followed by insertion of C_2H_4 into the W-H bond to generate the 16-electron species $(\eta^5\text{-}C_5H_5)W(CO)_2C_2H_5$. In CO matrices, however, the olefin was substituted by CO, and the corresponding hydrido carbonyl complex $(\eta^5\text{-}C_5H_5)W(CO)_3H$ is formed. The *cis* $\rightleftharpoons$ *trans* isomerisation and the insertion of C_2H_4 into a M-H bond are relevant to the understanding of hydroformylation reactions catalysed by transition metal hydrides.

Table 3.1 Infrared band positions (cm^{-1}) observed in the terminal CO-stretching region for $(\eta^5\text{-}C_5H_5)M(CO)_3H$ complexes (M = Cr, Mo, W) and *trans*-$(\eta^5\text{-}C_5H_5)W(CO)_2(C_2H_4)H$ and their photoproducts in various matrices at 12K.

Complex	CH_4	Ar	N_2	CO	5% C_2H_4/CH_4	3% C_2H_2/CH_4
$(\eta^5\text{-}C_5H_5)Mo(CO)_3H$	2029.8 1946.9) 1940.3)[a]	2033.4 1952.4) 1948.0)[a]	2029.2 1947.2) 1942.4)[a]	2029.2 1946.7) 1940.5)[a]	2028.2 1944.0) 1939.3)[a]	2027.7 1945.5) 1932.6)[a]
$(\eta^5\text{-}C_5H_5)W(CO)_3H$	2025.5 1939.5) 1935.1)[a]	2032.2 1946.1) 1942.1)[a]	2029.5 1942.5) 1932.3)[a]	2024.3 1936.1) 1931.1)[a]	2024.0 1932.5[b]	2024.6 1935.8) 1926.5)[a]
$(\eta^5\text{-}C_5H_5)Mo(CO)_2H$	1963.5 1885.2	1972.4 1892.4	c	d	1962.2 1882.7	1956.0 1880.8
$(\eta^5\text{-}C_5H_5)W(CO)_2H$	1956.4 1872.0	1967.0 1881.6	c	d	1956.0 1874.5	1957.3 1870.8
$(\eta^5\text{-}C_5H_5)Mo(CO)_2(N_2)H$[e]	-	-	1976.1 1912.8	-	-	-
$(\eta^5\text{-}C_5H_5)W(CO)_2(N_2)H$[e]	-	-	1972.7 1910.0	-	-	-
$(\eta^5\text{-}C_5H_5)Mo(CO)_3$	-	2012.8 1918.2	-	2008.9 1915.5) 1908.4)[f]	-	2000.5 1906.3

/continued

Table 3.1 (Continued)

Complex	CH_4	Ar	N_2	CO	5% C_2H_4/CH_4	3% C_2H_2/CH_4
$(\eta^5\text{-}C_5H_5)W(CO)_3^{\cdot}$	-	2004.2 1908.0	-	1999.3 1900.3)[f] 1896.5)[f]	-	1989.0 1903.5
$Mo(CO)_6$	-	-	-	1984.8	-	-
$W(CO)_6$	-	-	-	1979.7	-	-
$H^{12}CO/H^{13}CO$	-	-	-	1859.1/1817.0	-	-
trans-$(\eta^5\text{-}C_5H_5)Mo(CO)_2(C_2H_4)H$	-	-	-	-	1974.8 1901.3	-
cis-$(\eta^5\text{-}C_5H_5)W(CO)_2(C_2H_4)H$	1987.6 1928.5	-	-	1988.7 1931.4	1986.2 1927.8	-
trans-$(\eta^5\text{-}C_5H_5)W(CO)_2(C_2H_4)H$	1974.2 1897.2	-	-	1979.5 1902.1	1974.0 1897.5	-
$(\eta^5\text{-}C_5H_5)Mo(CO)_2C_2H_5$	-	-	-	-	1955.0 1872.5	-
$(\eta^5\text{-}C_5H_5)W(CO)_2C_2H_5$	1947.8 1861.1	-	-	1949.1 1862.2	1945.3 1859.3	-
$(\eta^5\text{-}C_5H_5)W(CO)(C_2H_4)H$	1904.0	-	-	-	1904.3	-
cis-$(\eta^5\text{-}C_5H_5)Mo(CO)_2(C_2H_2)H$	-	-	-	-	-	1981.5[g]

/Continued

Table 3.1 (Continued)

Complex	CH_4	Ar	N_2	CO	5% C_2H_4/CH_4	3% C_2H_2/CH_4
cis-$(\eta^5\text{-}C_5H_5)W(CO)_2(C_2H_2)H$	-	-	-	-	-	1979.2[g]
$(\eta^5\text{-}C_5H_5)Cr(CO)_3H$	2016.4 1941.8 1930.4	2021.2 1949.7 1939.0	2018.5 1945.4 1934.5	2016.7 1943.6 1932.7	2014.8 1941.6 1929.7	- - -
unknown	2048.5	2050.0	2050.0	2050.0	2046.8	-
Species (I)	1974.5 1883.0	1981.7 1888.0	1977.8 1885.4	1976.3 1885.2	1973.0 1881.4	- -
$(\eta^5\text{-}C_5H_5)Cr(CO)_2H$	1953.3 1855.5	-	-	-	-	-
$(\eta^5\text{-}C_5H_5)Cr(CO)_2(N_2)H$[h]	-	-	-	-	-	-
$(\eta^5\text{-}C_5H_5)Cr(CO)_2(C_2H_4)H$[i]	-	-	-	-	-	-
$(\eta^3\text{-}C_5H_5)Cr(CO)_4H$ Or $(\eta^4\text{-}C_5H_6)Cr(CO)_4$	-	-	-	2023.2[j] 1902.3	-	-
$Cr(CO)_6$	-	-	-	1976.3	-	-

/continued

Table 3.1 (Continued)

Complex	CH_4	Ar	N_2	CO	5% C_2H_4/CH_4	3% C_2H_2/CH_4
$(\eta^5\text{-}C_5H_5)Cr(CO)_3^{\cdot}$	-	1988.5 1913.3)[f] 1907.0)[f]	-	1986.3 1910.4	-	-
HCO	-	-	-	1859.2	-	-

[a] Overlapping A' and A" bands (see text).

[b] Broad unresolved band due to mixed matrix effect.

[c] $(\eta^5\text{-}C_5H_5)M(CO)_2H$ species (M = Mo, W) are not observed in N_2 matrices.

[d] $(\eta^5\text{-}C_5H_5)M(CO)_2H$ species (M = Mo, W) are not observed in CO matrices.

[e] ν_{NN} (Mo) at 2192.0 cm^{-1}; ν_{NN} (W) at 2163.5 cm^{-1}.

[f] Broad band split.

[g] Overlapping band.

[h] No reaction, since no $\nu_{N\equiv N}$ was observed.

[i] No reaction.

[j] Band at high energy obscured by the band of CO gas.

Table 3.2 Observed and calculated band positions (cm^{-1}) of terminal CO bands in an experiment with a ^{13}CO-enriched samples of $(\eta^5\text{-}C_5H_5)W(CO)_3H$ and $(\eta^5\text{-}C_5H_5)Cr(CO)_3H$ in various gas matrices.

Complex (symmetry point group)	ν(CO)	Observed	Calculated
$(\eta^5\text{-}C_5H_5)W(^{12}CO)_3H$ [a]	A'	2029.6	2028.9
(C_s)	A' + A"	1942.0	1941.1
$(\eta^5\text{-}C_5H_5)W(^{12}CO)_2(^{13}CO)H$	A'	2020.0	2020.5
(C_s) [b]	A"	1941.2 [d]	1941.1
	A'	1906.0	1905.9
	A	2016.0	2016.7
(C_1) [c]	A	1941.2 [d]	1941.1
	A	1908.6	1909.4
$(\eta^5\text{-}C_5H_5)W(^{12}CO)(^{13}CO)_2H$	A	2005.2	2006.1
(C_1) [f]	A	1920.8	1919.6
	A	1899.0	1897.9
	A'	1999.7	2001.0
(C_s) [g]	A'	e	1924.4
	A"	1897.0	1897.9
$(\eta^5\text{-}C_5H_5)W(^{13}CO)_3H$	A'	1983.4	1983.9
(C_s)	A' + A"	1897.1	1897.9
$(\eta^5\text{-}C_5H_5)W(^{12}CO)_2H$ [h]	A'	1965.9	1966.0
(C_s)	A"	1879.5	1879.7
$(\eta^5\text{-}C_5H_5)W(^{12}CO)(^{13}CO)H$	A	1950.1	1949.2
(C_1)	A	1854.5	1953.8
$(\eta^5\text{-}C_5H_5)W(^{13}CO)_2H$	A'	e	1922.3
(C_s)	A"	1837.6	1837.9

/Continued)

Table 3.2 (Continued)

Complex (symmetry point group)	ν(C)	Observed	Calculated
$(\eta^5\text{-}C_5H_5)W(^{12}CO)_2(N_2)H^i$	A'	1972.7	1972.7
(C_s)	A"	1910.0	1910.0
$(\eta^5\text{-}C_5H_5)W(^{12}CO)(^{13}CO)(N_2)H$	A	1957.2	1957.6
(C_1)	A	1882.3	1882.0
$(\eta^5\text{-}C_5H_5)W(^{13}CO)_2(N_2)H$	A'	1928.6	1928.9
(C_s)	A"	1866.4	1867.6
$(\eta^5\text{-}C_5H_5)W(^{12}CO)_3{}^j$	A_1	1999.7	1999.3
(C_{3v})	E	1899.5	1898.6
$(\eta^5\text{-}C_5H_5)W(^{12}CO)_2(^{13}CO)$.	A'	1987.8	1988.0
(C_s)	A"	1899.2	1898.7
	A'	1866.7	1867.0
$(\eta^5\text{-}C_5H_5)W(^{12}CO)(^{13}CO)_2$.	A'	1974.5	1974.3
(C_s)	A'	1880.5	1879.9
	A"	k	1856.5
$(\eta^5\text{-}C_5H_5)W(^{13}CO)_3$.	A_1	1954.4	1954.8
	E	1855.5	1856.4
$(\eta^5\text{-}C_5H_5)Cr(^{12}CO)_3H^l$	A'	2014.8	2014.5
(C_s)	A'	1939.8	1939.2
	A"	1929.4	1929.0
$(\eta^5\text{-}C_5H_5)Cr(^{12}CO)_2(^{13}CO)H$	A'	2004.8	2004.0
(C_s)[b]	A"	m	1937.1
	A'	1898.7	1898.1
(C_1)[c]	A	2003.0	2003.9
	A	n	1929.0
	A	1906.8	1906.2

/Continued

Table 3.2 (Continued)

Complex (symmetry point group)	ν(CO)	Observed	Calculated
$(\eta^5\text{-}C_5H_5)Cr(^{12}CO)(^{13}CO)_2H$			
$(\underline{C}_1)^f$	A	1990.3	1991.5
	A	1918.7	1918.0
	A	1885.7	1886.1
$(\underline{C}_s)^g$	A'	1989.1	1990.3
	A"	1912.5	1912.6
	A'	1893.5	1892.6
$(\eta^5\text{-}C_5H_5)Cr(^{13}CO)_3H$			
$(\underline{C}_s)$	A'	1969.5	1969.8
	A'	1895.5	1896.2
	A"	1885.7	1886.2
$(\eta^5\text{-}C_5H_5)Cr(^{12}CO)_2H$			
$(\underline{C}_s)$	A'	1953.3	
	A"	1855.5	

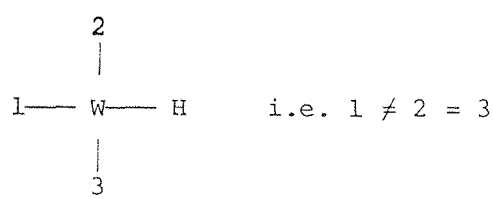

i.e. 1 ≠ 2 = 3

(a) Refined energy-factored force constants for $(\eta^5\text{-}C_5H_5)W(CO)_3(H)$: K_1 = 1559.3, K_2 = 1574.1, k_{12} = 43.9, and k_{23} = 51.9 Nm^{-1} as defined by the numbering in the diagram above.

(b) ^{13}CO in position 1.

(c) ^{13}CO in position 2.

(d) Band obscured by parent molecule band at 1942.0 cm^{-1}.

(e) Band obscured by band of ^{13}CO-enriched $(\eta^5\text{-}C_5H_5)W(CO)_3(H)$ at 1920.8 cm^{-1}.

(f) ^{12}CO in position 2.

(g) ^{12}CO in position 1.

(h) Refined energy-factored force constants for $(\eta^5\text{-}C_5H_5)W(CO)_2H$: K = 1494.5 and k_i = 67.0 Nm^{-1}.

Table 3.2 (Continued)

(i) Refined energy-factored force constants for *trans*-$(\eta^5\text{-}C_5H_5)W(CO)_2(N_2)H$: $K = 1523.0$ and $k_i = 49.2\ Nm^{-1}$; for Mo complex: $K = 1527.9$ and $k_i = 49.7\ Nm^{-1}$.

(j) Refined energy-factored force constants for $(\eta^5\text{-}C_5H_5)W(CO)_3$.: $K = 1509.2$ and $k_i = 52.8\ Nm^{-1}$ in a mixed $^{13}CO/^{12}CO$ (25:75) matrix.

(k) Band obscured by the band of $(\eta^5\text{-}C_5H_5)W(^{13}CO)_3$. at 1855.5 cm^{-1}.

(l) Refined energy-factored force constants for $(\eta^5\text{-}C_5H_5)Cr(CO)_3H$: $K_1 = 1560.3$, $K_2 = 1550.9$, $k_{12} = 40.3$, and $k_{23} = 47.3\ Nm^{-1}$.

(m) Bands obscured by parent molecule band at 1939.2 cm^{-1}.

(n) Bands obscured by parent molecule band at 1929.4 cm^{-1}.

3.5 REFERENCES

1. Y. Matsui and M. Orchin, *J. Organomet. Chem.*, 1982, 236, 381.

2. P. Renaut, G. Tainturier and B. Gantheron, *J. Organomet. Chem.*, 1978, 150, C9.

3. F.W.S. Benfield and M.L.H. Green, *J. Chem. Soc. Dalton*, 1974, 1324.

4. M.L.H. Green and R. Mahtab, *J. Chem. Soc. Dalton Trans.*, 1979, 262.

5. K.A. Mahmoud, A.J. Rest, H.G. Alt, M.E. Eichner and B.M. Jansen, *J. Chem. Soc. Dalton Trans.*, 1983 in press.

6. M. Orchin, *Acc. Chem. Res.*, 1981, 14, 259.

7. J. Halpern, *Inorg. Chim. Acta.*, 1981, 50, 11.

8. E.L. Muetterties, *Inorg. Chim. Acta.*, 1981, 50, 1.

9. V. Balzani, L. Moggi, M.F. Manfrin, F. Bolleta and M. Gleria, *Science*, 1975, 189, 855.

10. D.L. Reger and E.C. Culbertson, *J. Am. Chem. Soc.*, 1976, 98, 2789.

11. H.G. Alt and M.E. Eichner, *Angew. Chem. Int. Edn.*, 1982, 21, 78.

12. R.J. Kazlauskas and M.S. Wrighton, *J. Am. Chem. Soc.*, 1980, 102, 1727.

13. R. Bau, R.G. Teller, S.W. Kirtley and T.F. Koetzle, *Acc. Chem. Res.*, 1979, 12, 176.

14. J.A. Connor, M.T. Zatarani-Moattar, J. Bickerton, N.I. Elsaied, S. Suradi, R. Carson, G. Altakhin and H.A. Skinner, *Organometallics*, 1982, 1, 1166.

15. G.L. Geoffroy and M.S. Wrighton, *"Organometallic Photochemistry"*, Academic Press, London, 1979.

16. J. Chetwynd-Talbot, P. Grebenik and R.N. Perutz, *J. Chem. Soc. Chem. Commun.*, 1981, 452.

17. C. Giannotti and M.L.H. Green, *J. Chem. Soc. Chem. Commun.*, 1972, 1114.

18. E. Elmitt, M.L.H. Green, R.A. Forder, I. Jefferson and K. Prout, *J. Chem. Soc. Chem. Commun.*, 1974, 747.

19. L. Farrugia and M.L.H. Green, *J. Chem. Soc. Chem. Commun.*, 1975, 416.

20. G.L. Geoffroy and M.G. Bradley, *J. Organomet. Chem.*, 1977, 134, C27.

21. S.P. Church, M. Poliakoff, J.A. Timney and J.J. Turner, *J. Am. Chem. Soc.*, 1981, 103, 7515.

22. R.L. Sweany, *Inorg. Chem.*, 1980, 19, 3512; ibid., 1982, 21, 752.

23. G.L. Geoffroy and R. Pierantozzi, *J. Am. Chem. Soc.*, 1976, 98, 8054.

24. G.L. Geoffroy and M.G. Bradley, *Inorg. Chem.*, 1977, 16, 744.

25. J.K. Hoyano and W.A.G. Graham, *J. Am. Chem. Soc.*, 1982, 104, 3722.

26. N.W. Hoffman and T.L. Brown, *Inorg. Chem.*, 1978, 17, 613.

27. K.A. Mahmoud, R. Narayanaswany and A.J. Rest, *J. Chem. Soc. Dalton Trans.*, 1981, 2199.

28. B. Mayer, *"Low Temperature Spectroscopy"*, Elsevier, New York, 1970.

29. D.J. Taylor, *Ph.D. Thesis*, University of Southampton, 1980.

30. P.S. Braterman, *"Metal Carbonyl Spectra"*, Academic Press, London, 1975.

31. O. Crichton, A.J. Rest and D.J. Taylor, *J. Chem. Soc. Dalton Trans.*, 1980, 167.

32. A.J. Rest, J.R. Sodeau and D.J. Taylor, *J. Chem. Soc. Dalton Trans.*, 1978, 651.

33. D. Sellman, *Angew. Chem. Int. Ed.*, 1971, 10, 919.

34. A.J. Rest, *J. Organomet. Chem.*, 1972, 40, C76.

35. K.A. Mahmoud, A.J. Rest and H.G. Alt., *J. Organomet. Chem.*, 1983, 243, C5.

36. O. Crichton and A.J. Rest, *J. Chem. Soc. Dalton Trans.*, 1977, 986.

37. M.A. Graham, M. Poliakoff and J.J. Turner, *J. Chem. Soc. A.*, 1971, 2939.

38. K.A. Mahmoud, A.J. Rest and H.G. Alt, *J. Chem. Soc. Dalton Trans.*, 1983, in press.

39. E.O. Fisher, H. Hatner and H.O, Stahl, *Z. Anorg. Allg. Chem.*, 1955, 282, 47.

40. H.G. Alt, K.A. Mahmoud and A.J. Rest, *Angew. Chem. Int. Edn.*, 1983 in press.

41. D.S. Ginley and M.S. Wrighton, *J. Am. Chem. Soc.*, 1975, 97, 3533.

42. D. Sellmann and G. Maisel, *Z. Natureforsch Teil B*, 1972, 27, 465.

43. I. Fischler, K. Hildenbrand and E.A. Koerner von Gustorf, *Angew. Chem. Int. Edn.*, 1975, 14, 54.

44. D.E. Milligan and M.E. Jacox, *J. Chem. Phys.*, 1969, 51, 278.

45. M.E. Jacox, *J. Mol. Spec.*, 1973, 47, 14.

46. J.A. Connor, *Top. Curr. Chem.*, 1977, 71, 71.

47. A. Miyake and H. Kondo, *Angew. Chem. Int. Edn.*, 1968, 7, 880.

48. A. Miyake and H. Kondo, *Angew. Chem. Int. Ed. Engl.*, 1968, 7, 631.

49. J. Chetwynd-Talbot, P. Grebenik, R.N. Perutz and M.H.A. Powell, *Inorg. Chem.*, 1983 in press.

50. D.J. Fettes, R. Narayanaswamy and A.J. Rest, *J. Chem. Soc. Dalton Trans.*, 1981, 2311.

51. R.F. Heck, *Advan. Chem. Ser.*, 1965, 49, 181.

52. R.F. Heck, *Accounts. Chem. Res.*, 1969, 2, 10.

53. P.M. Treichel, J.H. Morris and F.G.A. Stone, *J. Chem. Soc.*, 1963, 720.

54. R.F. Heck and D.S. Breslow, *J. Am. Chem. Soc.*, 1961, 83, 4023.

55. R.B. King, *Organomet. Synth.*, 1963, 7, 136.

56. C.M. Masters, *"Homogenous Transition Metal Catalysis"*, Chapman and Hall, London, 1981.

57. H.G. Alt, K.A. Mahmoud and A.J. Rest, *J. Organomet Chem.*, 1983, 246, C37.

58. M.C. Baird, J.T. Mague, J.A. Osborn and G. Wilkinson, *J. Chem. Soc. A*, 1967, 1347.

59. Y. Iwashita, F. Tamura and H. Wakamatsu, *Bull. Chem. Soc. Jap.*, 1970, 43, 1520.

60. D.A. Harbourne, D.T. Rosevear and F.G.A. Stone, *Inorg. Nucl. Chem. Lett.*, 1966, 2, 247.

61. D.A. Harbourne and F.G.A. Stone, *J. Chem. Soc. A*, 1968, 1765.

62. H.G. Alt, *J. Organomet Chem.*, 1977, 127, 349.

63. M.D. Rausch, J.E. Gismondi, H.G. Alt and J.A. Schwarzle, *Z. Naturforsch. Teil B*, 1977, 32, 998.

64. G.L. Geoffroy, M.G. Bradley and R. Peirantozzi, *"Transition Metal Hydrides"*, 1978, Chap. 14, p.192.

65. K.L. Tangwong, J.L. Thomas and H.H. Brintzinger, *J. Am. Chem. Soc.*, 1974, 96, 3694.

66. L. Ricard, R. Weiss, W.E. Newton, G.J. Chen and J.W. McDonald, *J. Am. Chem. Soc.*, 1978, 100, 1318.

CHAPTER FOUR

PHOTOCHEMISTRY OF THE ALKYL COMPLEXES $(\eta^5-C_5H_5)W(CO)_3$alkyl (alkyl = ethyl, n-propyl, i-propyl, n-butyl, σ-allyl, benzyl, phenyl), $(\eta^5-C_5Me_5)W(CO)_3$ n-propyl AND OF $(\eta^5-C_5H_5)Mo(CO)_3$ ethyl IN GAS MATRICES AT 12K

4.1 INTRODUCTION

The photoinduced substitution of carbonyl ligands in complexes of the general formula $(\eta^5-C_5H_5)M(CO)_3R$ (M = Cr, Mo, W; R = alkyl) has been known for many years and has been proposed to proceed dissociatively via 16-electron $(\eta^5-C_5H_5)M(CO)_2R$ species [1 - 4]. Only recently, however, has it been recognised that $(\eta^5-C_5H_5)M(CO)_3CH_3$ complexes can be de-alkylated in solution [2, 5 - 8], if the solvent is not able to stabilise the 16-electron species $(\eta^5-C_5H_5)M(CO)_2CH_3$, formed initially or when a potential ligand is absent. For example, the photolysis of $(\eta^5-C_5H_5)M(CO)_3CH_3$ (M = Cr, Mo, W) complexes in solution results in the formation of CH_4 via hydrogen abstraction [5 - 9]. Radicals could be detected during the course of these photo-induced de-alkylation reactions [6, 9]. Derivatives with alkyl ligands that contain more than one carbon atom behave differently. For example the ethyl complex $(\eta^5-C_5H_5)W(CO)_3C_2H_5$ [4, 10, 11] and the n-pentyl complex $(\eta^5-C_5H_5)W(CO)_3C_5H_{11}$ [12] undergo photo-induced de-alkylation in alkane solution to form the same final metal-containing product, $[(\eta^5-C_5H_5)W(CO)_3]_2$. In this case the reaction is thought to involve β-hydrogen transfer and the formation of intermediate olefin hydrido species, e.g. $(\eta^5-C_5H_5)W(CO)_2(C_2H_4)(H)$.

The best documented processes involving hydrogens on carbon atoms of C_R chains bonded to metals are those generally described as "β-hydrogen elimination" and the most common type is intramolecular β-hydrogen abstraction by the metal. The most extensively studied example of intramolecular β-hydrogen abstraction is for $Pt(PPh_3)_2(n-C_4H_9)_2$ [13], (Equation 4.1).

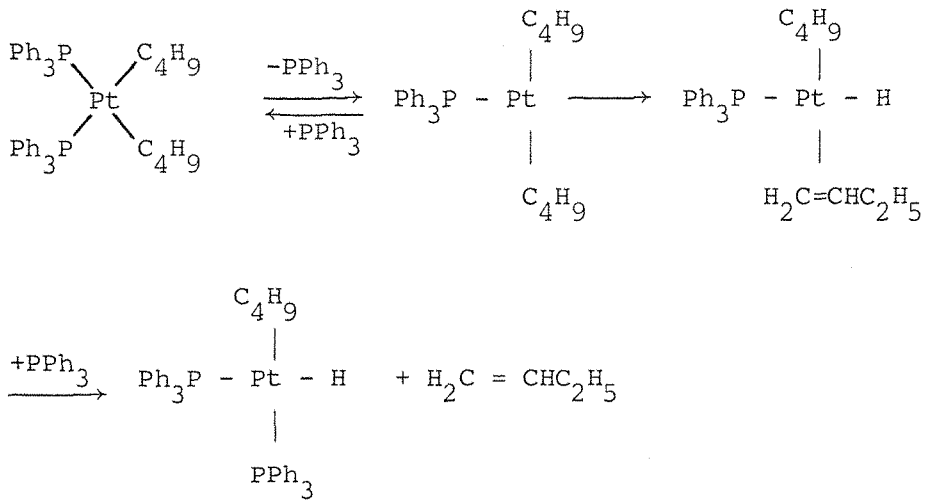

(4.1)

In the early transition metals, a nice example of β-hydrogen abstraction is the thermolysis of $(\eta^5\text{-}C_5H_5)_2\ NbC_2H_5$ to give isolable $(\eta^5\text{-}C_5H_5)_2Nb(C_2H_4)H$ [14] (Equation 4.2).

$$(\eta^5\text{-}C_5H_5)_2\ NbC_2H_5 \xrightleftharpoons{\Delta} (\eta^5\text{-}C_5H_5)_2\ Nb(C_2H_4)H \qquad (4.2)$$

Interestingly the thermolysis step is reversible and also $(\eta^5\text{-}C_5H_5)_2\ NbC_2H_5$ reacts further with C_2H_4 to give $(\eta^5\text{-}C_5H_5)_2\ Nb(C_2H_4)C_2H_5$ while $(\eta^5\text{-}C_5H_5)_2\ Nb(C_2H_4)H$ can be formed by the reaction of $(\eta^5\text{-}C_5H_5)_2\ Nb\ H$ with C_2H_4.

When the ligand R is a potential three-electron donor, e.g. σ-allyl, rearrangement of the ligand binding can take place on expulsion of a CO ligand. For example, photolysis of $Mn(CO)_5\ (\eta^1\text{-}C_3H_5)$ was one of the earliest reports of a re-organization of bonding between the metal and the hydrocarbon group induced by photodissociation of CO (Equation 4.3) [15].

$$Mn(CO)_5(\eta^1\text{-}C_3H_5) \xrightarrow[-CO]{h\nu} Mn(CO)_4(\eta^3\text{-}C_3H_5) \qquad (4.3)$$

The allyl group in $Mn(CO)_4(\eta^3\text{-allyl})$ may also be described as a π-allyl and is considered to be formed by the uncoordinated olefin of a σ-allyl taking the coordination site vacated by the ejected CO. Interesting consequences of CO dissociation from $(\eta^5\text{-}C_5H_5)Fe(CO)_2(\eta^1\text{-}C_3H_4R)$ include σ → π intramolecular rearrangements as shown in Equation 4.4 and *syn* and *anti* conformations of the R group [16].

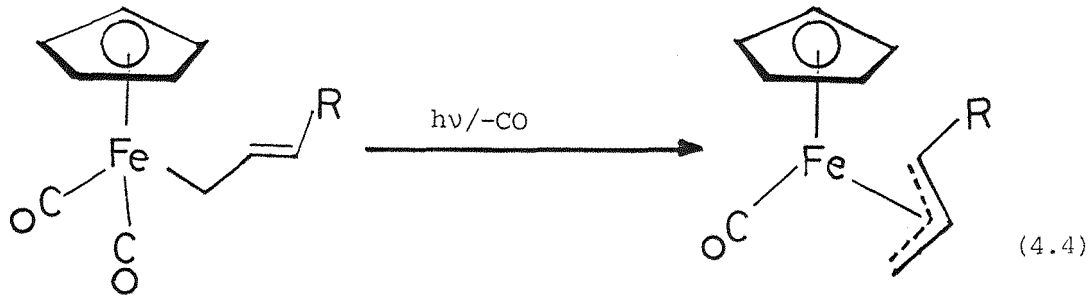

(4.4)

The matrix isolation technique has been shown to be very useful for investigating photochemical reactions and for characterising reactive species, in particular metal carbonyl species [17]. Using frozen gas matrices at 12K it has been shown (see Chapter 2) that the principal photoprocess for isolated $(\eta^5\text{-}C_5H_5)Mo(CO)_3CH_3$ molecules is ejection of CO to give the 16-electron species $(\eta^5\text{-}C_5H_5)Mo(CO)_2CH_3$, whose reactivity was demonstrated by its facile recombination with CO at ∿ 50K [18]. In polyvinyl chloride film matrices over the temperature range 12 - 293 K, however, infrared spectroscopic evidence was found for a photochemical reaction pathway involving radicals [19]. In order to gain a more detailed understanding of the mechanisms of photo-induced de-alkylation and de-arylation reactions of alkyl- and aryl-transition metal complexes a matrix isolation study of the photolysis of $(\eta^5\text{-}C_5R_5')W(CO)_3R$ complexes (R = C_2H_5, $\underline{n}\text{-}C_3H_7$, $\underline{i}\text{-}C_3H_7$, $\underline{n}\text{-}C_4H_9$, C_6H_5, $CH_2C_6H_5$, C_3H_5; R' = H, CH_3) in frozen gas matrices at 12 K was undertaken. The results in gas matrices are compared with photolysis studies in solution. A comparison with a metal in another series was effected by studying $(\eta^5\text{-}C_5H_5)Mo(CO)_3C_2H_5$ in gas matrices at 12K and in solution. Some matrix isolation studies had already been performed with $(\eta^5\text{-}C_5R_5')M(CO)_3R$ complexes (M = Mo, W; R = CH_3, C_2H_5, $\underline{n}\text{-}C_5H_{11}$; R' = H, CH_3) in paraffin matrices at 77K [11, 12]. From wide experience of the critical effects of temperature in matrix isolation studies [17], e.g. the recombination of $(\eta^5\text{-}C_5H_5)Mo(CO)_2CH_3$ with CO at ∿ 30K [18], it seemed probable that a study of $(\eta^5\text{-}C_5R_5')M(CO)_3R$ complexes in gas matrices at 12K might reveal additional species and processes compared to the study at 77K. A detailed study of the de-arylation of $(\eta^5\text{-}C_5H_5)W(CO)_3C_6H_5$ in solution and in gas matrices at 12K had not been carried out previously.

4.2 RESULTS

4.2.1 Photolysis of $(\eta^5\text{-}C_5H_5)M(CO)_3C_2H_5$ Complexes (M = Mo, W) in CH_4, N_2 and CO Matrices

The i.r. spectra of $(\eta^5\text{-}C_5H_5)M(CO)_3R$ complexes in solution show two terminal CO stretching bands whereas three bands are expected for a C_s $M(CO)_3R$ fragment. Similarly the i.r. spectra of C_s $(\eta^5\text{-}C_5H_5)Mo(CO)_3CH_3$ in gas matrices at 12K showed two i.r. active terminal CO stretching bands [18]. The C_s symmetry of the $Mo(CO)_3CH_3$ fragment was confirmed, however, by an energy-factored force-field fitting of the terminal CO stretching bands of matrix isolated $(\eta^5\text{-}C_5H_5)Mo(^{12}CO)_{3-n}(^{13}CO)_nCH_3$ [18]. The upper wavenumber band for $(\eta^5\text{-}C_5R_5')M(CO)_3R$ complexes in solution must, therefore, be the symmetric stretch (A', ca 2000 cm^{-1}) while the lower band arises from an accidental coincidence of A' and A" bands (ca 1920 cm^{-1}, Table 4.1). All the $(\eta^5\text{-}C_5R_5')M(CO)_3R$ complexes studied in matrices in this work showed a single upper wavenumber band and a split lower wavenumber band, e.g. the spectrum of $(\eta^5\text{-}C_5H_5)W(CO)_3C_2H_5$ (Figure 4.1a). The splittings of the lower wavenumber bands (ca 8 cm^{-1}) are of similar magnitude to those for matrix effects [20] and, therefore, in summarising the i.r. data for $(\eta^5\text{-}C_5R_5')M(CO)_3R$ complexes, the split bands (Tables 4.1 - 4.3) are assigned as A' + A" modes.

Irradiation of $(\eta^5\text{-}C_5H_5)W(CO)_3C_2H_5$ in CH_4 using a visible filter ($\lambda > 410$ nm), giving light corresponding to the long wavelength absorption band in the uv-vis spectrum (Figure 4.2a) produced free CO (ca 2138 cm^{-1}) and five new bands at 1988.5, 1977.4, 1948.7, 1899.7 and 1862.8 cm^{-1} (Figure 4.1b). A further period of irradiation ($\lambda > 370$ nm) showed an increase in free CO, increases in all the new bands, a decrease in the upper A' parent band, and a change in the splitting pattern of the combined parent A' + A" band (Figure 4.1c). The latter observation indicated that a further new band was growing (1929.6 cm^{-1}) under the parent A' + A" band. An extended period of irradiation confirmed this (Figure 4.1d) because the parent bands disappeared but a band remained at 1929.6 cm^{-1}. Comparison of the growth and disappearance of bands under various times of photolysis identified that there were three pairs of new bands (Figure 4.1): (1) at 1988.5 and 1929.2 cm^{-1}, (2) at 1977.4 and 1899.7 cm^{-1}, and (3) at 1948.7 and 1862.8 cm^{-1}.

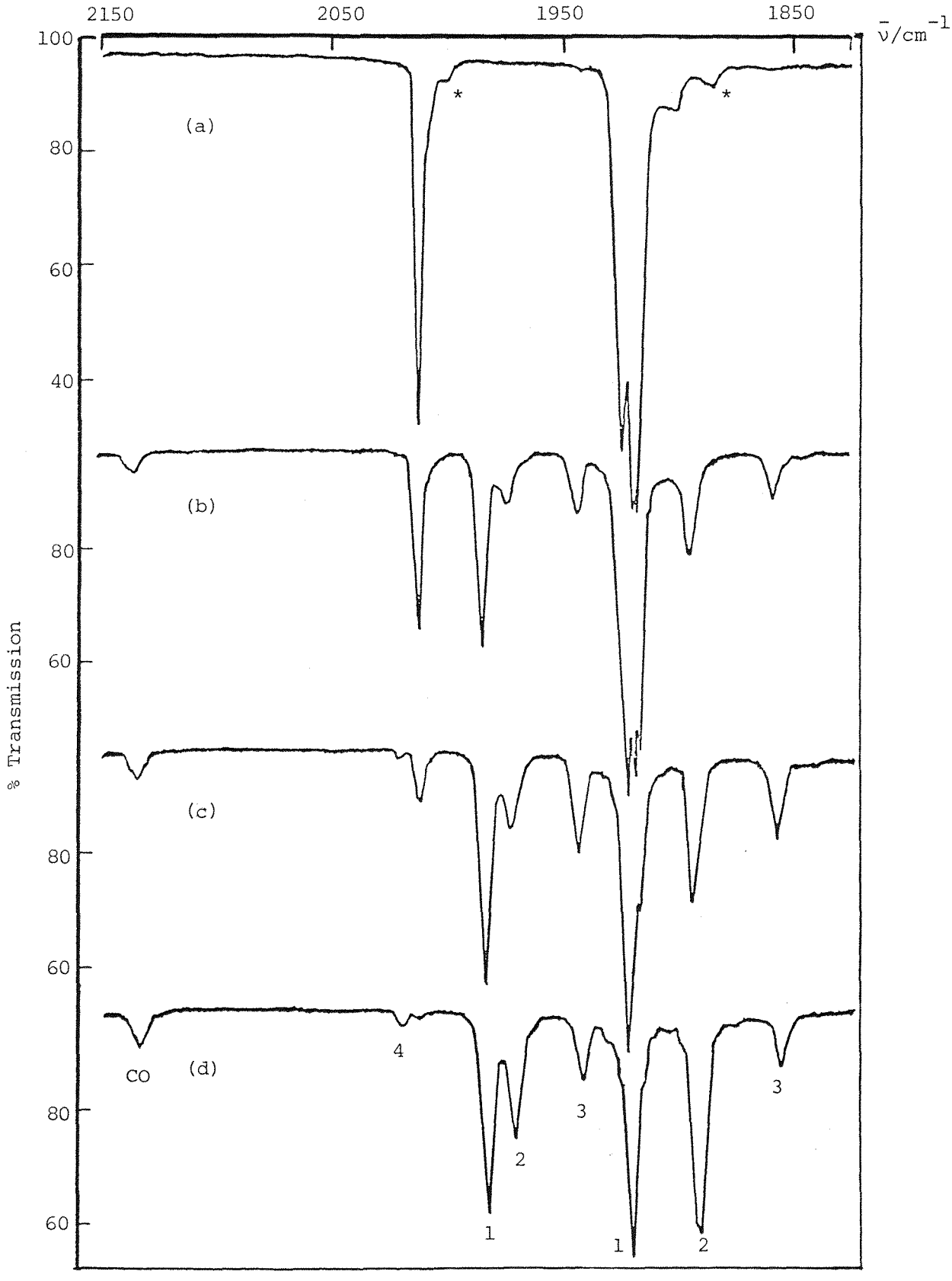

FIGURE 4.1 Infrared spectra from an experiment with $(\eta^5\text{-}C_5H_5)W(CO)_3C_2H_5$ isolated at high dilution in a CH_4 matrix at 12K: (a) after deposition, (b) after 60 min photolysis using $\lambda > 410$ nm radiation, (c) after 10 min photolysis using $\lambda > 370$ nm radiation, and (d) after further 75 min photolysis with $\lambda > 370$ nm radiation. Bands marked with (*) are due to $(\eta^5\text{-}C_5H_5)W(^{12}CO)_2(^{13}CO)C_2H_5$ in natural abundance. Bands marked (1) - (4) arise from photoproducts (see text).

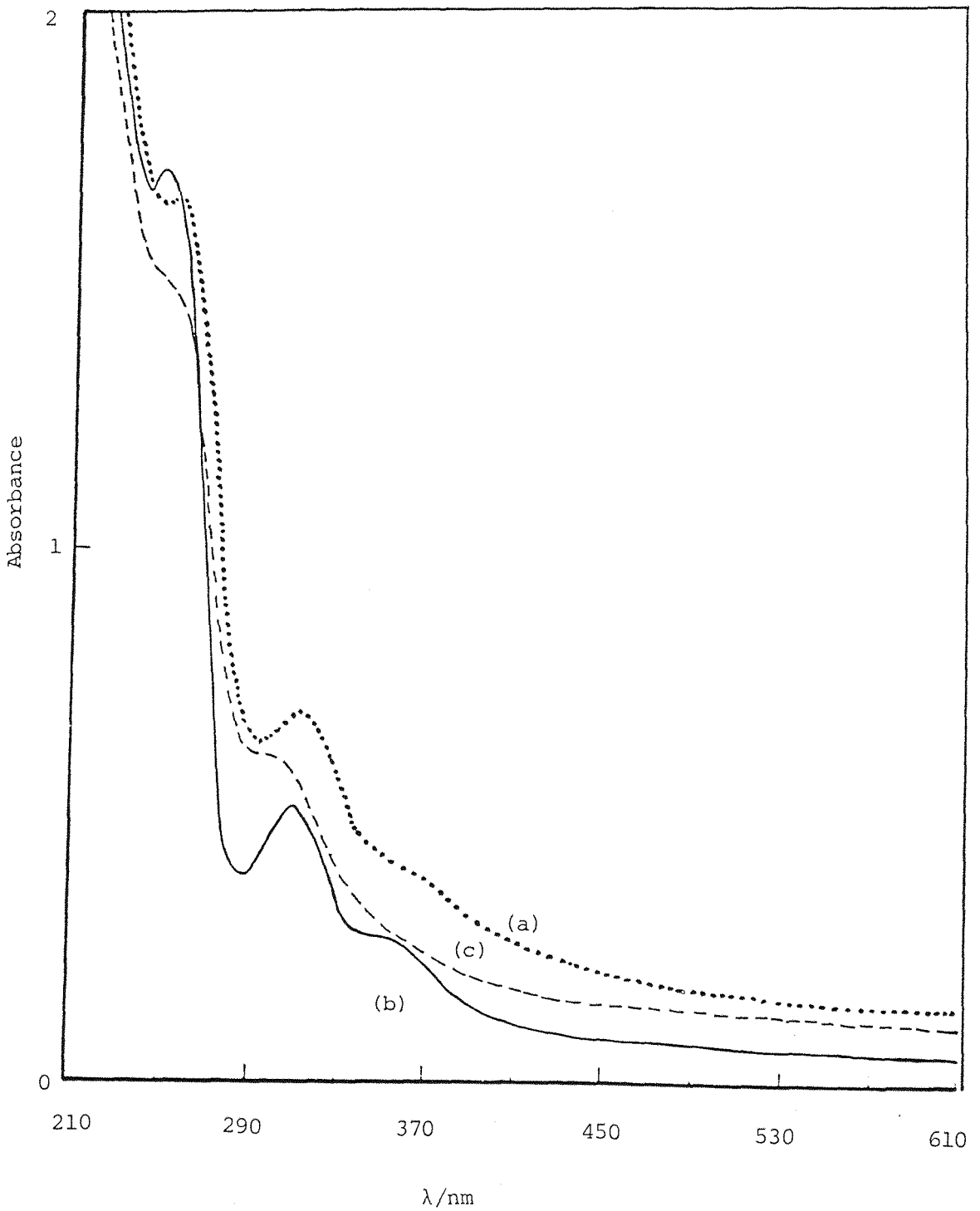

FIGURE 4.2 Ultraviolet-visible spectra from experiments with (a) $(\eta^5\text{-}C_5H_5)W(CO)_3C_2H_5$ and (b) $(\eta^5\text{-}C_5H_5)W(CO)_3(\underline{n}\text{-}C_3H_7)$ isolated at high dilution in CH_4 matrices at 12K and (c) after 60 min photolysis using $\lambda > 430$ nm.

The (2) pair (1977.4 and 1899.7 cm^{-1}) can be confidently assigned to *trans*-$(\eta^5\text{-}C_5H_5)W(CO)_2(C_2H_4)H$ by comparison with the bands for this complex in solution (1978 and 1903 cm^{-1}, Table 4.1) and in separate matrix isolation experiments (1974.2 and 1897.3 cm^{-1}) [21]. The (3) pair (1948.7 and 1862.8 cm^{-1}) may be assigned to the 16-electron species $(\eta^5\text{-}C_5H_5)W(CO)_2C_2H_5$ by analogy with the formation of $(\eta^5\text{-}C_5H_5)Mo(CO)_2CH_3$ (1966.0 and 1880.1 cm^{-1}) on photolysis of $(\eta^5\text{-}C_5H_5)Mo(CO)_3CH_3$ in gas matrices at 12K [18] and by comparison with the band positions of $(\eta^5\text{-}C_5H_5)W(CO)_2C_2H_5$ (1952 and 1865 cm^{-1}) in a paraffin wax matrix at 77K [11, 12]. The remaining pair of bands (pair (1), 1988.5 and 1929.2 cm^{-1}) must belong to a species with at least two CO ligands. The most likely candidates are $(\eta^5\text{-}C_5H_5)W(CO)_3H$ and *cis*-$(\eta^5\text{-}C_5H_5)W(CO)_2(C_2H_4)H$. Of these species, the former can be eliminated because it has bands at 2024.2, 1938.6 and 1934.4 cm^{-1} as shown in a separate matrix isolation study at 12K [21]; the upper band of $(\eta^5\text{-}C_5H_5)W(CO)_3H$ was observed to appear ((4), Figure 4.1c) and to grow (Figure 4.1d) on extended photolysis. Assuming the (1) pair belong to a $W(CO)_2$ fragment a bond angle OC-W-CO may be calculated from the expression $\tan^2 \theta/2 = I_{asym}/I_{sym}$ [22] and compared with that for *trans*-$(\eta^5\text{-}C_5H_5)W(CO)_2(C_2H_4)H$. Weighed tracings of the spectra of the two sets of bands in absorbance mode yielded values of ca 90° ((1) pair) and 110° ((2) pair). These values together with the similar band positions for pairs (1) and (2) suggest strongly that the (1) pair may be assigned to *cis*-$(\eta^5\text{-}C_5H_5)W(CO)_2(C_2H_4)H$. Additionally the energy-factored CO interaction force constant [22] for the (1) pair (k_i = 46.9 Nm^{-1}) is less than that for *trans*-$(\eta^5\text{-}C_5H_5)W(CO)_2(C_2H_4)H$ (k_i = 60.8 Nm^{-1}) and this is indicative of two *cis* CO groups in the (1) species.

Analogous results for $(\eta^5\text{-}C_5H_5)W(CO)_3C_2H_5$ were obtained for N_2 and CO matrices except that the amounts of the various species were different from those observed for CH_4 matrices and that a much higher yield of $(\eta^5\text{-}C_5H_5)W(CO)_3H$, was produced on extended photolysis in the case of CO matrices.

Photolysis of $(\eta^5\text{-}C_5H_5)Mo(CO)_3C_2H_5$ in CH_4 and CO matrices yielded all the species identified above for $(\eta^5\text{-}C_5H_5)W(CO)_3C_2H_5$ with the noteworthy exception of *cis*-$(\eta^5\text{-}C_5H_5)Mo(CO)_2(C_2H_4)H$, c.f. the failure to observe *cis*-$(\eta^5\text{-}C_5H_5)W(CO)_2(C_2H_4)H$ in paraffin wax matrices at 77K [11, 12]. Infrared data for all the species are collected in (Table 4.1).

In the study by Kazlauskas and Wrighton [12] using paraffin wax matrices at 77K, one of the most important species cited was the 16-electron dicarbonyl species, $(\eta^5\text{-}C_5H_5)M(CO)_2C_2H_5$, where it was proposed that a β-hydrogen became coordinated to the metal (I). The evidence for (I) was a large shift in the optical spectrum, e.g. λ_{max} at 405 and 535 nm, between species which were proposed to be dicarbonyls and were formed before β-elimination took place. We noticed no difference of colour in our matrices

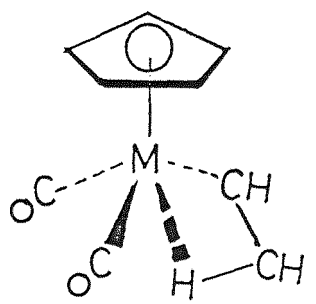

(I)

for $(\eta^5\text{-}C_5H_5)M(CO)_2C_2H_5$ species in CH_4, N_2 and CO matrices nor could we observe new absorptions in the uv-vis spectra on photolysis of $(\eta^5\text{-}C_5H_5)M(CO)_3C_2H_5$ complexes. It may well be that there was insufficient chromophore in the very thin gas matrices compared to the thicker and more concentrated paraffin wax matrices.

4.2.2 Photolysis of $(\eta^5\text{-}C_5R'_5)W(CO)_3R$ (R = n-C_3H_7, R' = H and CH_3; R = n-C_4H_9, R' = H) in CH_4 and CO Matrices

The photoreactions of the three complexes are typified by that of $(\eta^5\text{-}C_5H_5)W(CO)_3$n-$C_3H_7$, which is described in detail below.

The infrared spectrum of $(\eta^5\text{-}C_5H_5)W(CO)_3$(n-$C_3H_7$) isolated at high dilution in a CH_4 matrix in the terminal CO stretching region (Figure 4.3a, Table 4.2) is very similar to that already described for $(\eta^5\text{-}C_5H_5)W(CO)_3C_2H_5$.

Irradiation using the visible filter (λ > 430 nm), giving radiation corresponding to the long wavelength absorption band (Figure 4.2b), produced 'free' CO (2138 cm^{-1}) and new bands at 1986.0, 1978.6, 1970.3,

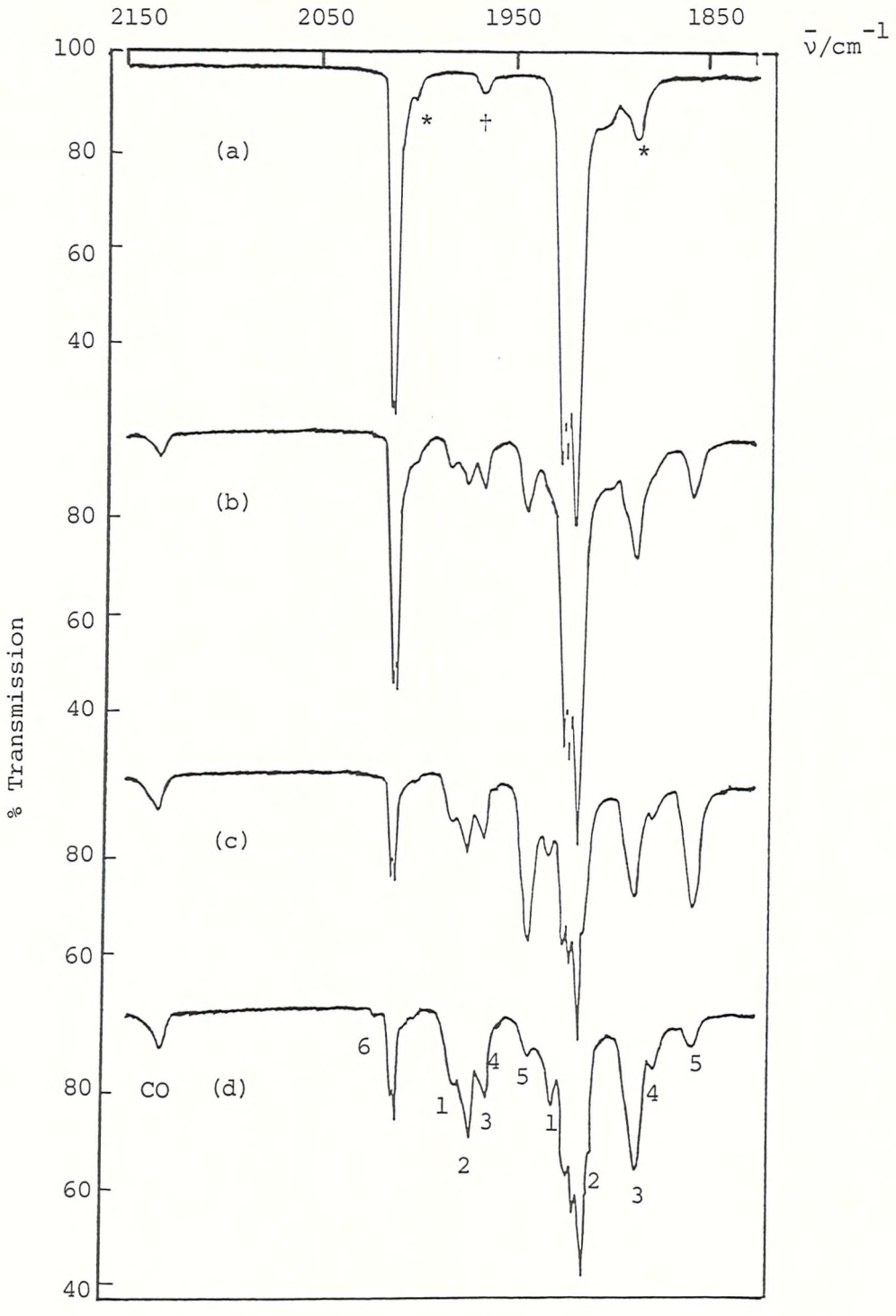

FIGURE 4.3 Infrared spectra from an experiment with $(\eta^5\text{-}C_5H_5)W(CO)_3(\underline{n}\text{-}C_3H_7)$ isolated at high dilution in a CH_4 matrix at 12K: (a) after deposition, (b) after 110 min photolysis using $\lambda > 430$ nm, (c) after 15 min photolysis using $\lambda > 370$ nm, and (d) after 100 min photolysis using $\lambda > 430$ nm. Bands marked (*) are due to $(\eta^5\text{-}C_5H_5)W(^{12}CO)_2(^{13}CO)(\underline{n}\text{-}C_3H_7)$ present in natural abundance and that marked (†) is due to $W(CO)_6$ present as a trace impurity. Bands marked (1) - (6) arise from photoproducts (see text).

1963.7, 1949.4, 1937.5, 1893.5, 1883.8 and 1863.5 cm^{-1} (Figure 4.3b). Further photolysis using slightly higher energy radiation ($\lambda > 370$ nm) caused a rapid increase in all the new bands (Figure 4.3c). When this was followed by a further period of long wavelength photolysis ($\lambda > 370$ nm) the bands at 1949.4 and 1863.5 cm^{-1} decreased dramatically (Figure 4.3d). At this stage the parent bands had almost disappeared. Comparison of the growth and disappearance of bands in several experiments and under various times of photolysis with different energies of radiation identified that there were five pairs of new bands (Figure 4.3): (1) at 1986.0 and 1939.5 cm^{-1}, (2) at 1978.6 and 1919.5 cm^{-1}, (3) at 1970.3 and 1893.5 cm^{-1}, (4) at 1963.7 and 1883.8 cm^{-1}, and (5) at 1949.4 and 1863.5 cm^{-1}. On extended photolysis a further band (6) begins to grow (Figure 4.3d).

The (5) pair (1949.4 and 1863.5 cm^{-1}) can confidently be assigned to the 16-electron coordinatively unsaturated species $(\eta^5\text{-}C_5H_5)W(CO)_2(\underline{n}\text{-}C_3H_7)$ by comparison with the bands for $(\eta^5\text{-}C_5H_5)W(CO)_2C_2H_5$ (1948.7 and 1862.8 cm^{-1}). The other bands, by analogy with *cis* and *trans* isomers for $(\eta^5\text{-}C_5H_5)W(CO)_2(C_2H_4)H$ in matrices (see above) are most probably due to *cis* and *trans* isomers of $(\eta^5\text{-}C_5H_5)W(CO)_2(\underline{1}\text{-}C_3H_6)H$. In solution *trans*-$(\eta^5\text{-}C_5H_5)W(CO)_2(\underline{1}\text{-}C_3H_6)H$ has terminal CO stretching bands at 1972 and 1899 cm^{-1} and these correlate well with the (3) pair (1970.3 and 1893.5 cm^{-1}). Taking the upper bands in pairs (1) + (2) (1986.0 and 1978.6 cm^{-1}) and (3) + (4) (1970.3 and 1963.7 cm^{-1}) it could be argued that each new pair represented a fundamental mode with a typical matrix splitting (0 - 10 cm^{-1}) [20], i.e. (1) + (2) belong to the *cis* isomer and (3) + (4) belong to the *trans* isomer. Treating the lower wavenumber bands in the same manner, giving pairs (1) + (2) (1937.5 and 1919.5 cm^{-1}) and (3) + (4) (1893.5 and 1883.8 cm^{-1}), shows that the matrix splitting explanation is false because the (1) + (2) pair have a splitting of 18 cm^{-1} which is well outside the range for matrix splittings. In solution at -80°C ^1H n.m.r. studies show that *trans*-$(\eta^5\text{-}C_5H_5)W(CO)_2(\underline{1}\text{-}C_3H_6)H$ exists as two rotamers (II and III). It seems reasonable, therefore, that rotamers of *cis*- and *trans*-$(\eta^5\text{-}C_5H_5)W(CO)_2(\underline{1}\text{-}C_3H_6)H$ should be formed and frozen out at 12K. We assign the (1) pair to *cis*-$(\eta^5\text{-}C_5H_5)W(CO)_2(\underline{1}\text{-}C_3H_6)H$, the (2) pair to *cis'*-$(\eta^5\text{-}C_5H_5)W(CO)_2(\underline{1}\text{-}C_3H_6)H$, the (3) pair to *trans*-$(\eta^5\text{-}C_5H_5)W(CO)_2(\underline{1}\text{-}C_3H_6)H$ and the (4) pair to *trans'*-$(\eta^5\text{-}C_5H_5)W(CO)_2(\underline{1}\text{-}C_3H_6)H$. On extended photolysis with high energy

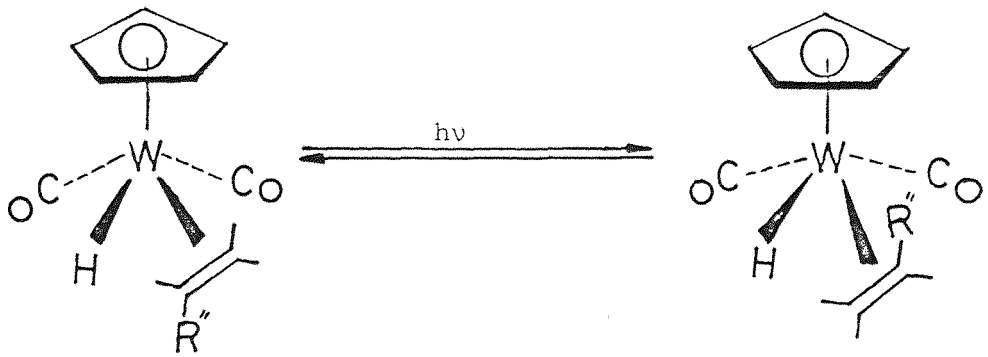

cis *cis'*

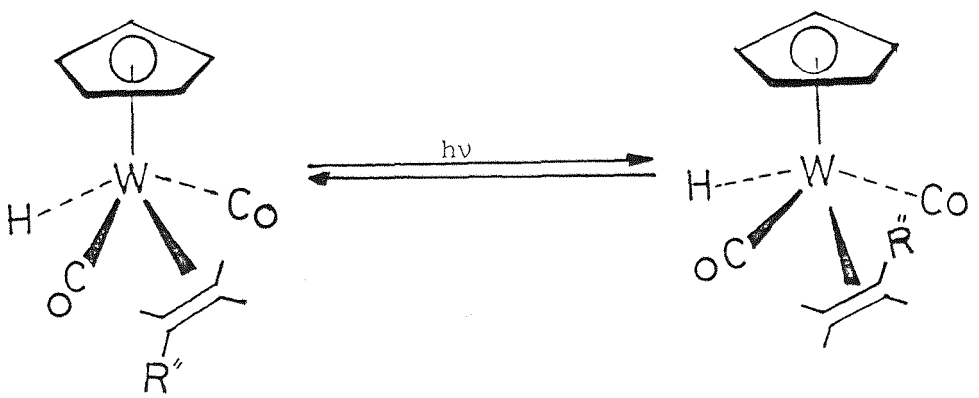

trans (II) *trans'* (III)

R" = CH_3, C_2H_5

radiation (λ = 310 - 370 nm) bands of $(\eta^5\text{-}C_5H_5)W(CO)_3H$ grew at the expense of those of the rotamers of $(\eta^5\text{-}C_5H_5)W(CO)_2(\underline{1}\text{-}C_3H_6)H$ and those of $(\eta^5\text{-}C_5H_5)W(CO)_2C_3H_7$.

Analogous results were obtained for $(\eta^5\text{-}C_5H_5)W(CO)_3(\underline{n}\text{-}C_3H_7)$ isolated in CO matrices except that bands due to $(\eta^5\text{-}C_5H_5)W(CO)_3H$ ((6) in Figure 4.3(d)) appeared after a much shorter period of irradiation. Similarly the photoreactions of $(\eta^5\text{-}C_5(CH_3)_3)W(CO)_3(\underline{n}\text{-}C_3H_7)$ and $(\eta^5\text{-}C_5H_5)W(CO)_3(\underline{n}\text{-}C_4H_9)$ in CH_4 and CO matrices followed the pattern described for $(\eta^5\text{-}C_5H_5)W(CO)_3(\underline{n}\text{-}C_3H_7)$ in CH_4. Infrared data for the new species are presented in (Table 4.2).

4.2.3 Photolysis of $(\eta^5\text{-}C_5H_5)W(CO)_3(\underline{i}\text{-}C_3H_7)$ in CH_4 and CO Matrices.

The infrared spectrum of $(\eta^5\text{-}C_5H_5)W(CO)_3(\underline{i}\text{-}C_3H_7)$ isolated at 12K in a CH_4 matrix before photolysis is analogous to those for other $(\eta^5\text{-}C_5R_5')W(CO)_3R$ complexes (Tables 4.1 and 4.2).

Irradiation of the matrix with long wavelength radiation (λ > 410 nm) for a similar length of time as that used initially for $(\eta^5\text{-}C_5H_5)W(CO)_3(\underline{n}\text{-}C_3H_7)$ produced bands due to 'free CO', pairs (1) - (5) seen previously for $(\eta^5\text{-}C_5H_5)W(CO)_3(\underline{n}\text{-}C_3H_7)$ (c.f. Figure 4.3b), and an additional band at 2024.2 cm^{-1} (c.f. (6) in Figure 4.3d). Further photolysis (λ > 370 nm) showed that the band at ca 1937 cm^{-1} grew out of proportion with the other band of the band (1) pair, i.e. there is another species with a band at 1937 cm^{-1}. Careful comparison of band intensities showed that the 1937 cm^{-1} band could be correlated with the band at 2024.2 cm^{-1} (6). The (6) pair can be identified as belonging to $(\eta^5\text{-}C_5H_5)W(CO)_3H$ by comparison with band position from separate experiments [21] (Table 4.1). In the experiments using CO matrices the production of $(\eta^5\text{-}C_5H_5)W(CO)_3H$ was even more predominant than for CH_4 matrices.

4.2.4 Photolysis of $(\eta^5\text{-}C_5H_5)W(CO)_3C_6H_5$ in CH_4, CO and 5% $^{13}CO/CH_4$ Doped Matrices

The infrared spectrum of $(\eta^5\text{-}C_5H_5)W(CO)_3C_6H_5$ isolated in a CH_4 matrix before irradiation is analogous to those for other $(\eta^5\text{-}C_5R_5')W(CO)_3R$ complexes (Figure 4.4a, Tables 4.1 and 4.2).

Irradiation of the matrices with long wavelength radiation (λ > 430 nm) produced new bands at 2138.0 ('free' CO), 1953.0 and 1869.7 cm^{-1} (Figure 4.4b, Table 4.3). A short period of higher energy irradiation (λ = 310 - 370 nm) produced marked increases in the new bands at the expense of the parent bands (Figure 4.4c). Irradiation then with longer wavelength radiation (λ > 490 nm) or annealing the matrix for 2 minutes to ca 30K caused the new product bands to decrease and those of the starting complex,

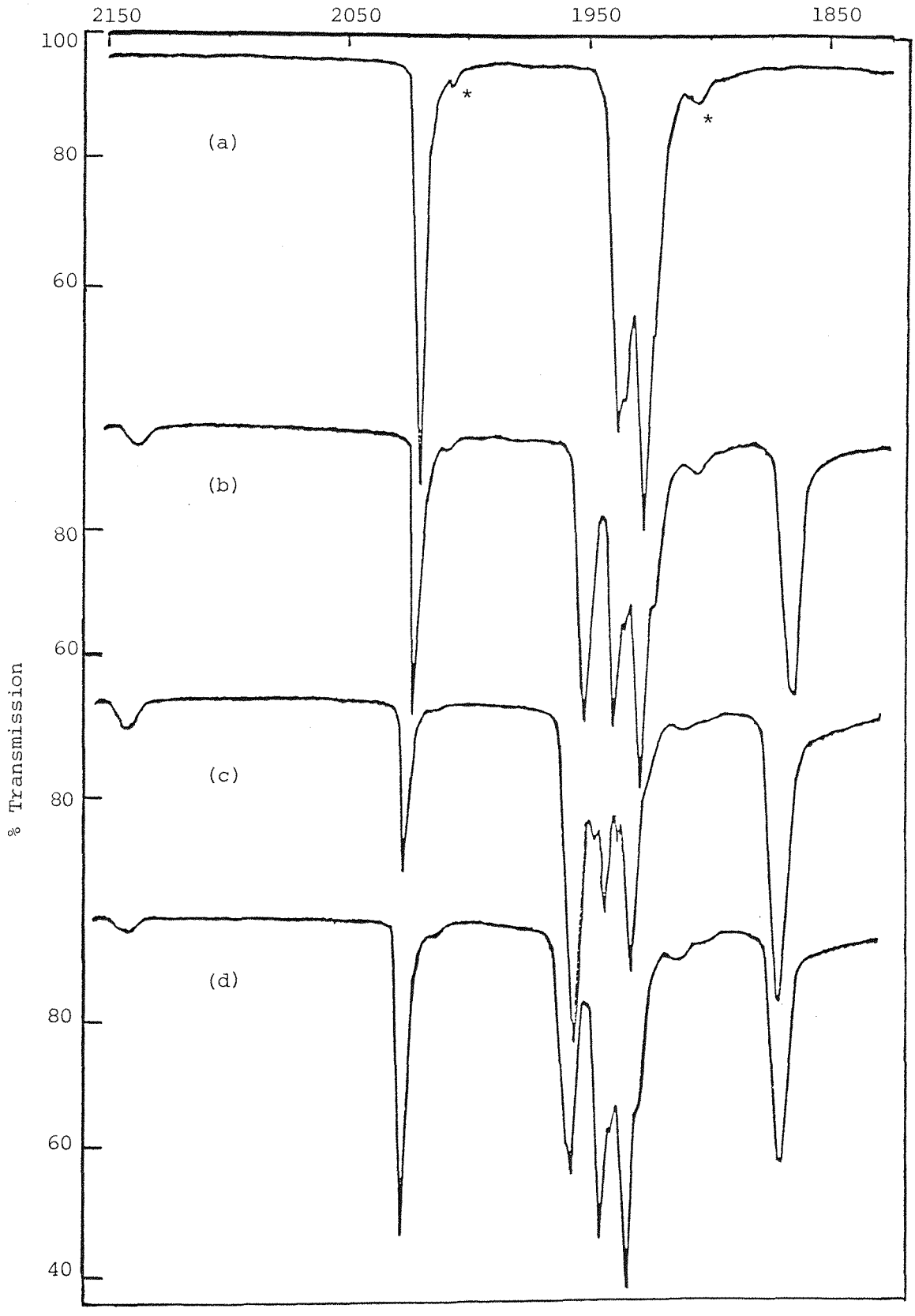

FIGURE 4.4 Infrared spectra from an experiment with $(\eta^5\text{-}C_5H_5)W(CO)_3C_6H_5$ isolated at high dilution in a CH_4 matrix at 12K: (a) after deposition, (b) after 30 min photolysis using $\lambda > 430$ nm, (c) after 5 min photolysis using $310 < \lambda < 370$ nm and (d) after 120 min photolysis using $\lambda > 530$ nm. Bands marked (*) are due to $(\eta^5\text{-}C_5H_5)W(^{12}CO)_2(^{13}CO)C_6H_5$ present in natural abundance.

$(\eta^5\text{-}C_5H_5)W(CO)_3C_6H_5$ to increase (Figure 4.4d). The relative intensity of the bands at 1955.0 and 1869.7 cm^{-1} remained constant under a variety of forward and reverse photolysis and annealing cycles indicating that the bands arose from a single product species. The dilution used, the absence of bands due to $[(\eta^5\text{-}C_5H_5)W(CO)_3]_2$ and the reversibility of the photoreaction enabled the new bands to be assigned to the 16-electron species $(\eta^5\text{-}C_5H_5)W(CO)_2C_6H_5$. This was confirmed using $(\eta^5\text{-}C_5H_5)W(^{12}CO)_n(^{13}CO)_{3-n}C_6H_5$ (see below). Analogous results were obtained for $(\eta^5\text{-}C_5H_5)W(CO)_3C_6H_5$ in CO matrices, i.e. an excess of CO does not prevent the photoejection of a CO ligand.

The i.r. spectrum of ^{13}CO-enriched $(\eta^5\text{-}C_5H_5)W(CO)_3C_6H_5$ (see Chapter 8) isolated in a CH_4 matrix showed bands due to the full range (n = 0 - 3) of $(\eta^5\text{-}C_5H_5)W(^{12}CO)_n(^{13}CO)_{3-n}C_6H_5$ species. A good correspondence was obtained between observed and calculated band positions using an energy-factored force-field fitting procedure [22] (Table 4.4).

Irradiation of the matrix with medium energy radiation ($\lambda > 410$ nm) gave new ^{13}CO-enriched product bands at 1936.3, 1910.2, 1839.1 and 1824.1 cm^{-1} in addition to the bands of the ^{12}CO species at 1954.0 and 1865.5 cm^{-1}. Subjecting these six bands to the energy-factored force-field fitting procedure gave an excellent fit for a $\underline{C_s}$ $W(CO)_2$ fragment (Table 4.4). Photoproducts produced with the liberation of 'free' CO and pairs of bands at ca 1950 and ca 1860 cm^{-1} can, therefore, be confidently assigned to structures $(\eta^5\text{-}C_5R_5')W(CO)_2R$.

The observed relative intensity of the two terminal CO bands for $(\eta^5\text{-}C_5H_5)W(CO)_2C_6H_5$, obtained by tracing and weighing the A' and A" bands from spectra run in absorbance units, was used to calculate a OC-W-CO bond angle of 90 ± 1° from the standard expression $I_{asymm}/I_{sym} = I_{A"}/I_{A'}$ (0.9966) $= \tan^2(\theta/2)$ [22].

4.2.5 Photolysis of $(\eta^5\text{-}C_5H_5)W(CO)_3C_6H_5$ in N_2 and 5% C_2H_4 Doped CH_4 Matrices

The infrared spectrum of $(\eta^5\text{-}C_5H_5)W(CO)_3C_6H_5$ isolated at high dilution in a 5% C_2H_4 doped CH_4 matrix shows very much broader bands than obtained in pure gas matrices (Figure 4.5a). The broadness of the bands is a common feature of all doped matrices and does not reflect a lack of isolation but rather that bulky substrate molecules are isolated in matrix cages with varying probabilities of dopant, orientations of substrate, and packing of host matrix molecules.

A period of photolysis of $(\eta^5\text{-}C_5H_5)W(CO)_3C_6H_5$ in a C_2H_4 doped CH_4 matrix using long wavelength radiation ($\lambda > 430$ nm) produced new bands at 2138.0, 1990.2, 1951.5 and 1861.5 cm^{-1} of which the band at 2138.0 cm^{-1} corresponds to CO liberated during photolysis (Figure 4.5b). A short period of higher energy photolysis ($\lambda > 370$ nm) caused all the product bands to increase while those of $(\eta^5\text{-}C_5H_5)W(CO)_3C_6H_5$ decreased (Figure 4.5c). Irradiation with much longer wavelength radiation ($\lambda > 490$ nm) (Figure 4.5d), or annealing the matrix to ca 30K (Figure 4.5e) revealed a band growing at 1922.5 cm^{-1} which was formerly obscurred by the bands of the parent molecule. Annealing the matrix also showed that the bands at 1951.5 and 1861.5 cm^{-1} (pair (1)) were not related to those at 1990.2 and 1922.5 cm^{-1} (pair (2)) because the former decreased in intensity whereas the latter increased, while there was little or no change in the intensities of the parent bands (Figure 4.5e). The more intense pair of bands, pair (2), (1951.5 and 1861.5 cm^{-1}, Figure 4.5b), which reversed on annealing and long wavelength photolysis, can be assigned to the coordinately unsaturated 16-electron species $(\eta^5\text{-}C_5H_5)W(CO)_2C_6H_5$ by comparison with those observed in CH_4 matrices (Table 4.3) and their analogous reversal behaviour. The pair of bands at higher wavenumbers, pair (1) (1990.2 and 1922.5 cm^{-1}, Figure 4.5e), are typical of a situation where a CO ligand has been replaced by another ligand, e.g. $(\eta^5\text{-}C_5H_5)Mo(CO)_2(N_2)CH_3$ (1969.7 and 1913.7 cm^{-1}) compared with $(\eta^5\text{-}C_5H_5)Mo(CO)_2CH_3$ (1972.8 and 1884.4 cm^{-1}) [18]. The bands can probably be assigned to the 18-electron species $(\eta^5\text{-}C_5H_5)W(CO)_2(C_2H_4)C_6H_5$. The band positions in the matrix (1990.2 and 1922.5 cm^{-1}) are,

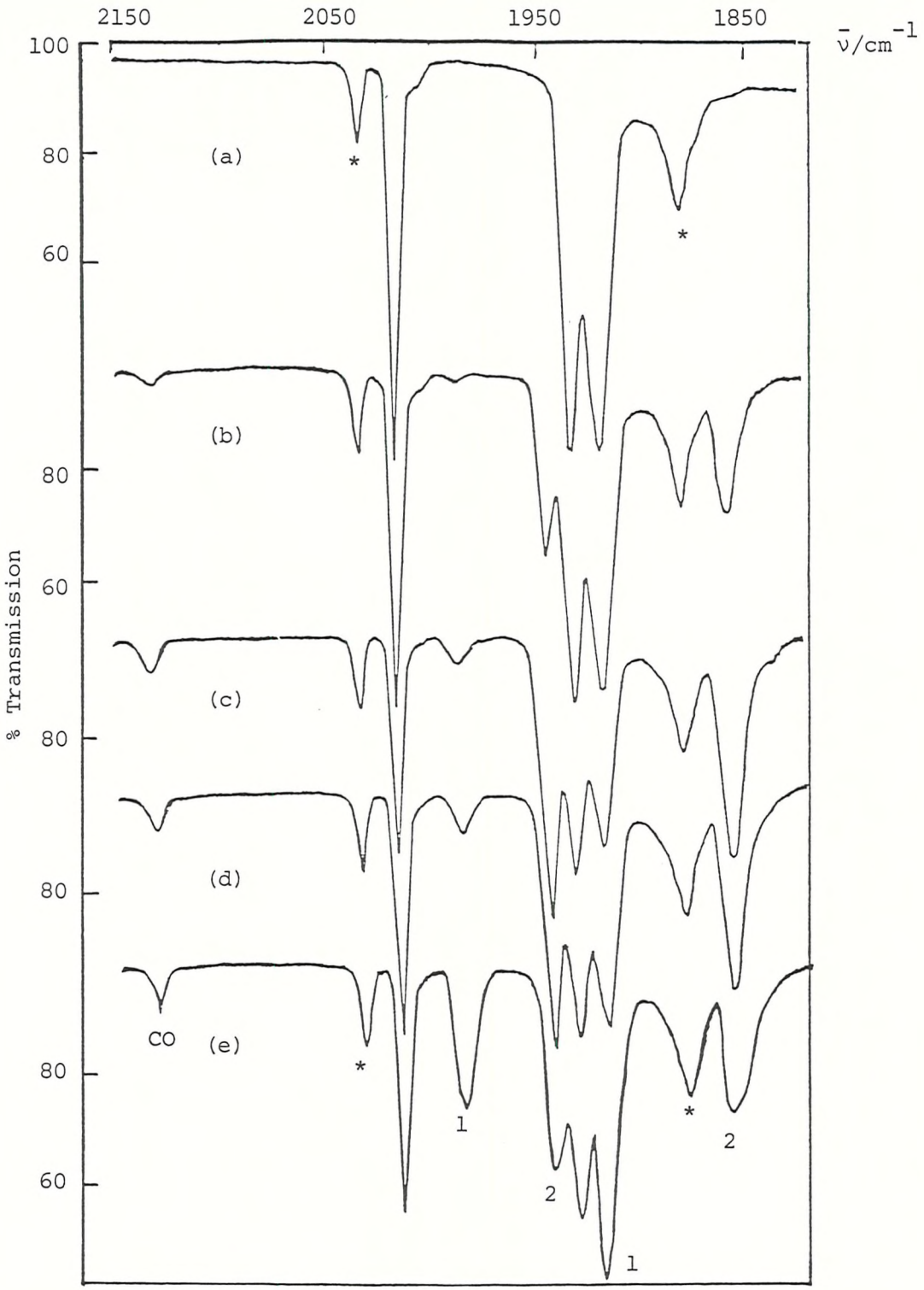

FIGURE 4.5 Infrared spectra from an experiment with $(\eta^5\text{-}C_5H_5)W(CO)_3C_6H_5$ isolated at high dilution in a 5% C_2H_4/CH_4 matrix at 12K: (a) after deposition, (b) after 45 min photolysis using $\lambda > 430$ nm, (c) after 2 min photolysis using $\lambda > 310$ nm, (d) after 120 min photolysis using $\lambda > 490$ nm and (e) after annealing the matrix to ca 30K for 2 min. Bands marked (*) are due to C_2H_4. Bands marked (1) and (2) arise from $(\eta^5\text{-}C_5H_5)W(CO)_2(C_2H_4)C_6H_5$ and $(\eta^5\text{-}C_5H_5)W(CO)_2C_6H_5$ respectively.

however, different from those of *trans*-$(\eta^5\text{-}C_5H_5)W(CO)_2(C_2H_4)C_6H_5$ observed in solution (1965 and 1883 cm^{-1} [31]. On the basis of other *cis* $\rightleftarrows$ *trans* isomers (see above) the bands at 1998.2 and 1922.5 cm^{-1} can be assigned to *cis*-$(\eta^5\text{-}C_5H_5)W(CO)_2(C_2H_4)C_6H_5$ because (a) the relative magnitude of the energy-factored CO interaction force constant for this species (53.5 Nm^{-1}) compared to that for the *trans* isomer (63.7 Nm^{-1}, solution), is similar to the relative magnitude of *cis* (46.9 Nm^{-1}) and *trans* (60.8 Nm^{-1}) interaction force constants for the isomers of $(\eta^5\text{-}C_5H_5)W(CO)_2(C_2H_4)H$ (Table 4.1), and (b) *cis* and *trans* isomers of $(\eta^5\text{-}C_5H_5)W(CO)_2$(olefin)H complexes are formed in matrices but only the *trans* isomers can be isolated as crystalline compounds.

Irradiation of $(\eta^5\text{-}C_5H_5)W(CO)_3C_6H_5$ in N_2 matrices with medium energy radiation ($\lambda > 430$ nm) produced two new strong bands at 1958.7 and 1873.6 cm^{-1}, which can be assigned to $(\eta^5\text{-}C_5H_5)W(CO)_2C_6H_5$ (see above and Table 4.3) and two weak bands at 1971.0 and 1902.3 cm^{-1}. Unfortunately the yield of these two bands was always low no matter what irradiation sources were employed. Comparison of these weak bands with those of $(\eta^5\text{-}C_5H_5)Mo(CO)_2(N_2)CH_3$ (see above) suggests that they may be assigned to the dinitrogen complex $(\eta^5\text{-}C_5H_5)W(CO)_2(N_2)C_6H_5$. Since NN stretching bands are always very much less intense than CO stretching bands it is perhaps not surprising that no new band in the 2200 cm^{-1} region could be observed, c.f. ν_{NN} at 2190.8 cm^{-1} for $(\eta^5\text{-}C_5H_5)Mo(CO)_2(N_2)CH_3$ [18].

Infrared data in the terminal CO stretching region for the new $(\eta^5\text{-}C_5H_5)W(CO)_2(C_2H_4)C_6H_5$ and $(\eta^5\text{-}C_5H_5)W(CO)_2(N_2)C_6H_5$ species is presented in Table 4.3

4.2.6 Photolysis of $(\eta^5\text{-}C_5H_5)W(CO)_3CH_2C_6H_5$ in CH_4, N_2, CO, 5% C_2H_4/CH_4 and of $(\eta^5\text{-}C_5H_5)W(CO)_3C_3H_5$ in CH_4 Matrices

Irradiation of $(\eta^5\text{-}C_5H_5)W(CO)_3(CH_2C_6H_5)$ in CH_4 and CO matrices produced analogous results to those described above for $(\eta^5\text{-}C_5H_5)W(CO)_3C_6H_5$, i.e. there was no evidence for the hydrides $(\eta^5\text{-}C_5H_5)W(CO)_2$(olefin)H and $(\eta^5\text{-}C_5H_5)W(CO)_3(H)$. There were, however, four new bands (not illustrated) at

1946.3, 1941.4, 1871.3 and 1859.5 cm^{-1} for species derived from $(\eta^5\text{-}C_5H_5)W(CO)_3CH_2C_6H_5$, in addition to a band due to 'free' CO, whereas only two new bands were observed in experiments starting from $(\eta^5\text{-}C_5H_5)W(CO)_3C_6H_5$. The four bands grew under various types of irradiation in such a way that two pairs could be identified: (1) at 1946.3 and 1871.3 cm^{-1} and (2) at 1941.4 and 1859.5 cm^{-1} of which the latter pair was much more intense. Surprisingly there was no reversal of the forward photolysis step on long wavelength irradiation ($\lambda > 530$ nm). The fact that two distinct species were involved was deduced from observations that the (1) pair and (2) pair had different relative intensities at various stages of irradiation and that the separation of the lower pair of bands (ca 12 cm^{-1}) is rather large for a matrix splitting (0 - 8 cm^{-1}).

The more intense pair of bands, pair (1) (1941.4 and 1859.5 cm^{-1}), are at similar positions to the bands of $(\eta^5\text{-}C_5H_5)W(CO)_2C_6H_5$ (1955.0 and 1869.7 cm^{-1}) and those of other 16-electron $(\eta^5\text{-}C_5R_5')W(CO)_2R$ species (Tables 4.1 and 4.2). The pair (1) bands, which grow with the growth of the band due to 'free' CO, can, therefore, be assigned to the coordinatively unsaturated 16-electron species $(\eta^5\text{-}C_5H_5)W(CO)_2(CH_2C_6H_5)$. There are two possible explanations for pair (2): (i) another conformation of an $\eta^1\text{-}CH_2C_6H_5$ ligand has been frozen out or (ii) the $CH_2C_6H_5$ ligand has changed its mode of coordination from a σ-bonded $\eta^1\text{-}CH_2C_6H_5$ to a π-bonded $\eta^3\text{-}CH_2C_6H_5$ configuration. Precedent for the latter type of bonding comes from the fact that $(\eta^5\text{-}C_5H_5)W(CO)_2(\eta^3\text{-}CH_2C_6H_5)$ is a known compound which has band positions (1952 and 1878 cm^{-1}, solution) [7] which are identical to those of pair (2) (1946.3 and 1871.3 cm^{-1}) if a 6 cm^{-1} solvent shift is allowed for. It seems most reasonable to assign the (2) pair of bands to $(\eta^5\text{-}C_5H_5)W(CO)_2(\eta^3\text{-}CH_2C_6H_5)$ especially since this is the major product formed when $(\eta^5\text{-}C_5H_5)W(CO)_3(\eta^1\text{-}CH_2C_6H_5)$ is photolysed in pentane solution (see Section 4.3). The same two product species were formed when $(\eta^5\text{-}C_5H_5)W(CO)_3(CH_2C_6H_5)$ was irradiated in CO and Ar matrices at 12K. The $\eta^1 \rightarrow \eta^3$ rearrangement process of $(\eta^5\text{-}C_5H_5)W(CO)_3(\eta^1\text{-}CH_2C_6H_5)$ complex is furthermore demonstrated by photolysis of the $(\eta^5\text{-}C_5H_5)W(CO)_3(\eta^1\text{-}C_3H_5)$ complex in CH_4 matrices.

The infrared spectrum of $(\eta^5\text{-}C_5H_5)W(CO)_3(\eta^1\text{-}C_3H_5)$ isolated in a CH_4 matrix (Figure 4.6) is very similar to that of $(\eta^5\text{-}C_5H_5)W(CO)_3(\eta^1\text{-}CH_2C_6H_5)$ complex. Before photolysis the spectrum shows three strong bands in the terminal CO stretching region at 2019.3, 1934.0 and 1924.8 cm^{-1} (Figure 4.6a and Table 4.3). Irradiation with (λ > 370 nm) produced four new bands at 1960.2, 1951.8, 1882.5 and 1886.5 cm^{-1} (Figure 4.6b) and the band of free CO at 2138 cm^{-1}. A further period of irradiation with (λ > 370 nm) caused an increase in free CO, increases in all the new bands, and a decrease in the bands due to the starting material $(\eta^5\text{-}C_5H_5)W(CO)_3(\eta^1\text{-}C_3H_5)$ (Figure 4.6c). The bands were demonstrated to belong to two different species by annealing and long wavelength photolysis experiments. The two bands at 1951.8 and 1866.5 cm^{-1} (bands (1)) can be assigned to the unsaturated 16-electron species $(\eta^5\text{-}C_5H_5)W(CO)_2(\eta^1\text{-}C_3H_5)$, by analogy with $(\eta^5\text{-}C_5R'_5)M(CO)_2R$ species, while the two bands at 1960.2 and 1882.5 cm^{-1} (bands (2)) may be identified with the saturated 18-electron species $(\eta^5\text{-}C_5H_5)W(CO)_2(\eta^3\text{-}C_3H_5)$, by comparison with solution data (1960 and 1880 cm^{-1}) [34]. Irradiation with u.v. light (λ = 320 - 390 nm) caused decreases in the bands due to the $(\eta^5\text{-}C_5H_5)W(CO)_2(\eta^3\text{-}C_3H_5)$ complex, and increases in the bands due to the 16-electron intermediate (Figure 4.6d and 4.6e).

No new bands assignable to $(\eta^5\text{-}C_5H_5)W(CO)_2(C_2H_4)(CH_2C_6H_5)$ and $(\eta^5\text{-}C_5H_5)W(CO)_2(N_2)(CH_2C_6H_5)$ species were observed when $(\eta^5\text{-}C_5H_5)W(CO)_3(CH_2C_6H_5)$ was photolysed in 5% C_2H_4 doped CH_4 and N_2 matrices respectively.

Infrared data in the terminal CO stretching region for all the new species is presented in (Table 4.3).

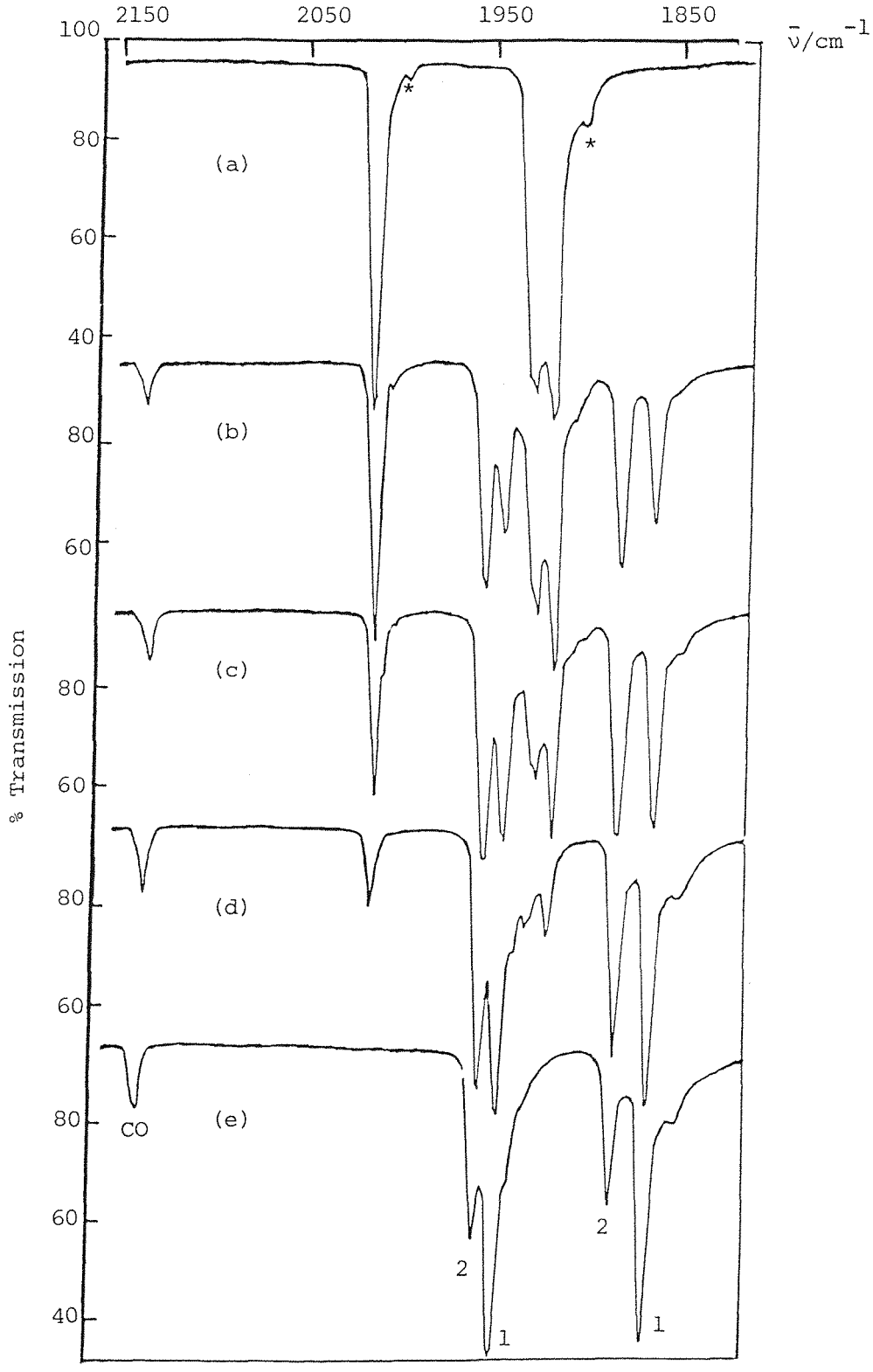

FIGURE 4.6 Infrared spectra from an experiment with $(\eta^5\text{-}C_5H_5)W(CO)_3(\eta^1\text{-}C_3H_5)$ isolated at high dilution in a CH_4 matrix at 12K: (a) after deposition, (b) after 10 min photolysis using $\lambda > 370$ nm, (c) after further 15 min photolysis with $\lambda > 370$ nm, (d) after 20 min photolysis using $\lambda = 320 - 390$ nm, and (e) after further 25 min photolysis with $\lambda = 320 - 390$ nm. Bands marked with (*) are due to $(\eta^5\text{-}C_5H_5)W(^{12}CO)_2(^{13}CO)(\eta^1\text{-}C_3H_5)$ in natural abundance. Bands marked (1) and (2) derive from photoproducts (see text).

4.3 DISCUSSION AND COMPARISON OF SOLUTION* AND MATRIX PHOTOCHEMISTRY

In the $(\eta^5\text{-}C_5R_5')M(CO)_3R$ complexes the dissociation energy of the transition metal carbon σ-bond is comparable with the bond strength of the metal carbonyl-carbon bond as determined calorimetrically [23]. In principle, therefore, both M-R and M-CO bonds could be cleaved by ultraviolet radiation ($\lambda > 300$ nm). The combination of solution and matrix isolation studies should provide a complete understanding of the mechanisms of the photo-induced CO substitution, de-alkylation and de-arylation reactions of $(\eta^5\text{-}C_5R_5')M(CO)_3R$ complexes because both final products and intermediates can be characterised.

The photoreactions of the $(\eta^5\text{-}C_5R_5')M(CO)_3R$ complexes (M = Mo, R = C_2H_5, R' = H; M = W, R = C_2H_5, n-C_3H_7, n-C_4H_9, i-C_3H_7, R' = H; M = W, R = n-C_3H_7, R' = CH_3) at high dilution in CH_4 and CO matrices are summarised in Scheme 4.1. The primary photoprocess in all cases is the ejection of a CO ligand. The resulting coordinatively unsaturated 16-electron species $(\eta^5\text{-}C_5R_5')M(CO)_2R$ can be identified in CH_4 and CO matrices at 12 - 30K and in paraffin wax matrices at 77K (M = Mo, W; R = CH_3, C_2H_5, n-C_5H_{11}; R' = H, CH_3) [11, 12] but not in n-pentane solutions at -30°C.

The fragments $(\eta^5\text{-}C_5R'_5)M(CO)_2R$ do not readily recombine with photo-ejected CO at 12K to reform the starting complexes $(\eta^5\text{-}C_5R'_5)M(CO)_3R$ (Equation 4.5); this is in striking contrast to the behaviour of $(\eta^5\text{-}C_5H_5)M(CO)_2CH_3$ fragments (M = Mo, W) [11, 12, 18, 19]. Instead the formation of the olefin-hydrido complexes $(\eta^5\text{-}C_5R'_5)M(CO)_2$(olefin)H is observed, i.e.

---

*Solution photochemical reactions performed by Dr. H.G. Alt of the University of Bayreuth, West Germany.

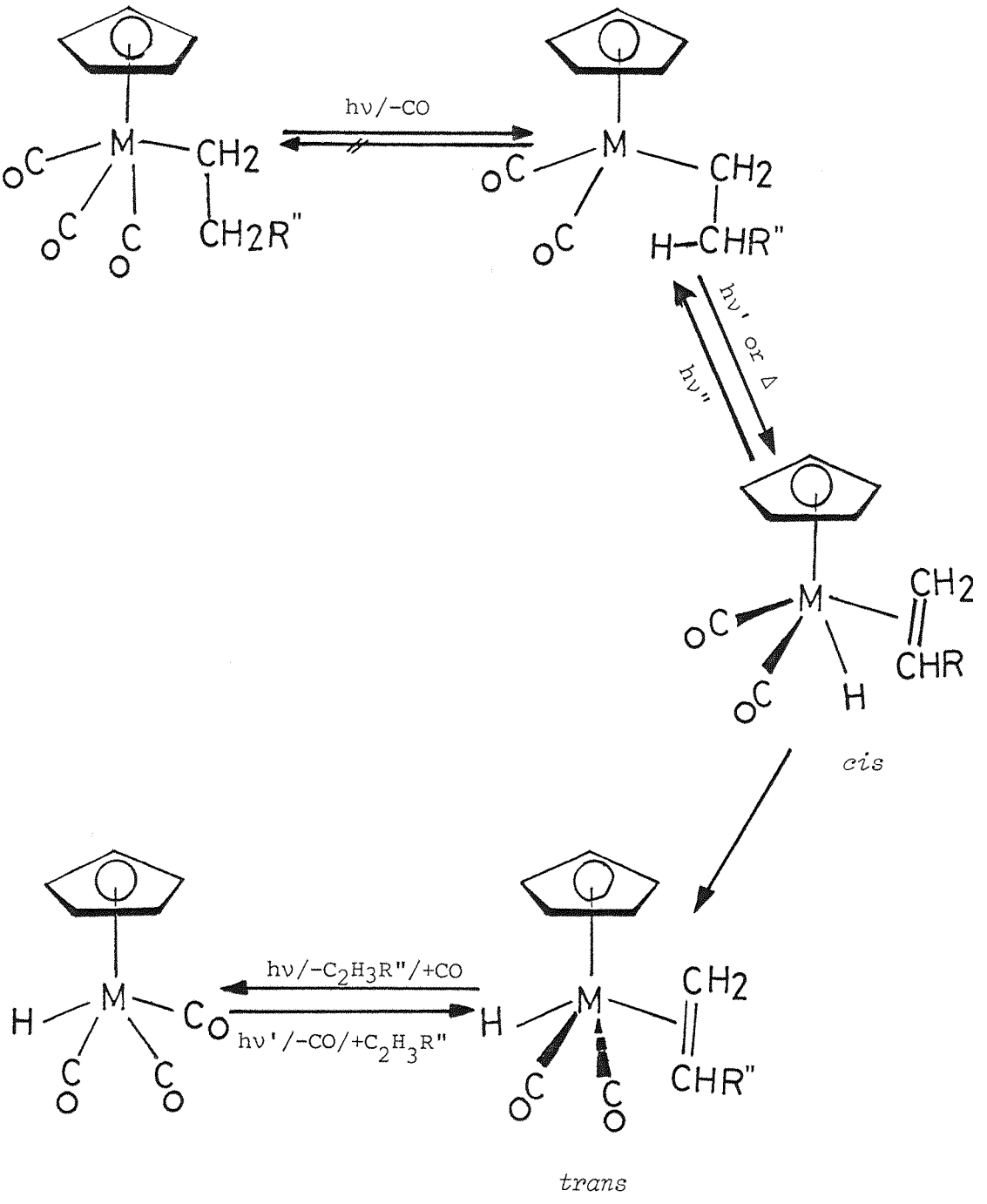

Scheme 4.1

M = Mo, R" = H

M = W, R" = H, CH_3, C_2H_5

$$(\eta^5\text{-}C_5H_5)M(CO)_3R \xrightarrow[\text{R > CH}_3]{h\nu/\text{-CO}} (\eta^5\text{-}C_5H_5)M(CO)_2R \qquad (4.5)$$

β-hydrogen transfer is a more favoured process than re-combination with photo-ejected CO. The growth and decay of the i.r. bands of $(\eta^5\text{-}C_5R'_5)M(CO)_2R$ and $(\eta^5\text{-}C_5R'_5)M(CO)_2(\text{olefin})H$ species suggests that there is a reversible reaction (Equation 4.6).

$$(\eta^5\text{-}C_5R'_5)M(CO)_2R \underset{h\nu'}{\overset{h\nu}{\rightleftharpoons}} (\eta^5\text{-}C_5R'_5)M(CO)_2(\text{olefin})H \qquad (4.6)$$

This was confirmed in separate experiments with $(\eta^5\text{-}C_5H_5)W(CO)_2(C_2H_4)H$ isolated in matrices at 12K when the formation of $(\eta^5\text{-}C_5H_5)W(CO)_2C_2H_5$ was observed [21].

It is important to note that in low temperature matrices at 12K both *cis* and *trans* isomers of $(\eta^5\text{-}C_5H_5)W(CO)_2(\text{olefin})H$ complexes can be observed. In the tungsten complex the photo-assisted isomerisation of ethylene-hydride complex is proposed to proceed as in Equations (4.7 - 4.9).

$$(\eta^5\text{-}C_5H_5)W(CO)_3C_2H_5 \xrightleftharpoons{h\nu/\text{-CO}} (\eta^5\text{-}C_5H_5)W(CO)_2C_2H_5 \qquad (4.7)$$

$$(\eta^5\text{-}C_5H_5)W(CO)_2C_2H_5 \xrightleftharpoons{h\nu} \textit{cis}\text{-}(\eta^5\text{-}C_5H_5)W(CO)_2(C_2H_4)H \qquad (4.8)$$

$$\textit{cis}\text{-}(\eta^5\text{-}C_5H_5)W(CO)_2(C_2H_4)H \longrightarrow \textit{trans}\text{-}(\eta^5\text{-}C_5H_5)W(CO)_2(C_2H_4)H \qquad (4.9)$$

In solution [10] and even in paraffin wax matrices at 77K [11, 12], however, only the *trans* isomer could be detected. The fact that $(\eta^5\text{-}C_5H_5)Mo(CO)_2(C_2H_4)H$ could only be detected as the *trans* isomer even at 12K reveals that the *cis* ⟶ *trans* isomerisation proceeds more rapidly and has a lower

activation energy barrier for Mo than for W. In all cases the formation of the *cis* isomer may be considered to be the first step; this was axiomatically assumed in the work of Kazlauskas and Wrighton [11, 12] although they detected only *trans*-$(\eta^5\text{-}C_5H_5)M(CO)_2(olefin)H$.

The hydride complexes $(\eta^5\text{-}C_5H_5)M(CO)_3H$ are generated by photo-substitution reaction of olefin by carbon monoxide in CO matrices, (Equation 4.10).

$$(\eta^5\text{-}C_5H_5)M(CO)_2(olefin)H + CO \xrightarrow[\text{-olefin}]{h\nu} (\eta^5\text{-}C_5H_5)M(CO)_3H \qquad (4.10)$$

Consistent with the mechanistic proposal represented by (Equations 4.7 - 4.9), we find that photolysis of $(\eta^5\text{-}C_5H_5)M(CO)_3H$ (M = Mo, W) complexes in 5% C_2H_4/CH_4 matrices yields the same products via reaction of the 16-electron intermediate $(\eta^5\text{-}C_5H_5)M(CO)_2H$ with C_2H_4 (see Chapter 3). This is consistent with the formation of $(\eta^5\text{-}C_5H_5)W(CO)_2(1\text{-pentene})H$ on irradiation of $(\eta^5\text{-}C_5H_5)W(CO)_3H$ in neat 1-pentene [11]. In solution the $(\eta^5\text{-}C_5R'_5)M(CO)_3H$ complexes can be photolysed to produce $[(\eta^5\text{-}C_5H_5)M(CO)_3]_2$ and H_2 or can react photochemically with unreacted starting material, $(\eta^5\text{-}C_5R_5')M(CO)_3R$, to give $[(\eta^5\text{-}C_5R_5')M(CO)_3]_2$ and the free alkane RH [21] (Scheme 4.2).

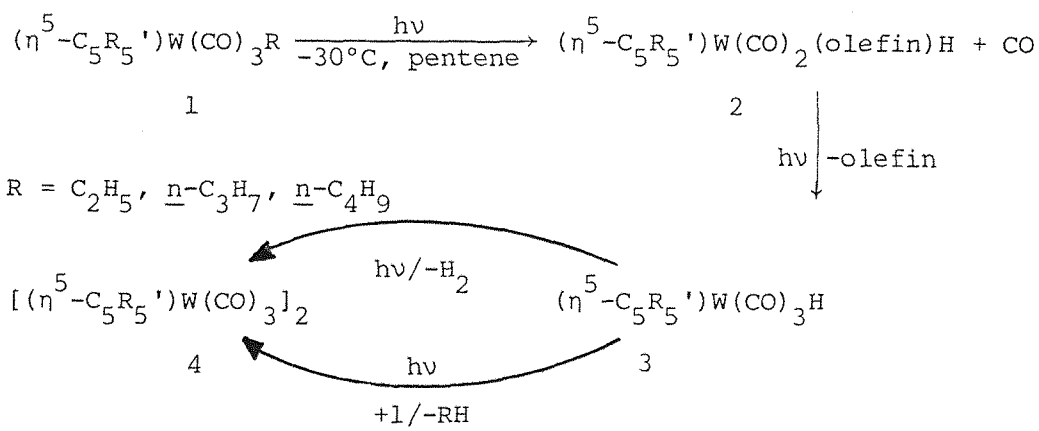

Scheme 4.2

The main organic photoproducts (see Scheme 4.2) were the olefins and free alkanes RH in the approximate ratio 3:1 together with a little CO and H_2.

In the cases of olefin-hydrido complexes with asymmetric olefins, e.g. $(\eta^5\text{-}C_5H_5)W(CO)_2(1\text{-}C_3H_6)H$ and $(\eta^5\text{-}C_5H_5)W(CO)_2(\underline{1}\text{-}C_4H_8)H$, the situation becomes more complicated because the *cis* and *trans* isomers can exist as rotamers, e.g. *cis* and *cis'* or *trans* and *trans'*. In fact all these four forms exist in an additional configuration, e.g. the *cis'* has a counterpart *cis"* with R" pointing away from the CO ligand. In theory it is possible to differentiate (Figure 4.3, Table 4.2) between R" near to H or to CO but, it was not feasible to assign whether R" was towards or away from H or CO in a particular species. In the solution studies two rotamers, (II) and (III), of the *trans* isomers can be observed and characterised at -80°C by ^1H and ^{13}C n.m.r. spectroscopy [31]. The barrier for the intramolecular rotation of the $\underline{1}$-propene and $\underline{1}$-butene ligands around the tungsten-olefin bond axis ($\Delta G^{\neq} \cong 50$ kJoule mol^{-1} in toluene-d_8) is approximately in the same range as that for the rotation of the C_2H_4 ligands in $(\eta^5\text{-}C_5H_5)W(CO)_2(C_2H_4)H$ and $(\eta^5\text{-}C_5H_5)W(CO)_2(C_2H_4)CH_3$ [24, 25]. Such a barrier indicates very strong metal-olefin back donation. In this situation the bonding may approximate to a metallocycle (IV) rather than the more conventional Chatt-Dewar representation (V). A metallocycle resonance form is suggested by the presence of $^{183}W\text{-}^{13}C$ (α) coupling constants ($J_{W,C}$ = 29 Hz) [25, 26] that are typical for W-C σ-bonds. The conversion of the olefin-hydrido species $(\eta^5\text{-}C_5R_5')M(CO)_2(\text{olefin})H$ to the coordinatively unsaturated species $(\eta^5\text{-}C_5R_5')M(CO)_2R$ ($\lambda > 370$ nm; CH_4 matrix) by olefin insertion is interesting because such a process is postulated as a step in the hydroformylation of olefins catalysed by metal carbonyl hydrides [27, 28].

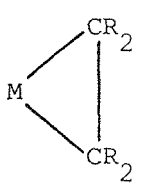

(IV)

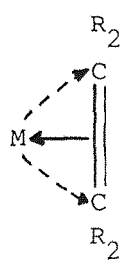

(V)

In the series of alkyl complexes $(\eta^5\text{-}C_5H_5)M(CO)_3R$ (R = alkyl) the *iso*-propyl derivative is noteworthy because of the very rapid appearance of bands due to $(\eta^5\text{-}C_5H_5)W(CO)_3H$ on photolysis, while there are modest yields of the $(\eta^5\text{-}C_5H_5)W(CO)_2(\underline{i}\text{-}C_3H_7)$ and $(\eta^5\text{-}C_5H_5)W(CO)_2(\underline{1}\text{-}C_3H_6)H$ species. Solution photolysis did not produce any $(\eta^5\text{-}C_5H_5)W(CO)_2(\underline{1}\text{-}C_3H_6)H$ but only $(\eta^5\text{-}C_5H_5)W(CO)_3H$. Since $(\eta^5\text{-}C_5H_5)W(CO)_3(\underline{i}\text{-}C_3H_7)$ has six hydrogens in the β-position of the alkyl ligand it should be a more favourable candidate for β-elimination than the $\underline{n}\text{-}C_3H_7$ derivative which has only two β hydrogens. Marks *et al.* [29, 30] have shown that $(\eta^5\text{-}C_5H_5)_3Th(\underline{i}\text{-}C_3H_7)$ can be readily photolysed in solution to give good yields of the complex $(\eta^5\text{-}C_5H_5)_3Th$. The organic products were propane and propene. When the reaction was carried out in frozen benzene the yields of propane and propene on thawing were in the ratio 26:74. In these reactions β-hydrogen transfer was considered to be the key process but no olefin-hydrido species could be detected. In the case of $(\eta^5\text{-}C_5H_5)W(CO)_3(\underline{i}\text{-}C_3H_7)$ the rapid generation of $(\eta^5\text{-}C_5H_5)W(CO)_3H$ is possibly caused by efficient generation of the olefin-hydrido species $(\eta^5\text{-}C_5H_5)W(CO)_2(\underline{1}\text{-}C_3H_6)H$ followed by secondary photolysis which photo-ejects $1\text{-}C_3H_6$ and adds a CO ligand.

In contrast to the alkyl complexes, the aryl complexes $(\eta^5\text{-}C_5H_5)W(CO)_3C_6H_5$ and $(\eta^5\text{-}C_5H_5)W(CO)_3(CH_2C_6H_5)$ do not undergo β-elimination reactions either in solution or in matrices. The complexes do, however, show photo-ejection of CO ligands to give $(\eta^5\text{-}C_5H_5)W(CO)_2C_6H_5$ and $(\eta^5\text{-}C_5H_5)W(CO)_2\text{-}(\eta^1\text{-}CH_2C_5H_5)$. A ^{13}CO-labelling study of $(\eta^5\text{-}C_5H_5)W(CO)_3C_6H_5$ established beyond doubt the formation of the coordinatively unsaturated 16-electron species $(\eta^5\text{-}C_5H_5)W(CO)_2C_6H_5$ in this case and for $(\eta^5\text{-}C_5R_5')M(CO)_2R$ species in general. The reactivity of the $(\eta^5\text{-}C_5H_5)W(CO)_2C_6H_5$ species was demonstrated by its ready recombination with CO, and its reaction with N_2 and C_2H_4 ligands. Surprisingly $(\eta^5\text{-}C_5H_5)W(CO)_2(\eta^1\text{-}CH_2C_6H_5)$ did not show reactions with N_2 and C_2H_4. In solution the photolysis of $(\eta^5\text{-}C_5H_5)W(CO)_3C_6H_5$ alone leads to the formation of $[(\eta^5\text{-}C_5H_5)W(CO)_3]_2$ and benzene, which presumably arises via hydrogen abstraction from the solvent or from a $\eta^5\text{-}C_5H_5$ ring [31] (Equation 4.11).

$$(\eta^5\text{-}C_5H_5)W(CO)_3C_6H_5 \xrightarrow[\text{pentane}]{h\nu} [(\eta^5\text{-}C_5H_5)W(CO)_3]_2 + C_6H_6 \qquad (4.11)$$

Evidence that β-hydrogen may be abstracted from an aryl ligand is provided by $(\eta^5\text{-}C_5H_5)_2Ti(C_6H_5)_2$ or its C_6D_5 analogue where either Ti or the phenyl ligand abstracts an *ortho* hydrogen to give benzene [32], (Equation 4.12).

$$(\eta^5\text{-}C_5H_5)_2Ti(C_6D_5)_2 \xrightarrow{C_6H_6,\ 80°C} (\eta^5\text{-}C_5H_5)_2Ti(C_6D_4) + C_6D_6 \qquad (4.12)$$

An interesting feature of the matrix photochemistry of the $(\eta^5\text{-}C_5H_5)W(CO)_3(\eta^1\text{-}C_3H_5)$ and $(\eta^5\text{-}C_5H_5)W(CO)_3(\eta^1\text{-}CH_2C_6H_5)$ complexes, was the observation of additional bands besides those assigned to the 16-electron species $(\eta^5\text{-}C_5H_5)W(CO)_2(\eta^1\text{-}C_3H_5)$ and $(\eta^5\text{-}C_5H_5)W(CO)_2(\eta^1\text{-}CH_2C_6H_5)$. In view of the fact that $(\eta^5\text{-}C_5H_5)W(CO)_2(\eta^3\text{-}C_3H_5)$ [33 - 35] and $(\eta^5\text{-}C_5H_5)W(CO)_2(\eta^3\text{-}CH_2C_6H_5)$ [7, 31] complexes are both well characterised in solution, the additional bands in low temperature matrices may be assigned to the formation of the π-allyl species. Therefore, irradiation of the allyl and benzyl complexes of $(\eta^5\text{-}C_5H_5)W(CO)_3(\eta^1\text{-}R)$ (R = C_3H_5 or $CH_2C_6H_5$) in gas matrices leads to isomerisation of the $\eta^1 \longrightarrow \eta^3$ in a reversible process (Equations 4.13, 4.14).

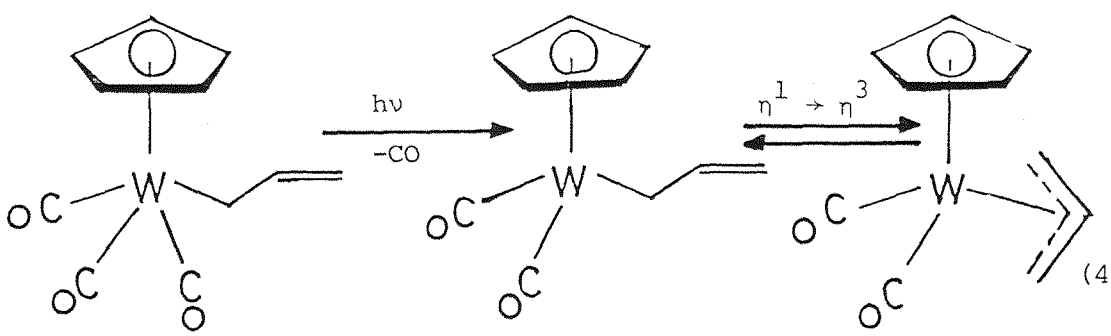

(4.13)

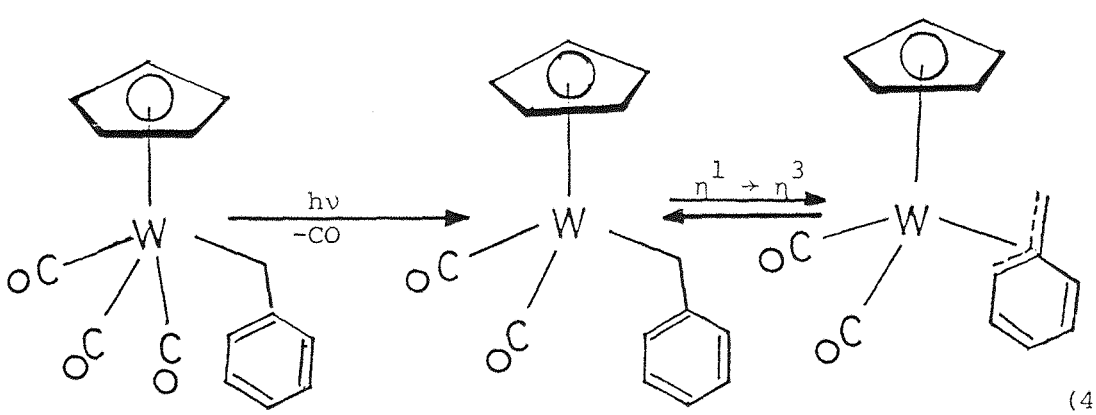

(4.14)

Similary Wrighton et al. [36], demonstrated that irradiation of $(\eta^5\text{-}C_5H_5)W(CO)_3CH_2CH_2C_6H_5$ leads to a blue 16-electron species at 77K which gives *trans*-$(\eta^5\text{-}C_5H_5)W(CO)_2$(styrene)H upon warming. The styrene-hydride rearranges slowly at 300K to form $(\eta^5\text{-}C_5H_5)W(CO)_2(\eta^3\text{-}CH(CH_3)C_6H_5)$ (Scheme 4.3).

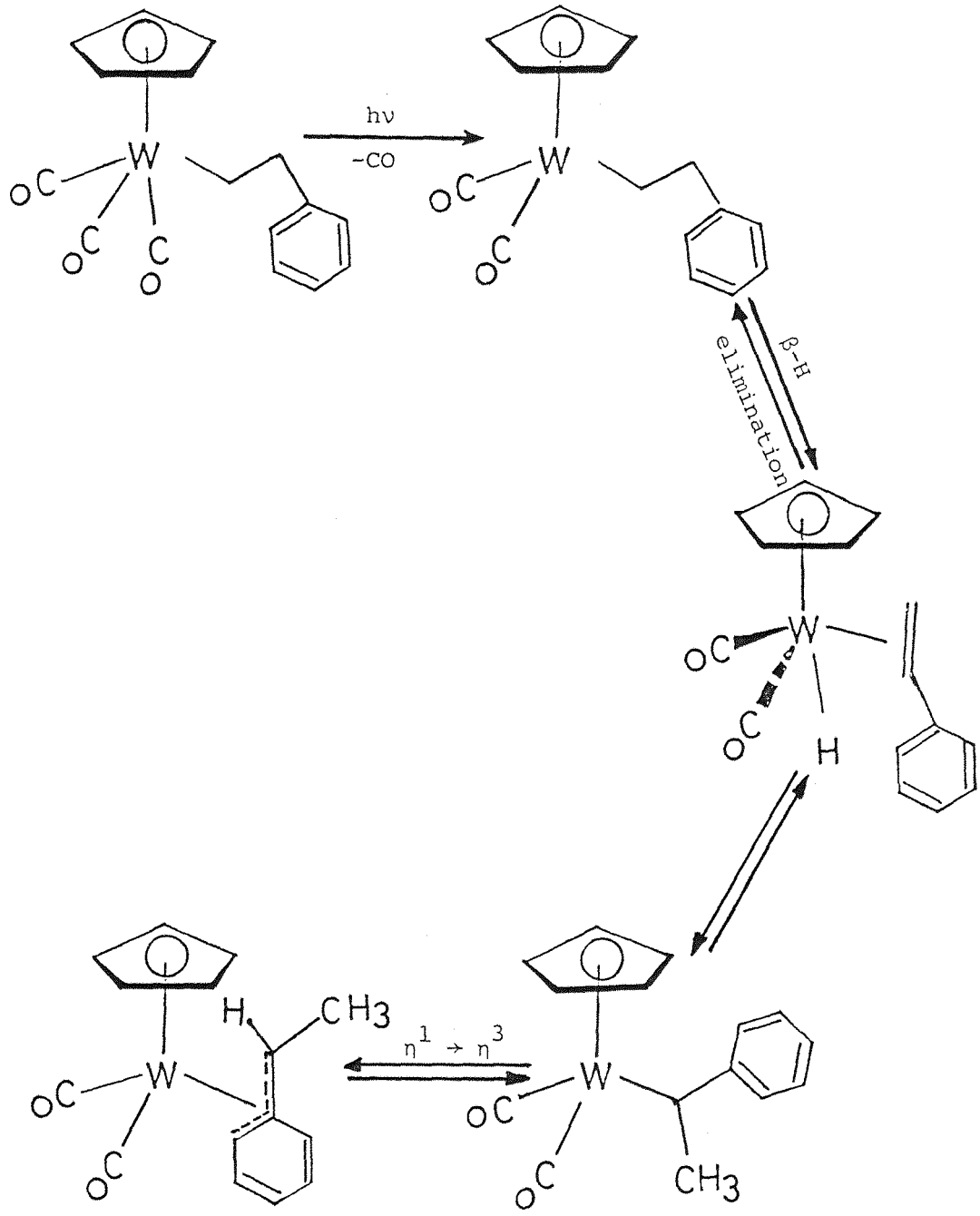

Scheme 4.3

In this case β-hydrogen migration is involved and the $\eta^1 \longrightarrow \eta^3$ process is reversible. The complex $(\eta^5\text{-}C_5H_5)W(CO)_2(\eta^3\text{-}CH(CH_3)C_6H_5)$ was also characterised from irradiation of $(\eta^5\text{-}C_5H_5)W(CO)_3H$ and styrene [37]. In previous work [38, 39] the presence of four carbonyl stretching bands in the i.r. spectrum of $(\eta^5\text{-}C_5H_5)Mo(CO)_2(\eta^3\text{-}C_3H_4R)$ (R = H or CH_3) was taken to suggest the existence of two different rotamers (VI and VII) in solution (Equation 4.15).

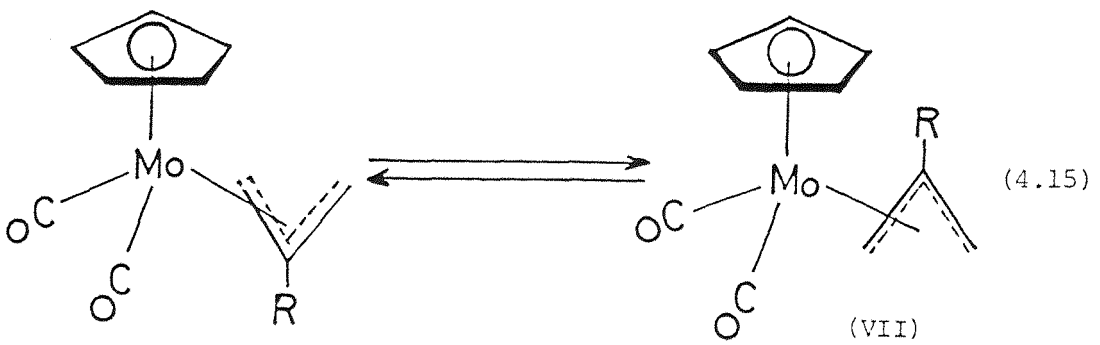

(VI) (VII) (4.15)

Similarly the *endo* isomer of $(\eta^5\text{-}C_5H_5)Ru(CO)(\eta^3\text{-}C_3H_5)$ thermally re-arranges to the more stable *exo* isomer [40], (Equation 4.16).

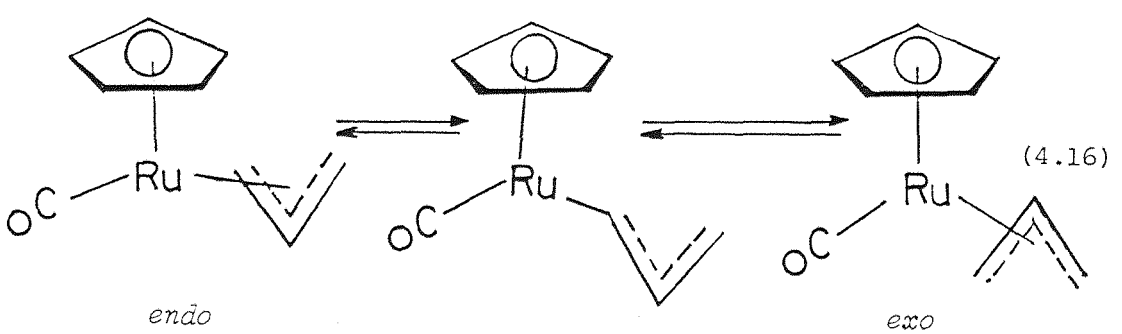

endo *exo* (4.16)

However, in the matrix it is not clear if the $(\eta^5\text{-}C_5H_5)W(CO)_2(\eta^3\text{-}R)$ (R = C_3H_5, $CH_2C_6H_5$) can exist in two rotamers, because the two strong bands attributed to these complexes are broad.

In contrast to the $(\eta^5\text{-}C_5H_5)W(CO)_3C_6H_5$ complex, irradiation of the $(\eta^5\text{-}C_5H_5)W(CO)_3(\eta^1\text{-}R)$ (R = C_3H_5, $CH_2C_6H_5$) complexes in the presence of the external ligands, e.g. N_2 or C_2H_4 did not lead to photosubstitution but rather to isomerisation. Irradiation of a cyclohexane solution of $(\eta^5\text{-}C_5H_5)W(CO)_3(\eta^1\text{-}CH_2C_6H_5)$ results in the formation of $(\eta^5\text{-}C_5H_5)W(CO)_2(\eta^3\text{-}CH_2C_6H_5)$ as the major photoproduct and of $[(\eta^5\text{-}C_5H_5)W(CO)_3]_2$ as the minor one [7]. Irradiation of $(\eta^5\text{-}C_5H_5)W(CO)_3(\eta^1\text{-}CH_2C_6H_5)$ in pentane solution in presence of C_2H_4 ligand gave primarily the $(\eta^5\text{-}C_5H_5)W(CO)_2(\eta^3\text{-}CH_2C_6H_5)$ and small amount of $(\eta^5\text{-}C_5H_5)W(CO)_2(C_2H_4)(\eta^1\text{-}CH_2C_6H_5)$ [31].

4.4 CONCLUSIONS

A combination of studies in solution at 243K and in gas matrices at 12K has confirmed that the primary step in the photoreactions of $(\eta^5\text{-}C_5R_5')M(CO)_3R$ (R = alkyl and aryl) complexes is the ejection of a CO ligand in agreement with studies using paraffin matrices [11, 12]. In contrast to the latter work, the lower temperatures used in the gas matrix work was instrumental in detecting the key secondary photoproduct *cis*-$(\eta^5\text{-}C_5H_5)W(CO)_2$(olefin)H, which was assumed to be formed in the 77K study and was crucial to the β-elimination mechanism proposed on that study. Additionally the gas matrix study revealed the existence of rotamers for olefin-hydrido species with asymmetric olefins; these were not observed in paraffin matrices at 77K. The importance of temperature in the design of experiments to trap and characterise unstable species, proposed as reaction intermediates, has been underlined. The only species detected in paraffin matrices at 77K and not detected in gas matrices at 12K was a species (I), where, on the basis of a large optical shift, it was proposed that a β-hydrogen became coordinated to the metal in $(\eta^5\text{-}C_5H_5)M(CO)_2C_2H_5$ species [11, 12]. No differences of colour in our matrices for $(\eta^5\text{-}C_5H_5)M(CO)_2C_2H_5$ in CH_4 and CO matrices could be detected nor could any new absorptions in the uv-vis spectra be recorded after photolysis. It may well be that there was insufficient chromophore in the very thin gas matrices compared to the thicker wax matrices.

Irradiation of $(\eta^5\text{-}C_5H_5)W(CO)_3(\eta^1\text{-}R)$ (R = C_3H_5, $CH_2C_6H_5$) complexes in gas matrices gave evidence that CO dissociation is the primary step in the

photochemistry of these complexes to generate the required vacant coordination site in the 16-electron intermediate $(\eta^5\text{-}C_5H_5)W(CO)_2(\eta^1\text{-}R)$, allowing subsequent intramolecular rearrangement to yield $(\eta^5\text{-}C_5H_5)W(CO)_2(\eta^3\text{-}R)$ complexes ($R = C_3H_5$, $CH_2C_6H_5$). Only one product, $(\eta^5\text{-}C_5H_5)W(CO)_2(\eta^3\text{-}R)$, was observed from irradiation of $(\eta^5\text{-}C_5H_5)W(CO)_3(\eta^1\text{-}R)$ complexes in solution [7, 33, 34].

Table 4.1 Infrared band positions (cm^{-1}) observed in the terminal CO-stretching region for $(\eta^5\text{-}C_5H_5)M(CO)_3C_2H_5$ complexes (M = Mo, W) and their photoproducts in CH_4 and CO matrices at 12K.

Complex	CH_4	CO
$(\eta^5\text{-}C_5H_5)Mo(CO)_3C_2H_5$	2019.5 1939.5 } a 1932.8	2019.3 1938.8 } a 1928.0
$(\eta^5\text{-}C_5H_5)W(CO)_3C_2H_5$	2016.8 1930.4 } a 1924.6	2016.0 1931.7 } a 1925.0
$(\eta^5\text{-}C_5H_5)Mo(CO)_2C_2H_5$	1957.8 1876.2	1956.6 1876.3
$(\eta^5\text{-}C_5H_5)W(CO)_2C_2H_5$	1948.7 1862.8	1949.8 1861.5
trans-$(\eta^5\text{-}C_5H_5)Mo(CO)_2(C_2H_4)H$ [b]	1977.4 1904.7	1980.0 1908.5
cis-$(\eta^5\text{-}C_5H_5)W(CO)_2(C_2H_4)H$ [c]	1988.5 1929.2	1988.1 1930.3
trans-$(\eta^5\text{-}C_5H_5)W(CO)_2(C_2H_4)H$ [d]	1977.4 1899.7	1976.7 1901.2
$(\eta^5\text{-}C_5H_5)Mo(CO)_3H$	2028.0 1947.6 } a 1940.3	2028.0 1947.1 } a 1941.3
$(\eta^5\text{-}C_5H_5)W(CO)_3H$	2024.8 1938.6 } a 1934.4	2026.4 1938.8 } a 1933.2

[a] Overlapping A' and A" bands (see text).

[b] Energy-factored CO force constants: K = 1522.0 and k_i = 57.0 Nm^{-1}.

[c] Energy-factored CO force constants: K = 1549.9 and k_i = 46.9 Nm^{-1}.

[d] Energy-factored CO force constants: K = 1518.2 and k_i = 60.8 Nm^{-1}.

Table 4.2 Infrared band positions (cm^{-1}) observed in the terminal CO-stretching region for $(\eta^5\text{-}C_5R_5')W(CO)_3R$ complexes (R' = H, R = n-C_3H_7, i-C_3H_7, n-C_4H_9; R' = CH_3, R = n-C_3H_7) and their photoproducts in CH_4 and CO matrices at 12K.

Complex	CH_4	CO
$(\eta^5\text{-}C_5H_5)W(CO)_3(n\text{-}C_3H_7)$	2016.6 1929.9 1923.2 } a	2016.6 1929.5 1921.8 } a
$(\eta^5\text{-}C_5H_5)W(CO)_3(i\text{-}C_3H_7)$	2014.1 1929.0 1919.3 } a	2013.2 1927.5 1915.2 } a
$(\eta^5\text{-}C_5(CH_3)_5)W(CO)_3(n\text{-}C_3H_7)$	2002.0 1908.7 1904.4 } a	2002.5 1909.0 1902.6 } a
$(\eta^5\text{-}C_5H_5)W(CO)_3(n\text{-}C_4H_9)$	2017.5 1930.2 1924.5 } a	2014.1 1925.8 1916.8 } a
$(\eta^5\text{-}C_5H_5)W(CO)_2(n\text{-}C_3H_7)$	1949.4 1863.5	1948.7 1862.5
$(\eta^5\text{-}C_5H_5)W(CO)_2(i\text{-}C_3H_7)$	1946.3 1860.8	1946.8 1862.0
$(\eta^5\text{-}C_5(CH_3)_5)W(CO)_2(n\text{-}C_3H_7)$	1932.2 1845.8	1931.8 1844.2
$(\eta^5\text{-}C_5H_5)W(CO)_2(n\text{-}C_4H_9)$	1948.2 1862.8	1945.0 1860.0
cis-$(\eta^5\text{-}C_5H_5)W(CO)_2(l\text{-}C_3H_6)H$	1986.0 1937.5	b 1936.2
cis'-$(\eta^5\text{-}C_5H_5)W(CO)_2(l\text{-}C_3H_6)H$	1978.6 1919.5	1982.7 1923.7
trans-$(\eta^5\text{-}C_5H_5)W(CO)_2(l\text{-}C_3H_6)H$	1970.3 1893.5	1971.4 1894.3
trans'-$(\eta^5\text{-}C_5H_5)W(CO)_2(l\text{-}C_3H_6)H$	1963.7 1883.8	c 1885.0
cis-$(\eta^5\text{-}C_5(CH_3)_5)W(CO)_2(l\text{-}C_3H_6)H$	d 1922.4	d 1924.5

...Continued/

Table 4.2 Continued

Complex	CH_4	CO
cis'-$(\eta^5$-$C_5(CH_3)_5)W(CO)_2(\underline{l}$-$C_3H_6)H$	1967.8 1904.0	1970.3 1910.5
trans-$(\eta^5$-$C_5(CH_3)_5)W(CO)_2(\underline{l}$-$C_3H_6)H$	1954.1 1875.2	1955.0 1875.3
trans'-$(\eta^5$-$C_5(CH_3)_5)W(CO)_2(\underline{l}$-$C_3H_6)H$	e 1860.0	e 1865.4
cis-$(\eta^5$-$C_5H_5)W(CO)_2(\underline{l}$-$C_4H_8)H$	1986.3 1937.3	1987.1 1937.4
cis'-$(\eta^5$-$C_5H_5)W(CO)_2(\underline{l}$-$C_4H_8)H$	1980.7 1921.8	1982.3 1922.6
trans-$(\eta^5$-$C_5H_5)W(CO)_2(\underline{l}$-$C_4H_8)H$	1971.1 1894.3	1969.7 1891.4
trans'-$(\eta^5$-$C_5H_5)W(CO)_2(\underline{l}$-$C_4H_8)H$	f 1882.5	f 1881.6
$(\eta^5$-$C_5H_5)W(CO)_3H$	2024.2 1937.5 1932.3 } a	2024.3 1936.8 1934.6 } a
$(\eta^5$-$C_5(CH_3)_5)W(CO)_3H$	2012.1 1922.2	2011.4 1923.2

[a]Overlapping $\underline{A}'$ and $\underline{A}''$ bands.

[b]Band obscurred by broad band at 1982.7 cm^{-1}.

[c]Band obscurred by broad band at 1971.4 cm^{-1}.

[d]Band obscurred by broad upper band of *cis'* isomer.

[e]Band obscurred by broad upper band of *trans* isomer.

[f]Band obscurred by broad upper band of *trans* isomer.

Table 4.3 Infrared band positions (cm^{-1}) observed in the terminal CO-stretching region for $(\eta^5\text{-}C_5H_5)W(CO)_3R$ complexes (R = C_3H_5, $CH_2C_6H_5$ and C_6H_5) and their photoproducts in a variety of matrices at 12K.

Complex	CH_4	Ar	CO	N_2	5% C_2H_4/CH_4
$(\eta^5\text{-}C_5H_5)W(CO)_3(\eta^1\text{-}CH_2C_6H_5)$	2014.1 1930.6 1919.3 }a	2021.4 1936.6 1925.8 }a	2015.0 1931.1 1917.1 }a	-	-
$(\eta^5\text{-}C_5H_5)W(CO)_3(\eta^1\text{-}C_3H_5)$	2019.3 1934.0 1924.8	-	-	-	-
$(\eta^5\text{-}C_5H_5)W(CO)_3C_6H_5$	2025.1 1944.3 1932.2 }a	-	2024.3 1938.9 1927.8 }a	2024.3 1941.7 1929.6 }a	2022.1 1938.0 1924.5 }a
$(\eta^5\text{-}C_5H_5)W(CO)_2(\eta^1\text{-}CH_2C_6H_5)$	1939.4 1857.5	1949.4 1868.5	1942.4 1859.3	-	-
$(\eta^5\text{-}C_5H_5)W(CO)_2(\eta^1\text{-}C_3H_5)$	1951.8 1866.5	-	-	-	-
$(\eta^5\text{-}C_5H_5)W(CO)_2C_6H_5$	1955.0 1869.7	-	1954.4 1865.7	1958.7 1973.6	1951.5 1861.5
$(\eta^5\text{-}C_5H_5)W(CO)_2(\eta^3\text{-}CH_2C_6H_5)$	1945.0 1871.3	d 1880.5	1946.2 1871.7		
$(\eta^5\text{-}C_5H_5)W(CO)_2(\eta^3\text{-}C_3H_5)$	1960.2 1882.5	-	-	-	-
$(\eta^5\text{-}C_5H_5)W(CO)_2(N_2)C_6H_5$ b	-	-	-	1971.0 1902.3	-
$(\eta^5\text{-}C_5H_5)W(CO)_2(C_2H_4)C_6H_5$ c	-	-	-	-	1990.2 1922.5

[a] Overlapping A' and A" bands.

[b] ν_{NN} too weak to observe.

[c] *Cis* isomer in matrices at 12K (K = 1546.0 and k_i (*cis*) = 53.5 Nm^{-1}) but *trans* isomer in solution (Table 1, K = 1495.6 and k_i (*trans*) = 63.7 Nm^{-1}).

[d] Band obscured by broad band of $(\eta^5\text{-}C_5H_5)W(CO)_2(\eta^1\text{-}CH_2C_6H_5)$ at 1949.4 cm^{-1}.

Table 4.4 Observed and calculated[a] band positions (cm^{-1}) of terminal CO-stretching bands in an experiment with a ^{13}CO-enriched sample of $(\eta^5\text{-}C_5H_5)W(CO)_3C_6H_5$ in a CH_4 matrix at 12K.

Complex (symmetry point group)	ν(CO)	Observed	Calculated
$(\eta^5\text{-}C_5H_5)W(^{12}CO)_3C_6H_5$	A'	2023.0	2023.1
(C_s)	A'	1940.0	1939.6
	A"	1930.0	1930.7
$(\eta^5\text{-}C_5H_5)W(^{12}CO)_2(^{13}CO)C_6H_5$	A'	2012.3	2012.8
(C_s)[b]	A"	1931.3	1930.7
	A'	1906.4	1906.2
	A	2010.0	2011.9
(C_1)[c]	A	1937.2	1937.8
	A	d	1900.0
$(\eta^5\text{-}C_5H_5)W(^{12}CO)(^{13}CO)_2C_6H_5$	A	1998.1	1998.8
(C_1)[e]	A	1914.4	1913.6
	A	d	1893.7
	A'	1996.7	1998.4
(C_s)[f]	A'	d	1919.9
	A"	1887.2	1887.8
$(\eta^5\text{-}C_5H_5)W(^{13}CO)_3C_6H_5$	A'	1978.2	1978.1
(C_s)	A'	1896.0	1896.4
	A"	1888.4	1887.8
$(\eta^5\text{-}C_5H_5)W(^{12}CO)_2C_6H_5$	A'	1954.0	1953.8
(C_s)	A"	1865.6	1865.5

...Continued/

Table 4.4 Continued

Complex (symmetry point group)	ν(CO)	Observed	Calculated
$(\eta^5\text{-}C_5H_5)W(^{12}CO)(^{13}CO)C_6H_5$ ($\underline{C}_1$)	$\underline{A}$	1936.3	1937.0
	$\underline{A}$	1839.1	1839.9
$(\eta^5\text{-}C_5H_5)W(^{13}CO)_2C_6H_5$ ($\underline{C}_s$)	$\underline{A}'$	1910.2	1910.4
	$\underline{A}''$	1824.1	1824.0

[a] Refined energy-factored force constants for $(\eta^5\text{-}C_5H_5)W(CO)_3C_6H_5$: $\underline{K}_1$ = 1562.8, $\underline{K}_2$ = 1558.2, $\underline{k}_{12}$ = 44.2 and $\underline{k}_{23}$ = 52.3 Nm^{-1} as defined by the number in the diagram below.

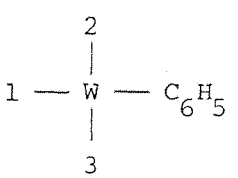

i.e. 1 ≠ 2 = 3

Refined energy-factored force constants for $(\eta^5\text{-}C_5H_5)W(CO)_2C_6H_5$: $\underline{K}$ = 1474.1 and $\underline{k}_i$ = 68.1 Nm^{-1}.

b ^{13}CO in position 1.

c ^{13}CO in position 2.

d Band obscured.

e ^{12}CO in position 2.

f ^{12}CO in position 1.

4.5 REFERENCES

1. K.W. Barnett and D.W. Slocum, *J. Organomet. Chem.*, 1972, 44, 1.

2. H.G. Alt, *Habilitationsschrift*, University of Bayreuth, 1979.

3. G.C. Geoffry and M.S. Wrighton, *'Organometallic Photochemistry'*, Academic Press, New York, 1979.

4. H.G. Alt and M.E. Eichner, *J. Organomet. Chem.*, 1981, 212, 397.

5. H.G. Alt, *J. Organomet. Chem.*, 1977, 127, 349.

6. M.D. Rausch, T.E. Gismondi, H.G. Alt and J.A. Schwärzle, *Z. Naturforsch, Teil B*, 1977, 32, 998.

7. R.G. Severson and A. Wojcicki, *J. Organomet. Chem.*, 1978, 157, 173.

8. D.R. Taylor, *Inorg. Chem.*, 1981, 20, 2257.

9. E. Samuel, M.D. Rausch, T.E. Gismondi, E.A. Mintz and C. Giannotti, *J. Organomet. Chem.*, 1979, 172, 309.

10. H.G. Alt and M.E. Eichner, *Angew. Chem. Int. Edn.*, 1982, 21, 78.

11. R.J. Kazlauskas and M.S. Wrighton, *J. Am. Chem. Soc.*, 1980, 102, 1727.

12. R.J. Kazlauskas and M.S. Wrighton, *J. Am. Chem. Soc.*, in press.

13. G.M. Whitesides, J.F. Gaasch and E.R. Stedronsky, *J. Am. Chem. Soc.*, 1972, 94, 5258.

14. F.N. Tebbe and G.W. Parshall, *J. Am. Chem. Soc.*, 1971, 93, 3793.

15. M.L.H. Green and P.L.T. Nagy, *Adv. Organomet. Chem.*, 1964, 2, 325.

16. M.L.H. Green and P.L.T. Nagy, *J. Chem. Soc.*, 1963, 189.

17. J.K. Burdett, *Coord. Chem. Rev.*, 1978, 28, 1.

18. K.A. Mahmoud, R. Narayanaswamy and A.J. Rest, *J. Chem. Soc. Dalton. Trans.*, 1981, 2199.

19. R.B. Hitam, R.H. Hooker, K.A. Mahmoud, R. Narayanaswamy and A.J. Rest. *J. Organomet. Chem.*, 1981, 222, C9.

20. J.K. Burdett and J.J. Turner, in *"Cryochemistry"*, Eds. M. Moskovits and G.A. Ozin, Wiley-Interscience, London, 1976.

21. K.A. Mahmoud, A.J. Rest and H.G. Alt, *J. Chem. Soc. Dalton. Trans.*, in press.

22. P.S. Braterman, *"Metal Carbonyl Spectra"*, Academic Press, London, 1975.

23. D.L.S. Brown, J.A. Connor and H.A. Skinner, *J. Organomet. Chem.*, 1974, 81, 403.

24. H.G. Alt, J.A. Schwärzle and C.G. Kreiter, *J. Organomet. Chem.*, 1978, 115, C65.

25. C.G. Kreiter, K. Nist and H.G. Alt., *Chem. Ber.*, 1981, 114, 1845.

26. F.H. Köhler, H.J. Kalder and E.O. Fischer, *J. Organomet. Chem.*, 1975, 85, C19; 1976, 113, 11.

27. J.P. Collman and L.S. Hegedus, *"Principles and Applications of Organotransition Metal Chemistry"*, University Science Books, Mill Valley, California, 1980, p292.

28. H.G. Alt, K.A. Mahmoud and A.J. Rest, *J. Organomet. Chem.*, 1983, in press.

29. D.G. Kalina, T.J. Marks and W.A. Wachter, *J. Am. Chem. Soc.*, 1977, 99, 3877.

30. D.G. Kalina and T.J. Marks, *Progr. Inorg. Chem.*, 1979, 25, 288.

31. K.A. Mahmoud, A.J. Rest, H.G. Alt, M.E. Eichner and B.M. Jansen, *J. Chem. Soc. Dalton. Trans.*, 1983, in press.

32. J. Dvorak, R.J. O'Brien and W. Santo, *J. Chem. Soc. Chem. Commun.*, 1970, 411.

33. R.B. King, W.C.Z. Zipperer and M. Ishaq, *Inorg. Chem.*, 1972, 11, 1361.

34(a) M.L.H. Green and A.N. Stear, *J. Organomet. Chem.*, 1964, 1, 230.

34(b) R.B. King and M.B. Bisnette, *J. Organomet. Chem.*, 1965, 4, 486.

35. R.B. King and A. Fronzaglia, *J. Am. Chem. Soc.*, 1966, 88, 709.

36. B. Klein, R.J. Kazlauskas and M.S. Wrighton, *Organometallics*, 1982, 1, 1338.

37. Shiu-Chin H. Su and A. Wojciki, *International Conference*, Toronto, 1980.

38. J.W. Faller and M.J. Incorvia, *Inorg. Chem.*, 1968, 7, 840.

39. R.B. King, *Inorg. Chem.*, 1966, 5, 2242.

40. A.N. Nesmeyanov, Z.L. Lutsenko, A.A. Bezrukova, A.V. Kisin, M.G. Kuznetsova, N.V. Alekseev and A.Z. Rubezhov, *Izv. Akad. Nauk. SSSR, Ser. Khim.*, 1981, 413.

CHAPTER FIVE

PHOTOCHEMISTRY OF $(\eta^5\text{-}C_5H_5)M(CO)_2R$ COMPLEXES (M = Fe, Ru; R = CH_3, C_2H_5) IN LOW TEMPERATURE GAS MATRICES AT 12K

5.1 INTRODUCTION

The photo-induced carbonyl substitution reactions of $(\eta^5\text{-}C_5H_5)Fe(CO)_2Me$ have been known for almost 20 years [1]. However, the first report on photolysis reactions of $(\eta^5\text{-}C_5H_5)Fe(CO)_2R$ complexes (R = Me, Et, Ph) in solution without any potential ligands present appeared only in 1979 [2]. The photolysis of these compounds in pentane or other non-coordinating solvents yielded $[(\eta^5\text{-}C_5H_5)Fe(CO)_2]_2$ as the sole metal-containing product. The reaction pathway of these photolysis reactions depends very much on R (Me, Et, Ph). In all three cases photo-induced dissociation of one carbonyl ligand and generation of a 16-electron species was assumed to be the first step in the reaction:

$$(\eta^5\text{-}C_5H_5)Fe(CO)_2R \underset{\text{solvent}}{\overset{h\nu}{\rightleftharpoons}} (\eta^5\text{-}C_5H_5)Fe(CO)R + CO$$

Support for this assumption came from the fact that two-electron ligands L, e.g. L = PR_3, were able to stabilise these $(\eta^5\text{-}C_5H_5)Fe(CO)R$ fragments. The composition of the organic photoproducts, i.e. CH_4 (for R = CH_3), C_2H_4, C_2H_6 and H_2 (for R = Et), and C_6H_6 and $(C_6H_5)_2$ (for R = C_6H_5), suggested a hydrogen abstraction pathway for R = Me and Ph, but a β-hydrogen-elimination pathway for R = Et. These results were confirmed by other groups recently [3, 4]. The photolysis of $(\eta^5\text{-}C_5H_5)Fe(CO)_2Me$ in a CO matrix at 12K, leading to $(\eta^3\text{-}C_5H_5)Fe(CO)_3Me$, revealed that also ring-slippage, i.e. $\eta^5 \rightarrow \eta^3\text{-}C_5H_5$, should also be considered as providing the basis for a reaction pathway [5].

In order to obtain more details about the mechanism of the photolysis of $(\eta^5\text{-}C_5H_5)Fe(CO)_2R$ compounds (R = Me, Et) experiments have been extended to include the ruthenium analogues $(\eta^5\text{-}C_5H_5)Ru(CO)_2R$ (R = Me, Et). From

similar reactions with the complexes $(\eta^5\text{-}C_5H_5)M(CO)_3R$ [6], (M = Mo, W; R = Me, Et, n-Pr, i-Pr, n-Bu, Ph) (see Chapter 4) it was found that the heavier homologues gave more stable intermediates upon photolysis. In this chapter the photolysis of $(\eta^5\text{-}C_5H_5)M(CO)_2R$ compounds (M = Fe, Ru; R = Me, Et) is described in various gas matrices at 12K without and in the presence of the potential ligands, e.g. N_2, CO and C_2H_4.

5.2 RESULTS

(a) Photolysis of $(\eta^5\text{-}C_5H_5)M(CO)_2Me$ complexes (M = Fe, Ru) in CH_4, ^{13}CO doped CH_4, N_2, C_2H_4 doped CH_4 and CO matrices at 12K

In contrast with the photoreactions of $(\eta^5\text{-}C_5H_5)Ru(CO)_2Me$ in a variety of matrices (see below), no evidence has been found [4,5] for the formation of the coordinatively unsaturated species $(\eta^5\text{-}C_5H_5)Fe(CO)Me$ on photolysis of $(\eta^5\text{-}C_5H_5)Fe(CO)_2Me$ in Ar, CH_4 and N_2 matrices, nor for $(\eta^5\text{-}C_5H_5)Fe(CO)(N_2)Me$ in N_2 matrices, nor for $(\eta^5\text{-}C_5H_5)Fe(CO)(COMe)$ in CO matrices. However, in ^{13}CO doped CH_4 matrices rapid exchange of CO ligands was observed [4, 5] and in pure CO matrices an expanded coordination-number species was observed, i.e. $(\eta^3\text{-}C_5H_5)Fe(CO)_3Me$ where ring slippage was proposed to occur [5].

The i.r. spectrum of $(\eta^5\text{-}C_5H_5)Ru(CO)_2Me$ isolated at high dilution in a CH_4 matrix shows two strong absorption bands in the terminal CO stretching region at 2018.9 and 1958.8 cm^{-1} (Figure 5.1(a), Table 5.1). Irradiation of the matrix with medium energy u.v. radiation ($290 < \lambda < 370$ nm) produced a new band at 1943.4 cm^{-1} together with a band due to free CO at 2138 cm^{-1} (Figure 5.1(b)). Annealing the matrix to a higher temperature (ca 30K), which allows the CO to diffuse in CH_4 caused reversal of the primary photolysis step (Figure 5.1(c)). The ejection of CO in the primary photolysis step, the recombination on annealing, and the observation of a single new band in the terminal CO stretching region suggested that the new species was $(\eta^5\text{-}C_5H_5)Ru(CO)Me$. This assignment was confirmed when $(\eta^5\text{-}C_5H_5)Ru(CO)_2Me$ was photolysed in a ^{13}CO doped (5%) CH_4 matrix. Initially rapid exchange occurred to produce $(\eta^5\text{-}C_5H_5)Ru(^{12}CO)(^{13}CO)Me$ and $(\eta^5\text{-}C_5H_5)Ru(^{13}CO)_2Me$ but

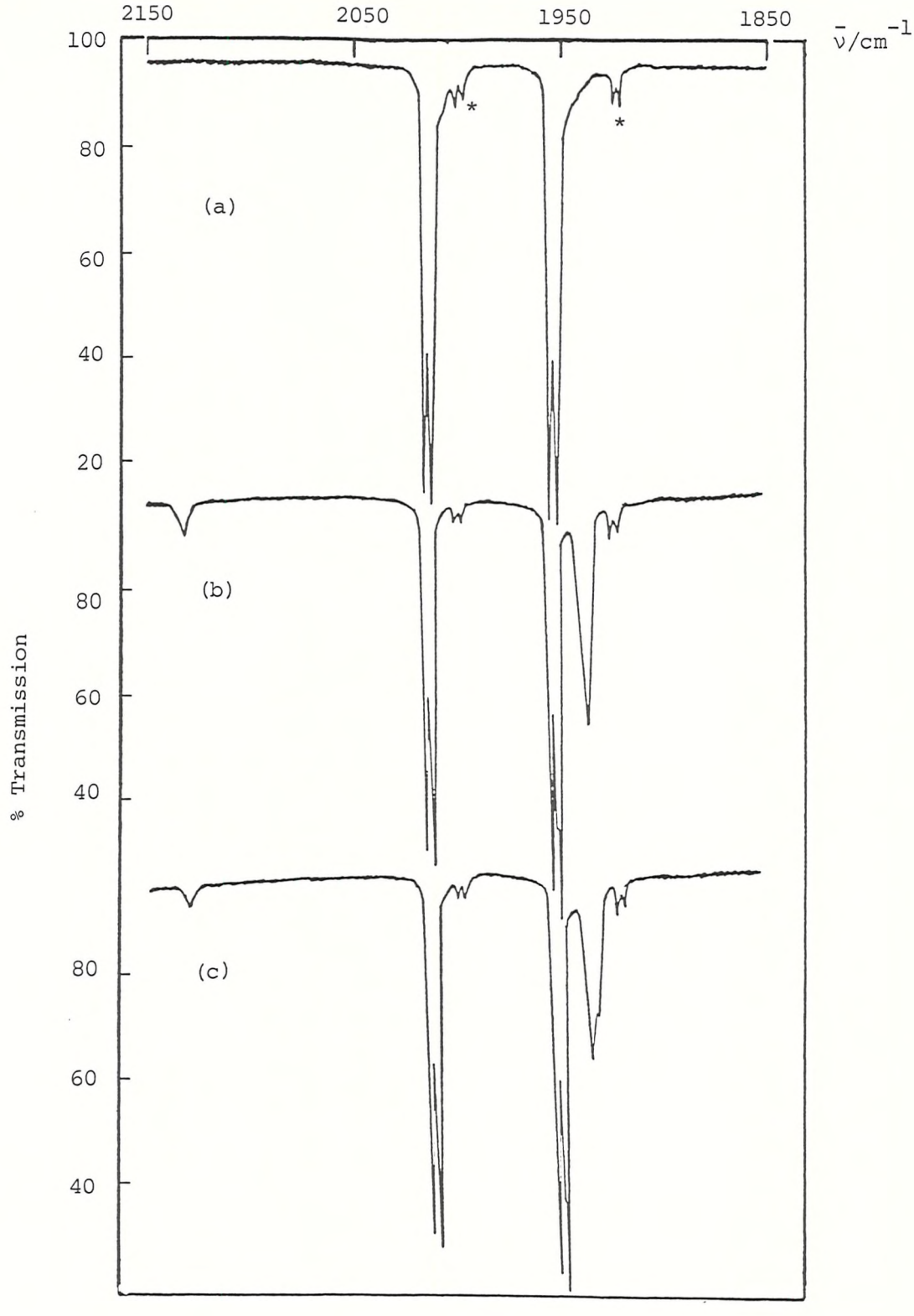

FIGURE 5.1 Infrared spectra from an experiment with $(\eta^5\text{-}C_5H_5)Ru(CO)_2Me$ isolated at high dilution in a CH_4 matrix at 12K: (a) after deposition, (b) after irradiation for 4 hr using $290 < \lambda < 370$ nm light, and (c) after 1 min annealing to ca 30K followed by cooling to 12K. Bands marked with an asterisk (*) are due to $(\eta^5\text{-}C_5H_5)Ru(^{12}CO)(^{13}CO)Me$ present in natural abundance.

then further bands assigned to $(\eta^5\text{-}C_5H_5)Ru(^{12}CO)Me$ and $(\eta^5\text{-}C_5H_5)Ru(^{13}CO)Me$ grew in. Excellent correspondence between observed and calculated band positions was found (Table 5.2) using the energy-factored force field approach [7, 8].

The reactivity of the 16-electron species $(\eta^5\text{-}C_5H_5)Ru(CO)Me$ was demonstrated by its reaction with N_2 and also C_2H_4 (see below). Irradiation of $(\eta^5\text{-}C_5H_5)Ru(CO)_2Me$ isolated at high dilution in a N_2 matrix (Figure 5.2(a)) produced new bands at 2188.6, 2152.5 and 1968.2 cm^{-1} together with a band due to free CO (Figure 5.2(b)). Longer times of photolysis showed that the band at 2152.5 cm^{-1} grew independently of the pair at 2188.6 and 1968.2 which maintained a constant relative intensity. Bands in the 2150 - 2300 cm^{-1} region are typical of ν_{NN} for N_2 bonded to transition metals in matrix isolation studies, e.g. $(\eta^5\text{-}C_5H_5)Co(CO)(N_2)$ (ν_{NN} at 2164.6 cm^{-1}) [8]. The species with the bands at 2188.6 and 1968.2 cm^{-1} can, therefore, be assigned to the species $(\eta^5\text{-}C_5H_5)Ru(CO)(N_2)Me$ (Table 5.1). In contrast to the photoproduct in a pure CH_4 matrix, $(\eta^5\text{-}C_5H_5)Ru(CO)Me$, the new dinitrogen species $(\eta^5\text{-}C_5H_5)Ru(CO)(N_2)Me$ is stable towards annealing to ca 30K (Figure 5.2(c)). In the same way that ^{13}CO from the matrix exchanges progressively with bound ^{12}CO ligands in $(\eta^5\text{-}C_5H_5)Ru(^{12}CO)_2Me$ it is likely that N_2 could behave similarly, i.e. the band at 2152.5 cm^{-1} may be assigned to the bis-dinitrogen complex $(\eta^5\text{-}C_5H_5)Ru(N_2)_2Me$.

In a C_2H_4 doped (5%) CH_4 matrix photolysis produces new bands at 1956.6 and 1941.7 cm^{-1} in addition a band due to free CO. The band at 1941.7 cm^{-1} corresponds with the 16-electron species $(\eta^5\text{-}C_5H_5)Ru(CO)Me$ (Table 5.1). On the basis of the similarity of the new band at 1956.6 cm^{-1} with the CO-stretching band of $(\eta^5\text{-}C_5H_5)Ru(CO)(N_2)Me$ it seems reasonable to assign the other new band to $(\eta^5\text{-}C_5H_5)Ru(CO)(C_2H_4)Me$. Similarly $(\eta^5\text{-}C_5H_5)Fe(CO)_2Me$ gave $(\eta^5\text{-}C_5H_5)Fe(CO)(C_2H_4)Me$.

The i.r. spectrum of $(\eta^5\text{-}C_5H_5)Ru(CO)_2Me$ isolated at high dilution in a CO matrix at 12K shows broader bands at 2020.7 and 1962.4 cm^{-1} (Figure 5.3 (a)) than for CH_4 matrices (Figure 5.1(a)). On irradiation ($270 < \lambda < 390$ nm) the bands of the starting material were reduced in intensity and a

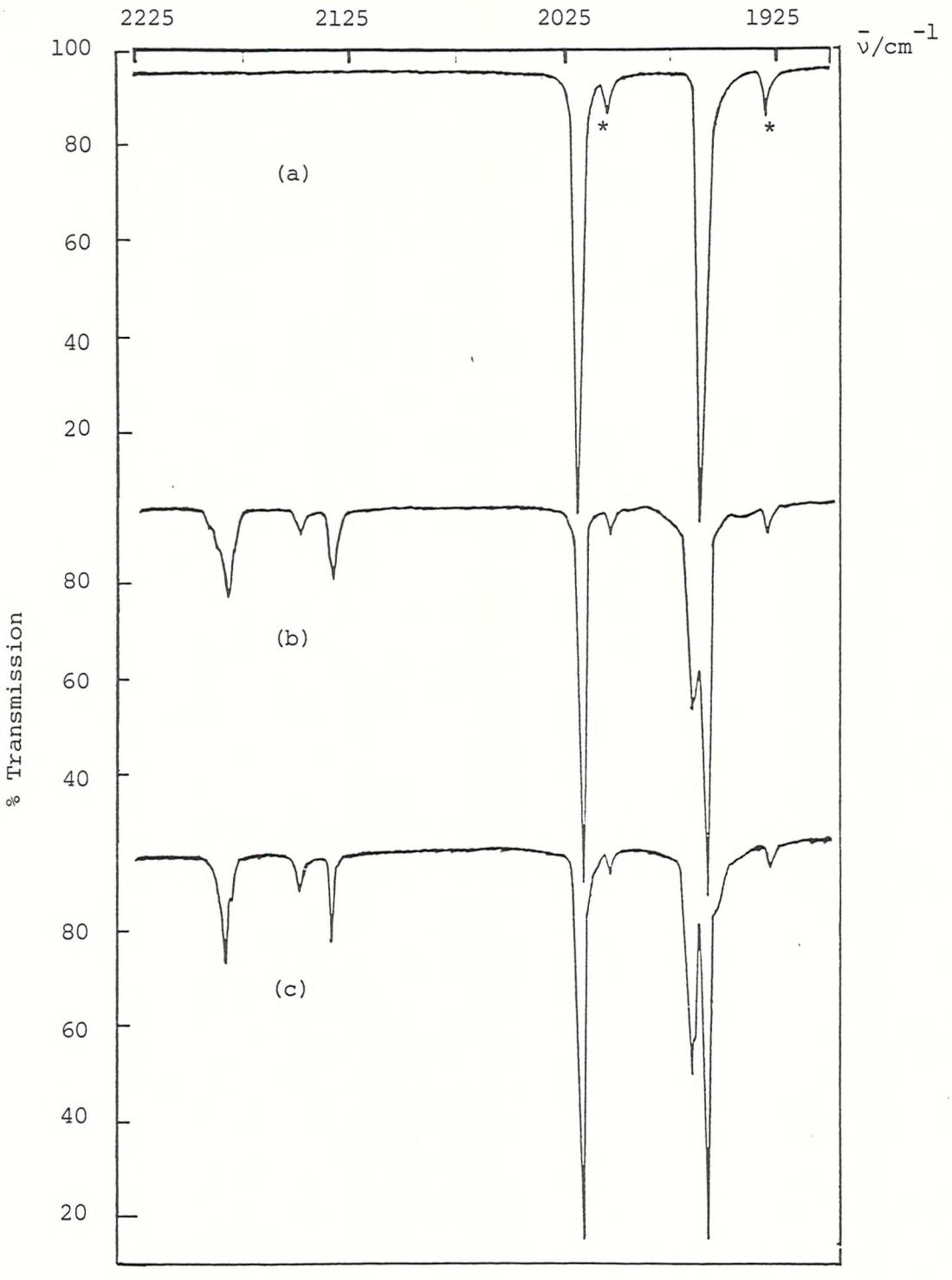

FIGURE 5.2 Infrared spectra from an experiment with $(\eta^5\text{-}C_5H_5)Ru(CO)_2Me$ isolated at high dilution in a N_2 matrix at 12K: (a) after deposition, (b) after 5 hr irradiation using $290 < \lambda < 370$ nm light, and (c) after 1 min annealing. Bands marked with an asterisk (*) are due to $(\eta^5\text{-}C_5H_5)Ru(^{12}CO)(^{13}CO)Me$ present in natural abundance.

number of new bands appeared (Figure 5.3(b); (1)-(3)). Prolonged photolysis with the same source resulted in the growth of two intense bands at 2038.1 and 1971.1 cm^{-1} (Figure 5.3(c); (4)) in addition to growth of the weaker bands at 2061.2 and 1993.5 cm^{-1} (Figure 5.3(c)). The spectrum obtained after further irradiation with u.v. light ($\lambda < 350$ nm; Figure 5.3 (d)) showed a significant increase in the bands at 2038.1, 1993.5 and 1971.1 cm^{-1} and of these the bands at 2038.1 and 1971.1 cm^{-1} increase with constant relative intensities. On the basis that a coordinatively expanded species has been observed for the iron analogue which shows ring slippage, i.e. $(\eta^3\text{-}C_5H_5)Fe(CO)_3Me$ (ν_{CO} at 2050.3, 1982.7 and 1975.1 cm^{-1}) [5] and that even a $\eta^5\text{-}C_5H_5$ ligand can be replaced by CO ligands in matrix isolation experiments, e.g. $(\eta^5\text{-}C_5H_5)NiNO \xrightarrow{h\nu/CO} (\eta^5\text{-}C_5H_5)Ni(CO)_2 \longrightarrow Ni(CO)_4$ [9] it seems likely that the species like $(\eta^3\text{-}C_5H_5)Ru(CO)_3Me$, $(\eta^1\text{-}C_5H_5)Ru(CO)_4Me$ and ultimately $Ru(CO)_5$ could possibly be produced. Support for this proposal is afforded by the observation of $Mo(CO)_6$ and $W(CO)_6$ on photolysis of $(\eta^5\text{-}C_5H_5)M(CO)_3R$ complexes (M = Mo, W; R = Me, Et) in polyvinyl chloride (pvc) film matrices at 12K [10]. Additionally $(\eta^5\text{-}C_5H_5)_2ReH$ is known to undergo metal-to-ring hydrogen transfer on photolysis at 12K [11] and $(\eta^4\text{-dimethylpentadiene})Fe(CO)_3$ is known to show ring-to-metal methyl migration [4]. Using i.r. terminal CO stretching band data for $(\eta^3\text{-}C_5H_5)Fe(CO)_3Me$, $Fe(CO)_5$ (ν_{CO} at 2034 and 2014 (gas) [12], 2022 and 2000 (n-heptane) [12] and 2028.0, 2003.7 and 1996.3 cm^{-1} (CO matrix) [13], and $Ru(CO)_5$ (ν_{CO} at 2035 and 1991 cm^{-1} (n-heptane)) [12] together with the growth and decay patterns of the bands in Figure 5.3 and the relative band positions for $(\eta^5\text{-}C_5H_5)Ru(CO)_2Me$ versus $(\eta^5\text{-}C_5H_5)Fe(CO)_2Me$ it was possible to assign the majority of the bands. For example, the shift to higher wavenumbers of the bands of the parent Ru complex compared to the Fe analogue suggests that bands due to $(\eta^3\text{-}C_5H_5)Ru(CO)_3Me$ would occur at higher wavenumbers than those of $(\eta^3\text{-}C_5H_5)Fe(CO)_3Me$ and, therefore, the 2061.2 cm^{-1} band (band (1)) could be assigned to $(\eta^3\text{-}C_5H_5)Ru(CO)_3Me$; other bands could be obscured. A comparison of the solution and CO matrix data for $Fe(CO)_5$ and $Ru(CO)_5$ suggests that the bands at 2003.6 and 1993.5 cm^{-1} (bands (3)) may be assigned to $Ru(CO)_5$; the upper band could be obscured by the intense band at 2038 cm^{-1}. The bands at 2029.4 and 1969.3 cm^{-1} (bands (2)) are analogues to the band positions of $(\eta^5\text{-}C_5H_5)Ru(CO)_2H$ (Table 5.1) though how such a methyl to hydride transformation could occur is not clear. An alternative explanation

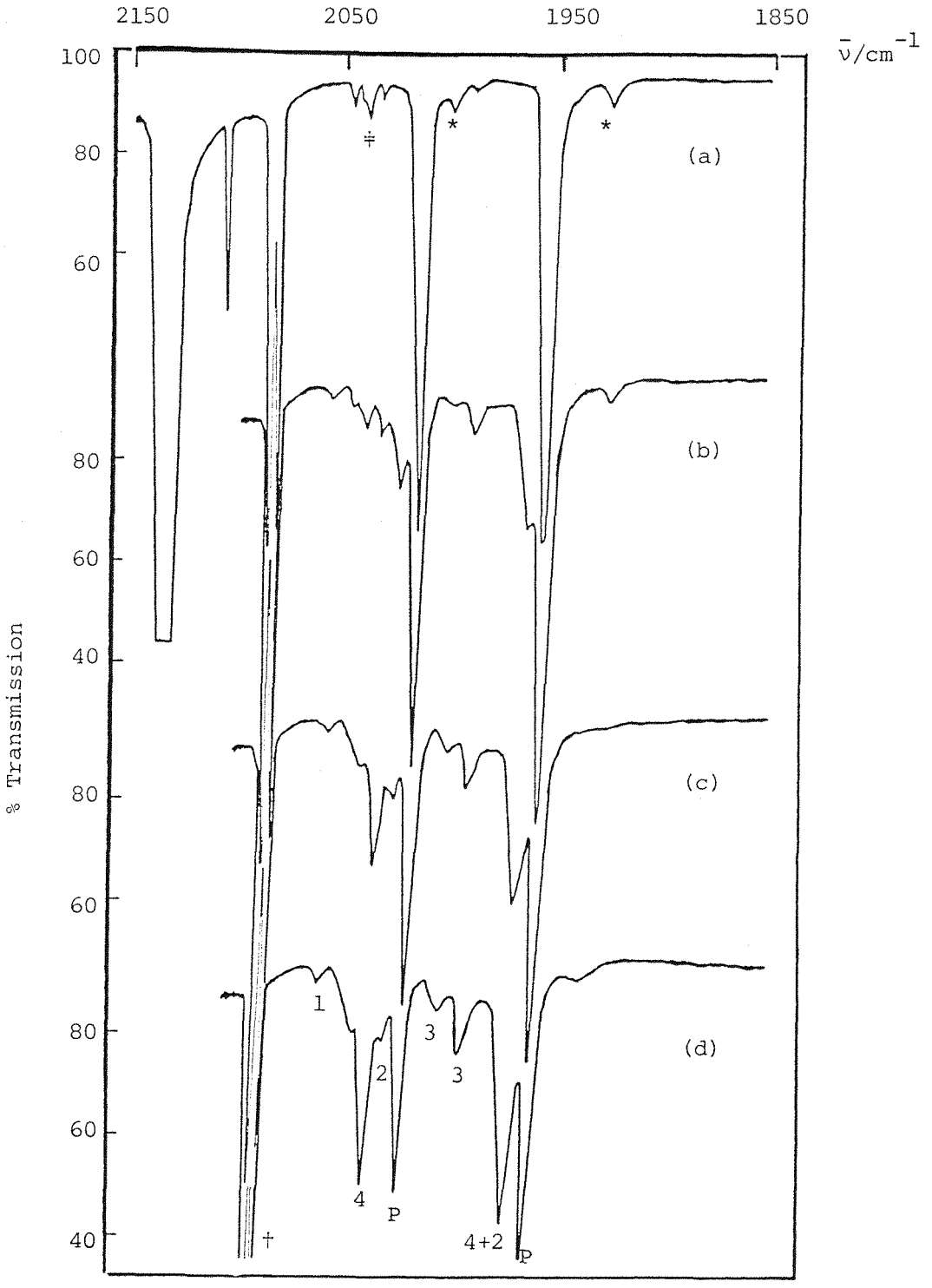

FIGURE 5.3 Infrared spectra from an experiment with $(\eta^5\text{-}C_5H_5)Ru(CO)_2Me$ (bands marked P) isolated at high dilution in a CO matrix at 12K: (a) after deposition, (b) after 100 min photolysis using $270 < \lambda < 350$ and $\lambda > 550$ nm radiation, (c) after 50 min photolysis with $270 < \lambda < 390$ nm light, and (d) after further 100 min photolysis using the same radiation. Bands marked with an asterisk (*) are due to $(\eta^5\text{-}C_5H_5)Ru(^{12}CO)(^{13}CO)Me$ present in natural abundance, those marked with a dagger (†) are due to other isotopically substituted CO molecules and those marked with a double dagger (‡) are due to a trace impurity. Bands marked (1) to (4) derive from photoproducts (see text).

could be that bands (2) are due to $(\eta^4\text{-}C_5H_5Me)Ru(CO)_3$, formed by metal-to-ring methyl transfer. The bands at 2038.1 and 1971.1 cm^{-1} (bands (4)), which grow in later, may then possibly be due to $(\eta^2\text{-}C_5H_5Me)Ru(CO)_4$ which ultimately gives $Ru(CO)_5$ (see above) and free C_5H_5Me. Definitive proof of these species via ^{13}CO labelling experiments seems remote because of the large number of products and overlapping bands.

(b) Photolysis of $(\eta^5\text{-}C_5H_5)M(CO)_2Et$ complexes (M = Fe, Ru) in CH_4, ^{13}CO doped CH_4, N_2, C_2H_4 doped CH_4 and CO matrices at 12K

The infrared spectrum of $(\eta^5\text{-}C_5H_5)Fe(CO)_2Et$ isolated at high dilution in a CH_4 matrix at 12K showed two intense terminal CO stretching bands at 2005.8 and 1947.2 cm^{-1} (Table 5.1). Irradiation of the matrix with medium energy u.v. light ($290 < \lambda < 370$ nm) led to the generation of two new bands at 2017.6 and 1958.5 cm^{-1}. Since these two bands continued to grow with the same relative intensity ratio they must arise from a species with two terminal carbonyl ligands. Such a species is $(\eta^5\text{-}C_5H_5)Fe(CO)_2H$, i.e. β-elimination has taken place. This is in agreement with the findings of Kazlauskas and Wrighton [3], who photolysed $(\eta^5\text{-}C_5H_5)Fe(CO)_2Et$ in glasses and paraffin wax matrices at 77K, and Gerhartz et al. [4], who photolysed $(\eta^5\text{-}C_5H_5)Fe(CO)_2Et$ in Ar at 10K. When the experiment was repeated with a ^{13}CO doped CH_4 matrix initial irradiation generated new bands which may be assigned to the species $(\eta^5\text{-}C_5H_5)Fe(^{12}CO)_2H$ and $(\eta^5\text{-}C_5H_5)Fe(^{12}CO)(^{13}CO)Et$, i.e. there is a competition between exchange and elimination. Prolonged photolysis resulted in bands which are attributed to $(\eta^5\text{-}C_5H_5)Fe(^{13}CO)_2Et$, $(\eta^5\text{-}C_5H_5)Fe(^{12}CO)(^{13}CO)H$ and $(\eta^5\text{-}C_5H_5)Fe(^{13}CO)_2H$ complexes on the basis of the excellent correspondence between the observed and calculated band positions produced by energy-factored force field fitting (Table 5.2).

Irradiation of $(\eta^5\text{-}C_5H_5)Fe(CO)_2Et$ in the reactive matrices N_2 and C_2H_4 doped CH_4 did not lead to the formation of the new species $(\eta^5\text{-}C_5H_5)Fe(CO)(N_2)Et$ and $(\eta^5\text{-}C_5H_5)Fe(CO)(C_2H_4)Et$ but to two bands seen previously in pure CH_4 matrices, i.e. formation of $(\eta^5\text{-}C_5H_5)Fe(CO)_2H$. This is in contrast to the formation of new N_2 and C_2H_4 substituted complexes for $(\eta^5\text{-}C_5H_5)Ru(CO)_2Et$ (see below). On photolysis ($290 < \lambda < 370$ nm) in pure CO matrices (Figure

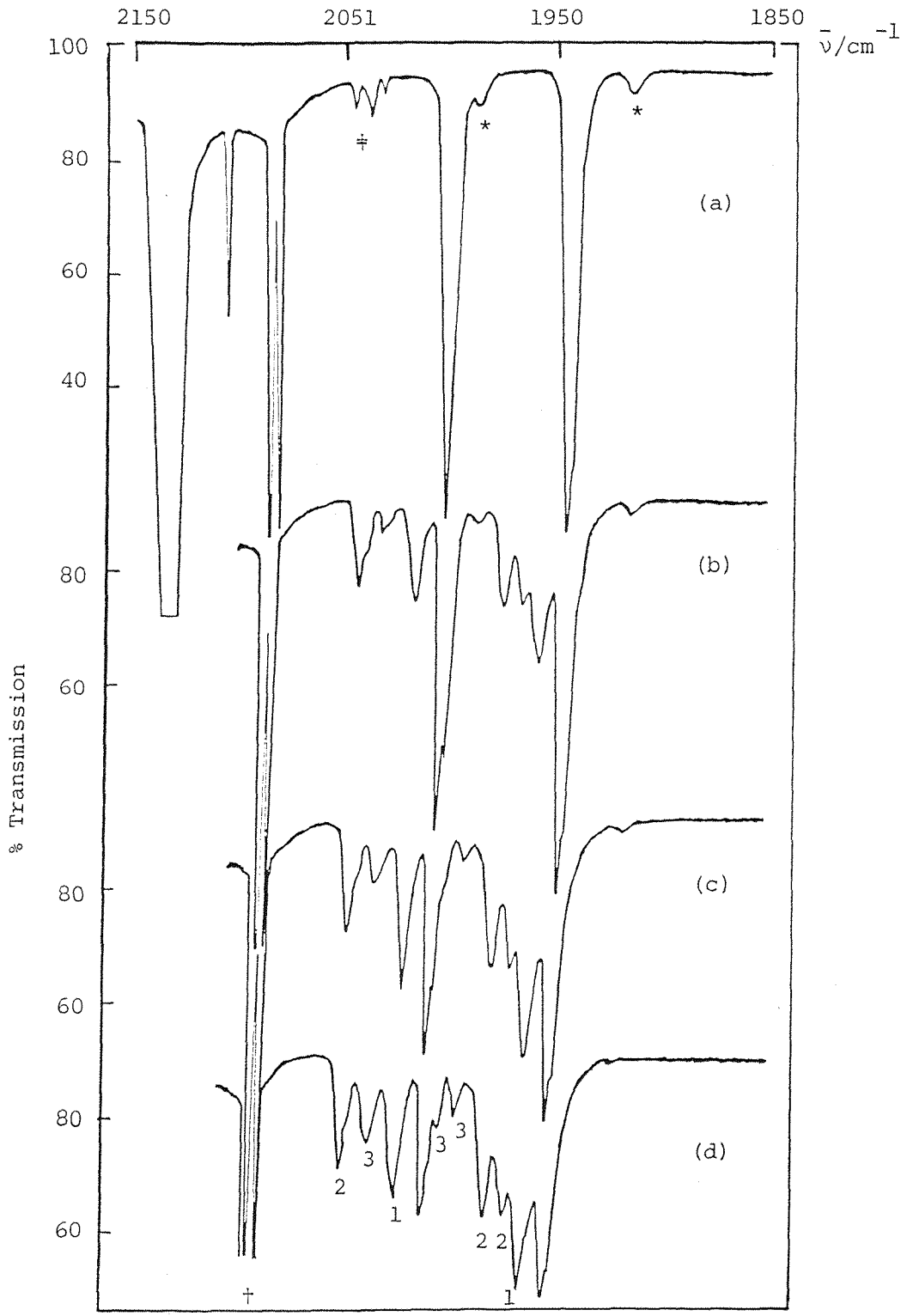

FIGURE 5.4 Infrared spectra from an experiment with $(\eta^5\text{-}C_5H_5)Fe(CO)_2Et$ (bands marked P) isolated at high dilution in a CO matrix at 12K: (a) after deposition, (b) after 4 hr photolysis using $290 < \lambda < 370$ nm light, (c) after 50 min photolysis with $270 < \lambda < 390$ nm light, and (d) after further 60 min photolysis with $270 < \lambda < 390$ nm light. Bands marked with an asterisk (*) are due to $(\eta^5\text{-}C_5H_5)Fe(^{12}CO)(^{13}CO)Et$ present in natural abundance, those marked with a dagger (†) are due to other isotopically substituted CO molecules and those marked with a double dagger (‡) are due to a trace impurity. Bands marked (1) to (3) derive from photoproducts (see text).

5.4), however, new bands were observed at 2046.0, 2020.8, 1978.7, 1969.3 and 1962.7 cm^{-1} (Figure 5.4(b)). The bands at 2020.8 and 1962.7 cm^{-1} (bands (1)) may be assigned to the known hydride complex, $(\eta^5\text{-}C_5H_5)Fe(CO)_2H$ by analogy with the behaviour of $(\eta^5\text{-}C_5H_5)Fe(CO)_2Et$ in CH_4, N_2 and C_2H_4 doped matrices. The other three bands (2046.0, 1978.7 and 1969.3 cm^{-1}; (bands (2)) show a clear similarity to the bands of $(\eta^3\text{-}C_5H_5)Fe(CO)_3Me$ (2050.3, 1982.7 and 1975.1 cm^{-1}; Table 5.1). Bearing in mind that the ordering of the CO bands for $(\eta^5\text{-}C_5H_5)Fe(CO)_2R$ complexes (R = H, Me, Et) is H > Me > Et and that the new product bands are at lower wavenumbers than those of $(\eta^3\text{-}C_5H_5)Fe(CO)_3Me$, the new photoproduct was, therefore, assigned as $(\eta^3\text{-}C_5H_5)Fe(CO)_3Et$. Such an assignment reveals the possibility that in CO matrices ring slippage ($\eta^5 \rightarrow \eta^3$) may be preferred over β-elimination. Prolonged photolysis with higher energy u.v. light ($270 < \lambda < 390$ nm) produced further new bands at 2035.2, 2005.5 and 1992.8 cm^{-1} (bands (3); Figures 5.4(c) and 5.4(d)), c.f. the additional bands observed on photolysis of $(\eta^5\text{-}C_5H_5)Ru(CO)_2Me$ in CO matrices (see above). Significantly, no bands were seen for HCO, MeCO and EtCO radicals in contrast to the photoreactions of $(\eta^5\text{-}C_5H_5)M(CO)_3H$ complexes (M = Mo, W) which generate the HCO radical [14].

The infrared spectrum of $(\eta^5\text{-}C_5H_5)Ru(CO)_2Et$ isolated at high dilution in a CH_4 matrix (Figure 5.5(a)) showed the same doublet splitting seen previously for $(\eta^5\text{-}C_5H_5)M(CO)_2Me$ complexes (M = Fe, Ru) in CH_4 matrices. A period of photolysis (45 min; $290 < \lambda < 370$ nm) led to the observation of three new bands at 2029.2, 1967.5 and 1960.3 cm^{-1} (Figure 5.5(b)) in addition to a band due to free CO. Continued photolysis with the same energy source showed that these three bands arise from two different species (Figure 5.5(c)). Since the relative intensity ratio of the bands at 2029.2 and 1967.5 cm^{-1} remained constant throughout the experiment, these bands originate with the same species, $(\eta^5\text{-}C_5H_5)Ru(CO)_2H$. The single CO stretching band at 1960.3 cm^{-1} probably arises from a monocarbonyl product since free CO is also observed. Comparison of the band position for $(\eta^5\text{-}C_5H_5)Ru(CO)Me$ with those of $(\eta^5\text{-}C_5H_5)Ru(CO)_2Me$ (Table 5.1) results in the prediction that a band for $(\eta^5\text{-}C_5H_5)Ru(CO)Et$ should occur at ca 1938 cm^{-1} which is at considerably lower wavenumbers than that observed (1960.3 cm^{-1}). An alternative

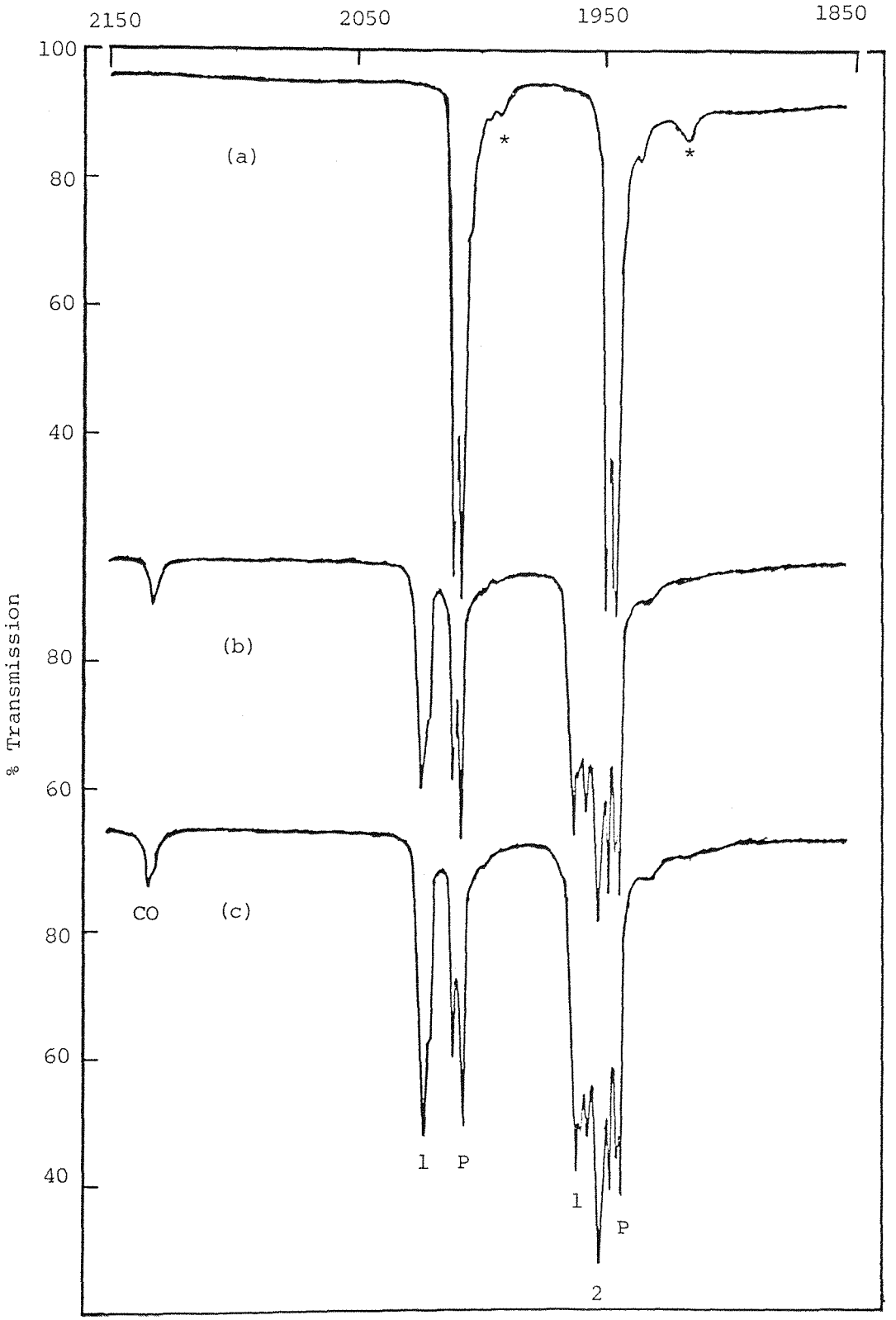

FIGURE 5.5 Infrared spectra from an experiment with $(\eta^5\text{-}C_5H_5)Ru(CO)_2Et$ (bands marked P) isolated at high dilution in a CH_4 matrix at 12K: (a) after deposition, (b) after 45 min photolysis using $290 < \lambda < 370$ nm radiation, and (c) after 20 min photolysis using the same filter. Bands marked with an asterisk (*) are due to $(\eta^5\text{-}C_5H_5)Ru(^{12}CO)(^{13}CO)Et$ present in natural abundance. Bands marked (1) and (2) derive from photoproducts (see text).

candidate is $(\eta^5\text{-}C_5H_5)Ru(CO)(C_2H_4)H$ and this assignment was proved correct when $(\eta^5\text{-}C_5H_5)Ru(CO)_2Et$ was photolysed in a C_2H_4 doped CH_4 matrix. The product with the single band at 1960.3 cm^{-1} was formed in high yield in addition to $(\eta^5\text{-}C_5H_5)Ru(CO)_2H$. In order to provide further evidence $(\eta^5\text{-}C_5H_5)Ru(CO)_2Et$ was photolysed in a ^{13}CO doped CH_4 matrix. The initial products were $(\eta^5\text{-}C_5H_5)Ru(^{12}CO)_2H$ and $(\eta^5\text{-}C_5H_5)Ru(^{12}CO)(C_2H_4)H$ together with a band due to free ^{12}CO. Prolonged photolysis with the same source ($290 < \lambda < 370$ nm) resulted in the growth of bands which were assigned to $(\eta^5\text{-}C_5H_5)Ru(^{12}CO)(^{13}CO)H$ and $(\eta^5\text{-}C_5H_5)Ru(^{13}CO)_2H$ on the basis of the excellent agreement between the observed and calculated bands using an energy-factored force field treatment (Table 5.2). Significantly no bands were observed for $(\eta^5\text{-}C_5H_5)Ru(^{12}CO)_{2-n}(^{13}CO)_nEt$ ($n = 0\text{-}2$) and $(\eta^5\text{-}C_5H_5)Ru(^{13}CO)(C_2H_4)H$.

Photolysis of $(\eta^5\text{-}C_5H_5)Ru(CO)_2Et$ in a N_2 matrix with medium energy u.v. radiation ($290 < \lambda < 370$ nm) led to the production of new photoproduct bands at 2194.8, 2033.2, 1979.8, 1971.4 and 1967.2 cm^{-1} in addition to the band of free CO. Further irradiation resulted in the growth of all the new bands at the expense of the parent complex. The two bands at 2033.2 and 1971.4 cm^{-1} are at similar positions to those obtained when $(\eta^5\text{-}C_5H_5)Ru(CO)_2Et$ was photolysed in CH_4 matrices (Table 5.1) and can be assigned to $(\eta^5\text{-}C_5H_5)Ru(CO)_2H$. Similarly the single band at 1967.2 cm^{-1} may be assigned to $(\eta^5\text{-}C_5H_5)Ru(CO)(C_2H_4)H$. The remaining bands at 2194.8 and 1979.8 cm^{-1} are typical of terminal ν_{NN} and ν_{CO} bands respectively so that the new photoproducts may be identified as $(\eta^5\text{-}C_5H_5)Ru(CO)(N_2)H$, c.f. $(\eta^5\text{-}C_5H_5)Ru(CO)(N_2)Me$. Prolonged photolysis ($290 < \lambda < 370$ nm) led to the growth of a further weak band at 2155.2 cm^{-1} which probably arises from $(\eta^5\text{-}C_5H_5)Ru(N_2)_2H$, c.f. $(\eta^5\text{-}C_5H_5)Ru(N_2)_2Me$ (Table 5.1).

Photolysis ($290 < \lambda$ 370 nm) of $(\eta^5\text{-}C_5H_5)Ru(CO)_2Et$ isolated at high dilution in a CO matrix resulted in the initial growth of three new bands at 2032.4, 1971.2 and 1966.3 cm^{-1}, which may be assigned to the species $(\eta^5\text{-}C_5H_5)Ru(CO)_2H$ and $(\eta^5\text{-}C_5H_5)Ru(CO)(C_2H_4)H$ (Table 5.1). Prolonged irradiation with the same source generated two further bands at 2059.2 and 1980.5 cm^{-1} which grow with constant relative intensities and hence arise

from a single species. By analogy with the band positions for $(\eta^3\text{-}C_5H_5)Fe(CO)_3Me$ (Table 5.1), the new species can be assigned as $(\eta^3\text{-}C_5H_5)Ru(CO)_3Et$. Upon further photolysis with higher energy u.v. light ($270 < \lambda < 390$ nm) some further new bands grew in at 2068.8 and 1983.4 cm^{-1} at the expense of the bands due to $(\eta^5\text{-}C_5H_5)Ru(CO)_2H$ which decreased in intensity. A comparison of the relative band positions for $(\eta^5\text{-}C_5H_5)Ru(CO)_2R$ complexes (R = H, Me, Et) gives an order H > Me > Et so that having assigned the Me and Et ring-slippage products it seems likely that the higher wavenumber bands for this new product can be assigned to $(\eta^3\text{-}C_5H_5)Ru(CO)_3H$ though the ethylene complex $(\eta^3\text{-}C_5H_5)Ru(CO)_2(C_2H_4)H$ cannot be ruled out. The weak band at 2041.5 cm^{-1} together with a band possibly obscured by the intense band at 1980.5 cm^{-1} may tentatively be assigned to $(\eta^4\text{-}C_5H_6)Ru(CO)_3$, by comparison with the band positions for $(\eta^4\text{-}C_5H_5Me)Ru(CO)_3$ (see above; 2038.1 and 1971.5 cm^{-1}), while the remaining weak bands at 2003.5 and 1993.5 cm^{-1} may be assigned to $Ru(CO)_5$ (see above).

5.3 DISCUSSION AND COMPARISON OF SOLUTION WITH MATRIX PHOTOCHEMISTRY

The mechanisms of the photoreactions of $(\eta^5\text{-}C_5H_5)M(CO)_2Me$ complexes in alkanes in the absence and presence of potential ligands have been proposed to involve dissociative loss of CO as the primary process following near-uv excitation [1, 2]. Recent experiments which showed that the quantum yield was independent of the incoming ligand and its concentration support the dissociative mechanism [3]. Similarly the varied photoreactions of $(\eta^5\text{-}C_5H_5)M(CO)_2Et$ complexes have all been proposed to start with the dissociative loss of a CO ligand [2, 3]. For such dissociative processes it has been proposed that $(\eta^5\text{-}C_5H_5)M(CO)R$ species (M = Fe, Ru; R = Me, Et) are reaction intermediates and low temperature studies have sought to trap the monocarbonyl species.

The photoreaction of $(\eta^5\text{-}C_5H_5)M(CO)_2R$ complexes (M = Fe, Ru; R = Me, Et) studied in pentane solutions at -30°C (243K)[†] and in gas matrices at

[†]Experiments carried out by Dr. H.G. Alt at the University of Bayreuth, West Germany.

12K are summarised in Schemes 5.1 and 5.2 respectively.

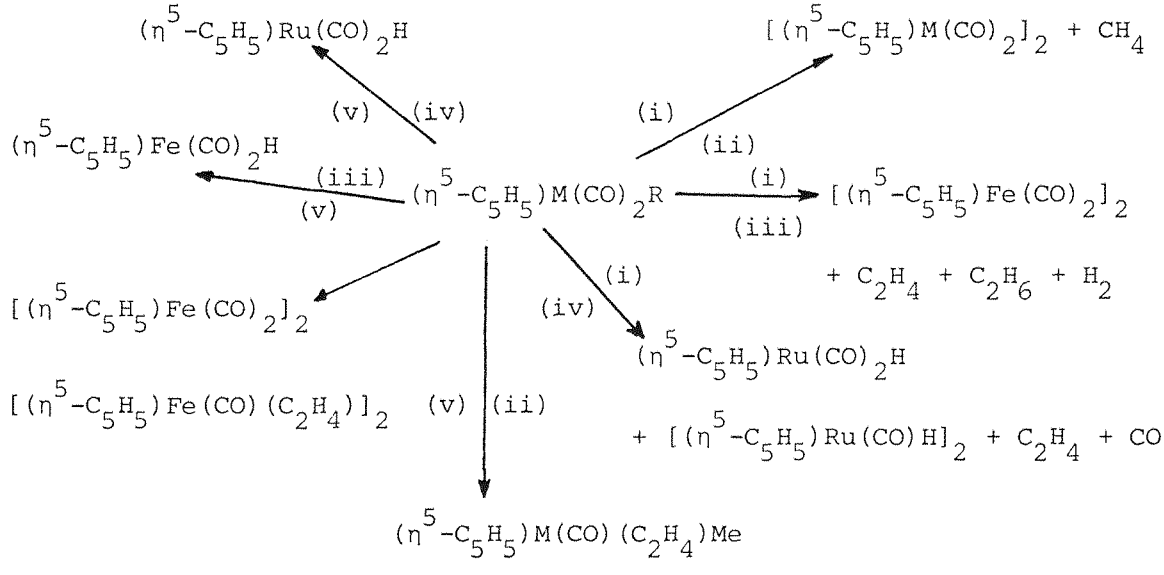

Scheme 5.1

(i) hν, pentane; (ii) M = Fe, Ru; R = Me; (iii) M = Fe; R = Et; (iv) M = Ru; R = Et; (v) hν, C_2H_4/pentane.

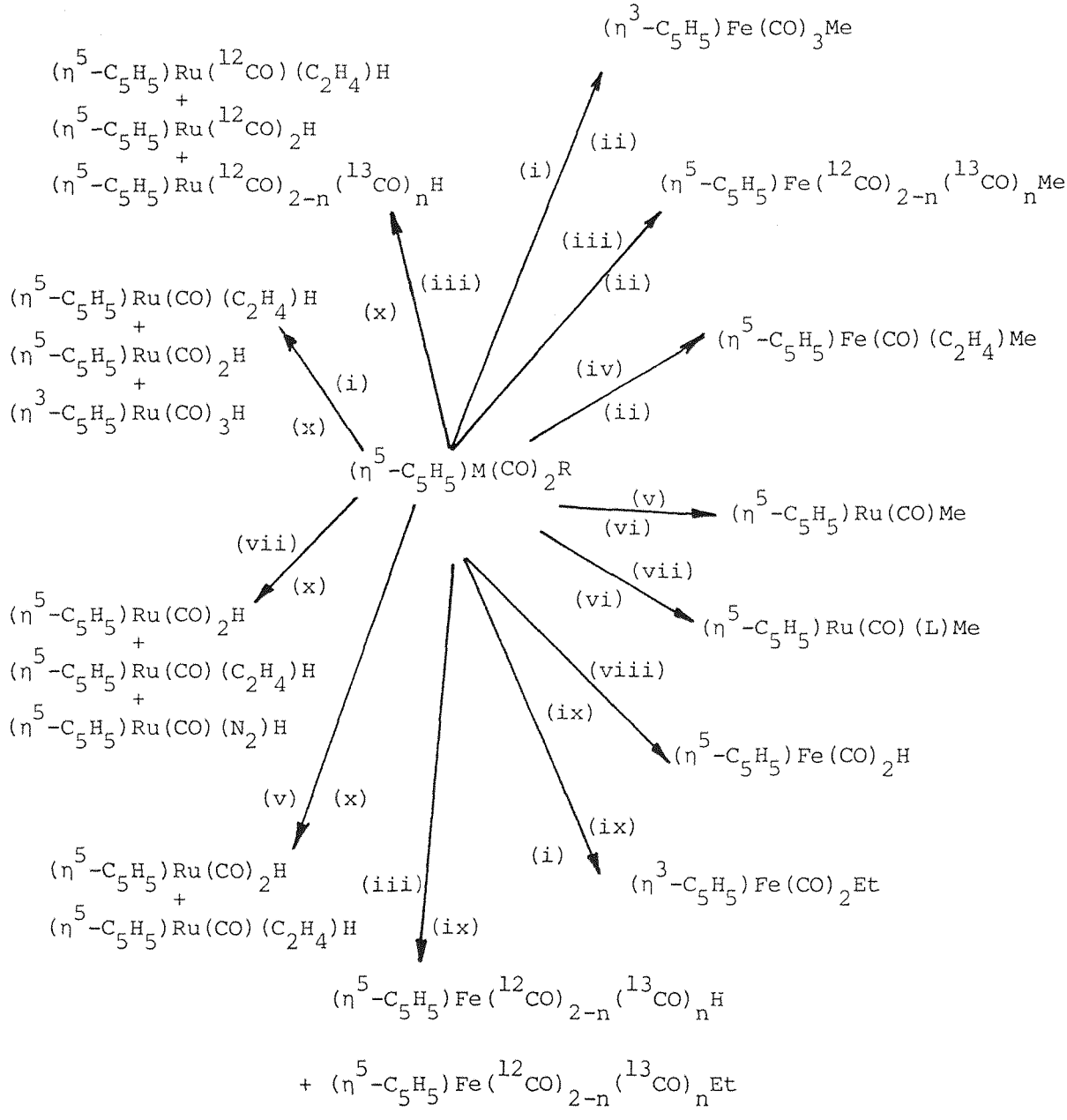

Scheme 5.2

(i) hν, CO; (ii) M = Fe, R = Me; (iii) hν, 5% $^{13}CO/CH_4$; (iv) hν, 5% C_2H_4/CH_4; (v) hν, CH_4; (vi) M = Ru, R = Me; (vii) hν, N_2, 5% C_2H_4/CH_4, 5% $^{13}CO/CH_4$; (viii) hν, CH_4, N_2; (ix) M = Fe, R = Et; (x) M = Ru, R = Et.

The formation of $[(\eta^5\text{-}C_5H_5)Ru(CO)_2]_2$ on photolysis of $(\eta^5\text{-}C_5H_5)Ru(CO)_2Me$ in pentane at -30°C parallels the finding for the iron analogue [2].

In contrast to this the photoreaction of $(\eta^5\text{-}C_5H_5)Fe(CO)_2Et$ at -30°C produced $[(\eta^5\text{-}C_5H_5)Fe(CO)_2]_2$ [2] whereas the ruthenium analogue gave $(\eta^5\text{-}C_5H_5)Ru(CO)_2H$ and the new dimer $[(\eta^5\text{-}C_5H_5)Ru(CO)H]_2$, a complex that contains a Ru = Ru double bond, (I). A similar dimeric Os-hydrido complex with pentamethylsubstituted cyclopentadienyl rings has been reported recently [15].

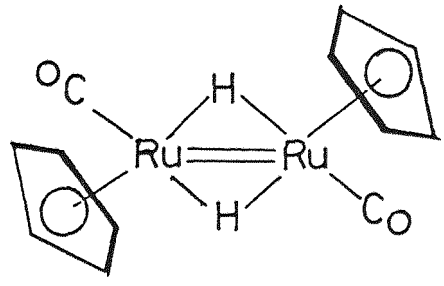

(I)

The composition of the photolysis gas of the photo-induced de-alkylation of $(\eta^5\text{-}C_5H_5)Ru(CO)_2Et$ depended on the length of photolysis. In the beginning ethylene was the dominant component besides a little ethane, but then the amount of carbon monoxide increased, and at the end of the reaction this was the main product. Although an ethylene hydrido complex of the composition $(\eta^5\text{-}C_5H_5)Ru(CO)(C_2H_4)H$ could not be detected in solution, it is apparent that a β-hydrogen transfer reaction is the key step in this reaction (Scheme 5.3) Support for this reaction sequence is afforded by the conversion of $(\eta^5\text{-}C_5H_5)Ru\{P(C_6H_5)_3\}_2\ C_2H_5$ to $(\eta^5\text{-}C_5H_5)Ru\{P(C_6H_5)_3\}(C_2H_4)H$ and subsequently to $(\eta^5\text{-}C_5H_5)Ru\{P(C_6H_5)_3\}_2H$ in solution at 80°C [16].

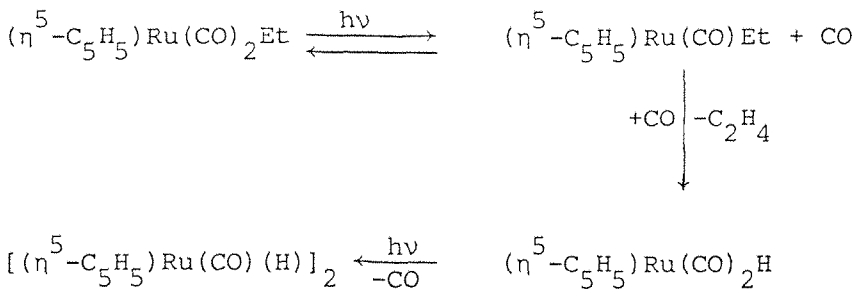

Scheme 5.3

At 25°C it was reported that photolysis of $(\eta^5\text{-}C_5H_5)M(CO)_2Et$ complexes (M = Fe, Ru) led to the formation of the mononuclear hydrides $(\eta^5\text{-}C_5H_5)M(CO)_2H$ [3].

The photo-induced reactions of $(\eta^5\text{-}C_5H_5)M(CO)_2Me$ complexes (M = Fe, Ru) in the presence of ethylene at -30°C results in the formation of the mono substitution products $(\eta^5\text{-}C_5H_5)M(CO)(C_2H_4)Me$. This is analogous to the behaviour of $(\eta^5\text{-}C_5H_5)Fe(C_2H_4)(CO)SnR_3$ and $(\eta^5\text{-}C_9H_7)Fe(CO)(C_2H_4)SnR_3$ complexes (R = Me, Ph) [17]. The reaction with the Fe derivatives is ca four times faster than the one with the Ru analogue. No other products could be detected. The Fe olefin complex was particularly temperature sensitive; it decomposed above -30°C.

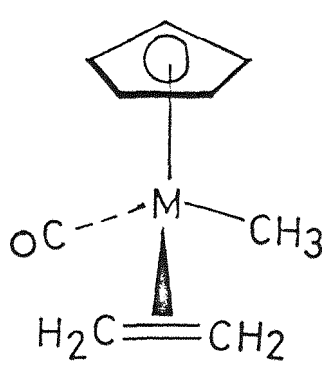

(II/III)

The rotation barrier around the metal-olefin bond axis in (II) and (III) was comparatively low, e.g. $\Delta G^{\dagger}$ = 41.3 KJ/mole and 36.4 KJ/mole for Fe and Ru respectively. The low barrier was explained as arising from weak back donation M → C_2H_4.

The preparation of the $(\eta^5\text{-}C_5H_5)Fe(CO)(C_2H_4)Me$ and $(\eta^5\text{-}C_5H_5)Ru(CO)(C_2H_4)Me$ complexes is noteworthy because they represent the first examples of Fe and Ru olefin alkyl derivatives. So far the known $(\eta^5\text{-}C_5H_5)M(CO)(L)Me$ species (M = Fe, Ru) have contained ligands L that are primarily n-donors, e.g. phosphines or phosphites. Differences between the first and second row metals emerge when the $(\eta^5\text{-}C_5H_5)M(CO)_2Et$ complexes are photolysed in pentane in the presence of C_2H_4. For example the metal-containing products in the case of Fe are $(\eta^5\text{-}C_5H_5)Fe(CO)_2H$, $[(\eta^5\text{-}C_5H_5)Fe(CO)_2]_2$, and the new dimer $[(\eta^5\text{-}C_5H_5)Fe(CO)(C_2H_4)]_2$ whereas $(\eta^5\text{-}C_5H_5)Ru(CO)_2H$ is the only product for the Ru, i.e. the Ru-H bond is less photochemically labile than the Fe-H bond. In neat 1-pentene at 77K, however, CO replacement was observed for $(\eta^5\text{-}C_5H_5)Ru(CO)_2H$ to give $(\eta^5\text{-}C_5H_5)Ru(CO)(1\text{-pentene})H$ [3] and in neat 1-pentene solution at -140°C the iron ethyl complex, $(\eta^5\text{-}C_5H_5)Fe(CO)_2Et$ gave $(\eta^5\text{-}C_5H_5)Fe(CO)(1\text{-pentene})(n\text{-pentyl})$ that was very substitution labile [3].

In Ar [4] and Ar, CH_4 and N_2 [5] matrices no evidence for the formation of $(\eta^5\text{-}C_5H_5)Fe(CO)Me$ was found on photolysis of $(\eta^5\text{-}C_5H_5)Fe(CO)_2Me$ although $(\eta^5\text{-}C_5H_5)Fe(CO)(COMe)$ was found [5] on photolysis of $(\eta^5\text{-}C_5H_5)Fe(CO)_2(COMe)$ and facile ^{13}CO exchange with $(\eta^5\text{-}C_5H_5)Fe(CO)_2Me$ was found [4, 5] for ^{13}CO-doped matrices. Photolysis of the Ru analogue provided the first direct evidence for the dissociative process when $(\eta^5\text{-}C_5H_5)Ru(CO)Me$ was formed in an alkane matrix at 77K [3]. Confirmation of this result is afforded by this work in matrices at 12K and in particular by the observation of bands for $(\eta^5\text{-}C_5H_5)Ru(^{12}CO)Me$ and $(\eta^5\text{-}C_5H_5)Ru(^{13}CO)Me$ in ^{13}CO doped matrices (Table 5.2). Differences in the stability of Fe and Ru species were also demonstrated by the detection (Table 5.2) of $(\eta^5\text{-}C_5H_5)Ru(CO)(N_2)Me$ and $(\eta^5\text{-}C_5H_5)Ru(CO)(N_2)H$ in N_2 matrices although both metals gave $(\eta^5\text{-}C_5H_5)M(CO)(C_2H_4)Me$ species in C_2H_4 doped CH_4 matrices.

In Ar (10K) [4], paraffin wax (77K) [3], and CH_4, N_2 and C_2H_4 doped CH_4 (12K, this work) matrices no evidence was found for the formation of $(\eta^5\text{-}C_5H_5)Fe(CO)Et$ but rather β-elimination and recapture of CO occurred to give $(\eta^5\text{-}C_5H_5)Fe(CO)_2H$; no evidence could be found either for the intermediate species $(\eta^5\text{-}C_5H_5)Fe(CO)(C_2H_4)H$. An indication that matters were more complex than just 'β-elimination and recapture of CO' was provided by the experiment involving a ^{13}CO doped CH_4 matrix when two ^{13}CO enriched products $(\eta^5\text{-}C_5H_5)Fe(^{12}CO)_{2-n}(^{13}CO)_nH$ (n = 0-2) and surprisingly $(\eta^5\text{-}C_5H_5)Fe(^{12}CO)_{2-n}(^{13}CO)_nEt$ (n = 0-2) (Table 5.2) were observed. In contrast to Fe, the Ru complex gave the species $(\eta^5\text{-}C_5H_5)Ru(CO)(C_2H_4)H$ and $(\eta^5\text{-}C_5H_5)Ru(CO)_2H$ in alkane matrices (77K) [3], and in CH_4 and N_2 matrices (12K; this work). Similarly, thermal and photochemical decomposition of $Fe_2(CO)_8(\mu\text{-}CHCH_3)$ [18], $Fe_2(CO)_8(\mu\text{-}C_3H_5R)$ and $[(\eta^5\text{-}C_5H_5)_2M_2(CO)_4\{\mu\text{-}(CH_2)_n\}]$ (M = Fe, n = 3-5; M = Ru, n = 3) resulted in evolution of hydrocarbons and olefins [19, 20]. The results were interpreted in terms of a transient dimetallocycle which decomposes via β-elimination and were suggested to be related to the mechanism of Fischer-Tropsch catalysis [21, 22]. The mechanism of formation of hydrides $(\eta^5\text{-}C_5H_5)M(CO)_2H$ (M = Fe, Ru) may be represented as shown in Scheme 5.4

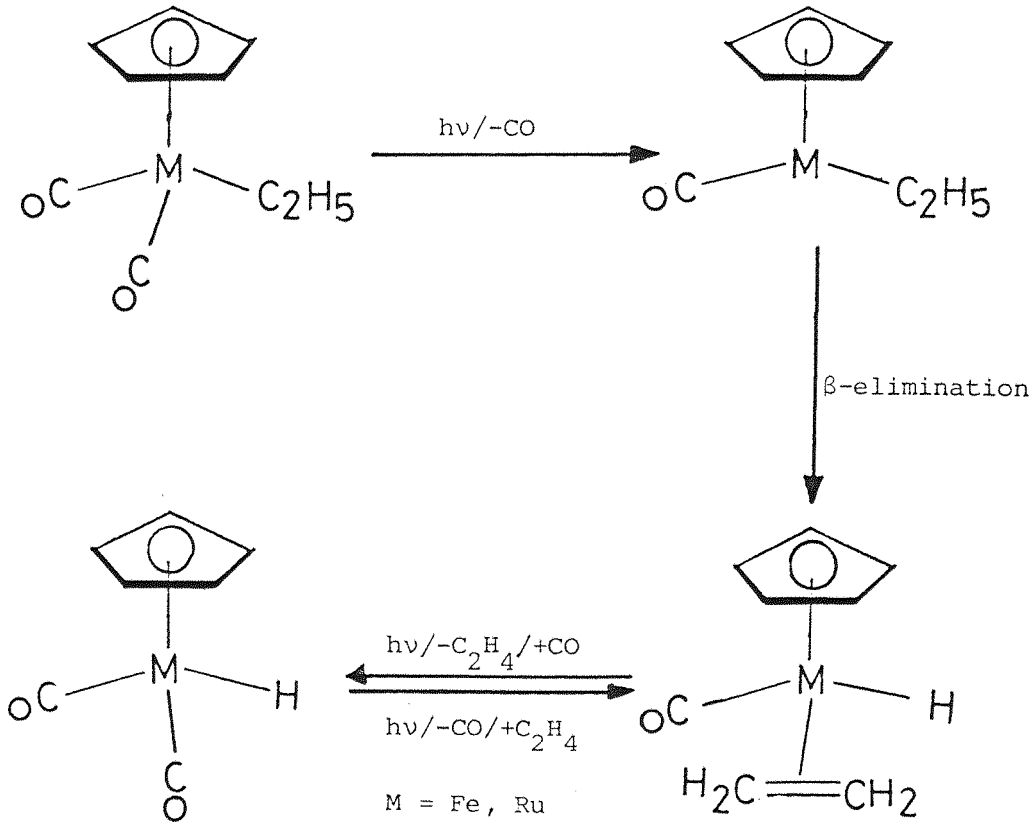

Scheme 5.4

Surprisingly, although the $(\eta^5\text{-}C_5H_5)Ru(CO)_2H$ species showed enrichment (Table 5.2) when $(\eta^5\text{-}C_5H_5)Ru(CO)_2Et$ was photolysed in a ^{13}CO doped matrix, no enrichment was observed for $(\eta^5\text{-}C_5H_5)Ru(CO)(C_2H_4)H$.

The photolysis of $(\eta^5\text{-}C_5H_5)Fe(CO)_2CH_3$ to give the ring-slippage product $(\eta^3\text{-}C_5H_5)Fe(CO)_3CH_3$ in CO matrices indicated [5] that the associative path should not be neglected. The existence of a $\eta^3\text{-}C_5H_5$ group has been demonstrated by an X-ray crystallographic study of $(\eta^3\text{-}C_5H_5)(\eta^5\text{-}C_5H_5)W(CO)_2$ [23]. Similarly, an expanded co-ordination number species $(\eta^3\text{-}C_5H_5)Fe(CO)_2(L)CH_3$ (L = CO or PR_3) accounts for the variety of products observed in the photochemical reactions of $(\eta^5\text{-}C_5H_5)Fe(CO)_2CH_3$ [24 - 27]. The u.v. irradiation possibly excites a metal-to-ligand charge-transfer (MLCT) transition [Fe → $(\eta^5\text{-}C_5H_5)$], which assists the attack of ligand L on Fe, with a concerted $\eta^5 \rightarrow \eta^3$ change in the mode of the ring co-ordination. Analogously, $(\eta^5\text{-}C_5H_5)Co(CO)_2$ exhibits a bimolecular substitution reaction [28], (Equation 5.2) which is explained by the intermediacy of a $Co(\eta^3\text{-}C_5H_5)$

$$(\eta^5\text{-}C_5H_5)Co(CO)_2 + L \longrightarrow (\eta^3\text{-}C_5H_5)Co(CO)_2(L) \qquad (5.2)$$

species [29]. Pertinent to this proposal was the presentation of infrared evidence for $(\eta^3\text{-}C_5H_5)Co(CO)_3$ in CO matrix at 12 K [8]. Transfer of electrons to the cyclopentadiene moiety was suggested to take place in the transition state. In case of $(\eta^5\text{-}C_5H_5)Ru(CO)_2CH_3$ the situation was more complicated. In addition to the low yield of $(\eta^3\text{-}C_5H_5)Ru(CO)_3CH_3$, irradiation of $(\eta^5\text{-}C_5H_5)Ru(CO)_2CH_3$ in CO matrices produced other species as major photoproducts. The presence of $Ru(CO)_5$ and $(\eta^3\text{-}C_5H_5)Ru(CO)_3CH_3$ complexes among the photoproducts suggests the following possible associative pathways (Scheme 5.5). Both steps (a) and (b) in Scheme 5.5 are possible. Recently structural evidence was found for cyclopentadiene ring slippage during phosphine substitution reactions at co-ordinatively saturated metal centres. For example, the reaction [30, 31] of $(\eta^5\text{-}C_5H_5)Re(NO)(CO)CH_3$ and $(\eta^5\text{-}C_5H_5)Re(CO)_3$ with $P(CH_3)_3$ at 25°C yielded the $(\eta^1\text{-}C_5H_5)Re(NO)(CO)[(P(CH_3)_3]_2CH_3$ and $(\eta^1\text{-}C_5H_5)Re(CO)_3[(P(CH_3)_3]_2$ complexes respectively, in which

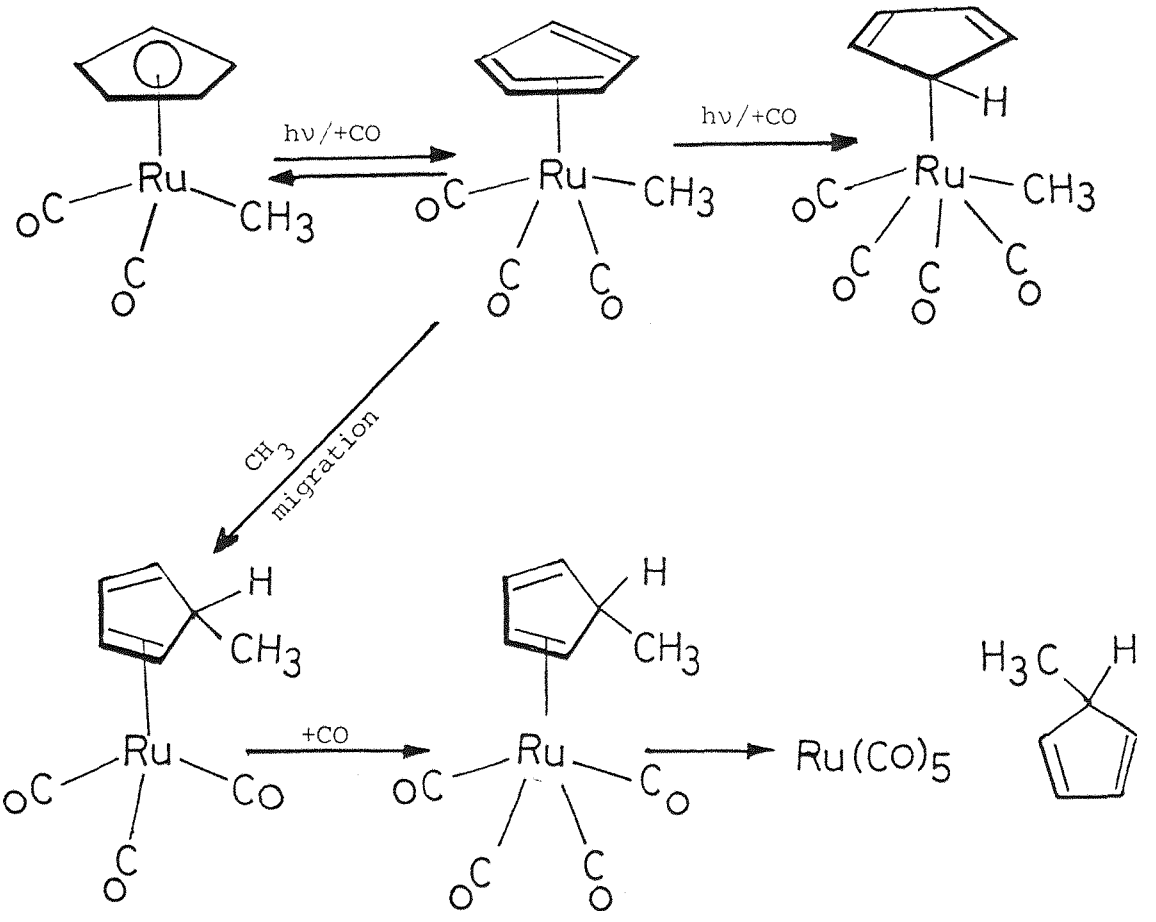

Scheme 5.5

the η^5-C_5H_5 ring has slipped all the way to an η^1-C_5H_5 configuration [32, 33]. The bands of (η^4-$C_5H_5CH_3$)$Ru(CO)_3$ at (2029.4 and 1969.3 cm^{-1}) are relatively similar to that of (η^4-butadiene)$Fe(CO)_3$ at (2028 and 1969 cm^{-1}) in Ar matrices [34]. However, metal-to-ring alkyl migration has only been observed under forcing conditions (50 atm, 50°C) for (η^5-C_5H_5)$_2$Mo(Et)Cl in the presence of CO [35], (Equation 5.3), whereas hydrogen transfer has been demonstrated to be facile in the reactions of (η^5-C_5H_5)$_2$ReH in low-temperature CO matrices [11]. Other authors [4, 36] who have examined ring $\rightleftharpoons$ metal hydrogen and alkyl migrations have often considered that

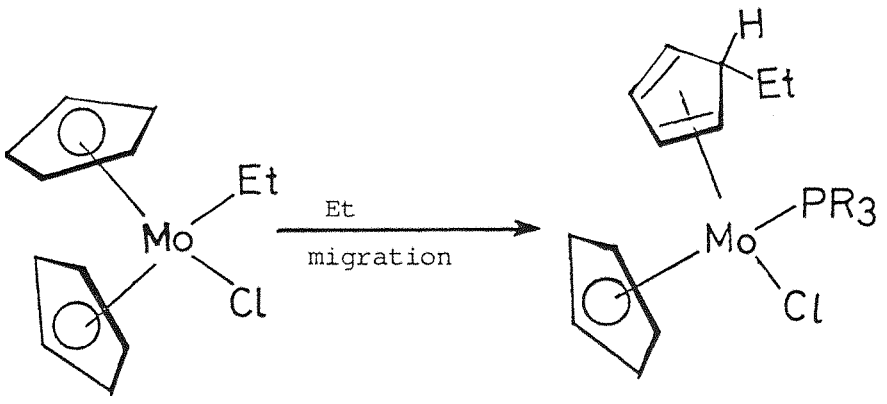

(5.3)

they may proceed via 16-electron intermediates (Equations 5.4 and 5.5), but such an intermediate has only been observed for $(\eta^5\text{-}C_5H_4Me)Fe(CO)_2Me$ [4], (Equation 5.5). In the alkyl transfer reaction of $(\eta^5\text{-}C_5H_5)_2Mo(Et)Cl$, a single step rather than a two step reaction seemed more plausible (Equation 5.3), [35].

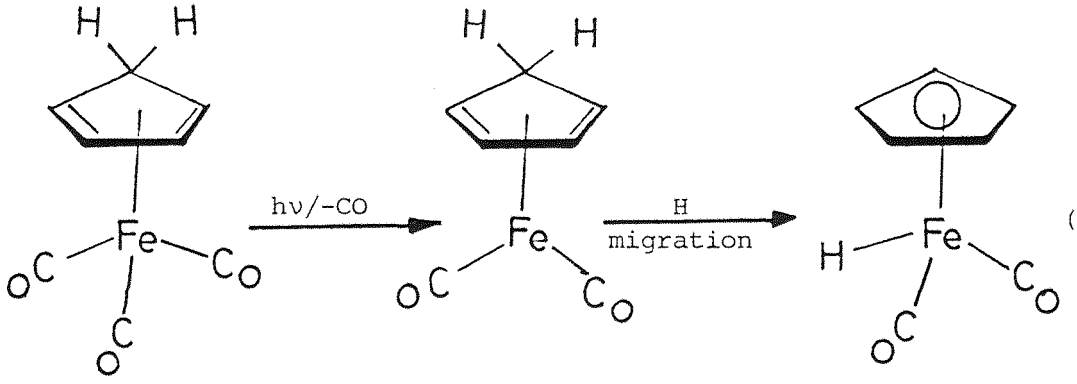

(5.4)

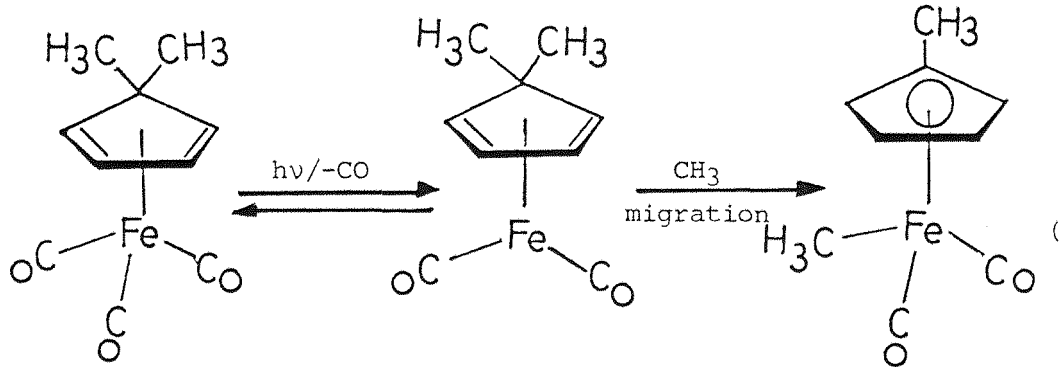

(5.5)

5.4 CONCLUSIONS

The importance of the CO dissociation path in the photoreactions of $(\eta^5\text{-}C_5H_5)M(CO)_2R$ complexes (M = Fe, Ru; R = Me, Et) has been confirmed by the detection of $(\eta^5\text{-}C_5H_5)Ru(^{12}CO)Me$ and $(\eta^5\text{-}C_5H_5)Ru(^{13}CO)Me$ in gas matrices at 12K and $(\eta^5\text{-}C_5H_5)Ru(CO)Me$ in alkane matrices at 77K [3]. The detection of ring-slippage products $(\eta^3\text{-}C_5H_5)M(CO)_3R$ (M = Fe, Ru; R = CH_3, H) and the nature of ^{13}CO exchange products in matrices at 12K indicates that there are a number of competing paths and that subtle differences occur between Fe and Ru and between methyl and ethyl derivatives. For example, it seems as though the ring-slippage process takes places after the primary processes of CO ejection and β-elimination for the ethyl complexes.

Table 5.1 I.r. band positions (cm^{-1}) observed in the CO stretching region for $(\eta^5\text{-}C_5H_5)M(CO)_2R$ complexes (M = Fe, Ru; R = Me, Et) and their photoproducts in various gas matrices at 12K.

Complex	CH_4	N_2	5% C_2H_4/ CH_4	CO
$(\eta^5\text{-}C_5H_5)Fe(CO)_2Me$[a]	2014.2)[b] 2010.3)	2017.0)[b] 2015.4)	2011.2	2015.4 2013.1
	1958.6)[b] 1954.3)	1963.4)[b] 1961.0)	1955.7	1961.0
$(\eta^5\text{-}C_5H_5)Fe(CO)_2Et$	2077.3)[b] 2003.5)	2009.6	2003.7	2008.3
	1952.1)[b] 1947.8)	1955.0	1947.1	1952.5
$(\eta^5\text{-}C_5H_5)Ru(CO)_2Me$	2020.1)[b] 2016.7)	2024.0	2016.5	2020.7
	1960.2)[b] 1956.4)	1966.7	1956.6	1962.4
$(\eta^5\text{-}C_5H_5)Ru(CO)_2Et$	2018.1)[b] 2015.2)	2019.8	2010.8	2018.2
	1956.4)[b] 1952.6)	1959.2	1949.7	1957.0
$(\eta^5\text{-}C_5H_5)Fe(CO)_2H$	2017.6 1958.5	2021.8 1964.1	2016.8 1957.5	2020.8 1957.5
$(\eta^3\text{-}C_5H_5)Fe(CO)_3Me$[a]				2050.3 1982.7 1975.1
$(\eta^3\text{-}C_5H_5)Fe(CO)_3Et$				2046.0 1978.7 1969.3
$(\eta^5\text{-}C_5H_5)Ru(CO)Me$	1943.4		1941.7	

/continued

Table 5.1 (Continued)

Complex	CH_4	N_2	5% C_2H_4/ CH_4	CO
$(\eta^5\text{-}C_5H_5)Ru(CO)(N_2)Me$[c]		1968.2		
$(\eta^5\text{-}C_5H_5)Ru(CO)(C_2H_4)Me$			1956.6[d]	
$(\eta^5\text{-}C_5H_5)Ru(CO)_2H$	2029.2 1967.5	2033.2 1971.4	2024.7 1961.2	2032.4 1971.2
$(\eta^5\text{-}C_5H_5)Ru(CO)(N_2)H$[e]		1979.8		
$(\eta^5\text{-}C_5H_5)Ru(CO)(C_2H_4)H$	1960.3	1967.2	1954.1	1966.3
$(\eta^3\text{-}C_5H_5)Ru(CO)_3Me$				2061.2 f
$(\eta^3\text{-}C_5H_5)Ru(CO)_3Et$				2059.2 1980.5
$(\eta^3\text{-}C_5H_5)Ru(CO)_3H$				2068.8 1983.4

[a] Data from Reference 5.

[b] Bands bracketed together arise from a single with matrix splitting unless otherwise stated.

[c] ν_{NN} at 2188.6 cm^{-1} for $(\eta^5\text{-}C_5H_5)Ru(CO)(N_2)Me$ and at 2152.5 cm^{-1} for $(\eta^5\text{-}C_5H_5)Ru(N_2)_2Me$.

[d] Band obscured initially by lower band of $(\eta^5\text{-}C_5H_5)Ru(CO)_2Me$.

[e] ν_{NN} at 2194.8 cm^{-1} for $(\eta^5\text{-}C_5H_5)Ru(CO)(N_2)H$ and at 2155.2 cm^{-1} for $(\eta^5\text{-}C_5H_5)Ru(N_2)_2H$.

[f] Band obscured by other photoproducts.

Table 5.2 Observed and calculated[a] band positions (cm^{-1}) of the terminal CO stretching bands of ^{13}CO-enriched (η^5-C_5H_5)$M(CO)_2R$ complexes (M = Fe, Ru; R = Me, Et) and their photoproducts in mixed $^{13}CO:CH_4$ (1:20) matrices at 12K.

Complex	Point Group	ν_{CO}	Observed bands	Calculated bands
(η^5-C_5H_5)Fe(^{12}CO)$_2$Et	C_s	A'	2003.8	2003.1
		A"	1946.3	1946.0
(η^5-C_5H_5)Fe(^{12}CO)(^{13}CO)Et	C_1	A	1987.5	1988.4
		A	1916.6	1916.8
(η^5-C_5H_5)Fe(^{13}CO)$_2$Et	C_s	A'	1957.7	1958.6
		A"	1902.2	1902.7
(η^5-C_5H_5)Ru(^{12}CO)$_2$Me	C_s	A'	2016.7	2016.7
			1956.3	1956.3
(η^5-C_5H_5)Ru(^{12}CO)(^{13}CO)Me	C_1	A	2011.7	2011.6
		A	1927.0	1927.3
(η^5-C_5H_5)Ru(^{13}CO)$_2$Me	C_s	A'	1971.0	1971.9
		A"	1912.1	1912.8
(η^5-C_5H_5)Ru(^{12}CO)$_2$Et	C_s	A'	2013.5	2013.5
		A"	1952.4	1952.4
(η^5-C_5H_5)Ru(^{12}CO)(^{13}CO)Et	C_1	A	b	1998.4
		A		1923.5
(η^5-C_5H_5)Ru(^{13}CO)$_2$Et	C_s	A'	b	1968.8
		A"		1909.0
(η^5-C_5H_5)Fe(^{12}CO)$_2$H	C_s	A'	2018.1	2018.4
		A"	1958.7	1958.2
(η^5-C_5H_5)Fe(^{12}CO)(^{13}CO)H	C_1	A	2003.8	2003.3
		A	1928.4	1929.2
(η^5-C_5H_5)Fe(^{13}CO)$_2$H	C_s	A'	1972.7	1973.5
		A"	1915.0	1914.7

/continued

Table 5.2 (Continued)

Complex	Point Group	ν_{NN}	Observed bands	Calculated bands
$(\eta^5\text{-}C_5H_5)Ru(^{12}CO)Me$	C_s	A'	1940.7	1940.7
$(\eta^5\text{-}C_5H_5)Ru(^{13}CO)Me$	C_s	A'	1895.8	1896.6
$(\eta^5\text{-}C_5H_5)Ru(^{12}CO)_2H$	C_s	A' A"	2027.6 1965.7	2027.7 1965.7
$(\eta^5\text{-}C_5H_5)Ru(^{12}CO)(^{13}CO)H$	C_1	A A	2012.5 1936.1	2012.3 1936.6
$(\eta^5\text{-}C_5H_5)Ru(^{13}CO)_2H$	C_s	A' A"	1981.0 1920.8	1981.6 1921.0
$(\eta^5\text{-}C_5H_5)Ru(^{12}CO)(C_2H_4)H$	C_1	A	1958.7	1958.7
$(\eta^5\text{-}C_5H_5)R(^{13}CO)(C_2H_4)H$	C_1	A	b	1914.2

[a]Refined energy factored CO stretching and interaction force constants (Nm^{-1}) are:

$(\eta^5\text{-}C_5H_5)Fe(CO)_2Me$, K = 1593.7 and k_i = 44.3 (Ref. 5);

$(\eta^5\text{-}C_5H_5)Fe(CO)_2Et$, K = 1575.4 and k_i = 45.6;

$(\eta^5\text{-}C_5H_5)Ru(CO)_2Me$, K = 1594.7 and k_i = 48.5;

$(\eta^5\text{-}C_5H_5)Ru(CO)_2Et$, K = 1589.0 and k_i = 49.0;

$(\eta^5\text{-}C_5H_5)Fe(CO)_2H$, K = 1597.5 and k_i = 48.3;

$(\eta^5\text{-}C_5H_5)Ru(CO)Me$, K = 1520.9;

$(\eta^5\text{-}C_5H_5)Ru(CO)_2H$, K = 1611.0 and k_i = 50.0.

[b]Enrichment competing with other photoprocesses which dominate in the course of the long photolysis times needed to produce these bands.

5.5 REFERENCES

1. P.M. Treichel, R.L. Shubkin, K.W. Barnett and D. Reichard, *Inorg. Chem.*, 1966, 5, 1177.

2. H.G. Alt, M. Herberhold, M.D. Rausch and B.H. Edwards, *Z.Naturforsch.*, 1979, 34b, 1970.

3. R.J. Kazlauskas and M.S. Wrighton, *Organometallics*, 1982, 1, 602.

4. W. Gerhartz, G. Ellerhorst, P. Dahler and P. Eilbracht, *Liebigs. Ann. Chem.*, 1981, 2311.

5. D.J. Fettes, R. Narayanaswamy and A.J. Rest, *J. Chem. Soc. Dalton Trans.*, 1981, 2311.

6. K.A. Mahmoud, A.J. Rest, H.G. Alt, M.E. Eichner and B.M. Jansen, *J. Chem. Soc. Dalton Trans.*, accepted for publication.

7. P.S. Braterman, *"Metal Carbonyl Spectra"*, Academic Press, London, 1975.

8. O. Crichton, A.J. Rest and D.J. Taylor, *J. Chem. Soc. Dalton Trans.*, 1980, 167.

9. O. Crichton and A.J. Rest, *J. Chem. Soc. Dalton Trans.*, 1977, 981.

10. R.H. Hooker and A.J. Rest, *J. Chem. Soc. Dalton Trans.*, accepted for publication.

11. J. Chetwynd-Talbot, P. Grebenik and R.N. Perutz, *J. Chem. Soc. Chem. Comm.*, 1981, 452; *Inorg. Chem.*, 1983, in press.

12. F. Calderazzo and F. L'Eplattenier, *Inorg. Chem.*, 1967, 6, 1220.

13. M. Poliakoff and J.J. Turner, *J. Chem. Soc. Dalton Trans.*, 1973, 1351.

14. K.A. Mahmoud, A.J. Rest and H.G. Alt, *J. Organomet. Chem.*, 1983, 246, C37; *J. Chem. Soc. Dalton Trans.*, accepted for publication.

15. J.K. Hoyano and W.A.G. Graham, *J. Am. Chem. Soc.*, 1982, 104, 3722; J.K. Hoyano, C.J. May and W.A.G. Graham, *Inorg. Chem.*, 1982, 21, 3095.

16. (a) H. Lehmkuhl, J. Grundke, R. Benn, G. Schroth and R. Mynott, *J. Organomet. Chem.*, 1981, 217, C5.

(b) H. Lehmkuhl, J. Grundke and R. Mynott, *Chem. Ber.*, 1983, 116, 159.

17. J.W. Faller, B.V. Johnson and C.D. Schaeffer Jr., *J. Am. Chem. Soc.*, 1976, 98, 1395.

18. C.E. Sumner, Jr., J.A. Collier and R. Pettit, *Organometallics*, 1982, 1, 1350.

19. M. Cooke, N.J. Forrow and S.A.R. Knox, *J. Organomet. Chem.*, 1981, 222, C21.

20. J.B. Keister, *J. Organomet. Chem.*, 1983, 245, 426.

21. R.C. Brady and R. Pettit, *J. Am. Chem. Soc.*, 1981, 103, 1287.

22. R.L. Pruett, *Adv. Organomet. Chem.*, 1979, 1, 17.

23. G. Huttner, H.H. Brintzinger, L.G. Bell, P. Friedrich, V. Bejenke and D. Neugebauer, *J. Organomet. Chem.*, 1978, 145, 329.

24. P.M. Treichel, R.L. Shubkin, K.W. Barnett and D. Reichard, *Inorg. Chem.*, 1966, 5, 1177.

25. C.R. Folkes and A.J. Rest, *J. Organomet. Chem.*, 1977, 136, 355.

26. S.R. Su and A. Wojciki, *J. Organomet. Chem.*, 1971, 27, 231.

27. A.C. Gingell and A.J. Rest, *J. Organomet. Chem.*, 1975, 99, C27.

28. H.G. Schuster-Woldan and F. Basolo, *J. Am. Chem. Soc.*, 1966, 88, 1657.

29. M.E. Revek and F. Basolo, *Organometallics.*, 1983, 2, 373.

30. C.P. Casey and W.D. Jones, *J. Am. Chem. Soc.*, 1980, 102, 6154.

31. A.B. Goel, S. Goel, D. Van der Veer and H.C. Clark, *Inorg. Chim. Acta.*, 1981, 53, L117.

32. C.P. Casey, J.M. O'Connor, W.D. Jones and K.J. Haller, *Organometallics.*, 1983, 2, 535.

33. C.P. Casey, W.D. Jones and S.G. Harsy, *J. Organomet. Chem.*, 1981, 206, C38.

34. G. Ellerhorst, W. Gerhartz and F.-W. Grevels, *Inorg. Chem.*, 1980, 19, 67.

35. F.W.S. Benfield and M.L.H. Green, *J. Chem. Soc. Dalton Trans.*, 1974, 1324.

CHAPTER SIX

PHOTOCHEMISTRY OF $(\eta^5\text{-}C_5H_5)M(CO)_3Cl$ (M = Mo, W) AND OF $(\eta^5\text{-}C_5H_5)M(CO)_2Cl$ (M = Fe, Ru) COMPLEXES IN LOW TEMPERATURE MATRICES AT 12K

6.1 INTRODUCTION

Previous investigations have illustrated that the $(\eta^5\text{-}C_5H_5)M(CO)_3X$ complexes (M = Mo, W; X = Cl, Br, I) react with a variety of ligands in solutions to yield derivatives of two types:

(i) Reactions in which CO only is displaced photochemically with a variety of two electron donor ligands (Equation 6.1).

$$(\eta^5\text{-}C_5H_5)M(CO)_3X + L \xrightarrow{h\nu} (\eta^5\text{-}C_5H_5)M(CO)_2(L)X + CO \quad (6.1)$$

Examples of such mono-substituted products are $(\eta^5\text{-}C_5H_5)Mo(CO)_2(L)Cl$ (L = PPh_3, $AsPh_3$, $SbPh_3$) and $(\eta^5\text{-}C_5H_5)Mo(CO)_2(L)I$ (L = PEt_3, PPh_3, $AsPh_3$, $AsMePh_2$, $SbPh_3$) [1]. Substituted derivatives of $(\eta^5\text{-}C_5H_5)M(CO)_3X$ have also been prepared by thermal reactions of the complexes with two electron donor ligands [2, 3]. Disubstituted complexes of general formula $(\eta^5\text{-}C_5H_5)M(CO)(L)_2X$ have been obtained by prolonged irradiation of $(\eta^5\text{-}C_5H_5)M(CO)_3X$ with excess ligand [1], which suggests that the mono substituted complexes are themselves susceptible to photosubstitution (Equation 6.2).

$$(\eta^5\text{-}C_5H_5)M(CO)_2(L)X + L \xrightarrow{h\nu} (\eta^5\text{-}C_5H_5)M(CO)(L)_2X + CO \quad (6.2)$$

Similarly $(\eta^5\text{-}C_5H_5)M(CO)_3X$ complexes are reported to react photochemically with the bidentate ligands $Me_2P(CH_2)_2PMe_2$ and *cis*-$Ph_2PCH = CHPPh_2$ ejecting two CO ligands and forming $(\eta^5\text{-}C_5H_5)M(CO)(\overline{L\quad L})X$ complexes [4].

(ii) Reactions in which the halide ion is displaced to yield ionic products, $(\eta^5\text{-}C_5H_5)M(CO)_3^+X^-$ (Equation 6.3).

$$(\eta^5\text{-}C_5H_5)M(CO)_3X \xrightarrow{h\nu} (\eta^5\text{-}C_5H_5)M(CO)_3^+ + X^- \qquad (6.3)$$

For example, $(\eta^5\text{-}C_5H_5)Mo(CO)_3Cl$ reacts with ammonia or hydrazine to afford the ionic derivatives $(\eta^5\text{-}C_5H_5)Mo(CO)_3(am)^+X^-$ (am = NH_3 or N_2H_4) [5]. Irradiation of $(\eta^5\text{-}C_5H_5)Mo(CO)_3Cl$ also promotes the formation of the ionic substitution compounds $(\eta^5\text{-}C_5H_5)Mo(CO)_2(L)_2^+Cl^-$ where (L = PEt_3, PPh_3, or L_2 = diphos) [7]. The tungsten complex $(\eta^5\text{-}C_5H_5)W(CO)_3Cl$ reacts with triphenyl and triethyl phosphine to afford $(\eta^5\text{-}C_5H_5)W(CO)_2(PR_3)_2^+Cl^-$ complexes (R = Ph, Et), where ionisation and CO substitution has occured [6].

The primary photochemical process for $(\eta^5\text{-}C_5H_5)Fe(CO)_2X$ complexes (X = Cl, Br, I) is claimed to be dissociative loss or exchange of a carbon monoxide ligand [8]. For example, irradiation of the bromo- or iodo-derivatives in the presence of PPh_3 leads to the formation of the covalent complexes $(\eta^5\text{-}C_5H_5)Fe(CO)(PPh_3)X$ (X = Br, I) [8] (Equation 6.4), while

$$(\eta^5\text{-}C_5H_5)Fe(CO)_2X + PPh_3 \xrightarrow[-CO]{h\nu} (\eta^5\text{-}C_5H_5)Fe(CO)(PPh_3)X \qquad (6.4)$$

photolysis of $(\eta^5\text{-}C_5H_5)Fe(CO)_2X$ (X = Cl, Br, I) in benzene solutions saturated with ^{13}CO yields $(\eta^5\text{-}C_5H_5)Fe(^{12}CO)(^{13}CO)X$. Other authors, however, have shown that irradiation of $(\eta^5\text{-}C_5H_5)Fe(CO)_2Cl$ results in the formation of $[(\eta^5\text{-}C_5H_5)Fe(CO)_2]_2$ [9] and Fe^{2+}, Cl^-, and ferrocene [10], depending upon the experimental conditions. The observation that photolysis of $(\eta^5\text{-}C_5H_5)Fe(CO)_2X$ (X = Cl, Br, I) at 336 or 436 nm in benzene or thf, resulted in no changes in the infrared or uv-vis spectra of the complexes, resulted in the conclusion that no detectable photochemical reactions take place in the absence of added nucleophiles in these solvents [8]. King et al. have reported [11] that u.v. irradiation of $(\eta^5\text{-}C_5H_5)Fe(CO)_2X$ complexes with an excess of the stronger π-acceptor phosphorous ligand $C_5H_{10}NPF_2$ yields the disubstitution products $(\eta^5\text{-}C_5H_5)Fe(PF_2NC_5H_{10})_2X$.

It should be noted that $(\eta^5\text{-}C_5H_5)Fe(CO)_2Cl$ reacts rapidly with PPh_3 in the dark at room temperature to produce a mixture of the covalent $(\eta^5\text{-}C_5H_5)Fe(CO)(PPh_3)Cl$ and ionic $(\eta^5\text{-}C_5H_5)Fe(CO)_2(PPh_3)^+Cl^-$ derivatives, precluding a detailed study of the photochemical substitution reactions of this complex [8].

This chapter describes an investigation of the photochemistry of $(\eta^5\text{-}C_5H_5)M(CO)_3Cl$ (M = Mo, W) and of $(\eta^5\text{-}C_5H_5)M(CO)_2Cl$ (M = Fe, Ru) complexes to determine whether dissociation of CO is the dominant photoprocess or whether photohomolysis of the M - Cl bond occurs as a major process in low temperature matrices at 12K. The results are related to the mechanisms of thermal and photochemical solution reactions.

6.2 RESULTS

6.2.1 Photolysis of $(\eta^5\text{-}C_5H_5)M(CO)_3Cl$ Complexes (M = Mo, W) in Ar and CH_4 Matrices at 12K

The i.r. spectrum of $(\eta^5\text{-}C_5H_5)Mo(CO)_3Cl$ isolated at high dilution in an Ar matrix (ca. 1:2000 - 1:5000) at 12K is shown in Figure 6.1(a). The spectrum shows that the $Mo(CO)_3Cl$ fragment has a C_s symmetry, with three i.r. bands in the terminal CO stretching region at 2062.5 (A'), 1989.5 (A'), and {1973.4, 1964.6} (A") cm^{-1} (Table 6.1).

Irradiation using visible light ($\lambda > 410$ nm) produced free CO (ca. 2138 cm^{-1}) and two new bands at 1981.2 and 1883.5 cm^{-1} (Figures 6.1(b) and 6.1(c)). The production of these two bands was accompanied by the decrease of bands of the parent and an increase in the band due to free CO. Annealing the matrix for 2 min. caused decreases in the intensities of the new photoproduct bands at 1981.2 and 1883.5 cm^{-1} with the regeneration of bands due to the starting material, $(\eta^5\text{-}C_5H_5)Mo(CO)_3Cl$ (Figure 6.1(d)). The relative intensities of the new terminal CO stretching bands remained constant under a variety of photolysis conditions (time and wavelength of radiation), indicating that the bands arose from a single mononuclear product species. This species may be assigned as $(\eta^5\text{-}C_5H_5)Mo(CO)_2Cl$ on the basis that the elimination of carbon monoxide from $(\eta^5\text{-}C_5H_5)Mo(CO)_3Cl$ could be reversed by annealing the matrix to ca. 35K. The assignment of the new bands to the 16-electron species $(\eta^5\text{-}C_5H_5)Mo(CO)_2Cl$ was confirmed by an experiment in which $(\eta^5\text{-}C_5H_5)Mo(CO)_3Cl$ was photolysed in a 5% ^{13}CO doped CH_4 matrix. Initially rapid exchange occured to produce bands due to the range of species $(\eta^5\text{-}C_5H_5)Mo(^{12}CO)_{3-n}(^{13}CO)_nCl$ (n = 1-3) but then further bands assigned to the ^{13}CO substituted 16-electron species

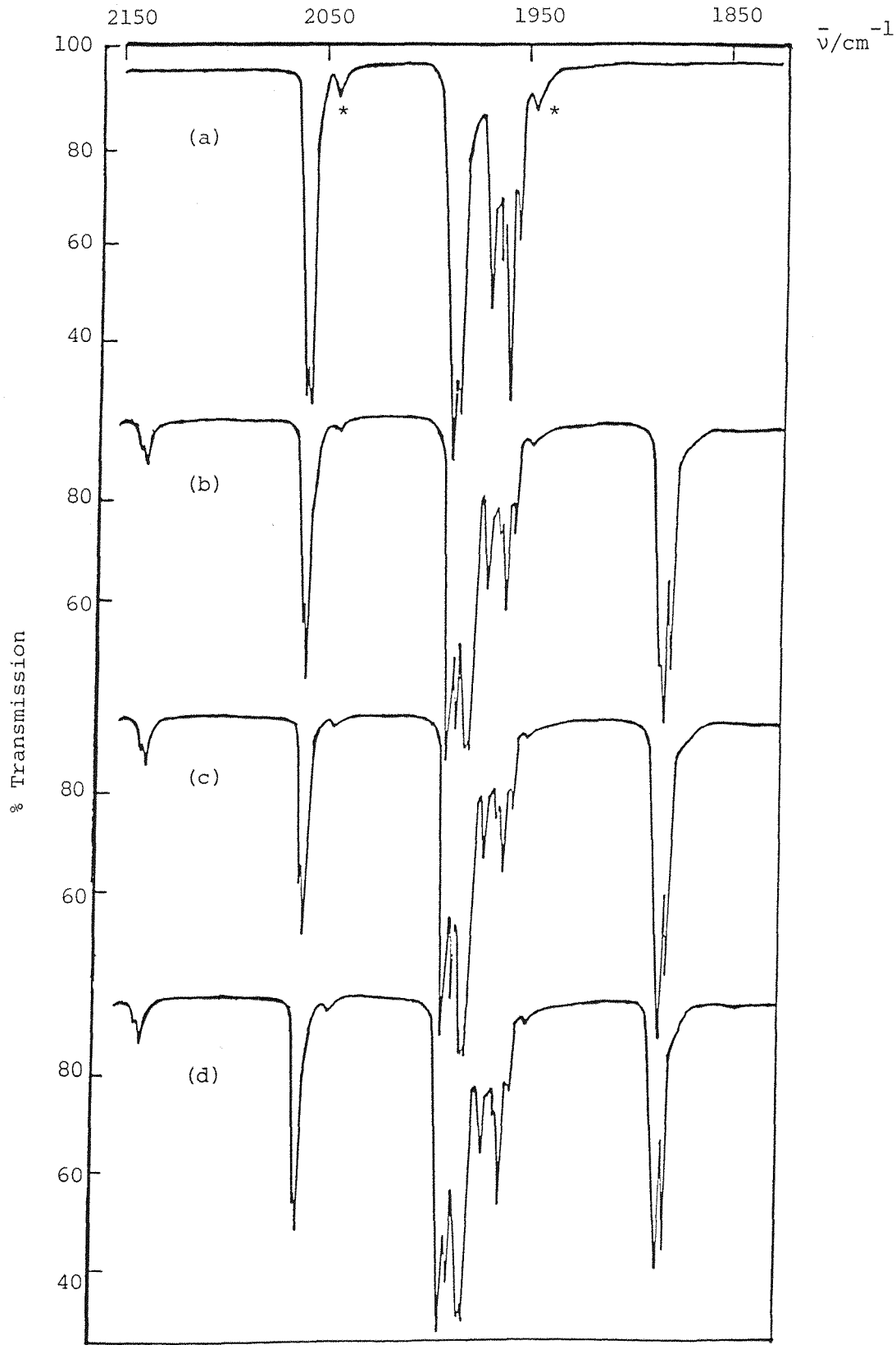

FIGURE 6.1 Infrared spectra from an experiment with $(\eta^5\text{-}C_5H_5)Mo(CO)_3Cl$ isolated at high dilution in an Ar matrix at 12K: (a) after deposition, (b) after 10 min. photolysis using λ > 270 nm, (c) after further 5 min. photolysis using the same radiation (λ > 370 nm) and (d) after 2 min. annealing. Bands marked (*) are due to $(\eta^5\text{-}C_5H_5)Mo(^{12}CO)_2(^{13}CO)Cl$ in natural abundance.

$(\eta^5\text{-}C_5H_5)Mo(CO)_2Cl$ grew in. Excellent correspondence between observed and calculated band positions was found for both $(\eta^5\text{-}C_5H_5)Mo(^{12}CO)_{3-n}(^{13}CO)_nCl$ (n = 0-3) and $(\eta^5\text{-}C_5H_5)Mo(^{12}CO)_m(^{13}CO)_{2-m}Cl$ (m = 0-2) using the energy-factored force-field approach [12] (Table 6.2).

Similar results were obtained for $(\eta^5\text{-}C_5H_5)Mo(CO)_3Cl$ in Ar matrices except that the photoreaction proceeded more slowly. The W analogue gave the same type of primary photoproduct as for Mo with an enhanced reaction rate.

Spectroscopic data are collected together in Table 6.1

6.2.2 Photolysis of $(\eta^5\text{-}C_5H_5)M(CO)_3Cl$ Complexes (M = Mo, W) in N_2 Matrices at 12K

Infrared spectra from an experiment with $(\eta^5\text{-}C_5H_5)Mo(CO)_3Cl$ isolated at high dilution in a nitrogen matrix at 12K are shown in Figure 6.2. Before photolysis the spectrum shows three strong bands in the terminal CO stretching region at 2058.0 (A'), 1983.7 (A'), and 1969.0 (A") cm^{-1}.

Visible irradiation with $\lambda > 410$ nm produced new infrared bands at 2240.8, 2138.0, 1999.4, 1938.5 and 1883.4 cm^{-1}, (Figure 6.2(b)), of which the band at 2138.0 cm^{-1} corresponds to free CO. Prolonged photolysis with the same energy light showed a further increase in free CO, increases in all the new bands, and decreases in the parent bands (Figures 6.2(b) and 6.2(c)). In these photolyses it was observed that the lower band of $(\eta^5\text{-}C_5H_5)Mo(CO)_3Cl$ at 1983.7 cm^{-1} decreased more slowly than the other two bands, indicating the growth of a new product band close to the position of a decreasing parent band (Figure 6.2(c)). Warming up the matrix to 35K and then re-cooling to 12K, caused increases in the intensities of the new photoproduct bands at 2240.8, 1999.4, 1938.5 cm^{-1} decreases in the intensities of bands at 1980.3 and 1883.4 cm^{-1} and little change in the parent band intensities (Figure 6.2(d)). Comparison of the growth and disappearance of bands under various times of photolysis identified two pairs of new terminal CO stretching bands: (1) at 1999.4, 1938.5 cm^{-1} and (2) at 1980.3, 1883.4 cm^{-1}. The (2) pair may be assigned to the coordinatively unsaturated 16-electron species $(\eta^5\text{-}C_5H_5)Mo(CO)_2Cl$ by virtue of the reversal on annealing and the correspondence of the band positions with those of the species obtained on photolysis of $(\eta^5\text{-}C_5H_5)Mo(CO)_3Cl$ in Ar and CH_4 matrices, (Section 6.2.1). The pair (1) also

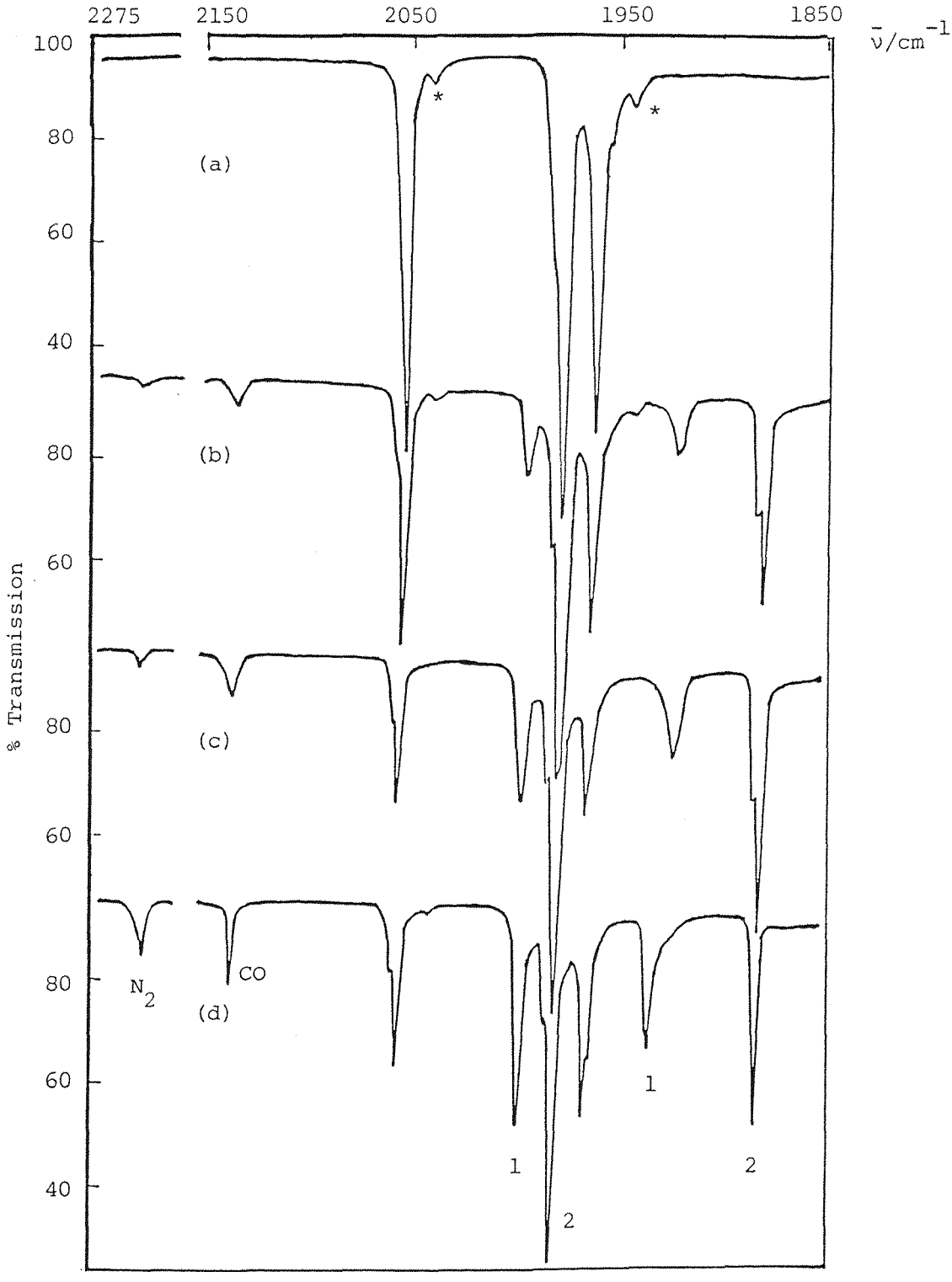

FIGURE 6.2 Infrared spectra from an experiment with $(\eta^5\text{-}C_5H_5)Mo(CO)_3Cl$ isolated at high dilution in a N_2 matrix at 12K: (a) after deposition, (b) after 30 min. photolysis using $\lambda > 410$ nm, (c) after further 50 min. photolysis using $\lambda > 410$ nm, and (d) after 2 min. annealing. Bands marked (*) are due to $(\eta^5\text{-}C_5H_5)Mo(^{12}CO)_2(^{13}CO)Cl$ occuring in natural abundance, and those marked (1) and (2) arise from photoproducts (see text).

correlate with a band at 2240.8 cm^{-1} which may be assigned as a $\nu_{N\equiv N}$ stretching mode of an end-on coordinated dinitrogen ligand by analogy with bands for $(\eta^4\text{-}C_4H_4)Fe(CO)_2(N_2)$ (ν_{NN} at 2206.8 cm^{-1}, N_2 matrix) [13], $Ni(CO)_3(N_2)$ (ν_{NN} at 2266 cm^{-1}, N_2 matrix) [14], $(\eta^5\text{-}C_5H_5)Mo(CO)_2(N_2)CH_3$ (ν_{NN} at 2190.8 cm^{-1}, N_2 matrix) [15] and, $RhH(N_2)[P(iso\text{-}Pr)_3]_2$ (ν_{NN} at 2140 cm^{-1}, hexane) [16]. The second new product, therefore contains at least two CO ligands and one NN ligand and may be assigned as $(\eta^5\text{-}C_5H_5)Mo(CO)_2(N_2)Cl$. Photolysis of ^{13}CO-enriched $(\eta^5\text{-}C_5H_5)Mo(CO)_3Cl$ in a N_2 matrix gave all the bands due to the species $(\eta^5\text{-}C_5H_5)Mo(^{12}CO)_{2-m}(^{13}CO)_m(N_2)Cl$ (m = 0-2; Table 6.2) to confirm the structural assignment of product (1) as $(\eta^5\text{-}C_5H_5)Mo(CO)_2(N_2)Cl$. Calculation of the OC-Mo-CO bond angle (θ = 78°) from relative band intensities [12] suggests that the two CO ligands in $(\eta^5\text{-}C_5H_5)Mo(CO)_2(N_2)Cl$ are *cis* to one another. The tungsten analogue, however, showed photo ejection of a CO ligand in N_2 matrices to give only the 16-electron species $(\eta^5\text{-}C_5H_5)W(CO)_2Cl$, i.e. no bands were observed for a $(\eta^5\text{-}C_5H_5)W(CO)_2(N_2)Cl$ species. Spectroscopic data for the new photoproducts are presented in Table 6.1.

6.2.3 Photolysis of $(\eta^5\text{-}C_5H_5)M(CO)_3Cl$ (M = Mo, W) in 5% C_2H_4 Doped CH_4 Matrices at 12K

Infrared spectra from an experiment with $(\eta^5\text{-}C_5H_5)W(CO)_3Cl$ isolated at high dilution in a 5% C_2H_4 doped CH_4 matrix are shown in Figure 6.3. Before photolysis the spectrum shows three bands in the CO stretching region at 2049.3, 1966.1 and 1948.4 cm^{-1} (Figure 6.3(a)).

Irradiation of the matrix using long wavelength radiation (λ > 410 nm), produced new bands at 2138.0, 2011.8, 1945.4 and 1861.5 cm^{-1} of which the band at 2138.0 cm^{-1} corresponds to CO liberated during photolysis (Figure 6.3(b)). Longer times of irradiation with the same energy wavelength (λ > 430 nm) revealed a band growing at 1962.4 cm^{-1}, which was formerly obscured by the bands of the parent molecule at 1966.1 cm^{-1}, and caused all the new product bands to increase in intensity while those of the parent molecule $(\eta^5\text{-}C_5H_5)W(CO)_3Cl$ decreased (Figure 6.3(c)). Annealing the matrix showed that the bands at 1962.4 and 1861.5 cm^{-1} were not related to those at 2011.8 and 1945.4 cm^{-1} because the former decreased in intensity whereas the latter

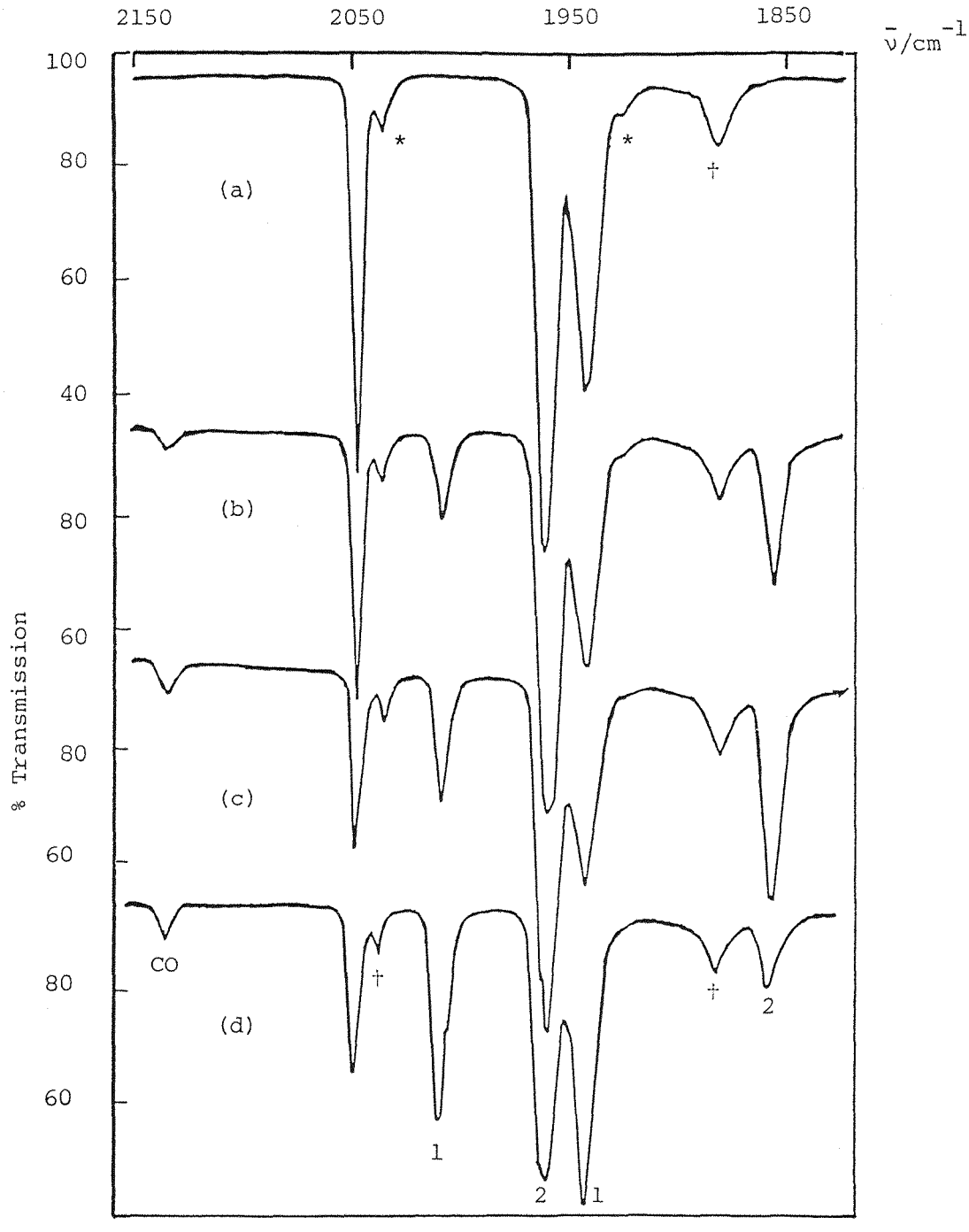

FIGURE 6.3 Infrared spectra from an experiment with $(\eta^5\text{-}C_5H_5)W(CO)_3Cl$ isolated at high dilution in C_2H_4 doped CH_4 (5%) matrix at 12K: (a) after deposition, (b) after 60 min. photolysis using $\lambda > 410$ nm, (c) after further 70 min. photolysis using $\lambda > 410$ nm, and (d) after 2 min. annealing. Bands marked (*) are due to $(\eta^5\text{-}C_5H_5)W(^{12}CO)_2(^{13}CO)Cl$ in natural abundance, bands marked (†) are due to C_2H_4, and those marked (1) and (2) arise from photoproducts (see text).

increased, while there was little or no change in the relative intensities of the parent bands (Figure 6.3(d)). The pair of bands at 1962.4 and 1861.5 cm^{-1} (bands (2)) which reversed on annealing can be assigned to the coordinatively unsaturated 16-electron species $(\eta^5\text{-}C_5H_5)W(CO)_2Cl$ by comparison with those observed in CH_4 matrix (Table 6.1) and their analogous reversal behaviour. The pair of bands at higher wavenumbers (2011.8 and 1945.4 cm^{-1}; bands (1)) are typical of a situation where a CO ligand has been replaced by another ligand, e.g. $(\eta^5\text{-}C_5H_5)W(CO)_2(C_2H_4)C_6H_5$ (1990.2 and 1922.5 cm^{-1}) compared with $(\eta^5\text{-}C_5H_5)W(CO)_2C_6H_5$ (1951.5 and 1861.5 cm^{-1}) (see Chapter 4). The two CO ligands in $(\eta^5\text{-}C_5H_5)W(CO)_2(C_2H_4)Cl$ are probably *cis* to one another, because the upper band of $(\eta^5\text{-}C_5H_5)W(CO)_2(C_2H_4)Cl$ is more intense than the lower band, i.e. $I_{asym}/I_{sym} < 1$ [12].

Analogous results were obtained with $(\eta^5\text{-}C_5H_5)Mo(CO)_3Cl$ isolated at high dilution in a 5% C_2H_4 doped CH_4 matrix. Spectroscopic data for the new species are presented in Table 6.1

6.2.4 Photolysis of $(\eta^5\text{-}C_5H_5)M(CO)_3Cl$ Complexes (M = Mo, W) in CO Matrices at 12K

The i.r. spectrum of $(\eta^5\text{-}C_5H_5)Mo(CO)_3Cl$ isolated at high dilution in a CO matrix is shown in Figure 6.4. Before photolysis, the spectrum (Figure 6.4(a)) showed bands in the CO stretching region at 2056.3, 1981.2 and {1967.0, 1958.5} cm^{-1} (Table 6.1).

An extended period of irradiation with visible light ($\lambda > 410$ nm) or a shorter period of irradiation with u.v. light (λ = 320-390 nm) produced at least three new bands (ν_{CO} at 2057.8, 1987.0 and 1955.2 cm^{-1}: Figure 6.4(b)). Annealing the matrix for 2 min. caused a rapid disappearance of the new photoproduct bands with the regeneration of the bands due to the starting material $(\eta^5\text{-}C_5H_5)Mo(CO)_3Cl$ (Figure 6.4(c)). The relative intensities of the new terminal CO stretching bands remained constant under a variety of photolysis conditions (time and wavelength of radiation), indicating that the bands arose from a single mononuclear product species. Interestingly these new photoproduct bands are at different wavenumbers

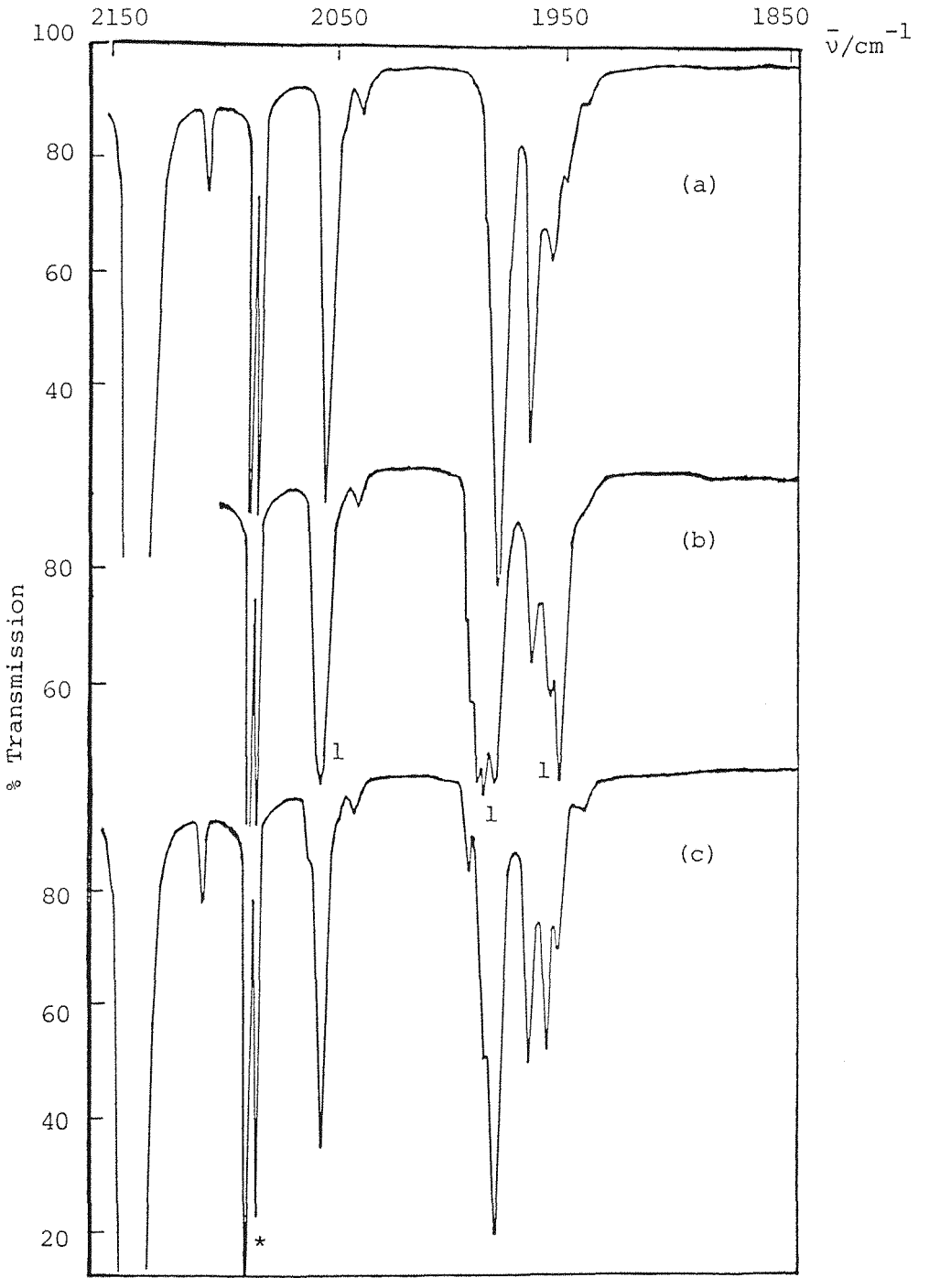

FIGURE 6.4 Infrared spectra from an experiment with $(\eta^5\text{-}C_5H_5)Mo(CO)_3Cl$ isolated at high dilution in a CO matrix at 12K: (a) after deposition, (b) after 20 min. photolysis using λ = 320 - 390 nm, and (c) after annealing the matrix for 2 min. Bands marked (l) are due to $(\eta^5\text{-}C_5H_5)Mo(CO)_3^+$, those marked (*) are due to other isotopically substituted CO molecules.

from those obtained for irradiation of $(\eta^5\text{-}C_5H_5)Mo(CO)_3Cl$ in CH_4 and Ar matrices.

Irradiation of $(\eta^5\text{-}C_5H_5)W(CO)_3Cl$ in CO matrices and under the same conditions produced two bands at 1964.8 and 1865.0 cm^{-1} which may be assigned to $(\eta^5\text{-}C_5H_5)W(CO)_2Cl$ (Table 6.1). Longer times of irradiation caused a reduction in the intensities of these two new bands, together with the appearance of three other new bands at 2052.0, 1972.8 and 1946.5 cm^{-1}, c.f. the bands obtained on irradiation of $(\eta^5\text{-}C_5H_5)Mo(CO)_3Cl$ in CO matrices.

There are three possible photochemical processes relevant to assigning the new photoproduct bands at 2057.8, 1987.2 and 1955.2 cm^{-1} and 2052.0, 1972.8 and 1946.5 cm^{-1} obtained from the irradiation of $(\eta^5\text{-}C_5H_5)Mo(CO)_3Cl$ and $(\eta^5\text{-}C_5H_5)W(CO)_3Cl$ complexes in CO matrices respectively (Equations 6.5 - 6.7).

$$(\eta^5\text{-}C_5H_5)M(CO)_3Cl \xrightleftharpoons{h\nu} (\eta^5\text{-}C_5H_5)M(CO)_3^{\cdot} + Cl^{\cdot} \qquad (6.5)$$

$$(\eta^5\text{-}C_5H_5)M(CO)_3Cl \xrightarrow{h\nu} (\eta^3\text{-}C_5H_5)M(CO)_3Cl \xrightarrow{+CO} (\eta^3\text{-}C_5H_5)M(CO)_4Cl \qquad (6.6)$$

$$(\eta^5\text{-}C_5H_5)M(CO)_3Cl \xrightleftharpoons{h\nu} (\eta^5\text{-}C_5H_5)M(CO)_3^{+} + Cl^{-} \xrightarrow{+CO}$$

$$(\eta^5\text{-}C_5H_5)M(CO)_4^{+} + Cl^{-} \qquad (6.7)$$

The first possibility, that is the formation of the radical species $(\eta^5\text{-}C_5H_5)M(CO)_3^{\cdot}$, can be eliminated because the bands attributed to these species are known in CO matrices ($(\eta^5\text{-}C_5H_5)Mo(CO)_3^{\cdot}$, 2008.9 and 1912.2 cm^{-1}; and $(\eta^5\text{-}C_5H_5)W(CO)_3^{\cdot}$, 1999.3 and 1898.4 cm^{-1}) (see Chapter 3). The second possibility, that is the ring slippage process can also be eliminated because

of the rapid and complete reversal of the new photoproduct bands to the starting material $(\eta^5\text{-}C_5H_5)M(CO)_3Cl$ on annealing the matrix from 12 to 35K. If this process occured it might also have led to the generation of the hexacarbonyl complexes $M(CO)_6$ (M = Mo, W), c.f. the generation of $M(CO)_6$ on irradiation of the $(\eta^5\text{-}C_5H_5)M(CO)_3H$ complexes (M = Cr, Mo, W) in CO matrices (see Chapter 3). However, no bands attributable to $M(CO)_6$ complexes were observed during irradiation of the $(\eta^5\text{-}C_5H_5)M(CO)_3Cl$ complexes in CO matrices. Therefore, the new bands probably arise from the cationic species $(\eta^5\text{-}C_5H_5)M(CO)_x^+$ (x = 3 or 4) as a result of heterolytic cleavage of the metal-halogen bond. The ionic species $(\eta^5\text{-}C_5H_5)M(CO)_4^+X^-$ (M = Mo, W) were first reported by Fischer and his coworkers [22], subsequently the related π-ethylene derivatives $(\eta^5\text{-}C_5H_5)M(CO)_3(\pi\text{-}C_2H_4)^+X^-$ (M = Mo, W) were described [5]. In this work bands at 2128, 2041 and 1980 cm^{-1} were assigned to the cationic species $(\eta^5\text{-}C_5H_5)Mo(CO)_4^+$ and bands at 2128, 2028 and 1965 cm^{-1} to the cationic species $(\eta^5\text{-}C_5H_5)W(CO)_4^+$. Comparison of the new bands at 2057.8, 1987.0 and 1955.2 cm^{-1} obtained from irradiation of $(\eta^5\text{-}C_5H_5)Mo(CO)_3Cl$ in a CO matrix with those of $(\eta^5\text{-}C_5H_5)Mo(CO)_4^+$ (ν_{CO} bands at 2128, 2041 and 1980 cm^{-1}; solution) and the new bands at 2052.0, 1972.8 and 1946.5 cm^{-1} obtained from irradiation of $(\eta^5\text{-}C_5H_5)W(CO)_3Cl$ in a CO matrix with those of $(\eta^5\text{-}C_5H_5)W(CO)_4^+$ (ν_{CO} bands at 2128, 2028 and 1965 cm^{-1}; solution) showed no correlation between the band positions in solution and those in CO matrices. In solution it was also suggested [19] that the loss of halide anions from $(\eta^5\text{-}C_5H_5)M(CO)_2Cl$ would result in formation of the 16-electron cationic complexes $(\eta^5\text{-}C_5H_5)M(CO)_3^+$ which should recombine rapidly to give the starting complexes [19], (Equation 6.7). In the presence of free carbon monoxide or PPh_3, the cations would be expected to react to give the coordinatively saturated complexes $(\eta^5\text{-}C_5H_5)M(CO)_4^+$ [22] or $(\eta^5\text{-}C_5H_5)M(CO)_3(PPh_3)^+$ [23]. If the reaction (Equation 6.7) went to completion in a matrix, however, it is unlikely that the modest thermal energy afforded by annealing the CO matrix would effect the reversal, i.e. replacement of CO by Cl^-.

It seems probable, therefore, that the new photoproduct bands resulting from irradiation of $(\eta^5\text{-}C_5H_5)M(CO)_3Cl$ complexes (M = Mo, W) in CO matrices are due to the formation of the 16-electron cationic species $(\eta^5\text{-}C_5H_5)M(CO)_3^+$ rather than the formation of the 18-electron cationic species $(\eta^5\text{-}C_5H_5)M(CO)_4^+$.

The use of ^{13}CO enriched isotopic labelling to support this assignment was not feasible because the large number of bands appearing in the spectrum due to the range of species $(\eta^5\text{-}C_5H_5)Mo(^{12}CO)_{3-n}(^{13}CO)_nCl$ (n = 0-3) (Table 6.2) and the overlapping of these bands with those of the cationic photoproduct species.

6.2.5 Photolysis of $(\eta^5\text{-}C_5H_5)M(CO)_2Cl$ Complexes (M = Fe, Ru) in CH_4, N_2, CO and 5% ^{13}CO Doped CH_4 Matrices

The infrared spectrum of $(\eta^5\text{-}C_5H_5)Fe(CO)_2Cl$ isolated at high dilution in a CH_4 matrix in the CO stretching region shows two bands at 2054.2 and 2010.2 cm^{-1} (Figure 6.5). These bands correspond to the symmetric (A') and antisymmetric (A") modes expected for a molecule with C_s symmetry together with two very weak bands (marked with an asterisk) arising from $(\eta^5\text{-}C_5H_5)Fe(^{12}CO)(^{13}CO)Cl$ present in natural abundance.

Irradiation of the matrix with u.v. light (λ = 290 - 370 nm) produced a single band at 1977.2 cm^{-1} in addition to the band of free CO at 2138 cm^{-1} (Figure 6.5(b)). Longer times of irradiation (λ = 290 - 370 nm) led to increases the single band at 1977.2 cm^{-1} and the band of free CO (Figure 6.5(c)). The band at 1977.2 cm^{-1} may be assigned to the unsaturated 16-electron $(\eta^5\text{-}C_5H_5)Fe(CO)Cl$ species on the basis that elimination of carbon monoxide from the parent $(\eta^5\text{-}C_5H_5)Fe(CO)_2Cl$ complex which can be reversed by annealing the matrix to higher temperatures (ca. 30K) which allow diffusion of CO. The validity of this assignment was demonstrated when $(\eta^5\text{-}C_5H_5)Ru(CO)_2Cl$ was photolysed in a 5% ^{13}CO doped CH_4 matrix (Figures 6.6(a) and 6.6(b)). Initially rapid exchange occured to produce $(\eta^5\text{-}C_5H_5)Ru(^{12}CO)(^{13}CO)Cl$ and $(\eta^5\text{-}C_5H_5)Ru(^{13}CO)_2Cl$ but on further photolysis bands assigned to $(\eta^5\text{-}C_5H_5)Ru(^{12}CO)Cl$ and $(\eta^5\text{-}C_5H_5)Ru(^{13}CO)Cl$ grew in. Excellent correspondence between observed and calculated band positions was found for ^{13}CO enriched $(\eta^5\text{-}C_5H_5)Ru(CO)_2Cl$ and $(\eta^5\text{-}C_5H_5)Ru(CO)Cl$ (Table 6.3) using the energy-factored force-field approach [12].

Irradiation of $(\eta^5\text{-}C_5H_5)M(CO)_2Cl$ complexes (M = Fe, Ru) in N_2 and CO matrices was expected to lead to the formation of $(\eta^5\text{-}C_5H_5)M(CO)(N_2)Cl$ and

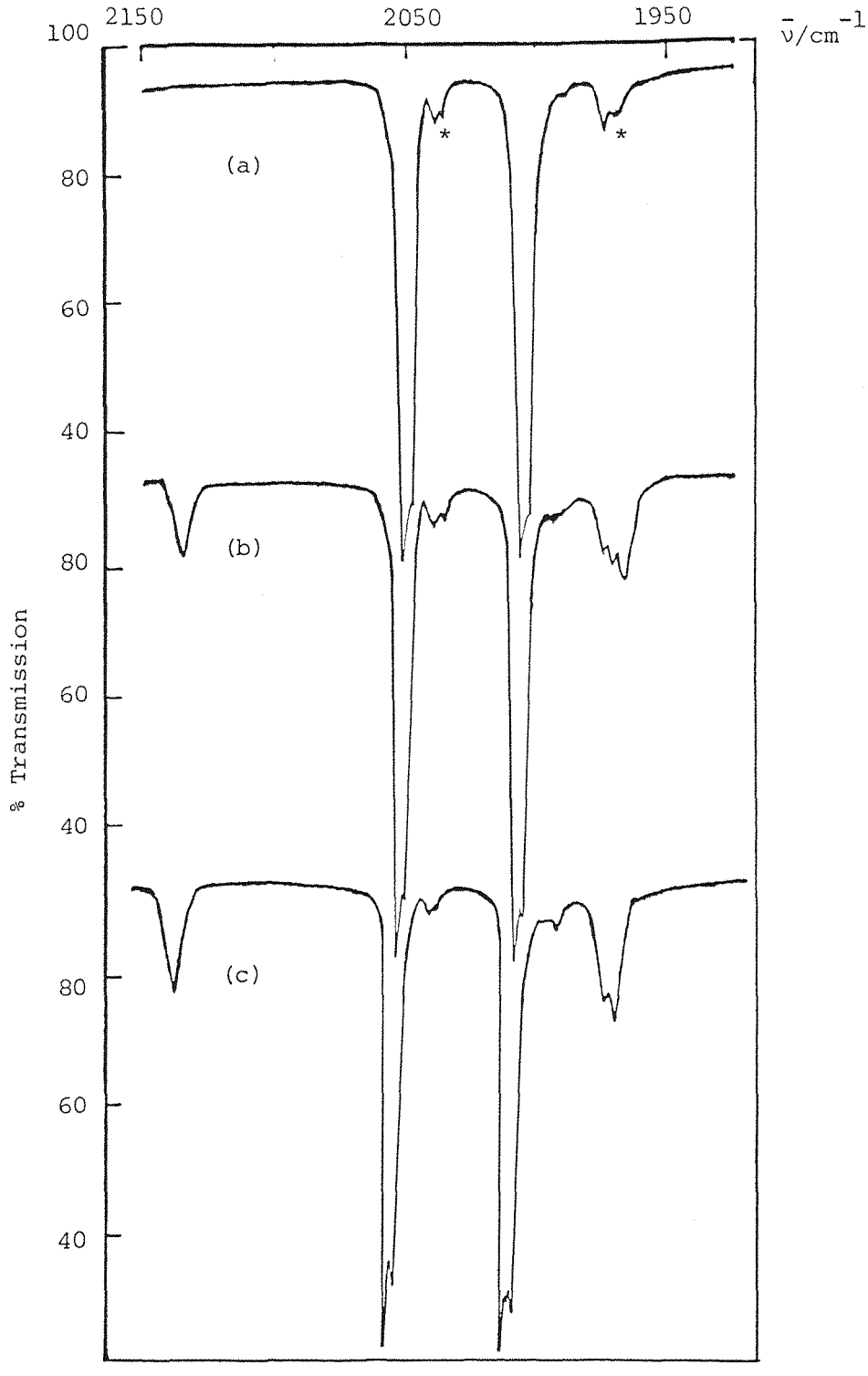

FIGURE 6.5 Infrared spectra from an experiment with $(\eta^5\text{-}C_5H_5)Fe(CO)_2Cl$ isolated at high dilution in CH_4 matrix at 12K: (a) after deposition, (b) after 30 min. photolysis using λ = 290 - 370 nm, and (c) after further 2 hours photolysis with the same energy source (λ = 290 - 370 nm). Bands marked (*) are due to $(\eta^5\text{-}C_5H_5)Fe(^{12}CO)(^{13}CO)Cl$ present in natural abundance.

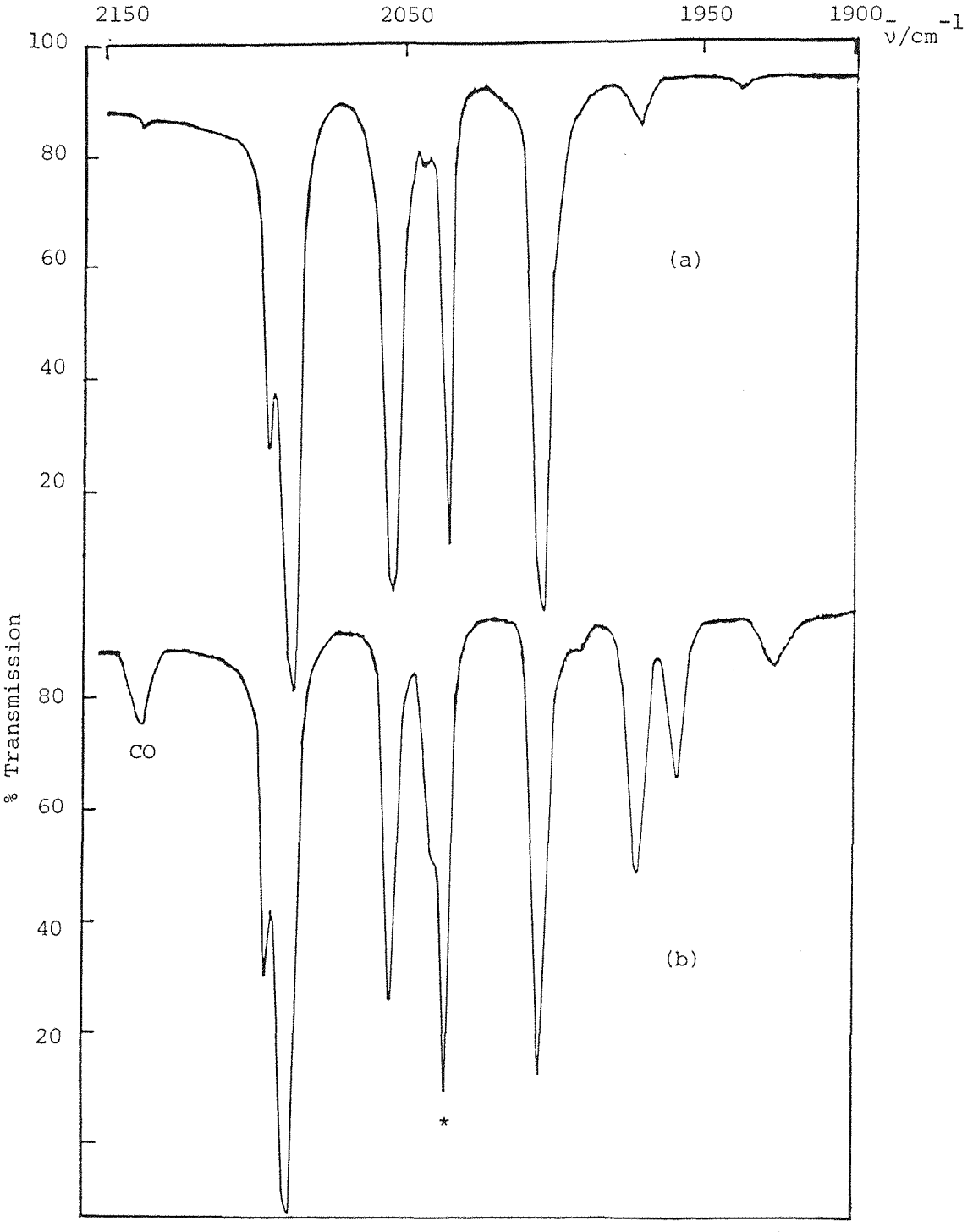

FIGURE 6.6 Infrared spectra from an experiment with $(\eta^5\text{-}C_5H_5)Ru(CO)_2Cl$ isolated at high dilution in 5% ^{13}CO doped CH_4 matrix at 12K: (a) after deposition, and (b) after 2 hours photolysis using λ = 290 - 370 nm. Bands marked (*) are due to other isotopically substituted CO molecules.

$(\eta^5\text{-}C_5H_5)M(CO)_2{}^+Cl^-$ complexes respectively. However, no such species were formed but only $(\eta^5\text{-}C_5H_5)M(CO)Cl$. Spectroscopic data for the new species are given in Table 6.1.

6.3 DISCUSSION

The photoreactions of $(\eta^5\text{-}C_5H_5)M(CO)_3Cl$ complexes (M = Mo, W), in frozen gas matrices (Ar, CH_4, N_2, CO and 5% C_2H_4 doped CH_4) are summarised in Scheme 6.1.

$$(\eta^5\text{-}C_5H_5)M(CO)_3Cl \underset{(iii)}{\overset{(i),\ (ii)}{\rightleftharpoons}} (\eta^5\text{-}C_5H_5)M(CO)_2Cl + CO$$

$$(ii)\downarrow (v) \qquad\qquad (ii)\downarrow (iv)$$

$$(\eta^5\text{-}C_5H_5)M(CO)_3{}^+Cl^- \qquad\qquad (\eta^5\text{-}C_5H_5)M(CO)_2(L)Cl$$

Scheme 6.1 (i) CH_4, Ar; (ii) hν (λ > 410 nm); (iii) hν (λ > 520 nm) or annealing; (iv) M = Mo, L = N_2 or C_2H_4; M = W, L = C_2H_4; (v) CO.

Previous investigations of the photolysis of $(\eta^5\text{-}C_5H_5)M(CO)_3X$ complexes (M = Mo, W; X = Cl, Br, I) in solution in the presence of PPh_3 have observed the formation of the monosubstituted complexes $(\eta^5\text{-}C_5H_5)M(CO)_2(PPh_3)X$ [2, 3]. Kinetic studies of the thermal substitution reactions of $(\eta^5\text{-}C_5H_5)Mo(CO)_3X$ with PPh_3 have shown [17, 18] that the reactions proceed by dissociative mechanism, with loss of carbon monoxide as the rate-determining step (Equations 6.8 and 6.9).

$$(\eta^5\text{-}C_5H_5)M(CO)_3X \xrightarrow{slow} (\eta^5\text{-}C_5H_5)M(CO)_2X + CO \qquad (6.8)$$

$$(\eta^5\text{-}C_5H_5)M(CO)_2X + PPh_3 \xrightarrow{fast} (\eta^5\text{-}C_5H_5)M(CO)_2(PPh_3)X \qquad (6.9)$$

Matrix isolation studies of $(\eta^5\text{-}C_5H_5)M(CO)_3Cl$ complexes (M = Mo, W) in different non-reactive gas matrices, e.g. CH_4 and Ar, have demonstrated the dissociative loss of one CO ligand and the formation of the unsaturated 16-electron species $(\eta^5\text{-}C_5H_5)M(CO)_2Cl$ as proposed [17, 18] in equation 6.8. Exchange of ^{13}CO for ^{12}CO during the photolysis of $(\eta^5\text{-}C_5H_5)M(CO)_3Cl$ complexes (M = Mo, W) in ^{13}CO doped CH_4 matrices at 12K confirms that photo-induced dissociation and exchange of CO ligands is taking place and indicates that similar processes occur during the irradiation in solution.

Irradiation of $(\eta^5\text{-}C_5H_5)M(CO)_3Cl$ complexes (M = Mo, W) in N_2 matrices affords the $(\eta^5\text{-}C_5H_5)Mo(CO)_2(N_2)Cl$ derivative, however, no reaction was observed for the $(\eta^5\text{-}C_5H_5)W(CO)_3Cl$ analogue. An interesting feature of $(\eta^5\text{-}C_5H_5)Mo(CO)_2(N_2)Cl$ complex is the *cis* stereochemistry deduced on the basis of OC-M-CO bond angle calculations ($\sim$ 78°) [12] (Equation 6.10).

$$(\eta^5\text{-}C_5H_5)Mo(CO)_3Cl + N_2 \xrightarrow{h\nu/-CO} cis\text{-}(\eta^5\text{-}C_5H_5)Mo(CO)_2(N_2)Cl \qquad (6.10)$$

This stereochemistry may be related to the photolysis of $(\eta^5\text{-}C_5H_5)M(CO)_3X$ complexes in the presence of PPh_3 to yield the monosubstituted complexes $(\eta^5\text{-}C_5H_5)M(CO)_2(PPh_3)X$. Although both *cis* and *trans* isomers of these derivatives are possible [19, 20], complexes with the *cis* geometry are formed stereospecifically by photosubstitution reactions (Equation 6.11)

$$(\eta^5\text{-}C_5H_5)M(CO)_3X + PPh_3 \xrightarrow[-CO]{h\nu} cis\text{-}(\eta^5\text{-}C_5H_5)M(CO)_2(PPh_3)X \qquad (6.11)$$

but *cis* and *trans*-$(\eta^5\text{-}C_5H_5)M(CO)_2(PPh_3)X$ complexes (M = Mo; X = Br, I; M = W, X = I) undergo geometric isomerisation upon 336 and 436 nm photolysis in benzene solutions (Equation 6.12).

$$cis\text{-}(\eta^5\text{-}C_5H_5)M(CO)_2(PPh_3)X \underset{h\nu'}{\overset{h\nu}{\rightleftharpoons}} trans\text{-}(\eta^5\text{-}C_5H_5)M(CO)_2(PPh_3)X \qquad (6.12)$$

It is interesting, however, that the chloro complexes *cis*-$(\eta^5\text{-}C_5H_5)Mo(CO)_2(PPh_3)Cl$ does not undergo photochemical isomerisation in benzene solutions to produce the *trans* isomer.

The photolysis of $(\eta^5\text{-}C_5H_5)M(CO)_3Cl$ complexes (M = Mo, W) in 5% C_2H_4 doped CH_4 matrices led to the formation of $(\eta^5\text{-}C_5H_5)M(CO)_2(C_2H_4)Cl$ complexes via the coordinatively unsaturated 16-electron species $(\eta^5\text{-}C_5H_5)M(CO)_2Cl$ (Equation 6.13). Overlapping of bands made it impossible to

$$(\eta^5\text{-}C_5H_5)M(CO)_3Cl + C_2H_4 \xrightarrow{h\nu} cis\text{-}(\eta^5\text{-}C_5H_5)M(CO)_2(C_2H_4)Cl \qquad (6.13)$$

calculate the bond angle OC-M-CO but a careful examination of the symmetric and antisymmetric band intensities of $(\eta^5\text{-}C_5H_5)M(CO)_2(C_2H_4)Cl$ showed that the two CO groups are in a *cis* position ($I_{antisym}/I_{sym} < 1$). Similarly *cis*-$(\eta^5\text{-}C_5H_5)M(CO)_2(C_2H_4)CH_3$ and *cis*-$(\eta^5\text{-}C_5H_5)W(CO)_2(C_2H_4)C_6H_5$ were generated when the complexes $(\eta^5\text{-}C_5H_5)M(CO)_3CH_3$ (M = Mo, W) and $(\eta^5\text{-}C_5H_5)W(CO)_3C_6H_5$ respectively were photolysed in 5% C_2H_4 doped CH_4 matrices (see Chapters 2 and 5). The reactivity of the $(\eta^5\text{-}C_5H_5)M(CO)_3Cl$ complexes toward the nitrogen ligand is less than that with the ethylene ligand as demonstrated by the higher yield of the latter photoproduct for the molybdenum derivatives.

Previous investigations have illustrated that the $(\eta^5\text{-}C_5H_5)M(CO)_3X$ derivatives of molybdenum and tungsten can react with a variety of ligands to yield a second type of derivatives in which the halide ion is displayed to yield an ionic products, e.g. $(\eta^5\text{-}C_5H_5)M(CO)_3(NH_3)^+Cl^-$ [5], $(\eta^5\text{-}C_5H_5)W(CO)_2(N_2H_4)^+Cl^-$ [5], and $(\eta^5\text{-}C_5H_5)W(CO)_2(PEt_3)_2^+Cl^-$ [21]. The loss of halide anions from $(\eta^5\text{-}C_5H_5)M(CO)_3X$ is proposed to result in formation of the 16-electron cationic complexes $(\eta^5\text{-}C_5H_5)M(CO)_3^+$ (Equation 6.14) which

$$(\eta^5\text{-}C_5H_5)M(CO)_3X \xrightarrow{h\nu} (\eta^5\text{-}C_5H_5)M(CO)_3^+ + X^- \qquad (6.14)$$

can capture a ligand (L = CO or PPh_3) to yield 18-electron complexes $(\eta^5\text{-}C_5H_5)M(CO)_4^+$ and $(\eta^5\text{-}C_5H_5)M(CO)_3(PPh_3)^+$ respectively [22, 23] (Equation 6.15).

$$(\eta^5\text{-}C_5H_5)M(CO)_3^+ + X^- \xrightarrow[L = CO,\ PPh_3]{h\nu} (\eta^5\text{-}C_5H_5)M(CO)_3(L)^+ + X^- \qquad (6.15)$$

In contrast to the formation of the 16-electron species $(\eta^5\text{-}C_5H_5)M(CO)_2Cl$, in CH_4, N_2 and Ar matrices, an alternative reaction path to CO ejection is observed in CO matrices which probably involves heterolytic cleavage of the metal-halogen bond (Equations 6.16 - 6.18).

$$(\eta^5\text{-}C_5H_5)Mo(CO)_3Cl \xrightarrow[\Delta]{h\nu/+CO} (\eta^5\text{-}C_5H_5)Mo(CO)_3^+ + Cl^- \qquad (6.16)$$

$$(\eta^5\text{-}C_5H_5)W(CO)_3Cl \rightleftharpoons \begin{cases} \xrightarrow{h\nu/+CO} (\eta^5\text{-}C_5H_5)W(CO)_3^+ + Cl^- & (6.17) \\ \xrightarrow{h\nu/-CO} (\eta^5\text{-}C_5H_5)W(CO)_2Cl & (6.18) \end{cases}$$

Comparing the photochemical reactivity of the molybdenum and tungsten complexes in CO matrices reveals that the generation of the $(\eta^5\text{-}C_5H_5)M(CO)_3^+$ cation is faster for Mo than for W complex using the same light source and the same period of irradiation. This suggests that the W-Cl bond may be stronger than the Mo-Cl bond.

The photoreactions of $(\eta^5\text{-}C_5H_5)M(CO)_2Cl$ complexes (M = Fe, Ru) in low temperature matrices (Ar, CH_4, N_2 and CO) are summarised in Scheme 6.2.

$$\begin{array}{ccc} (\eta^5\text{-}C_5H_5)M(CO)_2Cl & \underset{\text{annealing}}{\overset{h\nu}{\rightleftharpoons}} & (\eta^5\text{-}C_5H_5)M(CO)Cl + CO \\ \Big\downarrow h\nu/+CO & & \Big\downarrow h\nu/+N_2 \\ (\eta^5\text{-}C_5H_5)M(CO)_2^+Cl^- & & (\eta^5\text{-}C_5H_5)M(CO)(N_2)Cl \end{array}$$

Scheme 6.2

The primary photochemical process for $(\eta^5\text{-}C_5H_5)Fe(CO)_2X$ complexes (X = Cl, Br, I) in solution is dissociative loss of CO ligand [8]. For example, irradiation of the bromo- or iodo- derivatives in the presence of PPh_3 leads to the formation of the covalent complexes $(\eta^5\text{-}C_5H_5)Fe(CO)(PPh_3)X$ (X = Br, I) [8].

Matrix isolation studies of $(\eta^5\text{-}C_5H_5)M(CO)_2Cl$ complexes (M = Fe, Ru) in different gas matrices (Ar, CH_4, N_2, CO) have demonstrated the dissociative loss of one CO ligand and the formation of the unsaturated 16-electron species $(\eta^5\text{-}C_5H_5)M(CO)Cl$ as proposed in solutions. In a 5% ^{13}CO doped CH_4 matrix $(\eta^5\text{-}C_5H_5)Ru(CO)_2Cl$ shows rapid ^{13}CO exchange leading to $(\eta^5\text{-}C_5H_5)Ru(^{12}CO)_{2-n}(^{13}CO)_nCl$ (n = 1-2) species together with $(\eta^5\text{-}C_5H_5)Ru(^{12}CO)Cl$ and $(\eta^5\text{-}C_5H_5)Ru(^{13}CO)Cl$. This confirms that photoinduced dissociation and exchange of CO ligands taking place during u.v. irradiation of $(\eta^5\text{-}C_5H_5)M(CO)_2Cl$ (M = Fe, Ru) in low temperature matrices at 12K.

Irradiation of $(\eta^5\text{-}C_5H_5)M(CO)_2Cl$ complexes (M = Fe, Ru) in reactive nitrogen matrices produced also the 16-electron intermediate $(\eta^5\text{-}C_5H_5)M(CO)Cl$ but no reaction with nitrogen was observed. The failure of $(\eta^5\text{-}C_5H_5)M(CO)_2Cl$ to react with nitrogen at low temperature may be because the nitrogen ligand competes less effectively than the CO for $(\eta^5\text{-}C_5H_5)M(CO)Cl$ fragment [24 - 26].

Previous investigations have illustrated that the loss of halide anions from $(\eta^5\text{-}C_5H_5)Fe(CO)_2X$ is proposed to result in the formation of the 16-electron cationic complexes $(\eta^5\text{-}C_5H_5)Fe(CO)_2^+X^-$ [8]. This intermediate has been proposed to be susceptible to nucleophilic attack by two electron donor ligands [27] and should efficiently react with CO to produce 18-electron cationic complexes $(\eta^5\text{-}C_5H_5)Fe(CO)_3^+X^-$. No evidence for the formation of anions was found on photolysis of $(\eta^5\text{-}C_5H_5)M(CO)_2Cl$ complexes in CO matrices.

An alternative pathway involves breaking the iron-halogen bond homolytically. Homolytic cleavage of the metal-halogen bond would produce the radical species $(\eta^5\text{-}C_5H_5)M(CO)_2^{\cdot}$ and $X^{\cdot}$ and these radicals would yield the dimers $[(\eta^5\text{-}C_5H_5)M(CO)_2]_2$ and X_2 in solution. Indeed Kemp *et al.* have

reported [9] that the principal product on irradiation ($\lambda > 280$ nm) of $(\eta^5\text{-}C_5H_5)Fe(CO)_2Cl$ in the donor solvents pyridine and dimethyl sulfoxide is $[(\eta^5\text{-}C_5H_5)Fe(CO)_2]_2$, but no reaction was observed in cyclohexane or diethyl ether. Irradiation of $(\eta^5\text{-}C_5H_5)M(CO)_2Cl$ complexes (M = Fe, Ru) in CO matrices only resulted in CO ejection and the production of co-ordinatively unsaturated $(\eta^5\text{-}C_5H_5)M(CO)Cl$ species. This strongly suggests that homolytic iron-halogen bond cleavage is not an important pathway for the $(\eta^5\text{-}C_5H_5)M(CO)_2Cl$ complexes, in contrast to $(\eta^5\text{-}C_5H_5)M(CO)_3Cl$ complexes (M = Mo, W) (see above). The dimer $[(\eta^5\text{-}C_5H_5)Fe(CO)_2]_2$ was not expected nor observed in gas matrices because of the high dilution used in the experiments.

6.4 CONCLUSIONS

The photoreactions of $(\eta^5\text{-}C_5H_5)M(CO)_3Cl$ complexes (M = Mo, W) in Ar, CH_4, N_2 and 5% C_2H_4 doped CH_4 matrices at 12K indicate the principal reactive intermediate in the thermal and photochemical solution substitution reactions is the coordinatively unsaturated 16-electron species $(\eta^5\text{-}C_5H_5)M(CO)_2Cl$. The reaction is reversible (Equation 6.19).

$$(\eta^5\text{-}C_5H_5)M(CO)_3Cl \underset{\Delta}{\overset{h\nu}{\rightleftharpoons}} (\eta^5\text{-}C_5H_5)M(CO)_2Cl + CO \qquad (6.19)$$

Irradiation of $(\eta^5\text{-}C_5H_5)M(CO)_3Cl$ complexes (M = Mo, W) in CO matrices can suppress the CO loss photoreaction pathway and allow a second pathway to be observed (Equation 6.20). The formation of $(\eta^5\text{-}C_5H_5)M(CO)_3^+$ and Cl^-

$$(\eta^5\text{-}C_5H_5)M(CO)_3Cl \underset{\Delta}{\overset{h\nu/+CO}{\rightleftharpoons}} (\eta^5\text{-}C_5H_5)M(CO)_3^+ + Cl^- \qquad (6.20)$$

ions is indicative of photo-induced metal-chlorine bond homolysis.

Irradiation of $(\eta^5\text{-}C_5H_5)M(CO)_2Cl$ complexes (M = Fe, Ru) in CH_4, N_2 and CO matrices produced only the 16-electron species (Equation 6.21) and that CO dissociation rather than M - Cl bond homolysis is the principal reaction pathway.

$$(\eta^5\text{-}C_5H_5)M(CO)_2Cl \underset{\Delta}{\overset{h\nu}{\rightleftharpoons}} (\eta^5\text{-}C_5H_5)M(CO)Cl + CO \qquad (6.20)$$

Table 6.1 Infrared band positions (cm^{-1}) observed in the CO stretching region for $(\eta^5\text{-}C_5H_5)M(CO)_3Cl$ (M = Mo, W) and for $(\eta^5\text{-}C_5H_5)M(CO)_2Cl$ (M = Fe, Ru) complexes and their photoproducts in various gas matrices at 12K.

Complex	CH_4	Ar	CO	N_2	5% C_2H_4/CH_4
$(\eta^5\text{-}C_5H_5)Mo(CO)_3Cl$	2057.2 1983.0 1959.2	2062.5 1989.4 1973.4) 1964.6)[a]	2058.0 1982.7 1963.5	2058.0 1983.7 1969.0	2056.3 1982.7 1959.3
$(\eta^5\text{-}C_5H_5)W(CO)_3Cl$	2050.7 1967.0 1950.8		2052.0 1966.0 1951.2	2052.3 1968.3 1955.2	2049.3 1966.1 1948.4
$(\eta^5\text{-}C_5H_5)Mo(CO)_2Cl$	1976.7 1880.3	1981.2 1883.5	b	1980.3 1883.4	1979.2 1881.5
$(\eta^5\text{-}C_5H_5)W(CO)_2Cl$	1963.0 1863.0		1964.8 1865.0	1967.0 1867.0	1962.4 1861.5
$(\eta^5\text{-}C_5H_5)Mo(CO)_2(N_2)Cl$[c]				1999.4 1938.5	
$(\eta^5\text{-}C_5H_5)Mo(CO)_2(C_2H_4)Cl$					2015.5 1953.4
$(\eta^5\text{-}C_5H_5)W(CO)_2(C_2H_4)Cl$					2011.8 1945.4
$(\eta^5\text{-}C_5H_5)Mo(CO)_3^+$			2057.8 1987.0 1955.2		
$(\eta^5\text{-}C_5H_5)W(CO)_3^+$			2052.0 1972.8 1946.5		

.../Continued

Table 6.1 (Continued)

Complex	CH_4	Ar	CO	N_2	5% C_2H_4/CH_4
$(\eta^5\text{-}C_5H_5)Fe(CO)_2Cl$	2054.2 2010.2		2054.3 2010.6	2056.1 2013.7	
$(\eta^5\text{-}C_5H_5)Ru(CO)_2Cl$	2056.2 2009.2		2056.3 2009.5	2058.6 2010.3	
$(\eta^5\text{-}C_5H_5)Fe(CO)Cl$	1977.1		1974.5	1979.2	
$(\eta^5\text{-}C_5H_5)Ru(CO)Cl$	1967.7		1966.0	1969.5	

[a] Matrix splitting.

[b] Irradiation of $(\eta^5\text{-}C_5H_5)Mo(CO)_3Cl$ in CO matrices produced complete conversion to the cationic species $(\eta^5\text{-}C_5H_5)Mo(CO)_3^+$ whereas the W complex gave a mixture of the cationic species together with the coordinatively unsaturated 16-electron species $(\eta^5\text{-}C_5H_5)W(CO)_2Cl$ (see text).

[c] $\nu_{N\equiv N}$ at 2240.8 cm^{-1}.

Table 6.2 Observed and calculated[a] band positions (cm^{-1}) of terminal CO bands in an experiment with a ^{13}CO-enriched sample of $(\eta^5\text{-}C_5H_5)Mo(CO)_3Cl$ in N_2 matrix at 12K.

Complex	ν(CO)	Observed	Calculated
$(\eta^5\text{-}C_5H_5)Mo(^{12}CO)_3Cl$[a]	A'	2058.0	2057.3
(C_s)	A'	1983.7	1983.2
	A"	1969.0	1968.5
$(\eta^5\text{-}C_5H_5)Mo(^{12}CO)_2(^{13}CO)Cl$	A'	2053.5	2052.2
(C_s)[b]	A"	1969.2	1968.5
	A'	d	1944.2
	A	2044.1	2043.6
(C_1)[c]	A	1981.4	1981.6
	A	1938.7	1939.4
$(\eta^5\text{-}C_5H_5)Mo(^{12}CO)(^{13}CO)_2Cl$	A	2037.8	2036.5
(C_1)[e]	A	1948.5	1949.0
	A	d	1934.9
	A'	2025.6	2025.7
(C_s)[f]	A"	1970.3	1969.6
	A'	1924.3	1924.8
$(\eta^5\text{-}C_5H_5)Mo(^{13}CO)_3Cl$	A'	2011.3	2011.8
(C_s)	A'	1938.7	1939.2
	A"	1924.3	1924.8
$(\eta^5\text{-}C_5H_5)Mo(^{12}CO)_2Cl$	A'	1980.3	1980.3
(C_s)	A"	1883.4	1883.4
$(\eta^5\text{-}C_5H_5)Mo(^{12}CO)(^{13}CO)Cl$	A	d	1962.8
(C_1)	A	1857.2	1857.9

.../continued

Table 6.2 (Continued)

Complex	ν(CO)	Observed	Calculated
$(\eta^5\text{-}C_5H_5)Mo(^{13}CO)_2Cl$ [g]			
C_s	A'	d	1936.3
	A"	1841.0	1841.6
$(\eta^5\text{-}C_5H_5)Mo(^{12}CO)_2(N_2)Cl$ [h]			
C_s	A'	1999.4	1999.4
	A"	1938.5	1938.5
$(\eta^5\text{-}C_5H_5)Mo(^{12}CO)(^{13}CO)(N_2)Cl$			
C_1	A	d	1984.3
	A	d	1909.9
$(\eta^5\text{-}C_5H_5)Mo(^{13}CO)_2(N_2)Cl$			
C_s	A'	d	1955.0
	A"	1895.3	1895.5

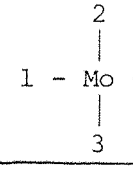

i.e. 1 ≠ 2 = 3.

[a] Refined energy-factored force constants for $(\eta^5\text{-}C_5H_5)Mo(CO)_3Cl$: K_1 = 1610.4, K_2 = 1627.2, k_{12} = 32.7, and k_{23} = 61.7 Nm^{-1} as defined by the numbering in the diagram above.

[b] ^{13}CO in position 1.

[c] ^{13}CO in position 2.

[d] Obscured bands

[e] ^{12}CO in position 2.

[f] ^{12}CO in position 1.

[g] Refined energy-factored force constants for $(\eta^5\text{-}C_5H_5)Mo(CO)_2Cl$: K = 1508.7 and k_i = 75.6 Nm^{-1}.

[h] Refined energy-factored force constants for $(\eta^5\text{-}C_5H_5)Mo(CO)_2(N_2)Cl$: K = 1566.7 and k_i = 48.5 Nm^{-1}.

Table 6.3 Observed and calculated[a] band positions (cm^{-1}) of $(\eta^5\text{-}C_5H_5)Ru(CO)_2Cl$ and its photoproducts in a 5% ^{13}CO doped CH_4 matrix.

Complex	Point Group	ν(CO)	Observed	Calculated
$(\eta^5\text{-}C_5H_5)Ru(^{12}CO)_2Cl$	C_s	A'	2056.2	2056.2
		A"	2009.2	2009.2
$(\eta^5\text{-}C_5H_5)Ru(^{12}CO)(^{13}CO)Cl$	C_1	A	2043.2	2042.5
		A	1977.5	1977.7
$(\eta^5\text{-}C_5H_5)Ru(^{13}CO)_2Cl$	C_s	A'	2011.0[b]	2010.5
		A"	1964.5	1964.6
$(\eta^5\text{-}C_5H_5)Ru(^{12}CO)Cl$	C_s	A'	1967.7[c]	
$(\eta^5\text{-}C_5H_5)Ru(^{13}CO)Cl$	C_s	A'	1923.2	1923.0

[a] Refined energy-factored force constants for $(\eta^5\text{-}C_5H_5)Ru(CO)_2Cl$: K = 1669.5 and k_i = 38.6 Nm^{-1}.
Refined energy-factored force constant for $(\eta^5\text{-}C_5H_5)Ru(CO)Cl$: K = 1563.6 Nm^{-1}.

[b] Band obscured under the lower band of $(\eta^5\text{-}C_5H_5)Ru(^{12}CO)_2Cl$.

[c] Band obscured under the lower band of $(\eta^5\text{-}C_5H_5)Ru(^{13}CO)_2Cl$, and it is calculated to be at 1967.7 cm^{-1} compared with that in a CH_4 matrix.

6.5 REFERENCES

1. R.J. Haines, R.S. Nyholm and M.H.B. Stiddard, *J. Chem. Soc. A.*, 1967 94.

2. D.L. Beach and K.W. Barnett, *J. Organomet. Chem.*, 1975, 97, C27.

3. D.L. Beach, M. Dattilo and K.W. Barnett, *J. Organomet. Chem.*, 1977, 47, 140.

4. R.B. King, L.W. Houk and K.H. Pannell, *Inorg. Chem.*, 1969, 8, 1042.

5. E.O. Fischer and E. Moser, *J. Organomet. Chem.*, 1964, 2, 230.

6. E.O. Rischer and E. Moser, *J. Organomet. Chem.*, 1966, 5, 63.

7. R.B. King, K.H. Pannell, C.A. Eggers and L.W. Houk, *Inorg. Chem.*, 1968, 7, 2353.

8. D.G. Alway and K.W. Barnett, *Inorg. Chem.*, 1978, 17, 2826.

9. L.H. Ali, A. Cox and T.J. Kemp, *J. Chem. Soc. Dalton Trans.*, 1973, 1475.

10. C. Giannotti and G. Merle, *J. Organomet. Chem.*, 1976, 97, 105.

11. R.B. King, W.C. Zipperer and M. Ishaq, *Inorg. Chem.*, 1972, 11, 1361.

12. P.S. Braterman, *"Metal Carbonyl Spectra"*, Academic Press, London, 1975.

13. A.J. Rest, J.R. Sodeau and D.J. Taylor, *J. Chem. Soc. Dalton Trans.*, 1978, 651.

14. A.J. Rest, *J. Organomet. Chem.*, 1972, 40, C76.

15. K.A. Mahmoud, N. Narayanaswamy and A.J. Rest, *J. Chem. Soc. Dalton Trans.*, 1981, 2199.

16. T. Yoshida, T. Okano, D.L. Thorn, T.H. Tulip, S. Otsuka and J.A. Ibers, *J. Organomet. Chem.*, 1979, 181, 183.

17. C. White and R.J. Mawby, *Inorg. Chima. Acta.*, 1970, 4, 261.

18. R.J. Mawby and C. White, *Chem. Commun.*, 1968, 312.

19. D.G. Alway and K.W. Barnett, *Inorg. Chem.*, 1980, 19, 1533.

20. D.G. Alway and K.W. Barnett, *J. Organomet. Chem.*, 1975, 99, C52.

21. R.B. King, *Inorg. Chem.*, 1963, 2, 936.

22. E.O. Fischer, K. Fichtel and K. Ofele, *Chem. Ber.*, 1962, 95, 249.

23. P.M. Treichel, K.W. Barnett and R.L. Shubkin, *J. Organomet. Chem.*, 1967, 7, 449.

24. J.L. Hughey IV, C.R. Bock and T.J. Meyer, *J. Am. Chem. Soc.*, 1975, 97, 4440.

25. A. Albini and H. Kisch, *J. Am. Chem. Soc.*, 1976, 98, 3869.

26. J.M. Kelly, D.V. Bent, H. Hermann, D. Schultefrohlinde and E. Koerner Von Gustorf, *J. Organomet. Chem.*, 1974, 69, 259.

27. J.A. Ferguson and T.J. Meyer, *Inorg. Chem.*, 1971, 10, 1025.

CHAPTER SEVEN

PHOTOCHEMISTRY OF METAL-METAL SIGMA-BONDED COMPLEXES OF THE TYPE $(\eta^5\text{-}C_5H_5)(CO)_3M\text{-}ER_2$ (M = Mo, E = As, Sb, R = Me; M = W, E = As, R = Me, i-Pr, t-Bu), AND OF $(\eta^5\text{-}C_5H_5)_2Fe_2(CO)_4$ IN LOW TEMPERATURE GAS MATRICES AT 12K

7.1 INTRODUCTION

Transition metal substituted phosphines, arsines and stibines undergo a variety of thermal and photochemical reactions. One of the most fundamental is the simple ejection of CO in benzene solution and the production of new complexes with double bonds (Equation 7.1). Interestingly a modest

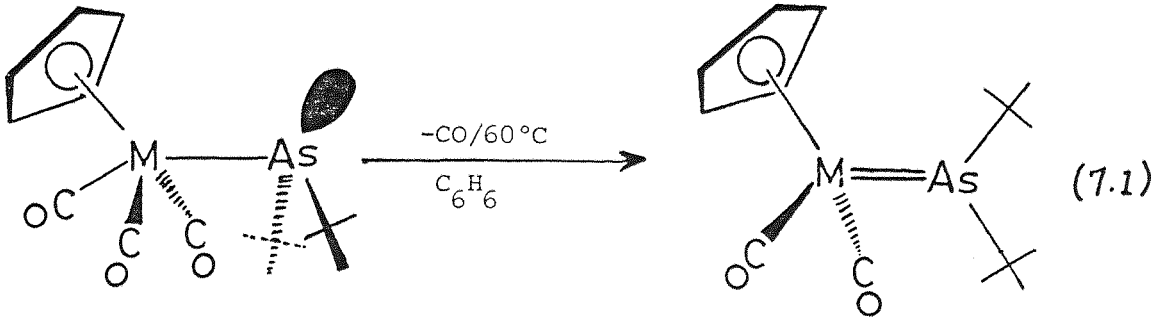

M = Mo, W (7.1)

pressure of CO at 25°C effects a reversal of the forward reaction [1]. In an endeavour to understand whether the forward reaction occurs in one or two stages, matrix isolation studies [2] have been carried out. In this chapter infrared spectroscopic evidence is presented for the formation of the 16-electron species $(\eta^5\text{-}C_5H_5)(CO)_2M\text{-}ER_2$, the dinitrogen substitution products $(\eta^5\text{-}C_5H_5)(CO)_2(N_2)M\text{-}ER_2$ and the double bonded species $(\eta^5\text{-}C_5H_5)(CO)_2M{=}ER_2$ (M = Mo, W; E = As, Sb; R = Me, i-Pr, t-Bu).

The results of recent photochemical and related [3 - 6] studies on transition-metal compounds containing metal-metal single bonds have been consistently interpreted by a principal primary photochemical act in which

homolytic cleavage of the metal-metal bond occurs (Equation 7.2), [3 - 6].

$$M - M \xrightarrow{h\nu} 2M^{\circ} \qquad (7.2)$$

Recent flash photolysis studies, however, of the photochemistry of the iron dimer, $(\eta^5\text{-}C_5H_5)_2Fe_2(CO)_4$ provided evidence for two distinct primary photo processes [7] (Equations 7.3 and 7.4). The identities of species $(\eta^5\text{-}C_5H_5)_2Fe_2(CO)_3$ and $(\eta^5\text{-}C_5H_5)Fe(CO)_2^{\cdot}$ were proposed on the basis of their life-times

$$(\eta^5\text{-}C_5H_5)_2Fe_2(CO)_4 \xrightarrow{h\nu} (\eta^5\text{-}C_5H_5)_2Fe_2(CO)_3 + CO \qquad (7.3)$$

$$(\eta^5\text{-}C_5H_5)_2Fe_2(CO)_4 \xrightarrow{h\nu} 2\ (\eta^5\text{-}C_5H_5)Fe(CO)_2^{\cdot} \qquad (7.4)$$

and uv-vis spectra together with the observation of a back reaction of $(\eta^5\text{-}C_5H_5)_2Fe_2(CO)_3$ with CO; $(\eta^5\text{-}C_5H_5)_2Fe_2(CO)_3$ was long lived and $(\eta^5\text{-}C_5H_5)Fe(CO)_2^{\cdot}$ was short lived. No definitive structural evidence for $(\eta^5\text{-}C_5H_5)Fe_2(CO)_3$ was presented.

The photoreactions of $(\eta^5\text{-}C_5H_5)_2Fe_2(CO)_4$ with phosphine and phosphite ligands [8] to give substitution products, e.g. $(\eta^5\text{-}C_5H_5)_2Fe_2(CO)_3(PPh_3)$ have been proposed to proceed via the CO-bridged intermediate $(\eta^5\text{-}C_5H_5)(CO)_2Fe(\mu\text{-}CO)Fe(CO)(\eta^5\text{-}C_5H_5)$ [9] and also via a radical pathway.

This chapter will also illustrate the photoreactions of $(\eta^5\text{-}C_5H_5)_2Fe_2(CO)_4$ in gas matrices at 12K and provide evidence for the generation of a novel dimeric species $(\eta^5\text{-}C_5H_5)_2Fe_2(\mu\text{-}CO)_3$ in CH_4 matrices. Additionally direct proof that the bridge-terminal interconversion of CO groups of the type (Equation 7.5), can occur very rapidly will be presented. The results

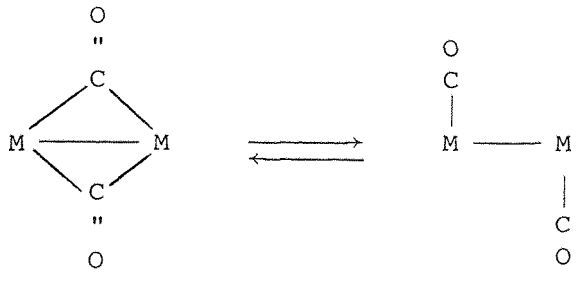

(7.5)

are related to the intermediates proposed in flash photolysis [7] and solution photochemistry [6, 9] studies.

7.2 RESULTS

7.2.1 Photolysis of $(\eta^5\text{-}C_5H_5)(CO)_3M\text{-}ER_2$ Complexes (M = Mo, W; E = As, Sb; R = Me, i-Pr, t-Bu) in CH_4 and N_2 Matrices at 12K

Infrared spectra from a matrix isolation experiment with $(\eta^5\text{-}C_5H_5)(CO)_3W\text{-}AsMe_2$ isolated at high dilution in a CH_4 matrix (ca 1:2000 - 1:5000) are shown in Figure 7.1. Before photolysis there are three strong absorption bands in the terminal CO stretching region at 1997.5 (A'), 1924.8 (A') and 1907.8 (A") cm^{-1} expected for a molecule with C_s symmetry (Figure 7.1(a), Table 7.1). Irradiation of the matrix with visible light ($\lambda > 410$ nm), giving light corresponding to the uv-vis spectrum (Figure 7.3(a)), produced free CO (2138 cm^{-1}) and four distinct new bands at 1971.8, 1941.8, 1887.6 and 1860.3 cm^{-1} (Figure 7.1(b)). A further period of photolysis with the same source showed (Figure 7.1(c)) all the new bands increasing at the expense of the parent bands (bands marked P). Annealing the matrix to 35K showed that the bands at 1941.8 and 1860.3 cm^{-1} (bands marked (3)) are not related to those at 1971.8 and 1887.6 cm^{-1} (bands marked (1)) because the pairs of bands changed their relative intensities (Figure 7.1(d)). Not only did the pair (1) bands decrease but new bands (bands marked (2)) appeared. The high dilution used, as indicated by the absence of any dimer product bands, i.e. $(\eta^5\text{-}C_5H_5)_2W_2(CO)_6$, and the reversibility of the bands at 1941.8 and 1860.3 cm^{-1} enabled these bands to be assigned to the 16-electron species $(\eta^5\text{-}C_5H_5)(CO)_2W\text{-}AsMe_2$. This behaviour is analogous to the formation of $(\eta^5\text{-}C_5H_5)M(CO)_2R$ species on photolysis of $(\eta^5\text{-}C_5H_5)M(CO)_3R$ complexes (M = Mo, W; R = Me, Et, n-Pr, i-Pr, n-Bu) [10, 11]. The other pairs of bands are assigned to two different rotamers of the W-As double bonded species $(\eta^5\text{-}C_5H_5)(CO)_2W{=}AsMe_2$, where the $AsMe_2$ group lies in or out of the plane bisecting the CO ligands. A precedent for such rotamers is found in the asymmetric olefin hydrido complexes $(\eta^5\text{-}C_5H_5)W(CO)_2(olefin)H$ together with facile *cis* $\rightleftarrows$ *trans* isomerisation of such complexes on annealing the matrices to 35K. Analogous results (Table 7.1) were obtained starting from other

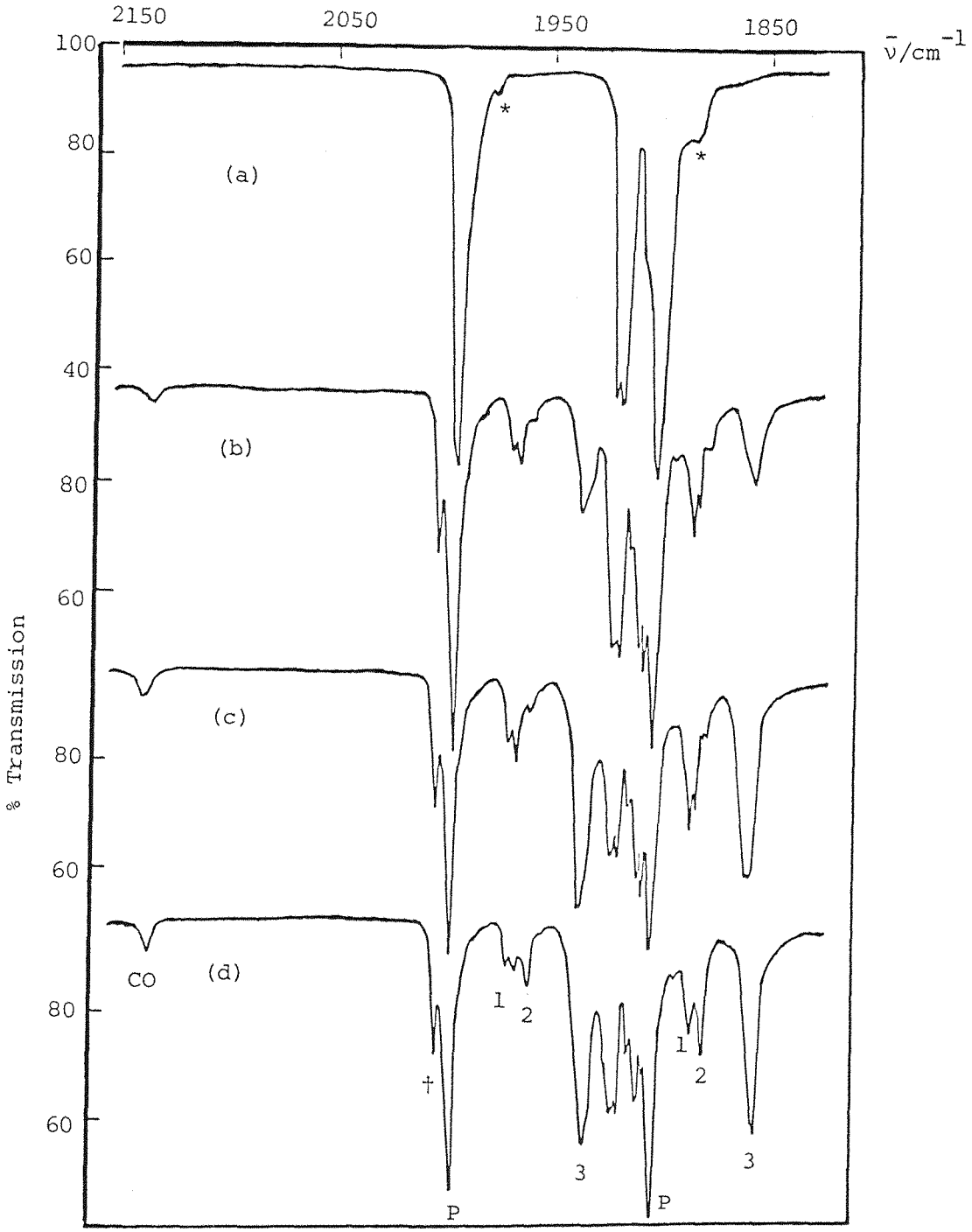

FIGURE 7.1 Infrared spectra from an experiment with $(\eta^5\text{-}C_5H_5)(CO)_3W\text{-}AsMe_2$ isolated at high dilution in a CH_4 matrix at 12K: (a) after deposition, (b) after 10 min. photolysis using $\lambda > 410$ nm, (c) after further 40 min. photolysis using the same source, and (d) after annealing to ca 30K for 2 min. Bands marked (†) are due to matrix splitting effects, those marked (*) are due to $(\eta^5\text{-}C_5H_5)(^{12}CO)_2(^{13}CO)W\text{-}AsMe_2$ present in natural abundance, and those marked (1) - (3) are due to new photoproducts (see text).

$(\eta^5\text{-}C_5H_5)(CO)_3M\text{-}ER_2$ complexes (M = Mo, W; E = As, Sb; R = i-Pr, t-Bu) in CH_4 matrices but the yields for Mo were much lower than for W analogues.

Photolysis of $(\eta^5\text{-}C_5H_5)(CO)_3M\text{-}ER_2$ complexes in N_2 matrices produced different results for Mo compared to W. For example, initial medium energy u.v. irradiation (λ > 370 nm) of $(\eta^5\text{-}C_5H_5)(CO)_3Mo\text{-}SbMe_2$ produced mainly $(\eta^5\text{-}C_5H_5)(CO)_2Mo\text{-}SbMe_2$, identified by analogy with the species produced in a CH_4 matrix (Table 7.1), with a small amount of $(\eta^5\text{-}C_5H_5)(CO)_2Mo{=}SbMe_2$. Reversal with long wavelength radiation (λ > 490 nm) resulted in the appearance of three new bands at 2183.6, 1942.6 and 1883.0 cm^{-1}, while bands due to $(\eta^5\text{-}C_5H_5)(CO)_2Mo\text{-}SbMe_2$ and $(\eta^5\text{-}C_5H_5)(CO)_2Mo{=}SbMe_2$ decreased in intensity. The band at 2183.6 cm^{-1} is in the region typical for NN terminal stretching modes, e.g. $(\eta^5\text{-}C_5H_5)Co(CO)(N_2)$ (ν_{NN} at 2161.6 cm^{-1} in N_2 matrix [12], $(\eta^5\text{-}C_5H_5)Mn(CO)_2(N_2)$ (ν_{NN} at 2175 cm^{-1} in N_2 matrix [13] and at 2169 cm^{-1} in n-hexane solution) [14], and $(\eta^5\text{-}C_5H_5)Mo(CO)_2(N_2)CH_3$ (ν_{NN} at 2191 cm^{-1} in N_2 matrix [10]). The bands at 1942.6 and 1883.0 cm^{-1} may be assigned as terminal CO stretching modes and, therefore, the product may be identified as $(\eta^5\text{-}C_5H_5)(CO)_2(N_2)Mo\text{-}SbMe_2$. Calculations [15] of the OC-Mo-CO bond angle (θ = 83°) from relative band intensities and the energy-factored CO interaction force constant ($\underline{k}_i$ = 46.0 Nm^{-1}) and comparison with data for *cis*-$(\eta^5\text{-}C_5H_5)Mo(CO)_2(N_2)CH_3$ (θ = 82° and $\underline{k}_i$ = 43.3 Nm^{-1}) [10] and $(\eta^5\text{-}C_5H_5)(CO)_3Mo\text{-}SbMe_2$ ($\underline{k}_{cis}$ = 37.3 and $\underline{k}_{trans}$ = 55.0 Nm^{-1}) suggests that the two CO ligands in $(\eta^5\text{-}C_5H_5)(CO)_2(N_2)Mo\text{-}SbMe_3$ are *cis* to one another. The As analogue, $(\eta^5\text{-}C_5H_5)(CO)_3Mo\text{-}AsMe_2$ also gave a dinitrogen complex (Table 7.1) but none of the parent W complexes gave N_2 substitution products; only the 16-electron species $(\eta^5\text{-}C_5H_5)(CO)_2W\text{-}ER_2$ were detected.

7.2.2 Photolysis of $(\eta^5\text{-}C_5H_5)_2Fe_2(CO)_4$ in a CH_4 Matrix at 12K

Infrared spectra from an experiment with $(\eta^5\text{-}C_5H_5)_2Fe_2(CO)_4$ (I, II) isolated at high dilution in a CH_4 matrix (ca 1:2000 - 1:5000) are shown in Figure 7.2. Before photolysis the spectrum contains bands at 2005.5, 1959.5, 1954.7 and 1936.3 cm^{-1} in the terminal CO stretching region and at 1802.1, 1780.0, 1753.6 and 1712.0 cm^{-1} in the bridging CO stretching region, which have been assigned [16, 17] to the *cis* (I) and *trans* (II) isomers of the bridged $(\eta^5\text{-}C_5H_5)_2Fe_2(CO)_4$ molecule (Figure 7.2(a), Table 7.2).

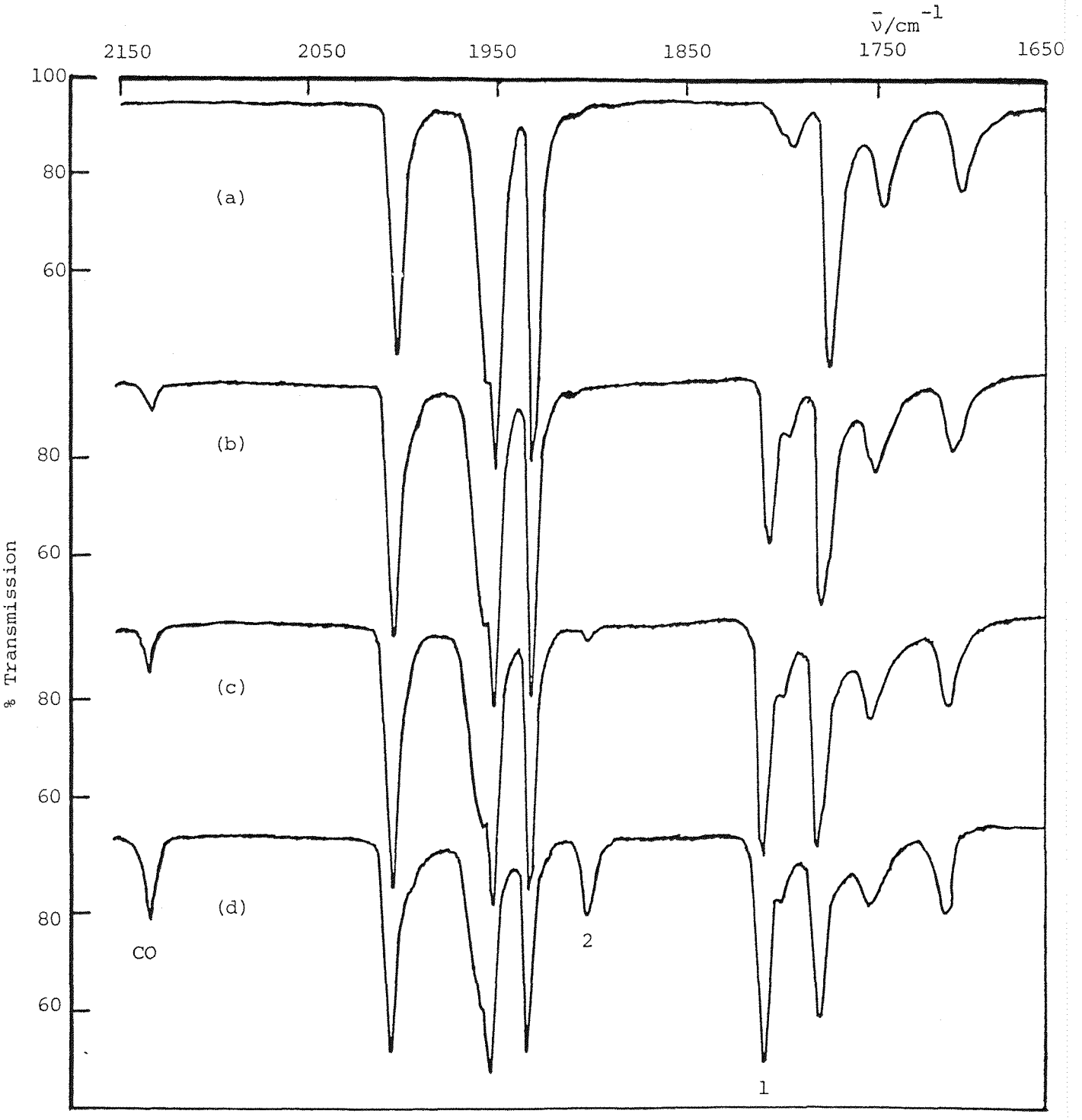

FIGURE 7.2 Infrared spectra from an experiment with $(\eta^5\text{-}C_5H_5)_2Fe_2(CO)_4$ isolated at high dilution in a CH_4 matrix at 12K: (a) after deposition, (b) after 30 min. photolysis using $\lambda > 430$ nm, (c) after further 75 min. photolysis using the same source, and (d) after further 40 min. photolysis using $\lambda = 310 - 390$ nm. Bands marked (1) and (2) arise from new photo-products (see text).

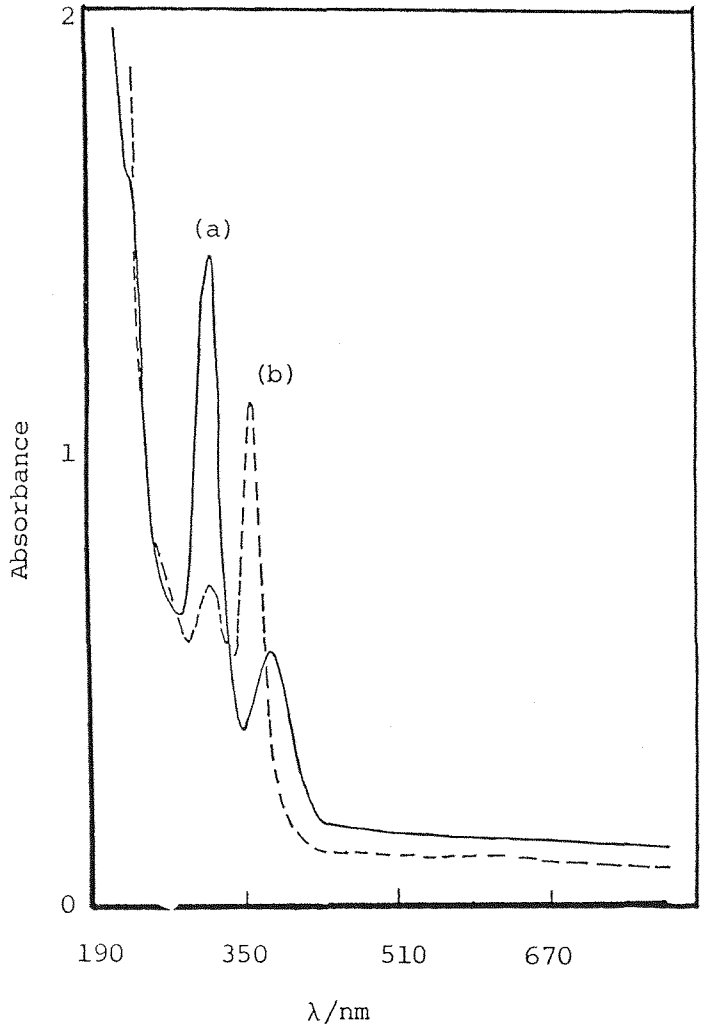

FIGURE 7.3 Ultraviolet-visible spectra from an experiment with $(\eta^5\text{-}C_5H_5)(CO)_3Mo\text{-}EMe_2$ isolated at high dilution in a CH_4 matrix at 12K: (a) after deposition, and (b) after 30 min. photolysis using $\lambda > 410$ nm.

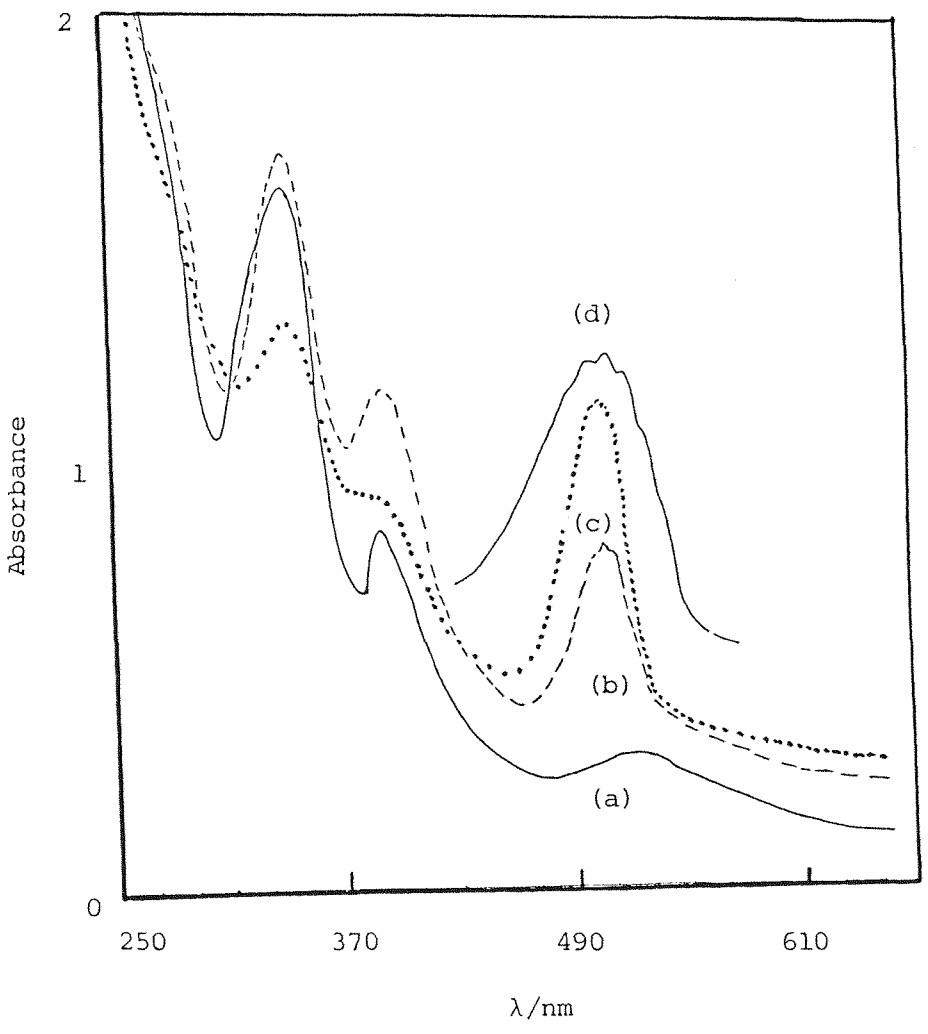

FIGURE 7.4 Ultraviolet-visible spectra from an experiment with $(\eta^5\text{-}C_5H_5)_2Fe_2(CO)_4$ isolated at high dilution in a CH_4 matrix at 12K: (a) after deposition, (b) after 30 min. photolysis using $\lambda > 430$ nm, (c) after further 40 min. photolysis using λ = 310 - 390 nm, and (d) the same as (c) repeated on an expanded scale.

Irradiation of the matrix with visible light (λ > 410 nm) giving light corresponding to the electronic absorption spectrum (Figure 7.4(a)) produced free CO (ca. 2138 cm^{-1}) and a single intense absorption band in the bridging CO stretching region at 1816.1 cm^{-1} (Figure 7.2(b)). A spectral subtraction [18] showed that there were no new photoproduct bands in the terminal CO stretching region and that only a slight reduction in the band of the *cis* (I) isomer of $(\eta^5\text{-}C_5H_5)_2Fe_2(CO)_4$ had occured. The photoproduct, which is also observed to be formed in p.v.c. films at 77K and in CH_4 matrices at 12K, has an electronic absorption band exhibiting vibronic fine structure (λ_{max} = 510 nm, $\bar{\nu}$ = 194 cm^{-1}; CH_4 matrix) (Figure 7.4(d)) which is indicative of a highly symmetric species, c.f. $(\eta^5\text{-}C_5H_5)_2W$ [19]. Prolonged irradiation with the same energy source (λ > 410 nm) showed a further increase in the intensity of the free CO band and the single absorption band at 1816.1 cm^{-1} (Figure 7.2(c)). Irradiation of the matrix with u.v. radiation (λ = 310 -390 nm) produced a further new band in the terminal CO stretching region at 1902.4 cm^{-1} and caused significant decreases in the bands of the parent molecule $(\eta^5\text{-}C_5H_5)_2Fe_2(CO)_4$ and in particular from the *cis* (I) isomer exclusively, with little or no increase in the single absorption band at 1816.1 cm^{-1} (Figure 7.2(d)). The band at 1902.4 cm^{-1} can be reversed to the starting material by using visible radiation (λ > 500 nm).

The photoproduct band at 1816.1 cm^{-1} is evidently formed by dissociative loss of CO from the parent molecule $(\eta^5\text{-}C_5H_5)_2Fe_2(CO)_4$ and in particular from the *trans* (II) isomer exclusively. The fact that it has only one bridging CO stretching band which is i.r. active and this band is at a higher wavenumber than those of $(\eta^5\text{-}C_5H_5)_2Fe_2(CO)_4$ in the bridging region suggests that the new species is $(\eta^5\text{-}C_5H_5)_2Fe_2(\mu\text{-}CO)_3$ (V) with three equivalent bridging CO ligands. The similarly symmetric dimer $Fe_2(CO)_9$ (VI) has one bridging CO stretching band at 1828 cm^{-1} [20] and $(\eta^5\text{-}C_5Me_5)_2Re_2(\mu\text{-}CO)_3$ (VII) has band (n-hexane) at 1748 cm^{-1} [21]. The product $(\eta^5\text{-}C_5H_5)_2Fe_2(\mu\text{-}CO)_3$ (V) is also similar to the photogenerated dimer $(\eta^4\text{-}C_4Ph_4)_2Fe_2(\mu\text{-}CO)_3$ (VIII) which is proposed to have an iron-iron triple bond [22].

Irradiation (λ > 430 nm) of $[(\eta^5\text{-}C_5H_5)Fe(^{12}CO)_{2-n}(^{13}CO)_n]_2$ (see Chapter 8 for preparation of this complex in a C_6H_{12}/thf mixture) in a CH_4 matrix gave new i.r. absorption bands at 1813, 1791, 1779 and 1772 cm^{-1}. The

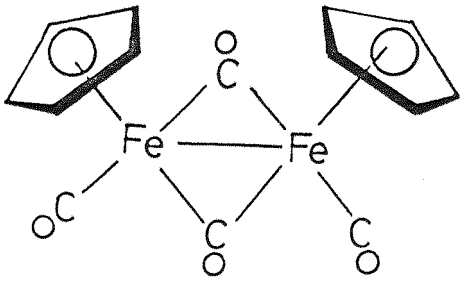

(I)

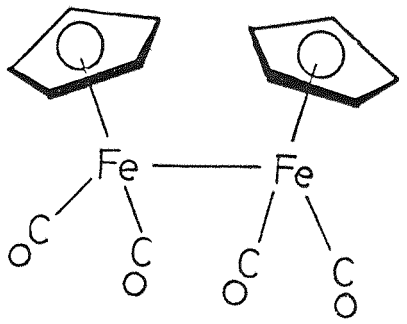

(III)

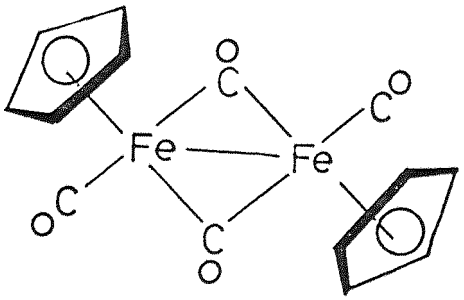

(II)

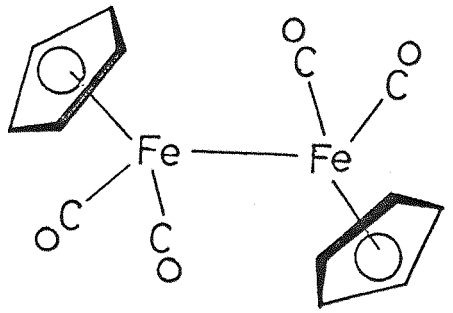

(IV)

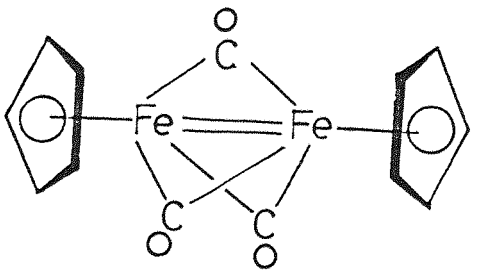

(V)

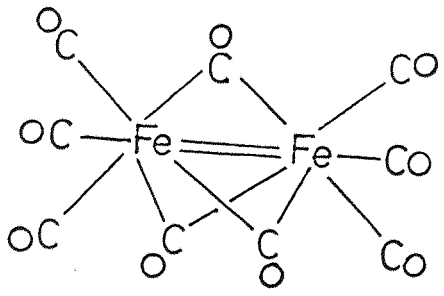

(VI)

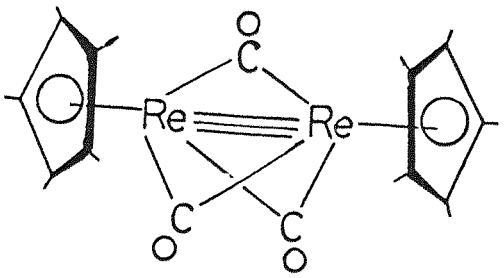

(VII)

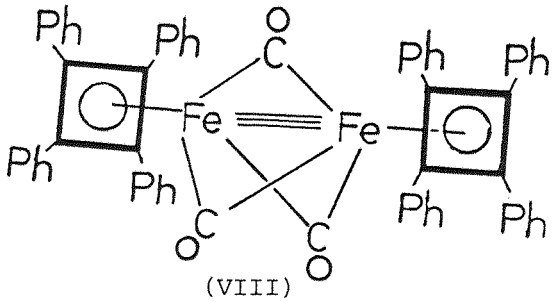

(VIII)

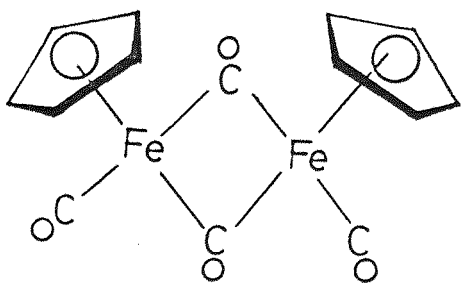

(IX)

intensity pattern and positions of these bands could be fitted [18] exactly by using an energy-factored force field for $\underline{D}_{3h}$ symmetry [23 - 25] and are consistent with the formation of the species $[(\eta^5\text{-}C_5H_5)_2Fe_2(\mu\text{-}^{12}CO)_{3-m}(\mu\text{-}^{13}CO_m]$ (m = 0-3), i.e. the structure of $(\eta^5\text{-}C_5H_5)_2Fe_2(CO)_3$ is established as (V). Similarly using X-ray crystallography it has been shown that the molecular structure of $(\eta^5\text{-}C_5Me_5)_2Re_2(\mu\text{-}CO)_3$ (VII) is highly symmetrical and approximately $\underline{D}_{3h}$ if only the metal atoms and the carbonyl groups are considered [21].

The band at 1902.4 cm^{-1} may prossibly arise from the formation of the radical species $(\eta^5\text{-}C_5H_5)Fe(CO)_2^{\cdot}$. If this species is formed in the matrix there should be another band in the terminal CO stretching region in addition to that observed at 1902.4 cm^{-1} (Figure 7.2(d)). Such a band could be hidden under other bands in the terminal CO stretching region. This possibility, can be eliminated, however, because the bands attributed to this species must fall at approximately 25 cm^{-1} lower than those of the parent molecule $(\eta^5\text{-}C_5H_5)_2Fe_2(CO)_4$ (ν_{CO} at 2005.5, 1959.5 and 1954.7 cm^{-1}, Table 7.2) on the basis of the comparison obtained on irradition of $(\eta^5\text{-}C_5H_5)M(CO)_3H$ complexes (M = Mo, W) in CO matrices ($(\eta^5\text{-}C_5H_5)Mo(CO)_3H$, 2029.2, 1946.7 and 1940.5 cm^{-1} and $(\eta^5\text{-}C_5H_5)Mo(CO)_3^{\cdot}$, 2008.9, 1915.5 and 1908.4 cm^{-1}; $(\eta^5\text{-}C_5H_5)W(CO)_3H$, 2024.3, 1936.1 and 1931.1 cm^{-1} and $(\eta^5\text{-}C_5H_5)W(CO)_3^{\cdot}$, 1999.3, 1900.3 and 1896.5 cm^{-1}; (see Chapter 3)).

Another possibility is that the band at 1902.4 cm^{-1} arises from a species (IX) where there are only the bridging CO groups in $(\eta^5\text{-}C_5H_5)_2Fe_2(CO)_4$ holding the two halves of the molecule together after electronic excitation cleaves the metal-metal σ-σ^* bond [9]. No new bands in the bridging CO stretching region were observed, however, for such a species (IX). At the present the assignment of the band at 1902.4 cm^{-1} in CH_4 matrices remains an enigma.

Analogous results were obtained for $(\eta^5\text{-}C_5H_5)_2Fe_2(CO)_4$ isolated at high dilution in N_2 matrices, but no bands were observed corresponding to the formation of the photosubstituted dinitrogen product $(\eta^5\text{-}C_5H_5)_2Fe_2(CO)_3(N_2)$. Spectroscopic data for the new species are given in Table 7.2.

7.2.3 Photolysis of $(\eta^5\text{-}C_5H_5)_2Fe_2(CO)_4$ in CO Matrices at 12K

Infrared spectra from an experiment with $(\eta^5\text{-}C_5H_5)_2Fe_2(CO)_4$ (I, II) isolated at high dilution in a CO matrix (ca. 1:2000 - 1:5000) are shown in Figure 7.5. Before photolysis the spectrum contains bands at 2004.8, 1989.4, 1958.4 and 1936.3 cm^{-1} in the terminal CO stretching region and 1802.0, 1779.2, 1951.5 and 1714.0 cm^{-1} in the bridging CO stretching region (Figure 7.5(a), Table 7.2). Irradiation of the matrix with visible radiation (λ > 430 nm) produced new photoproduct bands in the terminal CO stretching region at 2061.5, 2034.2, 1989.4 and 1954.2 cm^{-1} (Figure 7.5(b)). Prolonged irradiation with the same energy source (λ > 430 nm) increased in the intensity of the new bands and decreased the intensity of the parent bands (Figure 7.5(c)). Irradiation of the matrices with u.v. radiation (λ = 320 - 390 nm) decreased the bands of the parent molecule $(\eta^5\text{-}C_5H_5)_2Fe_2(CO)_4$ and in particular the bands of *cis* (I) isomer exclusively. Annealing the matrix for 2 minutes and then re-cooling to 12K caused reverse in the new photoproduct bands and regenerated the bands of the parent molecule. Unlike the species observed in a CH_4 matrix, irradiation of $(\eta^5\text{-}C_5H_5)_2Fe_2(CO)_4$ in a CO matrix produced no new bands in the CO bridging region. The disappearance of the terminal CO stretching and the bridging CO stretching bands and the growth of new photoproduct bands at higher energy than those of the starting material in the CO stretching region, indicates that non-bridging isomers are formed. In the series of $(\eta^5\text{-}C_5H_5)_2M_2(CO)_4$ complexes the $(\eta^5\text{-}C_5H_5)_2Os_2(CO)_4$ is non-bridged, the $(\eta^5\text{-}C_5H_5)_2Ru_2(CO)_4$ complex is a mixture of bridged and non-bridged isomers [26]. Comparison of the new bands at 2061.5, 2034.2, 1989.4, and 1954.2 cm^{-1} with those of the non-bridged $(\eta^5\text{-}C_5H_5)_2Os_2(CO)_4$ (ν_{CO} at 2040, 1986 and 1948 cm^{-1}; hexane) [26] and the non-bridged $(\eta^5\text{-}C_5H_5)_2Ru_2(CO)_4$ (ν_{CO} at 2021, 1972 and 1943 cm^{-1}; octane) [16] showed that some of the new photoproduct bands i.e. the bands at 2034.2, 1989.4 and 1954.2 cm^{-1} are in good correlation with those observed in solution for the non-bridged $(\eta^5\text{-}$

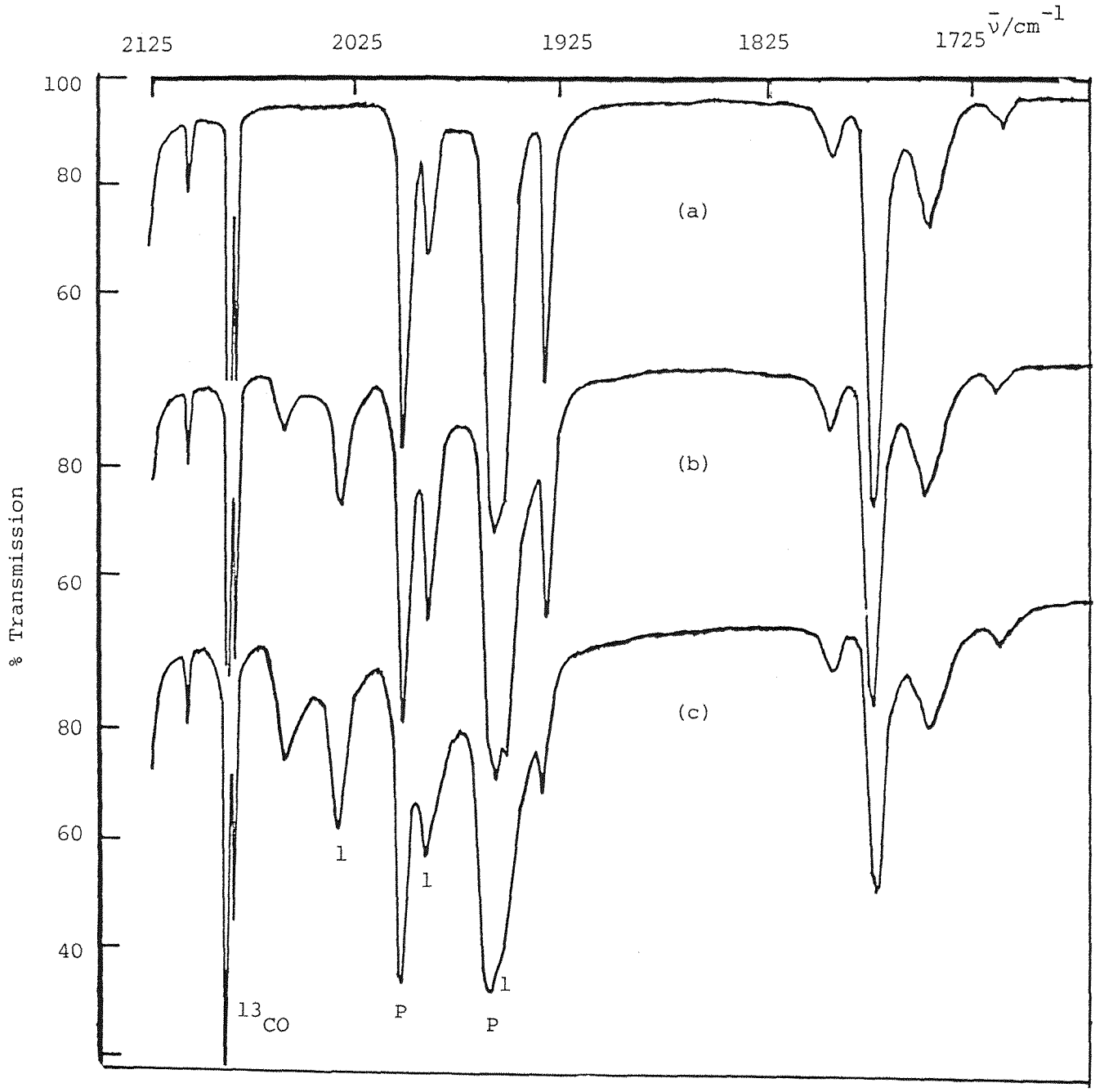

FIGURE 7.5 Infrared spectra from an experiment with $(\eta^5\text{-}C_5H_5)_2Fe_2(CO)_4$ isolated at high dilution in a CO matrix at 12K: (a) after deposition, (b) after 20 min. photolysis using $\lambda > 430$ nm and (c) after further 30 min. photolysis using the same source. Bands marked (P) are due to the parent molecule and those marked (1) arise from new photoproducts (see text).

$C_5H_5)_2Os_2(CO)_4$ and could be assigned to the *cis* (III) isomer of the non-bridged $(\eta^5\text{-}C_5H_5)_2Fe_2(CO)_4$. The band at 2061.5 cm^{-1} which did not increase in the same proportion as those at 2034.2, 1989.4 and 1954.2 cm^{-1} during u.v. irradiation could arise from a different species. However, this band was not always observed and, therefore, it has not been the subject of an assignment at this stage.

4.3 DISCUSSION

The photoreactions of the $(\eta^5\text{-}C_5H_5)(CO)_3M\text{-}ER_2$ complexes (M = Mo, W; E = As, Sb; R = Me, i-Pr, t-Bu) at high dilution in a CH_4 and N_2 matrices are summarised in Scheme 7.1. The primary photoprocess in all cases is the

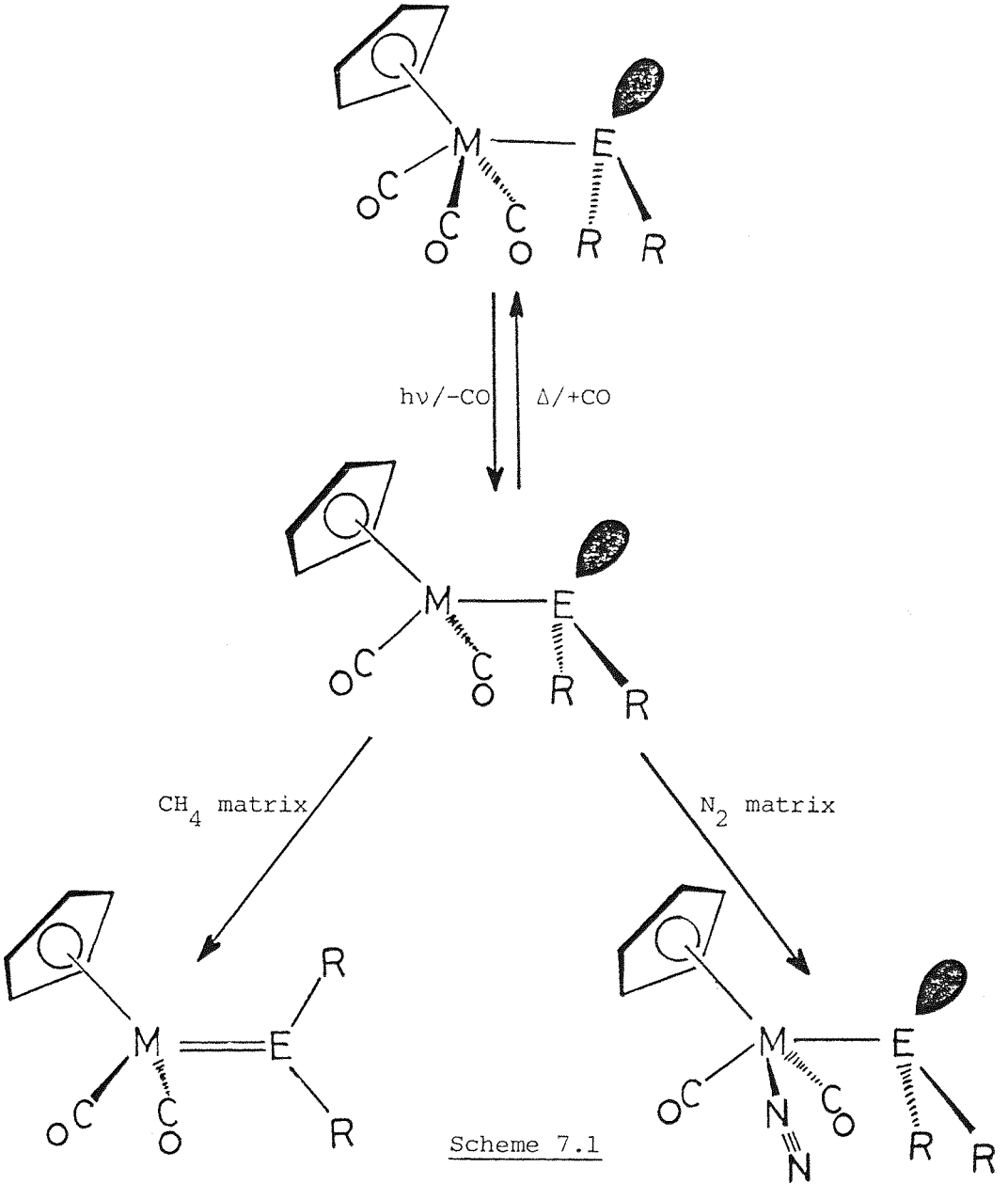

Scheme 7.1

dissociative loss of a CO ligand. The resulting coordinatively unsaturated 16-electron species $(\eta^5\text{-}C_5H_5)(CO)_2M\text{-}ER_2$ can be identified in CH_4 and N_2 matrices at 12-30K but not in benzene at 60°C [27 - 29]. This is similar to the behaviour of $(\eta^5\text{-}C_5H_5)M(CO)_3R$ complexes (M = Mo, W; R = H, CH_3, C_2H_5, Ph) where CO dissociation is the primary photoprocess (see Chapters 2, 3 and 4).

The formation of coordinatively unsaturated speices $(\eta^5\text{-}C_5H_5)(CO)_2M\text{-}ER_2$ was furthermore demonstrated by the detection of $(\eta^5\text{-}C_5H_5)(CO)_2(N_2)Mo\text{-}ER_2$ in nitrogen matrices, c.f. the production of $(\eta^5\text{-}C_5H_5)Mo(CO)_2(N_2)CH_3$ from $(\eta^5\text{-}C_5H_5)Mo(CO)_3CH_3$ [10]. Irradiation of $(\eta^5\text{-}C_5H_5)(CO)_3M\text{-}ER_2$ complexes in benzene solution [30 - 33] in presence of phosphine ligands (PMe_3, PEt_3, PPh_3) resulted in the formation of the photosubstituted derivatives (Equation 7.6). The solution studies, especially the results from the photolysis

$$(\eta^5\text{-}C_5H_5)(CO)_3M\text{-}ER_2 \xrightarrow[+PR_3]{h\nu/-CO} (\eta^5\text{-}C_5H_5)(CO)_2(PR_3)M\text{-}ER_2 \qquad (7.6)$$

of $(\eta^5\text{-}C_5H_5)(CO)_3M\text{-}AsMe_2$ complexes (M = Mo, W) suggested that photochemically generated 16-electron species $(\eta^5\text{-}C_5H_5)(CO)_2M\text{-}AsMe_2$ can also dimerises to form the $[(\eta^5\text{-}C_5H_5)M(CO)_2AsMe_2]_2$ complexes [34] (Equation 7.7).

$$2(\eta^5\text{-}C_5H_5)(CO)_3M\text{-}AsMe_2 \xrightarrow[h\nu]{-2CO}$$

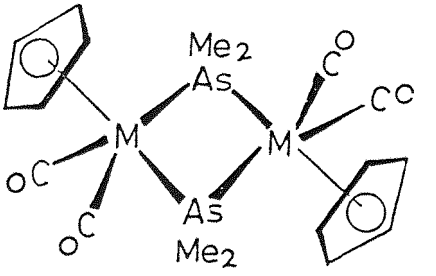

(7.7)

However, in CH_4 and N_2 matrices such a dimer $[(\eta^5\text{-}C_5H_5)(CO)_2M\text{-}AsMe_2]_2$ was not observed because of the high dilution of the experiments.

An interesting feature of the matrix photochemistry of $(\eta^5\text{-}C_5H_5)(CO)_3M\text{-}ER_2$ is the observation of additional bands besides those assigned to the 16-electron intermediates $(\eta^5\text{-}C_5H_5)(CO)_2M\text{-}ER_2$, and were not observed for

similar complexes irradiated under similar conditions e.g. $(\eta^5\text{-}C_5H_5)M(CO)_3CH_3$ (M = Mo, W) complexes [10]. In view of the fact that the metal-metal double bond of $(\eta^5\text{-}C_5H_5)(CO)_2M{=}ER_2$ is well characterised in solution [1], these additional bands are assigned to $(\eta^5\text{-}C_5H_5)(CO)_2M{=}ER_2$ species in low temperature matrices at 12K. A similar M=P double bond was demonstrated [35] in $(\eta^5\text{-}C_5H_5)(CO)_2Mo{=}P\overset{\downarrow}{N}(Me)CH_2CH_2\overset{\downarrow}{N}(Me)$ by X-ray crystallography. The presence of two $(\eta^5\text{-}C_5H_5)(CO)_2M{=}ER_2$ rotamers in the matrix suggesting that rotation relative to the metal-arsenic double bond is rapid [36] on warming up the matrix to room temperature.

Although extensive investigations have been carried out on the mechanisms of photochemical reactions of the dinuclear complexes $M_2(CO)_{10}$ (M = Mn, Re) [37 - 40], $(\eta^5\text{-}C_5H_5)M_2(CO)_6$ (M = Mo, W) [41 - 43] and $(\eta^5\text{-}C_5H_5)M_2(CO)_4$ (M = Fe, Ru) [4, 6, 7, 9] in solutions, when $(\eta^5\text{-}C_5H_5)_2Fe_2(CO)_4$ was irradiated with visible light in CH_4 matrix a novel dinuclear iron compound $(\eta^5\text{-}C_5H_5)_2Fe_2(\mu\text{-}CO)_3$ (V) was formed by dissociative loss of CO ligand (Equation 7.8). This complex $(\eta^5\text{-}C_5H_5)_2Fe_2(\mu\text{-}CO)_3$ is also a homologue of the iso-

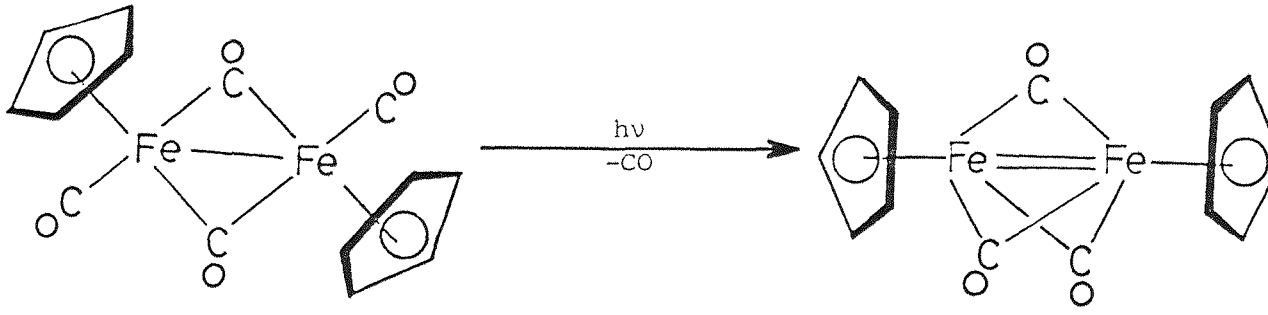

(II) (V) (7.8)

electronic series exemplified by $(\eta^4\text{-}C_4R_4)_2Fe_2(\mu\text{-}CO)_3$ (VIII) [22] (R = H, Ph) and $(\eta^6\text{-}C_6H_6)_2Cr_2(\mu\text{-}CO)_3$ [44] complexes. Similarly, Hoyano and Graham [21] prepared the novel complex $(\eta^5\text{-}C_5Me_5)_2Re_2(\mu\text{-}CO)_3$ (VII) by u.v. irradiation of the $(\eta^5\text{-}C_5Me_5)Re(CO)_3$ at 20°C in cyclohexane solution (Equation 7.9). The highly symmetrical structure, approximately $\underline{D_{3h}}$ was indicated

$$(\eta^5\text{-}C_5Me_5)Re(CO)_3 \xrightarrow{h\nu} (\eta^5\text{-}C_5Me_5)_2Re_2(\mu\text{-}CO)_3 + (\eta^5\text{-}C_5Me_5)_2Re_2(CO)_5 \qquad (7.9)$$

and the formulation as $(\eta^5\text{-}C_5Me_5)Re(\mu\text{-}CO)_3Re(\eta^5\text{-}C_5Me_5)$ (VII) was confirmed by X-ray crystallography.

In a more recent work [48], the complexes $(\eta^5\text{-}C_5R_5)_2Fe_2(CO)_4$ (R = H, Me) and $(\eta^5\text{-}C_5H_4Bz)_2Fe_2(CO)_4$ (Bz = CH_2Ph) have been photolyzed with near-u.v. light in rigid low temperature matrices of alkanes or 2-methyltetrahydrofuran. In the alkane media at 77K photolysis results in the loss of CO and the formation of a metal carbonyl complex having a single i.r. absorption in the CO stretching region. The metal-containing product is formulated as a triply CO bridged species based on the facts that only one band is observed in the bridging CO region and that only one CO is lost per molecule as established for the irradiation of $(\eta^5\text{-}C_5Me_5)_2Fe_2(CO)_4$. Only $(\eta^5\text{-}C_5Me_5)_2Fe_2(CO)_4$ reacts completely and this complex is significantly photosensitive in the 2-methyltetrahydrofuran matrix. The other two complexes each yield some of a triply CO bridged product in the alkane matrices, but i.r spectral changes show that only the *trans* isomer is photosensitive. The more polar 2-methyltetrahydrofuran matrix gives a mixture of isomers of the $(\eta^5\text{-}C_5H_5)_2Fe_2(CO)_4$ and the $(\eta^5\text{-}C_5H_4Bz)_2Fe_2(CO)_4$ that is very rich in the non-photosensitive *cis* isomer. This is consistent with the photochemical behaviour of $(\eta^5\text{-}C_5H_5)_2Fe_2(CO)_4$ in CH_4 matrices and p.v.c. films at 12K where the *trans* (II) isomer is highly photosensitive and *cis* (I) isomer is unreactive unless u.v. light is used.

From the results of Caspar and Meyer [7], the earlier results of Tyler et al. [9], and those of Abrahamson et al. [4], the overall reactivity which accounts for the observed photochemistry of $(\eta^5\text{-}C_5H_5)_2Fe_2(CO)_4$ can be represented as in Scheme 7.2. From its reactivity towards added ligands like CO or PPh_3, it is assumed that the intermediate $(\eta^5\text{-}C_5H_5)_2Fe_2(CO)_3$ is a CO loss product. In cyclohexane saturated with CO, a quantitative return to $(\eta^5\text{-}C_5H_5)_2Fe_2(CO)_4$ was observed following flash photolysis of the intermediate $(\eta^5\text{-}C_5H_5)_2Fe_2(CO)_3$ [7]. The electronic absorption band of (V) observed in CH_4 matrix is at the same wavelength (λ_{max} = 510 nm) as that of the CO loss species $(\eta^5\text{-}C_5H_5)_2Fe_2(CO)_3$ detected in the flash photolysis experiment [7]. It seems probable, therefore, that $(\eta^5\text{-}C_5H_5)_2Fe_2(CO)_3$, which has been proposed to have the stoichiometry shown in Scheme 7.2 is identical with (V).

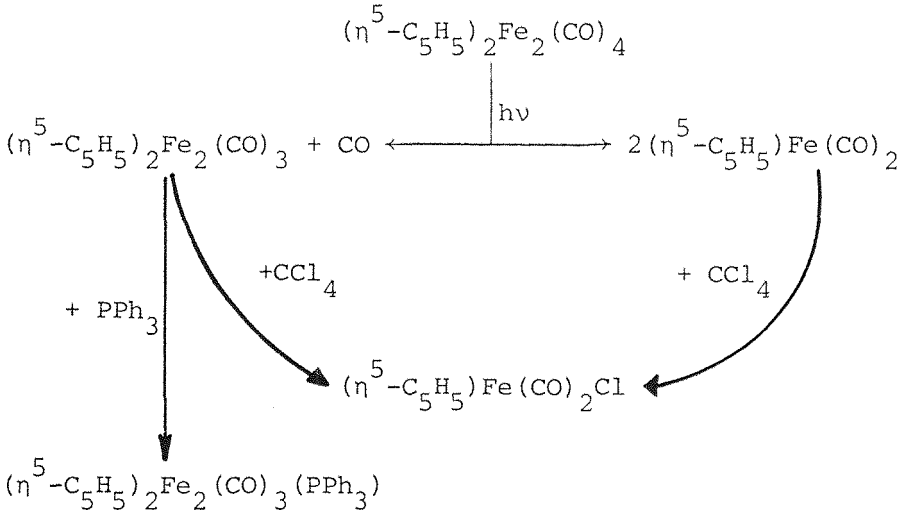

Scheme 7.2

Irradiation of $(\eta^5\text{-}C_5H_5)_2Fe_2(CO)_4$ in CO matrices produced new bands only in the terminal CO stretching region and were assigned to non-bridged isomers on the basis of the data available on the non-bridged $(\eta^5\text{-}C_5H_5)_2Os_2(CO)_4$ [16]. Analysis of the i.r. spectrum of $(\eta^5\text{-}C_5H_5)_2Fe_2(CO)_4$ in a range of solvents [45] and the low temperature ^1H n.m.r. spectrum [26, 46] has shown that in solution the compound behaves in a stereochemically non-rigid manner, i.e. an equilibrium between the *cis* (I) and *trans* (II) isomers of the compound (Scheme 7.3). Inter-conversion is proposed to occur via non-bridged forms of the type shown, but these intermediates themselves would appear to be almost totally absent in solutions of this particular compound, on the evidence of a lack of the absence of i.r. absorption bands assignable to these forms. There is strong evidence that the bridge $\rightleftharpoons$ non-bridged structure inter-conversions, of the type shown in Scheme 7.3 occurs with a low activation energy [26, 47]. It is possible, however, that the 12K temperature matrix technique stabilizes the non-bridged intermediates which were proposed as unstable intermediates in solution in the equilibirum (I) $\rightleftharpoons$ (II). In rigid media at low temperature matrices, however, the bridged *cis* (I) and *trans* (II) isomers do not thermally interconvert. The barrier to interconversion of *cis* (I) and *trans* (II) isomers of $(\eta^5\text{-}C_5H_5)_2Fe_2(CO)_4$ is of the order of 40 KJ /mol [26, 46]. However, in gas

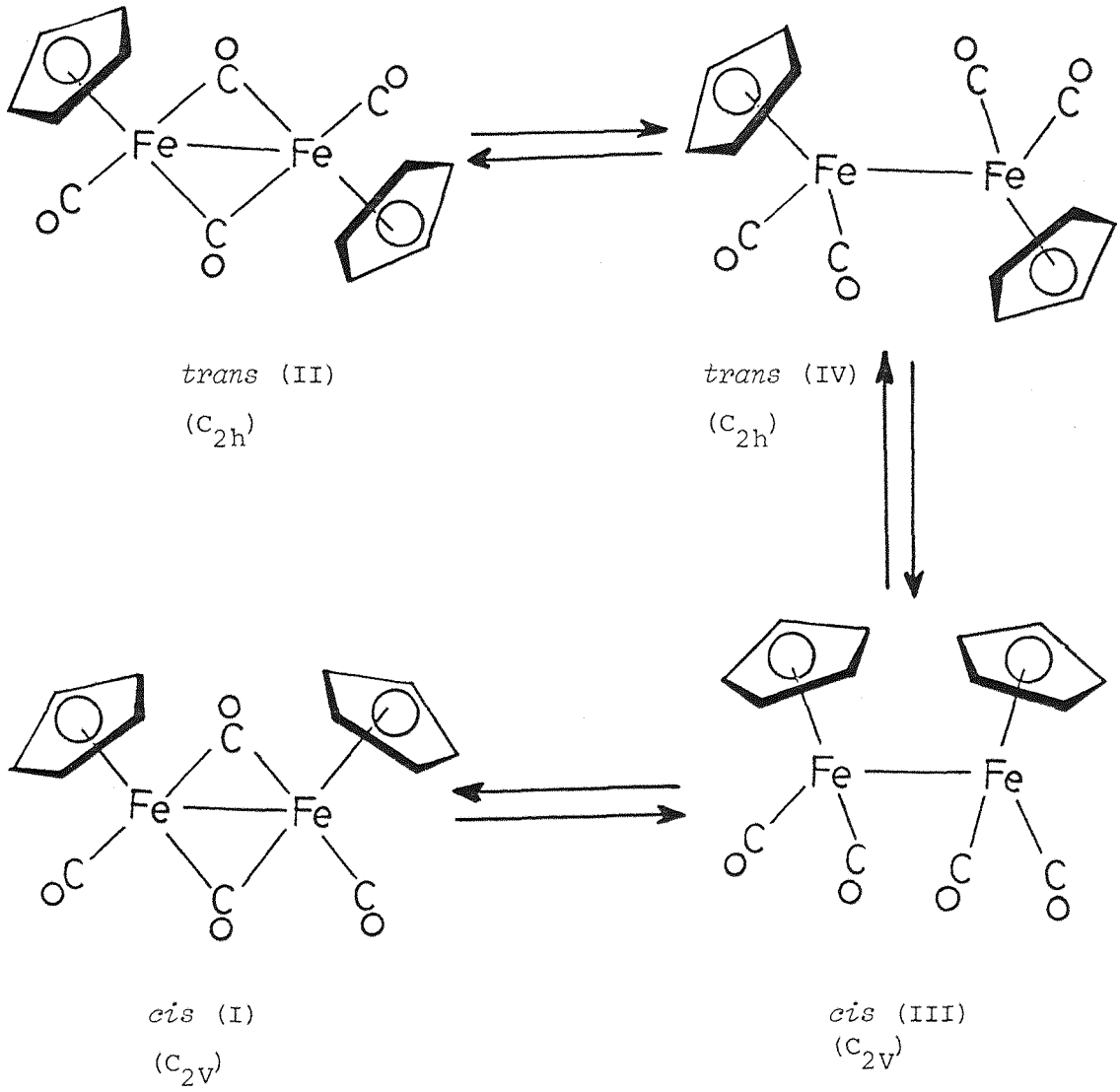

Scheme 7.3

matrices at 12K the interconversion of the non-bridged isomers *trans* (IV) $\rightleftharpoons$ *cis* (III) should be considered as an important pathway for the formation of the non-bridged *cis* (III) isomer in CO matrices.

7.4 CONCLUSIONS

The observation of high yields of the 16-electron coordinatively unsaturated species $(\eta^5\text{-}C_5H_5)(CO)_2M\text{-}ER_2$ (Scheme 7.1) may be taken to indicate that the reaction to form $(\eta^5\text{-}C_5H_5)(CO)_2M{=}ER_2$ species in solution (Equation 7.1) proceeds in two stages. This is supported by the formation of the $(\eta^5\text{-}C_5H_5)(CO)_2M\text{-}ER_2$ species in N_2 matrices followed by their reaction with N_2 to form 18-electron *cis*-$(\eta^5\text{-}C_5H_5)(CO)_2(N_2)Mo\text{-}ER_2$ complexes. The 16-electron coordinatively unsaturated species $(\eta^5\text{-}C_5H_5)(CO)_2M\text{-}ER_2$ would seem to be the most likely reaction intermediate in CO replacement reactions of $(\eta^5\text{-}C_5H_5)(CO)_3M\text{-}ER_2$ complexes.

Photolysis of the metal-metal bonded compound $(\eta^5\text{-}C_5H_5)_2Fe_2(CO)_4$ in CH_4 matrix leads to the formation of a novel species $(\eta^5\text{-}C_5H_5)_2Fe_2(\mu\text{-}CO)_3$ (V). Thus the work in low temperature matrices provides the <u>first</u> direct evidence for the structure of an intermediate proposed in the photochemical reactions of a metal-metal bonded dimer.

Photolysis of $(\eta^5\text{-}C_5H_5)_2Fe_2(CO)_4$ in CO matrices can suppress the principle CO loss photoreaction pathway and allow a second pathway, <u>vis</u> formation of a non-bridged isomer, to be observed (Scheme 7.3).

Table 7.1 Infrared band positions (cm^{-1}) observed in the terminal CO stretching region for $(\eta^5\text{-}C_5H_5)(CO)_3M\text{-}ER_2$ complexes (M = Mo, W; E = As, Sb; R = Me, i-Pr, t-Bu) and their photoproducts in CH_4 and N_2 matrices at 12K.

Complex	CH_4	N_2
$(\eta^5\text{-}C_5H_5)(CO)_3Mo\text{-}AsMe_2$	2001.5, 1933.2, 1913.0	2004.6, 1935.8, 1916.5
$(\eta^5\text{-}C_5H_5)(CO)_2Mo\text{-}AsMe_2$	1948.4, 1870.0	1950.5, 1875.4
$(\eta^5\text{-}C_5H_5)(CO)_2Me{=}AsMe_2$	1974.7, 1888.2	1976.3, 1892.7
$(\eta^5\text{-}C_5H_5)(CO)_2(N_2)Mo\text{-}AsMe_2$ [a]		1950.5, 1890.7
$(\eta^5\text{-}C_5H_5)(CO)_3Mo\text{-}SbMe_2$	1997.0, 1926.0, 1904.5	2001.0, 1931.4, 1908.0
$(\eta^5\text{-}C_5H_5)(CO)_2Mo\text{-}SbMe_2$	1940.3, 1866.6	1942.6, 1871.0
$(\eta^5\text{-}C_5H_5)(CO)_2Mo{=}SbMe_2$	1971.6, 1886.2	1970.8, 1885.5
$(\eta^5\text{-}C_5H_5)(CO)_2(N_2)Mo\text{-}SbMe_2$ [b]		1942.6, 1883.0
$(\eta^5\text{-}C_5H_5)(CO)_3W\text{-}AsMe_2$	1997.5, 1924.8, 1907.6	
$(\eta^5\text{-}C_5H_5)(CO)_2W\text{-}AsMe_2$	1941.8, 1860.3	
$(\eta^5\text{-}C_5H_5)(CO)_2W{=}AsMe_2$	1971.8, 1887.6 [c] 1963.5, 1882.5 [d]	
$(\eta^5\text{-}C_5H_5)(CO)_3W\text{-}As(\underline{i}\text{-}Pr)_2$	1995.9, 1918.6, 1902.8	1997.0, 1921.7, 1904.8
$(\eta^5\text{-}C_5H_5)(CO)_2W\text{-}As(\underline{i}\text{-}Pr)_2$	1933.4, 1855.2	1931.7, 1857.4
$(\eta^5\text{-}C_5H_5)(CO)_2W{=}As(\underline{i}\text{-}Pr)_2$	1963.0, 1884.0 [e]	1968.6, 1887.1
$(\eta^5\text{-}C_5H_5)(CO)_3W\text{-}As(\underline{t}\text{-}Bu)_2$	1994.5, 1919.6, 1895.0	1997.0, 1920.7, 1898.0
$(\eta^5\text{-}C_5H_5)(CO)_2W\text{-}As(\underline{t}\text{-}Bu)_2$	1933.2, 1853.8	1935.2, 1855.8
$(\eta^5\text{-}C_5H_5)(CO)_2W{=}As(\underline{t}\text{-}Bu)_2$	1962.0, 1881.6 [e]	1968.4, 1884.6

[a] ν_{NN} at 2183.6 cm^{-1}

[b] ν_{NN} at 2183.6 cm^{-1}

[c] Rotamer I

[d] Rotamer II

[e] Broad bands, only one rotamer observed.

Table 7.2 Infrared band positions (cm^{-1}) observed in the CO stretching region for $(\eta^5\text{-}C_5H_5)_2Fe_2(CO)_4$ and its photoproducts in various gas matrices at 12K.

Complex	CH_4	N_2	CO
$(\eta^5\text{-}C_5H_5)_2Fe_2(CO)_4$ [a]	2005.5	2007.5	2004.8
	1959.5	1964.5	1989.4
(I + II)	1954.7	1960.0	1958.4
	1936.3	1940.2	1936.3
	1802.1	1805.6	1802.0
	1780.0	1784.8	1779.2
	1753.6	1756.2	1751.5
	1712.0	1715.0	1714.0
$(\eta^5\text{-}C_5H_5)_2Fe_2(CO)_3$	1816.1	1818.5	b
(V)			
$(\eta^5\text{-}C_5H_5)_2Fe_2(CO)_4$ [d]	-	-	2034.2 [c]
			1989.4
(III + IV)			1954.2

[a] Bands are due to bridged isomers

[b] Not observed in CO matrix

[c] Bands due to the non-bridged isomer

[d] Only formed in CO matrix

7.5 REFERENCES

1. M. Luksza, S. Himmel and W. Malisch, *Angew. Chem. Int. Ed.*, 1983, in press.

2. A.J. Rest in *"Matrix Isolation Spectroscopy"*, A.J. Barnes, W.J., Orville-Thomas, A. Müller and R. Gaufrés (Eds.), NATO Advanced Study Institute Series, D. Reidel Publ. Co., Dordrecht, 1981; Chap. 9.

3. A. Hudson, M.F. Lappert and B.K. Nicholson, *J. Chem. Soc. Dalton Trans.*, 1977, 551.

4. H.B. Abrahamson, M.C. Palazotto, C.L. Reichel and M.S. Wrighton, *J. Am. Chem. Soc.*, 1979, 101, 4123.

5. R.M. Laine and P.C. Ford, *Inorg. Chem.*, 1977, 16, 4123.

6. M.S. Wrighton and D.S. Ginley, *J. Am. Chem. Soc.*, 1975, 97, 4246.

7. J.V. Caspar and T.J. Meyer, *J. Am. Chem. Soc.*, 1980, 102, 7794.

8. R.J. Haines and A.L. du Preez, *Inorg. Chem.*, 1969, 8, 1459.

9. H.B. Gray, M.A. Schmidt and D.R. Tyler, *J. Am. Chem. Soc.*, 1979, 101, 2753.

10. K.A. Mahmoud, R. Naranaswamy and A.J. Rest, *J. Chem. Soc. Dalton Trans.*, 1981, 2199.

11. K.A. Mahmoud, A.J. Rest, H.G. Alt, M.S. Eichner and B.M. Jansen, *J. Chem. Soc. Dalton Trans.*, 1983, in press.

12. O. Crichton, A.J. Rest and D.J. Taylor, *J. Chem. Soc. Dalton Trans.*, 1980, 167.

13. A.J. Rest, J.R. Sodeau and D.J. Taylor, *J. Chem. Soc. Dalton Trans.*, 1978, 651.

14. D.Sellmann, *Angew. Chem. Int. Ed.*, 1971, 10, 919.

15. P.S. Braterman, *"Metal Carbonyl Spectra"*, Academic Press, London, 1975.

16. R.D. Fischer, A. Vogler and K. Noack, *J. Organomet. Chem.*, 1967, 7, 135.

17. F.A. Cotton and G. Yagupsky, *Inorg. Chem.*, 1967, 7, 15.

18. R.H. Hooker, K.A. Mahmoud and A.J. Rest, *J. Chem. Soc. Chem. Commun.*, 1983, 1022.

19. J. Chetwynd-Talbot, P. Grebenik, R.N. Perutz and M.H.A. Powell, *Inorg. Chem.*, 1983, 22, 1675.

20. K.S. Pitzer and R.K. Sheline, *J. Am. Chem. Soc.*, 1950, 72, 1107.

21. J.K. Hoyano and W.A.G. Graham, *J. Chem. Soc. Chem. Commun.*, 1982, 27.

22. S.I. Murahashi, T. Mizoguchi, T. Hosokawa, I. Moritani, Y. Kai, M. Kohara, N. Yasuoka and N. Kasai, *J. Chem. Soc. Chem. Commun.*, 1974, 563.

23. E.B. Wilson, J.C. Decius and P.C. Cross, *"Molecular Vibrations"*, McGraw-Hill, New York, N.Y., 1955.

24. J.H. Darling and J.S. Ogden, *J. Chem. Soc. Dalton Trans.*, 1972, 2496.

25. H. Huber, E.P. Kündig, M. Moskovits and G.A. Ozin, *J. Am. Chem. Soc.*, 1973, 95, 332.

26. J.G. Bullitt, F.A. Cotton and T.J. Marks, *Inorg. Chem.*, 1972, 11, 671.

27. W. Malisch, R. Janta and G. Künzel, *Z. Naturforsch*, 1979, 34b, 599.

28. W. Malisch, H. Röbner, K. Keller and R. Janta, *J. Organomet. Chem.*, 1977, 133, C21.

29. W. Malisch, M. Luksza and W.S. Sheldrick, *Z. Naturforsch*, 1981, 36b, 1580.

30. W. Malisch and A. Meyer, *J. Organomet. Chem.*, 1980, 198, C29.

31. W. Malisch, R. Maisch, I.J. Colquhoun and W. McFarlane, *J. Organomet. Chem.*, 1981, 220, C1.

32. W. Malisch and R. Janta, *Angew. Chem.*, 1978, 90, 221.

33. U. Schubert, K. Ackermann, R. Janta, S. Voran and W. Malisch, *Chem. Ber.*, 115, 2003.

34. W. Malisch, M. Kuhn, W. Albert and H. Röbner, *Chem. Ber.*, 1980, 113, 3318.

35. L.D. Hutchins, R.T. Paine and C.F. Campana, *J. Am. Chem. Soc.*, 1980, 102, 4521.

36. B.E.R. Schilling, R. Hoffmann and D.L. Lichtenberger, *J. Am. Chem. Soc.*, 1979, 101, 585; B.E.R. Schilling, R. Hoffmann and J.W. Faller, *ibid*, 1979, 101, 592.

37. M.S. Wrighton and D.S. Ginley, *J. Am. Chem. Soc.*, 1975, 97, 2065.

38. M.S. Wrighton and D. Bredesen, *J. Organomet. Chem.*, 1973, 50, C35.

39. R.A. Levenson, H.B. Gray and G.P. Ceasar, *J. Am. Chem. Soc.*, 1970, 92, 3653.

40. B.H. Byers and T.L. Brown, *J. Am. Chem. Soc.*, 1977, 99, 2527.

41. B.H. Byers and T.L. Brown, *J. Am. Chem. Soc.*, 1975, 97, 3260 and *ibid*, 1977, 99, 2527.

42. D.S. Ginley and M.S. Wrighton, *J. Am. Chem. Soc.*, 1975, 97, 3533.

43. R.H. Hooker, K.A. Mahmoud and A.J. Rest, *J. Organomet. Chem.*, 1983, in press.

44. L. Knoll, K. Reiss, J. Schäfer and P. Klüfers, *J. Organomet. Chem.*, 1980, 193, C40.

45. A.R. Manning, *J. Chem. Soc., A*, 1968, 1319.

46. J.G. Bullitt, F.A. Cotton and T.J. Marks, *J. Am. Chem. Soc.*, 1970, 92, 2155.

47. K. Noack, *J. Organomet. Chem.*, 1967, 7, 151.

48. A.F. Hepp, J.P. Blaha, C. Lewis and M.S. Wrighton, *J. Am. Chem. Soc.*, 1983, in press.

CHAPTER EIGHT

EXPERIMENTAL

8.1 CRYOGENICS

Cryogenic temperatures (ca. 12K) were obtained using an Air Products and Chemical Inc. Displex closed cycle helium refrigeration systems (models CSW 202 and CSA 202). The apparatus (Plate 1) consists of a portable air cooled compressor module (C) and a two stage expander module (E) interlinked by two helium gas lines. The expander module plus vacuum shroud is mounted on a portable trolley complete with vacuum equipment capable of producing a high vacuum (ca. 10^{-7} Torr). The whole apparatus, trolley and compressor combined, allows a high degree of experimental flexibility.

The first and second stages of the expander module are surrounded by a two part shroud containing the outer spectroscopic windows (Figure 8.1) which allows evacuation of the interspace to a working pressure of 10^{-7} Torr. Orientation of the central cold window may be altered relative to the outer spectroscopic windows by rotation about a vacuum seal interconnecting the two parts of the vacuum shroud. This flexibility allows the cold window to be in the correct orientation for gas spray-on, sample photolysis, infrared and ultra violet spectroscopy.

8.2 DEPOSITION SYSTEMS

As the compounds used in this work had varying volatilities it was necessary to use two different spray-on techniques. For materials with high vapour pressures at normal temperatures, i.e. a few Torr in the region -20° to 20°C, it was sufficient to make up gas mixtures of known composition and deposit these by the pulsed method, as suggested by Rochkind [1]. However, for materials with lower vapour pressures, it was necessary to use a slow deposition method where the sample was co-condensed on to the cold window along with the matrix gas. A list of compounds investigated in this

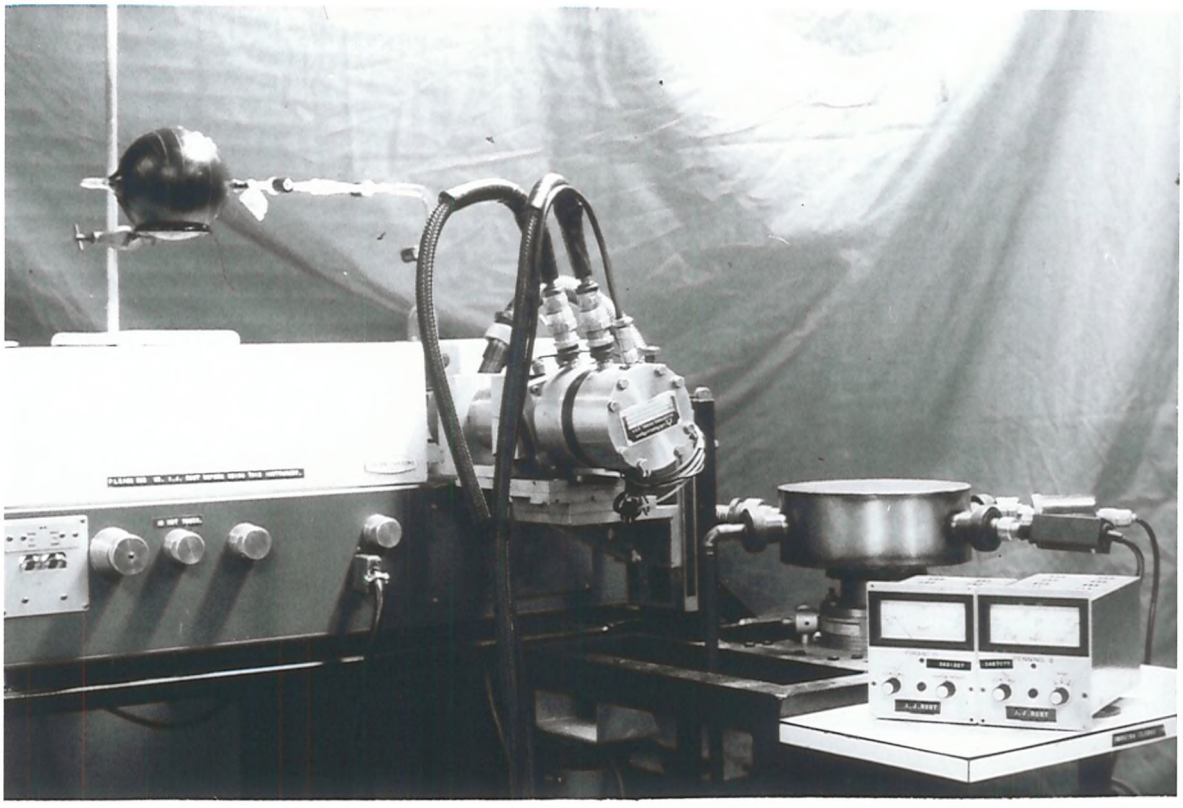

Plate 1

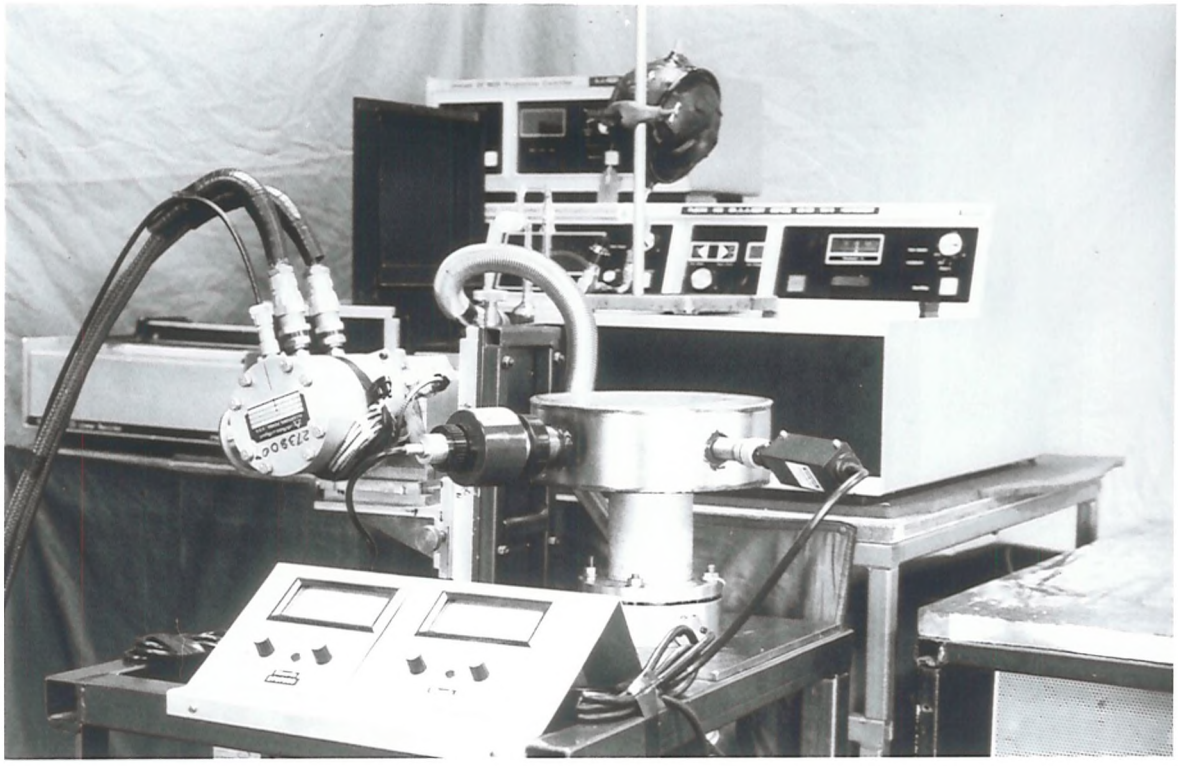

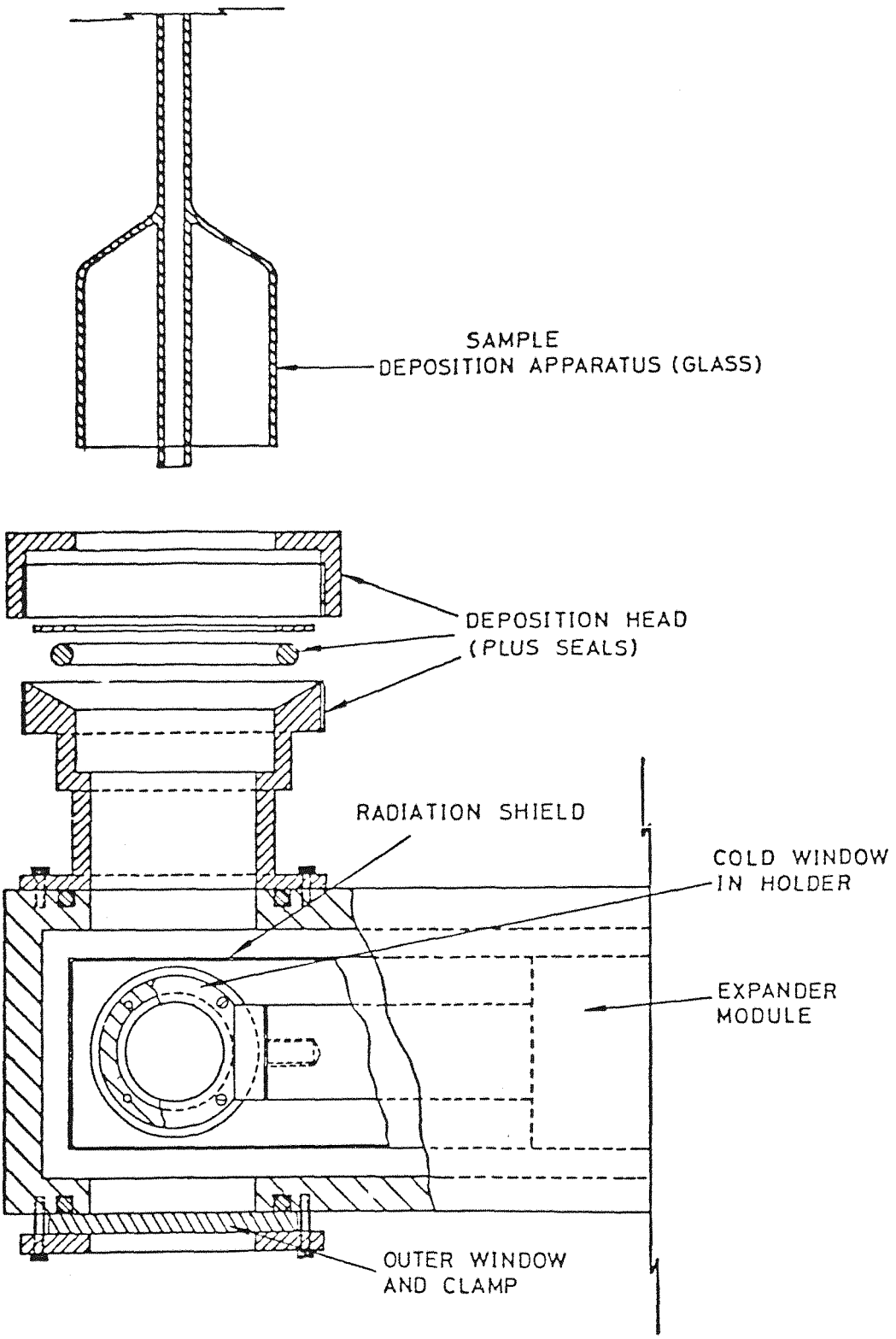

Figure 8.1 Side view of the cryostat tip, vacuum shield, radiation shield and deposition head.

work, method of spray-on and deposition conditions is given in Table 8.1.

Gas phase mixtures of the compounds with matrix gases were made up by the following procedure (Figure 8.2a). Consistent pressures of the 'guest' sample compound in the region 10^{-2} to 10^{-3} Torr were obtained by filling a small volume of a vacuum line (ca. 10 m^3) with the vapour pressure of the compound at a suitable temperature and then allowing the contents to expand into an evacuated bulb (1 litre). For compounds with lower vapour pressures this procedure was repeated several times. 'Host' matrix gas was then introduced into the bulb to give a total pressure of ca. 100 Torr and a dilution of the sample between 1:2000 and 1:10,000. By masking the bulb with black tape or aluminium foil it was possible to keep light sensitive gas mixtures stable for many hours. Once made up, the matrix bulb could be transferred to the cryogenic apparatus (Figure 8.2b) where the interspace could be evaluated using the vacuum system prior to cooling down the spectroscopic window.

The pulsed deposition system was arranged so that two taps on the glass spray-on head enclosed a small volume (ca. 10 cm^3) which, at the total pressure of 100 Torr, was found to be a suitable pulsing volume. Successive opening and closing of the two taps in sequence allowed the small volume of gas mixture into the apparatus and this was condensed onto the cold spectroscopic window. Provided the pulsing rates were controlled, i.e. a fresh pulse was not deposited until the matrix temperature and sublimation pressure had stabilised, it was possible to obtain matrices with suitable ultraviolet and infrared optical properties. With a 1:2000 - 1:5000 mixture, adequate infrared absorptions were generally obtained after 20 - 30 pulses, but provided the cold window was perfectly clean and the sample was not deposited too rapidly, as many as 100 pulses could be deposited without any detectable loss in transmission.

For less volatile compounds a co-condensation deposition method was used (Figure 8.2c) which incorporated different glass heads appropriate for the varying physical and chemical natures of the compounds. Arrangements which proved suitable for these compounds (Table 8.1) are shown in Figure 8.3 and essentially stem from an initial central design (Figure 8.3a). For

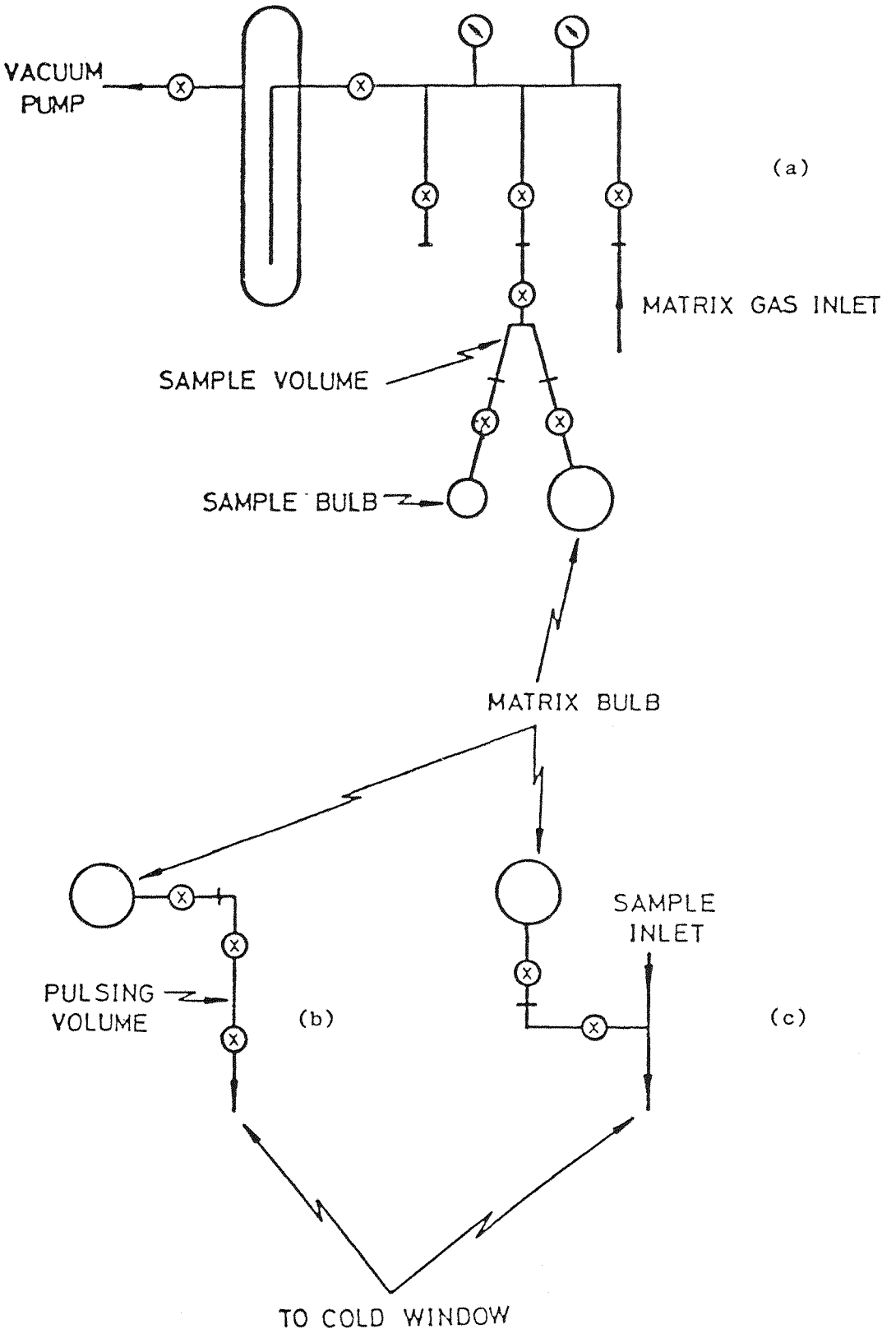

Figure 8.2 Schematic diagram for (a) vacuum line matrix gas preparation, (b) pulsed deposition, and (c) slow deposition methods.

systems with volatilities only marginally too low for the pulsed deposition method the sample could be stored in a finger and maintained at a low temperature (-30° to 25°C) which could be varied depending on the requirements of the sample (Figure 8.3b). After deposition, the line could be sealed using a greaseless tap and, if necessary, the finger and sample could be removed. For other low volatility compounds the sample could be held in one of three glass heads (Figures 8.3c - 8.3e) which reduced the distance between sample and the cold spectroscopic window. By the use of a temperature bath (Figure 8.3e) and an induction heater (Figures 8.3c and 8.3d) the sample could be maintained at a specific temperature within the range -10° to 100°C.

Matrix gases were introduced directly onto the cold window from a detachable bulb via a needle valve and a metal capillary line. The matrix gas bulb (1 litre) was prefilled to a total pressure of ca. 150 Torr and transferred to the experimental apparatus prior to cool-down. With a gas bulb pressure of 150 Torr and an optimised sample arrangement, a gas flow rate of 1.5 m mole h^{-1} for 2 hours gave a matrix with about 1 m mole of sample plus gas deposited on the window. This is may be compared with the pulsed spray-on method where deposition of 2 m mole in the course of 50 pulses gives a total deposition of around 1 m mole actually on the sample window.

8.3 SPECTROSCOPY

a) Infrared spectra: Most infrared spectra were obtained by using a Grubb-Parsons Spectromajor in conjunction with two Oxford Instruments 3000 chart recorders (one linear and one logarithmic) (Plate 1). This instrument was designed to cover the 8500 to 400 cm^{-1} spectral region in the ranges 8500 to 2000 cm^{-1} and 2000 to 400 cm^{-1} and in the course of the study both ranges were used. However, to give an uninterrupted scan in the terminal carbonyl stretching region the monochrometer has been modified to give an added facility of a grating change at 1800 cm^{-1}. The Grubb-Parsons performed adequately giving a resolution of better than 1 cm^{-1} throughout the spectral region and an accuracy of ca. ± 1.0 and ± 0.5 cm^{-1} for the ranges 8500 to 2000 and 2000 to 400 cm^{-1} respectively. Calibration was regularly carried

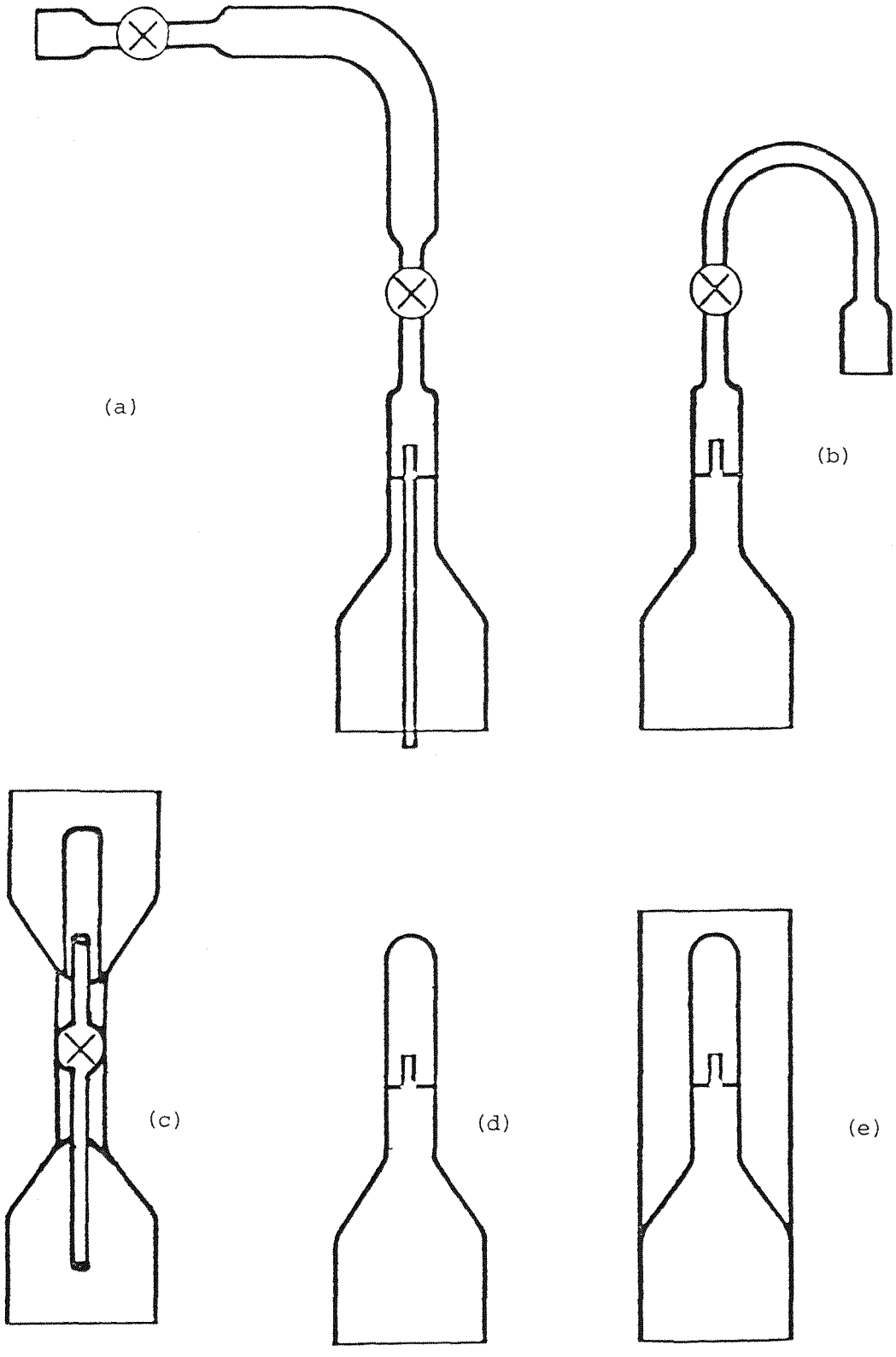

Figure 8.3 Section diagrams for the deposition heads (glass) used in this work: (a) pulsed deposition (volatile complexes), (b) slow deposition (semi-volatile complexes (-20 to 25°C)), (c) slow deposition (25 - 40°C using induction heater), (d) slow deposition (45 - 100°C using induction heater) and (e) slow deposition (less volatile complexes -20 to 25°C).

out using the gas phase absorptions of HCl, DCl, CO and the atmospheric absorption bands of H_2O [2]. In case of overlapping bands, infrared spectra were obtained by using a Nicolet 7199 Fourier Transform Infrared spectrometer which was accurate to ± 0.05 cm^{-1} and covered the range 4000 - 400 cm^{-1} (Plate 2).

Different spectral windows were used depending on the type of study and the infrared spectral region under study (Table 8.2), but generally a combination of CsI, CaF and KBr windows (purchased from BDH Limited) were used. Under certain circumstances a filter had to be used to prevent photosensitive photoproducts from being destroyed by visible radiation emitted by the Nernst glowbar of the infrared spectrometer. Two coated germanium interference filters (Ocli Optical Coatings) were employed which covered the ranges 2500 to 1400 cm^{-1} and 1400 to 600 cm^{-1}.

b) Ultraviolet-visible spectroscopy: Electronic absorption spectra were recorded on a Pye-Unicam SP 1800 B spectrometer (Plate 1). The SP 1800 B records the absorbance or concentration over the spectral region 190 - 850 nm, includes scale expansion facilities, and has a limiting resolution of 0.1 nm with precision of 0.5 nm and accuracy of ± 0.5 nm. All spectra were recorded using a bandwidth setting of 0.6 nm.

8.4 PHOTOLYSIS CONDITIONS

Photolysis of the transition metal complexes under investigation was achieved by the use of a water cooled medium pressure mercury lamp (Phillips HPK 125 watt) which gave an intense, effectively continuum source over the required uv-vis range. As many of the observed reactions of the matrix isolated complexes depended critically on the wavelength used for photolysis it was necessary to create a number of filters (Table 8.3) which enabled selective photolysis within defined limits throughout the wavelength range 200 to 650 nm. Two types of filter were used for selective photolysis:

(i) Gas cells.

(ii) Glass.

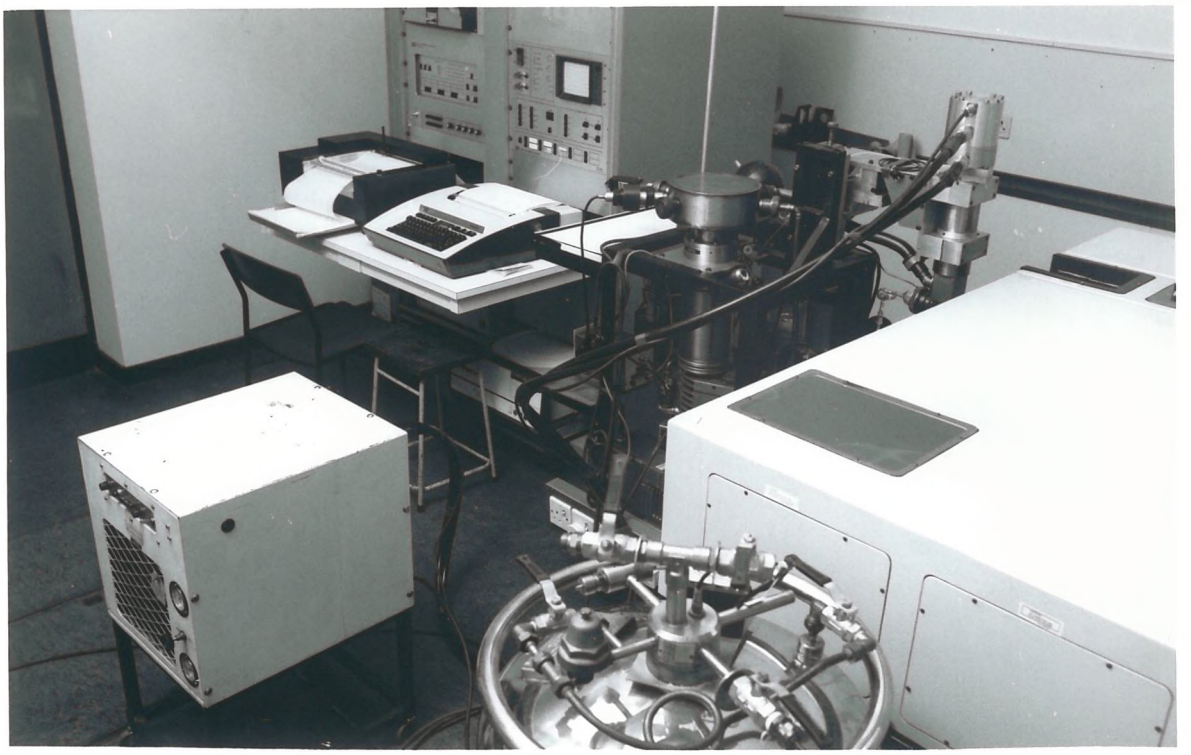

Plate 2

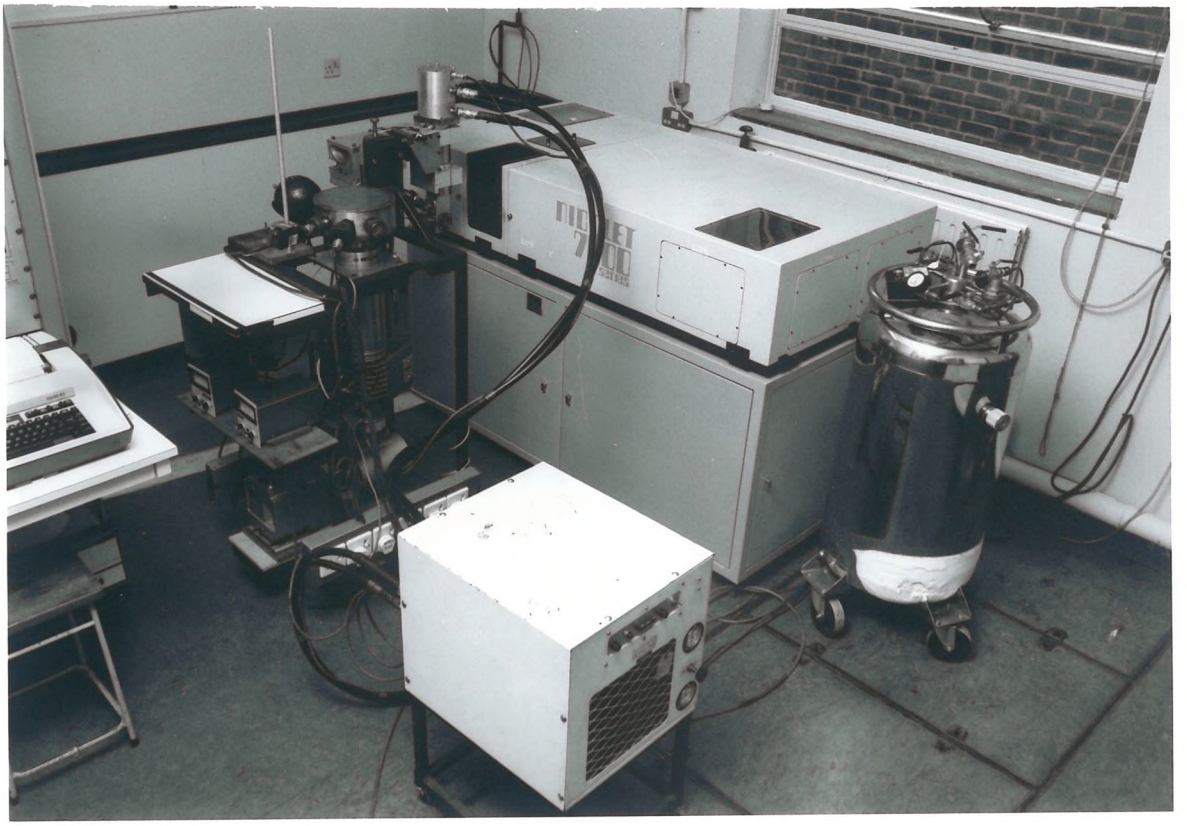

The gas cell filters were made by sealing chlorine gas (2 atmospheres) and bromine vapour (vapour pressure at 20°C) into quartz glass cells (25 mm pathlength). The glass filters were Corning color filters and were used as thin discs of different thicknesses.

8.5 MATRIX GASES

Generally argon, methane, nitrogen ($^{14}N_2$) carbone monoxide (^{12}CO) were used as the matrix gases, however, sometimes mixed matrices of these with ethylene, acetylene and isotopic carbon monoxide (^{13}CO) were used. Bulk gases were of BOC Grade 'X' (Research Grade) standard and used from cylinders. Isotopic gas ^{13}CO (99%) purchased in 1 litre bulbs.

8.6 PREPARATION OF COMPOUNDS

The samples $(\eta^5\text{-}C_5H_5)Mo(CO)_3CH_3$, $(\eta^5\text{-}C_5H_5)Mo(CO)_3CF_3$ and $(\eta^5\text{-}C_5H_5)Mo(CO)_3(COCF_3)$ were prepared according to the literature procedures and purified by sublimation [3, 4]. All other complexes were obtained as gifts or from commercial sources and all were purified by sublimation.

^{13}CO enriched complexes were prepared in a quartz sublimation apparatus (Figure 8.4) containing the complex to be enriched dissolved in an appropriate solvent. The entire apparatus was vacuum tight and contained, with the complex solution, an atmosphere of carbon monoxide at the required isotopic concentration. Substitution of ^{12}CO by ^{13}CO could be achieved thermally or photochemically. Solvent was removed by a vacuum pump and the complex purified by subliming directly onto the cold (-196°C) finger.

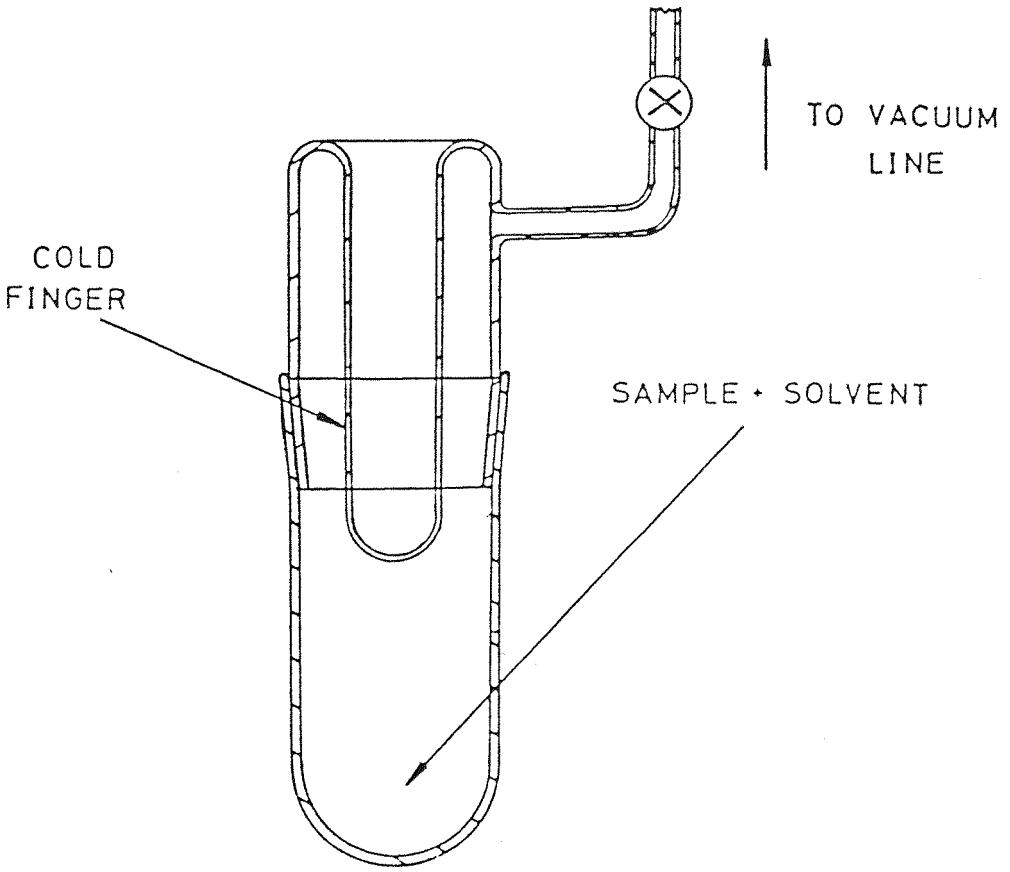

Figure 8.4 Quartz sublimation apparatus for the ^{13}CO enrichment of carbonyl complexes.

Table 8.1 Deposition conditions for various transition metal carbonyl complexes.

Complex	Deposition Method	Sample Head (Figure)	Sample (Temperature °C)[a]
$(\eta^5\text{-}C_5H_5)Cr(CO)_3CH_3$	Co-condensation	8.6b	10
$(\eta^5\text{-}C_5H_5)Mo(CO)_3CH_3$	Co-condensation	8.6b	10
$(\eta^5\text{-}C_5H_5)W(CO)_3CH_3$	Co-condensation	8.6c	20
$(\eta^5\text{-}C_5H_5)Mo(CO)_3CF_3$	Co-condensation	8.6c	25[b]
$(\eta^5\text{-}C_5H_5)Mo(CO)_3(COCF_3)$	Co-condensation	8.6c	25[b]
$(\eta^5\text{-}C_5H_5)Cr(CO)_3H$	Co-condensation	8.6b	5
$(\eta^5\text{-}C_5H_5)Mo(CO)_3H$	Co-condensation	8.6b	10
$(\eta^5\text{-}C_5H_5)W(CO)_3H$	Co-condensation	8.6b	15
$(\eta^5\text{-}C_5H_5)W(CO)_2(C_2H_4)H$	Co-condensation	8.6c	25[b]
$(\eta^5\text{-}C_5H_5)Mo(CO)_3C_2H_5$	Co-condensation	8.6b	15
$(\eta^5\text{-}C_5H_5)W(CO)_3C_2H_5$	Co-condensation	8.6c	30[b]
$(\eta^5\text{-}C_5H_5)W(CO)_3(\underline{n}\text{-}C_3H_7)$	Co-condensation	8.6c	30[b]
$(\eta^5\text{-}C_5H_5)W(CO)_3(\underline{i}\text{-}C_3H_7)$	Co-condensation	8.6c	30[b]
$(\eta^5\text{-}C_5Me_5)W(CO)_3(\underline{n}\text{-}C_3H_7)$	Co-condensation	8.6c	30[b]
$(\eta^5\text{-}C_5H_5)W(CO)_3(\underline{n}\text{-}C_4H_9)$	Co-condensation	8.6c	30[b]
$(\eta^5\text{-}C_5H_5)W(CO)_3C_3H_5$	Co-condensation	8.6c	30[b]
$(\eta^5\text{-}C_5H_5)W(CO)_3C_6H_5$	Co-condensation	8.6e	45[b]
$(\eta^5\text{-}C_5H_5)W(CO)_3CH_2C_6H_5$	Co-condensation	8.6e	50[b]
$(\eta^5\text{-}C_5H_5)Fe(CO)_2CH_3$	Pulsed	8.6a	25
$(\eta^5\text{-}C_5H_5)Fe(CO)_2C_2H_5$	Pulsed	8.6a	25
$(\eta^5\text{-}C_5H_5)Ru(CO)_2CH_3$	Pulsed	8.6a	25
$(\eta^5\text{-}C_5H_5)Ru(CO)_2C_2H_5$	Pulsed	8.6a	25
$(\eta^5\text{-}C_5H_5)Fe(CO)_2Cl$	Co-condensation	8.6c	40[b]
$(\eta^5\text{-}C_5H_5)Ru(CO)_2Cl$	Co-condensation	8.6d	50[b]
$(\eta^5\text{-}C_5H_5)Mo(CO)_3Cl$	Co-condensation	8.6d	50[b]
$(\eta^5\text{-}C_5H_5)W(CO)_3Cl$	Co-condensation	8.6d	50[b]
$(\eta^5\text{-}C_5H_5)Mo(CO)_3As(Me)_2$	Co-condensation	8.6d	45[b]
$(\eta^5\text{-}C_5H_5)Mo(CO)_3Sb(Me)_2$	Co-condensation	8.6d	45[b]
$(\eta^5\text{-}C_5H_5)W(CO)_3As(Me)_2$	Co-condensation	8.6d	55[b]
$(\eta^5\text{-}C_5H_5)W(CO)_3Sb(Me)_2$	Co-condensation	8.6d	55[b]

/continued

Table 8.1 (Continued)

Complex	Deposition Method	Sample Head (Figure)	Sample (Temperature °C)[a]
$(\eta^5\text{-}C_5H_5)W(CO)_3As(\underline{n}\text{-}C_3H_7)_2$	Co-condensation	8.6d	60[b]
$(\eta^5\text{-}C_5H_5)W(CO)_3As(\underline{i}\text{-}C_3H_7)_2$	Co-condensation	8.6d	60[b]
$(\eta^5\text{-}C_5H_5)W(CO)_3As(\underline{t}\text{-But})_2$	Co-condensation	8.6d	80[b]
$(\eta^5\text{-}C_5H_5)(CO)_2W{=}As(\underline{t}\text{-But})_2$	Co-condensation	8.6d	80[b]
$[(\eta^5\text{-}C_5H_5)Fe(CO)_2]_2$	Co-condensation	8.6d	100[b]

[a]Sample temperatures for the pulsed deposition method represent the temperatures required to generate the right vapour pressure in matrix gas preparation (Figure 8.2a). For co-condensation of the sample and matrix gas, the sample temperature represents the temperature required to control volatilisation of the complex.

[b]For temperatures > 25 °C an induction heater was used.

Table 8.2 Some optical materials, their properties and suitability for matrix infrared (IR) and UV-visible (UV-vis) spectroscopy.

Material	Optical Range (nm)	Suitability
Soda glass	330 - 2700	Vis
Quartz glass	200 - 4500	UV-vis
Sodium Chloride	250 - 15000	Vis and IR
Sodium Bromide	300 - 40000	IR
Sodium Iodide	350 - 70000	IR
Potassium Chloride	250 - 25000	IR
Potassium Bromide	250 - 60000	Vis and IR
Potassium Iodide	350 - 70000	IR
Cesium Bromide	250 - 80000	IR
Cesium Iodide	300 - 90000	IR
Lithium Fluoride	150 - 10000	UV-vis and IR
Calcium Fluoride	160 - 10000	UV-vis and IR
Magnesium Fluoride	150 - 10000	UV-vis and IR
Barium Fluoride	150 - 15000	UV-vis and IR
Strontium FLuoride	150 - 70000	UV-vis and IR
Silver Chloride	400 - 30000	IR
KRS-5	600 - 40000	IR

Table 8.3 Approximate ultraviolet-visible transmission ranges for filters used in conjunction with a medium pressure mercury arc.

Filter	Description	Transmission (> 50%)
A	Quartz gas cell (pathlength 30 mm) containing Cl_2 gas (2 atm.) + quartz cell containing Br_2 (300 Torr)	$\lambda < 285$, $\lambda > 500$ nm
B	Quartz gas cell (pathlength 25 mm) containing Br_2 gas (300 Torr) + pyrex disc 7 mm thick.	λ = 290 - 370 nm
C	Quartz gas cell (pathlength 25 mm) containing Br_2 gas (300 Torr)	$\lambda < 350$, $\lambda > 550$ nm
D	Corning glass filter C.S. 3-73	$\lambda > 430$ nm
E	Corning glass filter C.S. 3-74	$\lambda > 410$ nm
F	Corning glass filter C.S. 0-51	$\lambda > 370$ nm
G	Corning glass filter C.S. 3-70	λ = 490 - 513 nm
H	Corning glass filter C.S. 7-54	λ = 230 - 420 nm
I	Corning glass filter C.S. 7-60	λ = 290 - 390 nm
J	Corning glass filter C.S. 7-39	λ = 310 - 410 nm

REFERENCES

1. M.M. Rochkind, *Spectrochim. Acta.*, 1971, 27A, 547.

2. *"International Union of Pure and Applied Chemistry. Tables of wavenumbers for the calibration of infrared spectrometers".* Butterworths (1961).

3. R.B. King, *"Organometallic Synthesis"*, Academic Press, N.Y., 1965, Vol. 1, p145.

4. R.B. King and M.B. Bisenette, *J. Organomet. Chem.*, 1964, 2, 15.